The hydrogen-dependent CO_2 reductase from *Acetobacterium woodii* and *Thermoanaerobacter kivui*: Capture and storage of hydrogen and carbon dioxide in formic acid by acetogenic bacteria

Dissertation
zur Erlangung des Doktorgrades
der Naturwissenschaften

vorgelegt beim Fachbereich Biowissenschaften
der Johann Wolfgang Goethe-Universität
in Frankfurt am Main

von

Fabian M. Schwarz

aus Mannheim

Frankfurt am Main, 2021
(D30)

vom Fachbereich Biowissenschaften der
Johann Wolfgang Goethe-Universität als Dissertation angenommen.

Dekan:	Prof. Dr. Sven Klimpel
1. Gutachter:	Prof. Dr. Volker Müller
2. Gutachter:	Prof. Dr. Eric J. N. Helfrich

Datum der Disputation:

This thesis is based on the following publications:

1. **Schwarz, F.M.** and Müller, V. (2020) Whole-cell biocatalysis for hydrogen storage and syngas conversion to formate using a thermophilic acetogen. Biotechnol. Biofuels 13: 32. – accepted and published

2. **Schwarz, F.M.**, Ciurus, S., Jain, S., Baum, C., Wiechmann, A., Basen, M. and Müller, V. (2020) Revealing formate production from carbon monoxide in wild type and mutants of Rnf- and Ech-containing acetogens, *Acetobacterium woodii* and *Thermoanaerobacter kivui*. Microb. Biotechnol. 13: 2044-2056. – accepted and published

3. **Schwarz, F.M.**, Oswald, F. and Müller, V. (2021) Acetogenic conversion of H_2 and CO_2 into formic acid and *vice versa* in a fed-batch operated stirred tank bioreactor. ACS Sustain. Chem. Eng. 9: 6810-6820. – accepted and published

Table of contents

1. Summary

Global warming and climate change belong to the most serious concerns of humankind. Therefore, the implementation of global political regulations, CO_2 mitigation strategies as well as strategies to replace fossil-fuel-based energy carriers are urgently needed. Carbon capture and storage (CCS) and also carbon capture and utilization (CCU) technologies have gained more and more attention over the last years, covering chemical as well as biological routes to reduce the impact of CO_2 emissions on the environment. One way, which captures CO_2 and also stores molecular H_2, is the way of direct hydrogenation of CO_2 into the liquid organic hydrogen carrier (LOHC) formic acid. Since the compound formic acid directly addresses major challenges in the field of energy storage and (bio)-chemical production, the formate bioeconomy and its popularity are more and more growing.

This thesis describes a biological route for the conversion of H_2 and CO_2 to formic acid using the two acetogenic bacteria *Acetobacterium woodii* and *Thermoanaerobacter kivui* as biocatalysts. These two organisms contain a novel enzyme complex which directly uses molecular hydrogen as electron donor for the reduction of CO_2 to formic acid, the hydrogen-dependent carbon dioxide reductase (HDCR). The purified enzyme showed remarkable catalytic activities, by far exceeding any known chemical and biological catalyst. To take advantage of using whole cells instead of the purified enzyme, the thesis describes a whole-cell approach using *A. woodii* and *T. kivui* cells as biocatalyst to catalyze a chemically challenging reaction. Therefore, growth was decoupled from the HDCR reaction by lowering the intracellular amount of ATP using specific inhibitors or ionophores. As a result, the typical intermediate formic acid which is produced by many acetogens transiently during acetogenesis from H_2 and CO_2 becomes the predominant product. After the establishment, characterization and optimization of a whole-cell approach, energetically “uncoupled” *T. kivui* cells showed the highest specific formic acid production rates (~150 mmol g_{CDW}^{-1} h^{-1}) which were so far reported in the literature for biological systems.

But not only the conversion of H_2 and CO_2 was shown, moreover, the biotechnological interesting gas feed stock synthesis gas, a combination of H_2,

CO_2 and CO as well as CO alone, were converted to formic acid. To understand the HDCR-based CO utilization in the two bioenergetically different classes of 'Rnf'- and 'Ech-acetogens' with the representatives of *A. woodii* and *T. kivui*, respectively, wild-type and mutant strains of both organisms were investigated for their ability to convert CO into the bulk chemicals acetic acid and formic acid. Again, CO-based formic acid production rates were among the highest rates ever reported. Furthermore, mutants with deficiencies in key enzyme activities of the central metabolism such as Δ*hdcr*, Δ*cooS*, Δ*hydBA*, Δ*rnf* and Δ*ech2* allowed the postulation of two different CO utilization pathways in the bioenergetic model organisms *A. woodii* and *T. kivui*.

For future biotechnological applications of acetogenic bacteria in carbon capture and H_2 storage, the upscaling feasibility of the established whole-cell system was also shown in a fed-batch operated stirred tank bioreactor, converting H_2 and CO_2 into formic acid and *vice versa.* The process showed an efficiency of 100% for the CO_2 conversion to formic acid and notably no other products such as acetic acid were co-produced in the process. To release the stored H_2 from formic acid and to close the H_2 storage cycle, H_2 production from formic acid was also shown with a conversion efficiency of almost 100% and more than 2.1 M of formic acid was oxidized in the process. Not only catalytic rates, yields and final product concentrations were determined, moreover, important parameters such as turnover frequency (TOF) and turnover number (TON) were also identified for the whole-cell system. After both reaction directions were proven in bioreactor experiments, a new bioreactor application was designed for the biological hydrogen storage and release through multiple cycles of reversible hydrogenation of CO_2 to formic acid in a single process unit. Therefore, multiple day/night cycles were simulated with the aim to store H_2 in excess-energy times and to release the stored H_2 in energy-lean times. The process was running over two weeks and whole cells from *A. woodii* facilitated the conversion of H_2 and CO_2 to formic acid as well as the reverse reaction of formic acid oxidation to H_2 and CO_2 in a single bioreactor. In sum, 330 (± 85) mM formic acid could be produced and re-oxidized within two weeks and the cells showed a solid robustness in the applied process.

This thesis concludes, that the two HDCR containing bacteria *A. woodii* and *T. kivui* are promising biocatalysts to capture inorganic carbon and to store molecular hydrogen in the soluble and liquid C1 compound formic acid. Additionally, *A. woodii* cells were proven as biocatalyst for formic acid-driven H_2 production to enable the release of previously stored H_2 from formic acid. First bioreactor applications and a process design were also given to demonstrate the potential and future outlook of the whole-cell system. Therefore, acetogenic bacteria could provide a future biological route for the two challenging reactions of CO_2 hydrogenation to formic acid and *vice versa*, especially when many chemical catalysts strongly rely on high pressure or temperature, need very expensive additives or suffer from low TON/TOF in the CO_2 hydrogenation process.

2. Introduction

2.1. CO_2 reduction and formate dehydrogenases of acetogenic bacteria

The global carbon cycle describes the transformations and fluxes of carbon between four major reservoirs of the Earth system: the atmosphere, the lithosphere, the biosphere and the hydrosphere. Carbon is a fundamental building block of all life on planet earth, but anthropogenic activities over the past century have perturbed the balance of the entire system (Hansen et al., 2007; Ramanathan and Feng, 2008). Since the Industrial Revolution huge amounts of carbon dioxide (CO_2) have been emitted from various industries, resulting in a 30% increase of the atmospheric CO_2 partial pressure from 280 ppm to 400 ppm (Pearson and Palmer, 2000; Sarmiento and Gruber, 2002). Inorganic gaseous carbon such as CO_2, but also methane (CH_4), have important greenhouse properties that directly effect the global climate system (Houghton et al., 1996; Cox et al., 2000). The increased atmospheric CO_2 concentrations are linked to an increase of the global average temperature, therefore, causing global warming and climate change (Allen et al., 2009; Meinshausen et al., 2009; Solomon et al., 2009). As a result, CO_2 emissions have to be reduced and new technologies are needed to capture, store, and utilize CO_2. Strategies for CO_2 utilization are of particular interest since CO_2 can be used as a versatile feedstock to produce various organic products such as chemicals, fuels, and polymers (Olah et al., 2009; Venkata Mohan et al., 2016; Grignard et al., 2019). Among chemical approaches for carbon capture and storage (CCS) and carbon capture and utilization (CCU) also biological solutions apply (Leung et al., 2014; Cheah et al., 2016; Kumar et al., 2018). Here, a special group of non-phototrophic, anaerobic CO_2-fixing bacteria, the group of acetogenic bacteria, have recently attracted scientific and commercial interest (Daniell et al., 2012; Bengelsdorf et al., 2016; Liew et al., 2016b). This group of bacteria shows promising capabilities for industrial applications to develop carbon-neutral technologies by producing different biofuels and biochemicals from inorganic carbon such as the greenhouse gas (GHG) CO_2. (Latif et al., 2014; Daniell et al., 2016; Liew et al., 2016b).

In nature, there are seven ways of CO_2-fixation which enable autotrophic organisms to fix inorganic carbon in their metabolisms. Among these organisms are plants, cyanobacteria, algae, green and purple bacteria but also some non-phototrophic, anaerobic bacteria and archaea (Berg, 2011; Fuchs, 2011). They all use one of the known biological routes for CO_2 fixation such as the reductive pentose phosphate cycle (known as Calvin–Benson–Bassham cycle) (Calvin and Benson, 1948), the reductive acetyl-CoA pathway (known as Wood-Ljungdahl pathway) (Wood et al., 1986; Wood and Ljungdahl, 1991), the reductive tricarboxylic acid cycle (reductive TCA cycle) (Evans et al., 1966), the 3-hydroxypropionate/4-hydroxybutyrate cycle (Berg et al., 2007), the 3-hydroxypropionate bi-cycle (Holo, 1989; Herter et al., 2002; Zarzycki et al., 2009) and the dicarboxylate/4-hydroxybutyrate cycle (Huber 2008). Recently, even a seventh CO_2 fixation pathway was discovered in the sulfate-reducing bacterium *Desulfovibrio desulfuricans* named as reductive glycine pathway (Sánchez-Andrea et al., 2020). Nevertheless, all pathways exhibit one of two different strategies of carbon fixation - namely carboxylation or CO_2 reduction. In dependence of the used substrate, the involved enzymes are either carboxylases or CO_2 reductases which either accept inorganic carbon in form of HCO_3^- or CO_2. The Wood-Ljungdahl pathway (WLP) of acetogenic bacteria demonstrates the strategy of CO_2 reduction using formate dehydrogenases as CO_2 reductases (E.C. 1.17.1.9) to catalyze the reversible 2-electron reduction of CO_2 to formic acid/formate[1] (eq. 1).

$$\mathrm{CO_2 + 2H^+ + 2e^- \rightleftharpoons HCOO^- + H^+} \qquad \mathrm{E^{0\prime} = -430\ mV} \qquad (1)$$

In general, formate dehydrogenases (FDHs) are a group of heterogeneous enzymes which can display different subunit compositions and which harbor metal or no metal redox centers in their active sites. Based on their metal content/structure and consequent catalytic strategies, FDHs can broadly be classified into metal-independent and metal-dependent (molybdenum- and tungsten containing) enzymes (Maia et al., 2015). The class of metal-independent FDHs harbors no redox cofactors or metal ions and therefore a

[1] Formate is the conjugated base of formic acid which has an pK_a of 3.75. Therefore, the formate anion is the prevailing species under physiological conditions and will be representatively named for formic acid in this thesis.

direct hydride transfer from formate to the electron acceptor NAD^+ is suggested (Tishkov et al., 1996; Castillo et al., 2008). These NAD^+-dependent FDHs belong to the D-specific dehydrogenases of the 2-oxyacid family (Vinals et al., 1993; Balnokin and Popova, 1994), and representative enzymes of this class are extremely slow in the direction of CO_2 reduction (Tishkov and Popov, 2006; Choe et al., 2015; Cotton et al., 2018). The classified NAD^+-dependent FDH enzymes of *Candida boidinii*, *Candida methylica*, *Chaetomium thermophulum* and *Myceliphthora thermophile* showed only a small fraction of the catalytic turnover rate (k_{cat}) for CO_2 reduction compared to the metal-containing FDHs of *Desulfovibrio vulgaris*, *Cupriavidus necator* (formerly known as *Ralstonia eutropha*), *Rhodobacter capsulatus* or *Syntrophobacter fumaroxidans*, to name just a few (Moon et al., 2020). In contrast to the metal-independent FDHs which are more widespread and found in aerobic bacteria, yeasts, fungi and plants, the metal-dependent FDHs exist only in various prokaryotes such as acetogenic bacteria and methanogenic archaea. Here, the corresponding FDHs belong to the molybdenum and tungsten-containing enzyme families (Fig. 1) which harbor either a molybdenum (Mo) or tungsten (W) atom in the active site that mediates the formate oxidation (Grimaldi et al., 2013; Maia et al., 2015).

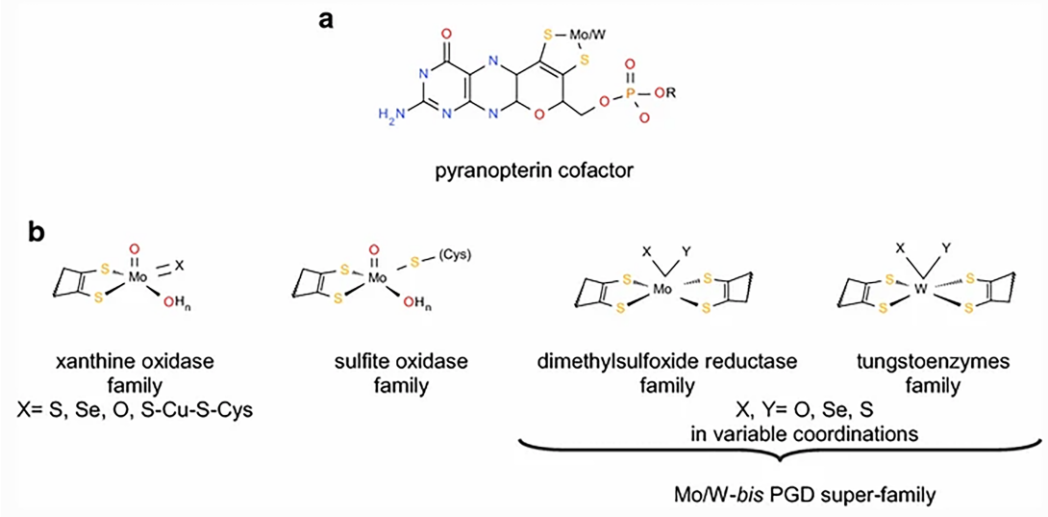

Fig. 1 Active site structures of molybdenum- and tungsten-containing enzymes (Maia et al., 2015). (a) Pyranopterin cofactor which binds the molybdenum or tungsten atom. In Eukaryotes the residue (R) is a hydrogen atom while in prokaryotes several nucleotides such as guanosine-, cytidine- or adenosine monophosphate are present. **(b)** Molybdenum and tungsten-containing enzyme families. Molybdoenzymes (containing Mo) can be divided into the three big families of xanthine oxidase, sulfite oxidase and dimethylsulfoxide reductase (DMSOR) families. The DMSOR family comprises different procaryotic enzymes such as DMSOR itself, Mo-containing formate deyhdrogenases (FDHs) and dissimilatory/assimilatory nitrate reductases. Due to the structural and functional similarities between the DMSOR family enzymes and tungstoenzymes, containing homologous Mo-FDHs and W-FDHs, respectively, both families can be gathered to the molybdenum/tungsten-*bis* pyranopterin guanosine dinucleotide super-family (Mo/W-*bis* PGD).

Moreover, metal-dependent FDHs are quite efficient in the direction of CO_2 reduction (Maia et al., 2017; Moon et al., 2020), thereby having an important role as non-photosynthetic CO_2 utilizing enzymes in various prokaryotes. Additionally, the enzyme group can be used as electrocatalyst (Reda et al., 2008; Schlager et al., 2016; Amao, 2018). The metal-dependent Fdh1 of *Syntrophobacter fumaroxidans* and FdhH of *Escherichia coli* were already used as electroactive enzymes in electroenzymatic approaches to catalyze the reduction of CO_2 to formate with electrons supplied from an electrode (Reda et al., 2008; Bassegoda et al., 2014). Since the CO_2/formate couple has a low redox potential with $E^{0'}$ of −430 mV (Thauer et al., 1977; Buckel and Thauer, 2013), energy-rich reducing equivalent such as reduced ferredoxin, NADPH or H_2 are required to drive the reduction of CO_2 to formate in nature (Thauer et al., 1977; Scherer and Thauer, 1978; Yamamoto et al., 1983; Wang et al., 2013b). So far, only a few formate dehydrogenases were purified and characterized from acetogenic bacteria which use this enzyme class to fix inorganic CO_2 in their metabolisms *via* the Wood-Ljungdahl pathway (WLP). However, the purified and characterized FDHs from acetogenic bacteria clearly demonstrate the diversity in subunit composition and the diversity of used reductants of this enzyme class.

In the 1970s the soluble ferredoxin-dependent formate dehydrogenase of the acetogenic bacterium *Clostridium pasteurianum* was purified (Scherer and Thauer, 1978). The molybdenum-containing enzyme complex, which consist of two major subunits, catalyzed the reversible reduction of CO_2 to formate with reduced ferredoxin. The Fd_{red}:CO_2 oxidoreductase activity as well as the formate:Fd_{ox} oxidoreductase activity was 35 U/mg and 22.5 U/mg (1 U = 1 µmol/min), respectively (Scherer and Thauer, 1978). The reduction of CO_2 with reduced ferredoxin as electron donor is quite favorable, since the standard redox potential $E^{0'}$ of the Fd_{ox}/Fd_{red} couple is around −400 mV and the redox potential is even expected to be more negative under physiological conditions (E' = ~ −500 mV) (Thamer et al., 2003; Thauer et al., 2008; Buckel and Thauer, 2013). This assumption is mainly based on the fact, that many ferredoxin-driven reactions operate at very low redox potentials in anaerobic bacteria such as the pyruvate:ferredoxin oxidoreductase reaction ($E^{0'}$ = −500 mV) (Uyeda and Rabinowitz, 1971; Thauer et al., 1977) or the CO dehydrogenase reaction ($E^{0'}$ = −520 mV) (Thauer et al., 1977). But this

assumption has been controversially debated (Bar-Even, 2013). Nevertheless, it has to be kept in mind, that the reduction potential of ferredoxins can greatly vary between different anaerobic organisms and that they can have different midpoint potentials (Smith and Feinberg, 1990; Smith et al., 1991; Boll et al., 2000; Bender and Ragsdale, 2011).

In 1982, the NADP-dependent formate dehydrogenase from the thermophilic acetogen *Moorella thermoacetica* (formerly known as *Clostridium thermoaceticum*) was purified and the enzyme complex catalyzed the reversible reduction of CO_2 to formate using NADPH as the electron donor (Yamamoto et al., 1983). The complex consists of two different subunits, most likely forming a heterodimer ($\alpha_2\beta_2$). Tungsten could be detected as cofactor in the purified enzyme. Nevertheless, molybdenum and tungsten may substitute for each other since both metals could be incorporated in the active enzyme (Yamamoto et al., 1983). That molybdenum and tungsten can replace each other was also supported by the observation of other FDHs which were active with each metal in the active site (Brondino et al., 2004; Brondino et al., 2006). The reduction of CO_2 with NADPH is quite unfavorable since the standard redox-potential ($E^{0'}$) of the $NADP^+$/NADPH couple is around −320 mV. But in living cells, the $NADP^+$/NADPH ratio is around 1/40, therefore changing the redox potential to a more negative value of around E' = −380 mV (Bennett et al., 2009). The state of the chemical equilibrium can further be affected by prevailing environmental and cellular conditions, thus allowing NADPH-driven CO_2 reduction *in vivo*.

A few years later, in 2013, a multimeric enzyme complex for the reduction of CO_2 to formic acid was discovered in the acetogenic bacterium *Clostridium autoethanogenum* (Wang et al., 2013b). Here, an electron-bifurcating [FeFe]-hydrogenase forms a complex with a tungsten-containing formate dehydrogenase and additional [FeS]-cluster-containing subunits (Fig. 2). The overall complex consists of seven different subunits which harbors 60 mol of iron, 0.3 mol of tungsten, 0.6 mol of selenium, and 0.63 mol of FMN per mol of enzyme. The enzyme complex catalyzes multiple redox reactions, such as the H_2-dependent CO_2 reduction to formate (41 U/mg), the reversible reduction of Fd_{ox} and $NADP^+$ with H_2 (29.2 U/mg) or formate (15.2 U/mg) as well as the reversible formation of H_2 and CO_2 from formate (40 U/mg). However, it has been

postulated that the reduction of CO_2 with NADPH and reduced ferredoxin is the preferred activity in cells growing on CO (Wang et al., 2013b).

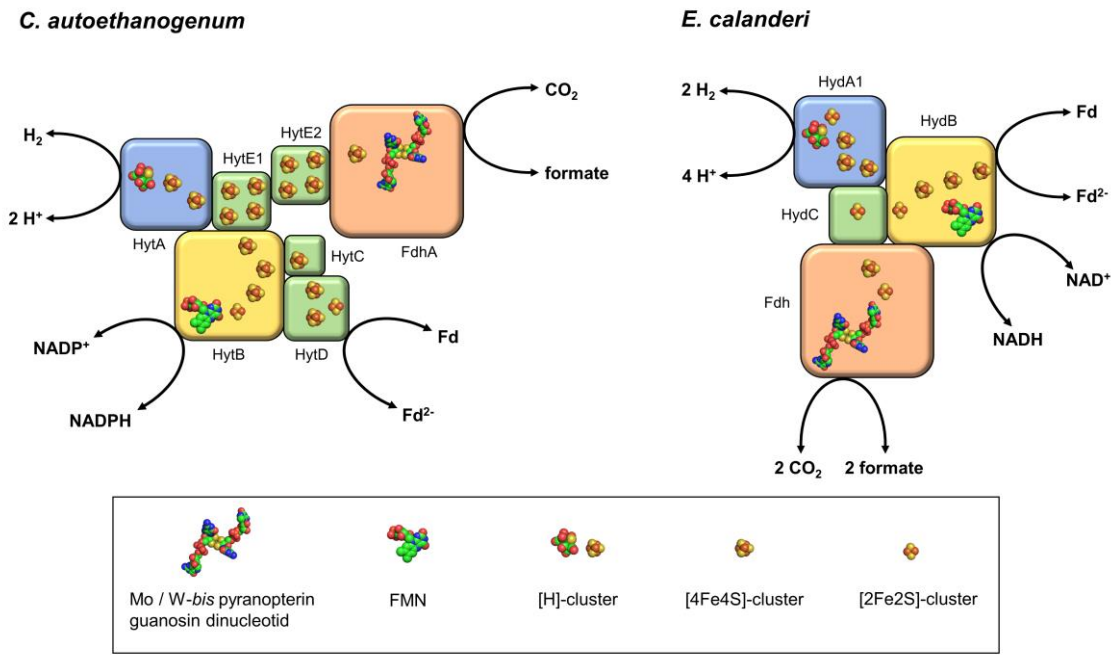

Fig. 2 Model of the electron bifurcating hydrogenase-formate dehydrogenase complex from *C. autoethanogenum* and *E. calanderi*. Both enzymes consist of a [FeFe]-hydrogenase, a formate dehydrogenase and multiple [FeS]-cluster-containing subunits. Additionally, both enzymes are capable of flavin-based electron bifurcation (FBEB). Mo, molybdenum; W, tungsten; FMN, flavin mononucleotide.

Recently, a similar electron bifurcating hydrogenase-formate dehydrogenase complex was identified in the acetogenic bacterium *Eubacterium callanderi* KIST612 (Dietrich et al., 2021). The purified enzyme complex consists of 4 subunits (Fdh, HydA1, HydB and HydC), again, combining an FMN-containing bifurcating [FeFe]-hydrogenase with a formate dehydrogenase subunit (Fig. 2). The enzyme complex also catalyzed H_2-dependent CO_2 reduction to formate and formate-driven H_2 production with a specific activity of 30 mU/mg and 0.84 U/mg, respectively (Dietrich et al., 2021). However, the activity (formate production; H_2 evolution) was highest if the soluble reducing equivalents NAD^+ and Fd_{ox} were present, indicating the involvement of these electron carriers *in vivo*. It is assumed, that excess electrons can be released by the enzyme *via* H_2 evolution during cellular electron imbalance as previously proposed for the enzyme complex of *C. autoethanogenum* (Wang et al., 2013b; Dietrich et al., 2021). However, both enzyme complexes are capable of flavin-based electron bifurcation (FBEB). The mechanism of FBEB is a newly discovered mechanism

in which a two-electron donor such as NAD(P)H, H_2, or format is oxidized to reduce two different electron acceptors, one with a more negative reduction potential and one with a more positive reduction potential (Buckel and Thauer, 2018a). In this mechanism a flavin bound cofactor (FMN or FAD) splits the electron pair of the donor into one electron with a more negative reduction potential and one with a more positive reduction potential, and the electrons are simultaneously transferred and tightly coupled to the reduction of the acceptors (Buckel and Thauer, 2013; Chowdhury et al., 2014). Here, the exergonic reduction of one acceptor always drives the endergonic reduction of the other acceptor. FBEB is a highly important mechanism for microorganisms to generate low-potential electrons for the reduction of ferredoxins (Fd) and flavodoxins (Fld) which are in turn required for redox reactions and energy conservation in the metabolism. If the mechanism operates in the reverse reaction, it is called electron confurcation (Schut and Adams, 2009; Buckel and Thauer, 2018a). Many enzymes involved in FBEB were purified over the last decade from various anaerobic bacteria and archaea also including many enzymes from the acetogenic model organism *Acetobacterium woodii* i.e., the Fd- and NADH-dependent caffeyl-CoA reductase (CarCDE) (Bertsch et al., 2013), the Fd- and NAD-dependent lactate dehydrogenase (LctBCD) (Weghoff et al., 2015) and the Fd- and NAD-dependent [FeFe]-hydrogenase (HydABC) (Schuchmann and Müller, 2012). The importance of flavin-based electron bifurcation in the energy metabolism, the general metabolic function as well as the enzymatic mechanism were already discussed in many excellent review articles (Buckel and Thauer, 2013, 2018a, b; Müller et al., 2018).

In 2013 and 2019, a novel enzyme complex for the reduction of CO_2 was discovered in the two acetogenic bacteria *A. woodii* and *Thermoanaerobacter kivuii* (Schuchmann and Müller, 2013; Schwarz et al., 2018). This enzyme complex has a simpler architecture than the enzyme from *C. autoethanogenum*, is not involved in energetic coupling by electron bifurcation and directly uses molecular hydrogen ($E^{0'}$ = −414 mV) as the electron donor for the reduction of CO_2 to formate. Therefore, the enzyme was named "H_2-dependent CO_2 reductase" (HDCR). The HDCR was purified and characterized from both organisms and consists of 4 subunits: the catalytic subunits of hydrogenase (HydA) and formate dehydrogenase (FdhF) and two putative

electron-transferring subunits (HycB). The electron-transferring subunits are rich in [4Fe4S]-clusters, most likely interlinking the electron transfer from one catalytic site to the other. The hydrogenase belongs to the group of [FeFe]-hydrogenases and shows a characteristic [H]-cluster in its active site, whereas the formate dehydrogenase contains a molybdenum/tungsten-*bis* pyranopterin guanosine dinucleotide (Mo/W-*bis* PGD) cofactor. Molybdenum (Mo) was found in the *A. woodii* enzyme whereas tungsten (W) was present in the isolated HDCR from *T. kivui* (Schuchmann and Müller, 2013; Schwarz et al., 2018) (Fig. 3).

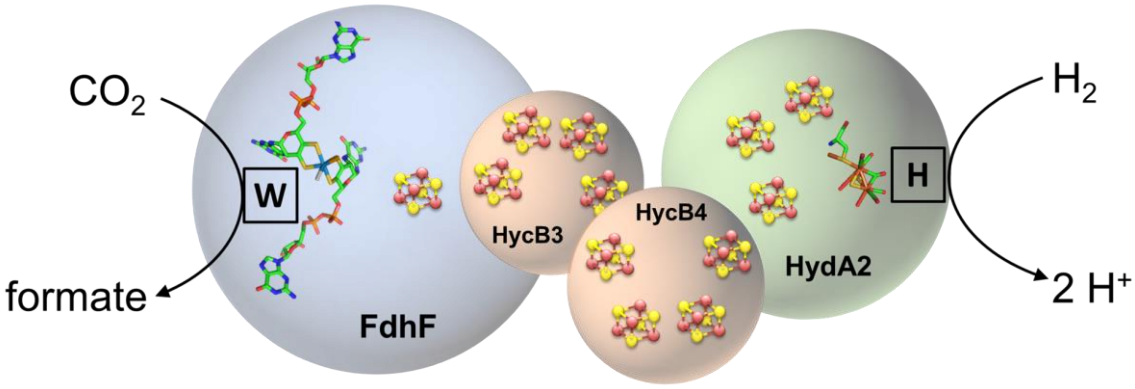

Fig. 3 Model of the hydrogen-dependent CO_2-reductase of *T. kivui* (Schwarz et al., 2018). The enzyme complex harbors two catalytic subunits of formate dehydrogenase (FdhF) and hydrogenase (HydA2). The formate dehydrogenase subunit belongs to the W-*bis* PGD super family reductase family and the hydrogenase subunit belongs to the group of [FeFe]-hydrogenases which contains the conserved regions of H-cluster binding. Coupling is putatively achieved by two electron-transferring subunits (HycB3/B4) which contains multiple [4Fe4S]-clusters. W, tungsten; H, H-cluster.

Another difference between the two HDCR complexes is the presence of two isoenzymes of the HDCR formate dehydrogenases in *A. woodii*, either containing selenocysteine or cysteine at the amino acid position 139 (Schuchmann and Müller, 2013). *T. kivui* harbors only a cysteine-containing FdhF in the HDCR complex and is probably not able to assemble selenoproteins due to the missing of the essential *selABC* gene cluster in the genome (Hess et al., 2014). Generally, selenocysteine is found in many metal-dependent FDHs but can be replaced by cysteine, mostly affecting the catalytic activity of the enzymes (Jones and Stadtman, 1981; Axley et al., 1991). The incorporation of cysteine instead of selenocysteine in the formate dehydrogenase H of *E. coli* dramatically decreased the formate dehydrogenase activity by two orders of magnitude (Axley et al., 1991). The HDCR from *A. woodii* and *T. kivui* catalyzed the direct hydrogenation of CO_2 to formic acid with a specific activity of 10 U/mg and 900 U/mg,

respectively (Schuchmann and Müller, 2013; Schwarz et al., 2018). Moreover, the reverse reaction, formate oxidation with simultaneous evolution of H_2 and CO_2, was catalyzed by the HDCRs. Here, a specific activity of 14 and 930 U/mg was demonstrated for the *A. woodii* and *T. kivui* enzyme (Schuchmann and Müller, 2013; Schwarz et al., 2018). Interestingly, electron microscopy studies of the purified enzyme from *A. woodii* revealed the formation of ordered filamentous structures with a length up to 200 nm *in vitro* (Schuchmann et al., 2016). The reversible polymerization of the HDCR into ordered filaments was dependent on the presence of divalent cations and the enzymatic activity was connected to the quaternary structure of the HDCR, showing the highest activity in the filamentous form (Schuchmann et al., 2016). First indications of the presence of HDCR filaments are also given for the HDCR of *T. kivui* (unpublished data). Interestingly, the filamentation of enzymes is increasingly recognized as an important phenomenon to affect function, regulation, signaling and activity of enzymes within the cell. The particular biological role of enzyme filamentation are diverse but many enzymes are already known to form filaments *in vitro* and *in vivo* (Park and Horton, 2019).

As mentioned, the HDCRs from *A. woodii* and *T. kivui* showed remarkable catalytic activities for the direct hydrogenation of CO_2 and *vice versa*, substantially exceeding any known chemical catalysts (Müller, 2019). In case of CO_2 hydrogenation, the enzymes are even 30- (*A. woodii*) and 1200- (*T. kivui*) times faster than any chemical catalyst under comparable moderate reaction conditions. Because of the catalyzed reactions and the remarkable catalytic activities in hydrogen-driven CO_2 reduction as well as formate oxidation, the HDCRs seem to be a promising biological catalyst for the capture and storage of CO_2 and H_2. To understand the physiological function of formate dehydrogenases in general and of HDCR enzymes in particular, the biochemistry and bioenergetics of the WLP for CO_2 fixation will be discussed in the following sections in greater detail.

2.2. Biochemistry of the Wood-Ljungdahl pathway

The ability to fix inorganic carbon into organic material (autotrophy) is a primeval life style that exists across all domains of life (Fuchs, 2011). The diverse and specialized group of acetogenic bacteria uses the linear, two branched Wood-Ljungdahl pathway (WLP) to reduce two molecules of CO_2 to acetyl-CoA (Wood et al., 1986). The formed acetyl-CoA can then be used for cell carbon synthesis or can be further converted to different products. In most cases, acetate[2] is formed but the end product can vary (Ljungdahl, 1986). The WLP can also operate in the oxidative direction, thus, allowing a great metabolic flexibility of acetogenic bacteria to utilize a vast variety of different organic substrates (organoheterotrophy) such as hexoses, pentoses, alcohols, methyl groups and formate (Drake et al., 1997; Schuchmann and Müller, 2016). Besides of acetogenic bacteria, the WLP was also identified in methanogenic archaea as well as sulfate reducers (Stupperich et al., 1983; Schauder et al., 1988; Spormann and Thauer, 1988; Ljungdahl, 1994). In general, the WLP can be divided into the two branches of methyl branch and carbonyl branch which are the entry points of CO_2 and/or CO (Fig. 4).

[2] The formed product is acetic acid (pK_a of 4.75). However, the prevailing species at physiological conditions is the conjugated base acetate. Therefore, this work refers to this species.

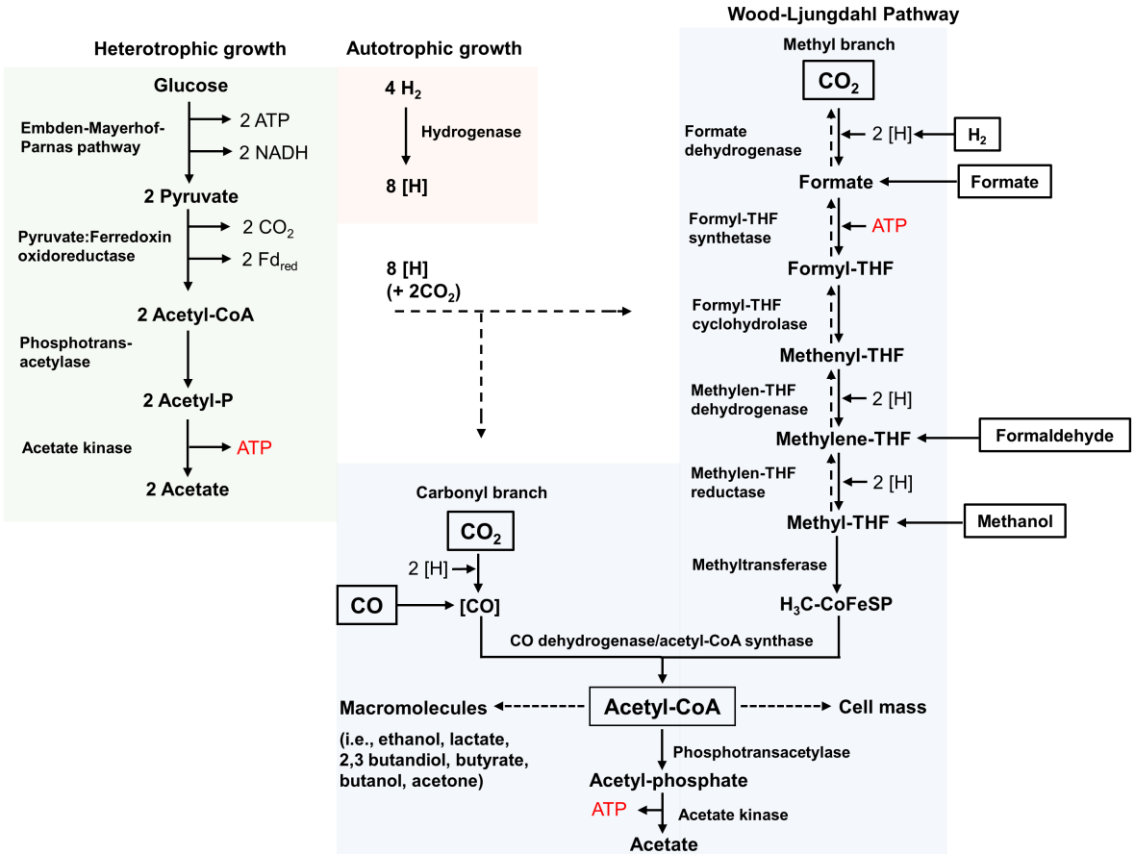

Fig. 4 Biochemistry of the heterotrophic and autotrophic metabolism of acetogenic bacteria (modified after Schuchmann and Müller, 2014). Under heterotrophic growth condition (green box), glucose is oxidized *via* the Embden-Mayerhof-Parnas pathway to pyruvate which is further converted to acetate. The generated reducing equivalents [H] (equals 1 H^+ and 1 e^-) from substrate oxidation are used to fix two CO_2 molecules in acetate by the Wood-Ljungdahl pathway (WLP, blue box). Under autotrophic growth conditions (pink box), the necessary reducing equivalents to drive the redox reactions of the WLP for CO_2 fixation can be obtain, for example, from H_2 oxidation. The net ATP yield of the WLP is zero. THF, tetrahydrofolic acid; CoFeSP, corrinoid iron-sulfur protein; Fd^{2-}, reduced ferredoxin.

In the initial step of the methyl branch, one molecule of CO_2 is reduced with a two-electron donor to formate, catalyzed by the previously mentioned enzyme group of FDHs. As stated, the used electron donor for the reduction of CO_2 to formate can be divers and differs within the group of acetogenic bacteria (Scherer and Thauer, 1978; Yamamoto et al., 1983; Schuchmann and Müller, 2013; Wang et al., 2013a). The intermediate compound formate is subsequently bound with the help of a N^{10}-formyl-THF synthetase and the expense of 1 mol ATP to the cofactor tetrahydrofolic acid (THF) to form N^{10}-formyl-THF (Himes and Harmony, 1973; MacKenzie, 1984). N^{10}-formyl-THF is then reduced in a sequence of tetrahydrofolate (THF)- and cobalamin-dependent reactions to N^5-methyl-THF. First, the N^5,N^{10}-methenyl-THF cyclohydrolase catalyzes the cyclization of N^{10}-formyl-THF to N^5,N^{10}-methenyl-THF (Clark and Ljungdahl, 1982) which is subsequently reduced by a N^5,N^{10}-methylene-THF dehydrogenase to N^5,N^{10}-

methylene-THF (Moore et al., 1974; Ragsdale and Ljungdahl, 1984). In the last step, a reductase catalyzes the formation of the THF-bound methyl group of N^5-methyl-THF (Clark and Ljungdahl, 1984; Wohlfarth et al., 1990). Before this methyl group is transferred to the bifunctional CO dehydrogenase/acetyl-CoA synthase (CODH/ACS) of the carbonyl branch, a methyltransferase catalyzes the methyl group transfer from N^5-methyl-THF to a cobalamin-bound cobalt ion of the corrinoid-iron-sulfur protein (Hu et al., 1984; Ragsdale et al., 1987).

In the carbonyl branch, a second molecule of CO_2 is reduced by the bifunctional CODH/ACS complex to an enzyme-bound carbonyl group, followed by the condensation of coenzyme A and the corrinoid-iron-sulfur protein bound methyl group of the methyl-branch to form acetyl-CoA (Pezacka and Wood, 1984a, b; Ragsdale and Wood, 1985). In the first step, the CODH/ACS catalyzes the reduction of CO_2 to enzyme-bound CO by using two low-potential electrons. Important to note, that this reduction reaction is the largest thermodynamic barrier in the WLP since the CO_2/CO redox couple has a very low standard redox potential ($E^{0'}$) of –520 mM (Thauer et al., 1977). The generated CO at the Ni-Fe-S center (called the C-cluster) of the CODH subunit is then transferred *via* a hydrophobic channel in the enzyme complex to a second Ni-Fe-S center (called the A-cluster) of the ACS subunit (Seravalli et al., 1997; Maynard and Lindahl, 1999; Seravalli and Ragsdale, 2000; Doukov et al., 2002) to prevent the cell metabolism from potentially toxic exposure of CO. The CODH/ACS from the acetogenic bacterium *M. thermoacetica* has been proposed to have one of the longest enzyme channels with a size of 138 A to allow intermolecular CO transport (Doukov et al., 2002). After the migration of CO through the inter-subunit channel, CO is bound to the Ni_p (proximal Ni) site in the A-cluster to form an organometallic complex, called the NiFeC species (Ragsdale, 2004; Brunold, 2004). At the A-cluster, the three different substrates CO, methyl group and coenzyme A are combined *via* a methylation reaction, a carbonylation reaction, and the synthesis of a high-energy thioester bond to form acetyl-CoA (Ragsdale, 1991; Ragsdale, 2008). Acetyl-CoA is converted to acetate as the end product, generating 1 mole of ATP (Diekert and Wohlfarth, 1994a, b). If acetate is formed, the phosphotransacetylase catalyzes the acetyl-group transfer of acetyl-CoA to free phosphate which results in the formation of acetyl phosphate. Finally, an acetate kinase catalyzes the conversion of acetyl phosphate to acetate and one

mole of ATP is produced by substrate level phosphorylation (Schaupp and Ljungdahl, 1974).

The overall stoichiometry ([H] corresponds to one electron plus one proton) of the WLP for the synthesis of acetate from two molecules of CO_2 is shown in eq. 2 (Fischer et al., 1932):

$$2\,CO_2 + 8\,[H] \rightleftharpoons CH_3COO^- + H^+ + 2\,H_2O \qquad \Delta G^{0\prime} = -95\,kJ/mol \qquad (2)$$

Four steps in the WLP require the input of electrons to enable the fixation of two CO_2 molecules. The necessary electrons which are required for the multiple reduction steps can be provided from different organic or inorganic compounds. Heterotrophic acetogenesis using hexoses as substrate leads to the formation of acetate as the only end product. This metabolism was first discovered in the thermophilic model acetogen *M. thermoacetica* where one mol of glucose was converted to three mol of acetate in stoichiometric amounts (eq. 3), therefore named homoacetogenesis (Fontaine et al., 1942). Here, the standard Gibbs free energy change ($\Delta G^{0\prime}$) per mole of acetate is −104 kJ (Drake, 1994).

$$C_6H_{12}O_6 \rightarrow 3CH_3COO^- + 3H^+ \qquad \Delta G^{0\prime} = -104\,kJ/mol \qquad (3)$$

The consumed glucose is oxidized in the Embden-Meyerhof-Parnas pathway (known as glycolysis), yielding two mol of pyruvate, two mol of ATP and two mol of the reducing equivalents NADH (Barker and Kamen, 1945). Each pyruvate is further oxidized by a pyruvate:ferredoxin oxidoreductase to acetyl-CoA and CO_2. The electrons are transferred to the electron acceptor ferredoxin (Ragsdale, 2003). At the end, the two molecules of acetyl-CoA are converted by a phosphotransacetylase and acetate kinase to two molecules of acetate as previously described. The acetate kinase reaction leads to the formation of two additional mol of ATP by substrate-level phosphorylation which provides additional energy for the cell. The remaining two CO_2 molecules are fixed by the WLP with electrons derived from glucose oxidation to produce the third molecule of acetate (Barker and Kamen, 1945; Wood and Ljungdahl, 1991). Besides of carbohydrate utilization (hexoses or pentoses) (Drake et al., 1997), acetogenic bacteria can also grow on a wide range of other organic compounds such as alcohols (i.e., ethanol, propanol, butanol) (Eichler and Schink, 1984; Drake and

Daniel, 2004; Schuchmann et al., 2015), carboxylic acids (i.e., lactate, pyruvate, citrate) (Yang et al., 1987; Weghoff et al., 2015), amino acids (i.e., alanine) (Dönig and Müller, 2018), C1 compounds (i.e., formate, methanol) (Beaty and Ljungdahl, 1991; Kremp et al., 2018; Dietrich et al., 2021; Moon et al., 2021) and C1 groups of methylated compounds (i.e., glycine betaine) (Lechtenfeld et al., 2018), making the group of acetogenic bacteria to the most metabolic diverse group of anaerobes (Drake et al., 1997; Schuchmann and Müller, 2016). Here, in few cases, the reactions of the WLP have to work in the reverse (oxidative) direction to provide necessary reducing equivalents for the WLP and to maintain redox homeostasis of the cell (Schuchmann and Müller, 2016). Examples for this scenario are the utilization of methanol and formate (Kremp et al., 2018; Moon et al., 2021). Acetogenesis from methanol was revealed in detail in the acetogenic model organism *A. woodii*, where a methyltransferase system is involved in the methyl group transfer from methanol to the cofactor THF yielding methyl-THF. The formed methyl-THF enters the WLP and is oxidized to CO_2 in the reverse direction of the methyl-branch (Banerjee and Ragsdale, 2003; Kremp et al., 2018). Thereby, the necessary reducing equivalents are produced to allow growth on methanol and to allow CO_2 fixation in the WLP.

Electrons can also be derived from the oxidation of inorganic compounds such as H_2. In this case, acetate is formed from H_2 and CO_2 as the sole electron and carbon source according to eq. 4

$$4H_2 + 2CO_2 \rightleftharpoons CH_3COO^- + H^+ + 2H_2O \qquad \Delta G^{0\prime} = -95\ \mathrm{kJ/mol} \qquad (4)$$

The standard Gibbs free energy change $\Delta G^{0\prime}$ of this reaction equals −95 kJ/mol acetate (Thauer et al., 1977). The derived electrons from H_2 oxidation, catalyzed by hydrogenases, are transferred to soluble electron carriers such as NAD(P)H and ferredoxin which are in turn channeled to the WLP (Drake, 1982) to get re-oxidized on the way of CO_2 reduction to acetate (Drake et al., 2008; Ragsdale and Pierce, 2008).

2.3. Bioenergetics of acetogenic bacteria

The formation of acetate from two moles of CO_2 by using H_2 as the reductant (lithotrophy) is energy-neutral. One ATP molecule is consumed in the N^{10}-formyl-THF synthetase reaction to activate formate whereas another ATP molecule is produced in the later acetate kinase reaction *via* substrate-level phosphorylation due to the phosphate-transfer from acetyl-phosphate to ADP (Schaupp and Ljungdahl, 1974). Therefore, the net ATP formation in the WLP is zero (Hugenholtz and Ljungdahl, 1990; Müller, 2003). However, since acetogens can grow with acetate formation on H_2 + CO_2, there has to be net ATP synthesis. In case of a heterotrophic life-style using hexoses as substrate, additional ATP is generated by the oxidation of glucose to pyruvate *via* glycolysis. The subsequent conversion of pyruvate to acetate also forms ATP. The generated 8 electrons in form of reducing equivalents are fed to the WLP which is primarily functioning as an electron sink to maintain redox homeostasis in the cell (Schuchmann and Müller, 2016). If H_2 is used as electron donor, the glycolysis reactions are missing and no ATP is provided. Here, a chemiosmotic mechanism using an energized membrane is responsible for additional ATP generation to allow growth under lithoautotrophic conditions (Hugenholtz et al., 1987; Heise et al., 1989; Müller, 2003; Poehlein et al., 2012). The respiratory enzymes which are involved in the generation of an electrochemical ion gradient are either the Rnf or the Ech complex, and the translocated ions are either Na^+ (sodium ions) or H^+ (protons) (Biegel and Müller, 2010; Schölmerich and Müller, 2019). Based on the distinct enzymes responsible for energy conservation, acetogens can be bioenergetically classified in ‘Rnf-’ and ‘Ech-acetogens’ with the subclasses of H^+- and Na^+-dependent organisms (Schuchmann and Müller, 2014).

In earlier days, the presence of membrane-bound corrinoid-containing proteins (methyltransferases) or the presence of membrane-bound electron-transferring proteins (cytochromes) were suggested to be involved in chemiosmotic energy conservation of acetogenic bacteria (Dangel et al., 1987; Müller, 2003). But the presence of such enzyme complexes could not be validated in different representatives of the acetogenic group such as *A. woodii* and *Clostridium ljungdahlii*. Even for *M. thermoacetica*, an organism which harbors cytochromes and quinones, the participation of these proteins in a membrane-

based electron transport chain was questionable. Evidence was neither given from an experimental point of view nor from genome data (Pierce et al., 2008; Huang et al., 2012; Mock et al., 2014). The enigma of energy conservation during acetogenesis could firstly be answered in the mesophilic acetogen *A. woodii*. In this organism, a membrane-integral ferredoxin:NAD^+-oxidoreductase was discovered, called the Rnf complex. This multi-subunit enzyme complex catalyzes the exergonic electron transfer from reduced ferredoxin to NAD^+ (Biegel et al., 2009; Biegel and Müller, 2010; Westphal et al., 2018). This reaction should provide sufficient amounts of energy ($\Delta G^{0\prime}$ = –25 kJ per mole; assuming $E^{0\prime}$ of the ferredoxin couple [Fd/Fd^{2-}] of –450 mV and $E^{0\prime}$ [NAD^+/NADH] of −320 mV) to translocate ions across the cytoplasmic membrane. Indeed, the reaction is coupled to the generation of a transmembrane Na^+-ion gradient that in turn drives a membrane-bound ATP synthase to generate ATP (Müller et al., 2001; Müller, 2003; Hess et al., 2013). The membrane-integral F_1F_O ATP synthase was identified to be specific for Na^+ ions and a conserved Na^+-binding motif consisting of the amino acid sequence Q...ES/T is also present (Heise et al., 1992; Rahlfs et al., 1999; Müller et al., 2001; Meier et al., 2009). Additional to three ATP synthesizing centers, structural studies revealed the presence of ten ion-binding sites in the *c*-subunit ring of the *A. woodii* ATP synthase (Fritz et al., 2008; Matthies et al., 2014), thus resulting in the use of 3.3 moles of Na^+ ions to generate 1 mole of ATP (Brandt and Müller, 2015).

In conclusion, the acetogenic model organism *A. woodii* belongs the class of Na^+-dependent Rnf-acetogens. *C. ljungdahlii* also contains a Rnf-complex that is involved in energy conservation (Köpke et al., 2010). But growth and chemiosmotic ATP synthesis was not dependent on Na^+ ions but rather connected to the generation of an electrochemical H^+ gradient (Köpke et al., 2010; Tremblay et al., 2012). Moreover, the conserved Na^+-binding amino acid motif of the ATP synthase is lacking (Rahlfs et al., 1999; Meier et al., 2006). Therefore, *C. ljungdahli* is assumed to be a representative of the class of H^+-dependent Rnf-acetogen.

However, some acetogens such as *M. thermoacetica* and *T. kivui* lack the genes coding for the Rnf complex that is the only coupling site for Na^+-translocation and energy conservation (Biegel and Müller, 2010; Biegel et al., 2011; Hess et al.,

2013). Thus, a second mode of energy conservation has to exist in acetogenic bacteria and a further membrane-bound, ion-translocating enzyme complex that is linked to energy conservation was identified. This energy-converting [NiFe]-hydrogenase was named as Ech complex (Pierce et al., 2008; Huang et al., 2012; Oehler et al., 2012; Hess et al., 2014; Schuchmann and Müller, 2014). The Ech complex catalyzes the exergonic electron transfer from reduced ferredoxin to H^+, resulting in the evolution of molecular H_2 (Hedderich and Forzi, 2005) (Schoelmerich and Müller, 2020). Additionally, the redox energy is used to translocated ions across the cytoplasmic membrane which can subsequently drive ADP phosphorylation to ATP *via* a membrane-bound F_1F_O ATP synthase. That the Ech complex forms a functional respiratory enzyme complex, which generates a transmembrane electrochemical ion gradient, was experimentally verified in the thermophilic acetogen *T. kivui* (Schölmerich and Müller, 2019). Interestingly, the genome of *T. kivui* harbors two Ech gene clusters, coding for two putative functioning Ech-type complexes. Although they differ in subunit composition, both Ech complexes have all cofactors and catalytic domains to potentially catalyze the previously mentioned reaction (Hess et al., 2014). Additionally, both gene clusters were highly upregulated during autotrophic growth (Schölmerich and Müller, 2019). Noteworthy, experiments with inverted membrane vesicles (IMVs) clearly demonstrated that the Ech activity was not only coupled to the translocation of one sort of ion, instead a Na^+ ion gradient as well as a $\Delta\mu_H{}^+$ was established across the cytoplasmic membrane (Schölmerich and Müller, 2019). Bioinformatic analysis of the membrane-integral subunits of both Ech complexes revealed highest sequence similarities to Na^+/H^+ antiporters. However, purified Ech enzymes would be required to further elucidate the enzyme mechanistic (i.e., sequence and mechanism of ion translocation) in greater detail. Since the ATP synthase of *T. kivui* does not contain a conserved Na^+ binding motif and the dependency on H^+ ions were experimentally verified (Hess et al., 2014; Schölmerich and Müller, 2019), the Ech activity is clearly linked to a H^+-dependent F_1F_O ATP synthase. Therefore, *T. kivui* is a representative of the class of H^+-dependent Ech-acetogens.

Both respiratory enzymes, Rnf and Ech use reduced ferredoxin as electron donor. The reduced ferredoxin could be obtained from oxidative reactions such as sugar oxidation or from the oxidation of H_2 and CO. The membrane-bound

enzyme complexes of Rnf and Ech do not only translocate ions across the cell membrane to generate a primary electrogenic ion potential, moreover, they are involved in redox balancing due to the conversion of reduced ferredoxin into the reducing equivalents of NADH and H_2 (Schuchmann and Müller, 2016). The reversibility of the Rnf activity (endergonic reaction) of *A. woodii* was demonstrated, catalyzing the reverse electron transfer from NADH to oxidized ferredoxin at the expense of the electrochemical ion potential (Hess et al., 2013). Therefore, redox balancing is maintained *via* the respiratory enzyme complexes Rnf and Ech, additional to electron-bifurcating enzymes. In general, the metabolism of acetogenic bacteria demonstrates a modular construction, harboring an oxidative module (i.e., glycolysis) which supply reducing power, a reductive module (WLP) which serve as electron sink and a redox balancing module (Rnf, Ech and electron-bifurcating enzymes) which interconnects the different modules to provide the correct electron carriers in the right stoichiometry within the cell (Schuchmann and Müller, 2016; Katsyv and Müller, 2020).

To sum up, the WLP is the only known CO_2 fixation pathway that is energy neutral and the pathway is considered to be one of the oldest biochemical pathways that enabled biomass and ATP formation under chemolithoautotrophic conditions in a primordial world (Martin and Russell, 2007; Wächtershäuser, 2007; Martin et al., 2014). Because of the unique carbon fixation strategy, which enables acetogenic bacteria to use CO_2 as the terminal electron acceptor and H_2 as the reductant, the acetogenic group has gained more and more commercial interest to produce biocommodities from waste gases consisting of H_2 and CO_2 (Bengelsdorf et al., 2018). This interest was even more stimulated by the discovery that some acetogens can not only use H_2 but also CO as electron donor for CO_2 reduction (Diender et al., 2015). The aim is the production of sustainable and value-added biocommodities and biofuels from H_2, CO_2 and/or CO, a highly abundant and low-cost gas composition that is called synthesis gas (Bengelsdorf and Dürre, 2017).

2.4. Biocommodities production by acetogenic bacteria

Historically, biotechnological production plants for the production of biofuels (first-generation biofuels) such as biodiesel, bioethanol and biogas were based on sugars (i.e., sugarcane, corn and wheat) (Naik et al., 2010). But the approach is questionable due to the source of feedstock and its potentially impact on biodiversity and land use. Here, the used substrate is in direct conflict with the production of food for mankind (Fargione et al., 2008; Ajanovic, 2011) and the process emits CO_2. The concerns about environmental impacts, carbon balances and the food-versus-fuel debate set limits to the commercial production of biofuels of the first generation (Naylor et al., 2007; Melillo et al., 2009; Ajanovic, 2011; Murphy et al., 2011).

The second-generation biofuels are based on lignocellulosic biomass that can be supplied on a large-scale basis from different low-cost raw materials such as wood and agricultural residues (Naik et al., 2010; Brown and Brown, 2013; Kucharska et al., 2018). But again, the process is not CO_2 neutral and multiple pretreatment and hydrolysis steps are necessary to break down non-fermentable polysaccharides into fermentable monosaccharides (Geddes et al., 2011; Kucharska et al., 2018), making biofuels production rarely cost-effective. Therefore, most projects of this kind were put on hold because of technical and non-technical barriers (Padella et al., 2019).

Another possibility of biomass utilization is its conversion into gaseous compounds by gasification which can then be used by microorganisms as substrate. This gas mixture which is fed to microorganisms mainly consists of H_2, CO_2, and CO and are called synthesis gas or syngas. The exact gas composition can vary strongly and depends on the used resources/feedstocks and technologies to produce syngas (Molino et al., 2018), but CO is typically the most abundant carbon species in syngas (van der Drift et al., 2001). Syngas can be obtained i.e., from gasification of biomass and waste streams (such as sewage sludge, organic industrial waste and municipal solid waste) (Hammerschmidt et al., 2011; Rokni, 2015), from industrial exhaust gases (such as steel mill off-gas) (Köpke et al., 2011b) or reformed biogas (Liew et al., 2016b). Therefore, the production of third-generation biofuels is based on carbon oxides as feedstock, and instead of producing CO_2, gas fermentation captures and stores CO_2 in the

form of value-added biochemicals or biofuels, thus making syngas-fermentation a sustainable and promising approach for CO_2 sequestration (Fig. 5).

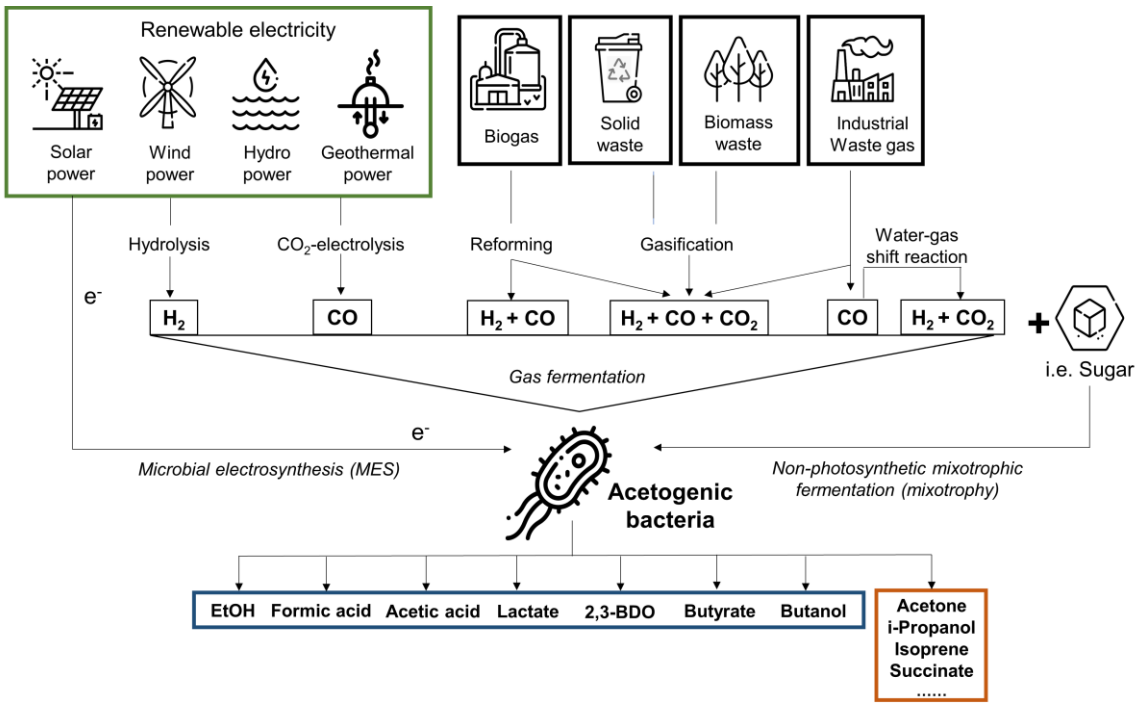

Fig. 5 Overview of feedstock options for acetogenic bacteria in CO_2-sequestration. Gas fermentation is a flexible platform to produce biofuels and biochemicals from waste and renewable feedstocks. In non-photosynthetic mixotrophic fermentations (mixotrophy) additional substrates such as sugars can be added to the process to increase the ATP yield. In case of microbial electrosynthesis (MES), reducing power is supplied *via* electrons directly from an electrode to the organisms. Native products of acetogenic bacteria are indicated in the blue box. Synthetic products that were produced through genetic modification of the organisms are indicated in the orange box. e^-, electrons; 2,3-BDO, 2,3-butanediol.

Numerous microbes are known to convert syngas into chemicals (Henstra et al., 2007b; Bengelsdorf et al., 2013; Bengelsdorf et al., 2018), but with the exception of some methanogens, the vast majority of syngas fermenting organism were found in the group of acetogenic bacteria (Latif et al., 2014). Acetogens are known to produce acetate as the sole metabolic end product but some strains are also able to produce ethanol in addition to acetate (Najafpour and Younesi, 2006; Maddipati et al., 2011; Bertsch and Müller, 2015b) such as *Clostridium carboxidivorans* (Liou et al., 2005), *C. ljungdahlii* (Tanner et al., 1993; Köpke et al., 2010) and *C. autoethanogenum* (Abrini et al., 1994). Noteworthy, the acetogenic bacterium *C. autoethanogenum* is already used as a biocatalyst to produce ethanol from syngas on an industrial scale (Köpke and Simpson, 2020). But not only the production of acetate and ethanol was demonstrated by gas fermentation. Moreover, some bacterial strains naturally produce minor amounts of butyrate, 2,3-butanediol or lactate (Liou et al., 2005; Köpke et al.,

2011b; Jeong et al., 2015). Recent improvements in the genetic tool box for acetogenic bacteria enable genetic manipulations, metabolic engineering and synthetic biology of this bacterial group (Tracy et al., 2012; Leang et al., 2013; Bengelsdorf et al., 2018). This leads to the production of many new products like acetone, butanol, 3-hydroxybutyrate and 2-propanol (isopropanol) with the help of recombinant strains (Köpke et al., 2010; Banerjee et al., 2014; Jones et al., 2016; Bengelsdorf et al., 2018).

Additionally, some microorganisms can also grow on carbon monoxide as sole carbon and electron source, named as “carboxydotrophs” or “carboxydotrophic” microorganisms. The trait of utilizing CO exists in the group of bacteria as well as archaea. Examples for anaerobic carboxydotrophic organisms are the hyperthermophilic archaeon *Thermococcus onnurineus* (Bae et al., 2006), the methanogenic archaeon *Methanosarcina barkeri* (O'Brien et al., 1984) and also the thermophilic acetogenic bacterium *M. thermoacetica* (Diekert and Thauer, 1978). Depending on the end product formed, the organisms are either hydrogenogenic, methanogenic or acetogenic (Diender et al., 2015). Many acetogens grow on carbon monoxide as sole carbon and electron source according to eq. 5:

$$4\mathrm{CO} + 2\mathrm{H_2O} \leftrightarrow \mathrm{CH_3COO^-} + \mathrm{H^+} + 2\mathrm{CO_2} \qquad \Delta G_0' = -165.6\ \mathrm{kJ/mol} \qquad (5)$$

In this case, CO is first oxidized to CO_2 which is subsequently reduced to acetate with electrons derived from CO oxidation (Diekert and Thauer, 1978; Diender et al., 2015). Further representatives of the acetogenic group which can grow on CO are for example *Eubacterium limosum* (Genthner and Bryant, 1982), *C. ljungdahlii* (Tanner et al., 1993), *T. kivui* (Weghoff and Müller, 2016) and *Blautia producta* (Lorowitz and Bryant, 1984). All these carboxydotrophic organisms harbor the capability to catalyze the oxidation of CO to CO_2, to use the derived electrons from CO oxidation for growth, to re-assimilate parts of the formed CO_2 *via* CO_2 fixating pathways (i.e., the WLP or ribulose bisphosphate cycle) and to withstand CO inhibition (Meyer and Schlegel, 1983). The CO molecule is oxidized by CO dehydrogenases (CODH) in the biological water-gas shift reaction as shown in eq. 6.

$$CO + H_2O \rightleftharpoons CO_2 + 2H^+ + 2e^- \qquad E^{0\prime} = -520\ mV \qquad (6)$$

The CODH enzymes which enable organisms to utilize CO can either be mono- or bi-functional, the latter includes the previously described key enzyme CODH/ACS complex of the WLP. The crystal structure of several CODHs (mono- or bifunctional) from different organisms have already been determined (Dobbek et al., 2001; Drennan et al., 2001), including the bifunctional CODH/ACS complex of *M. thermoacetica* (Doukov et al., 2002; Darnault et al., 2003). Large differences can be observed in the group of CO-utilizing acetogenic bacteria with regard to growth parameters such as growth rate and yields (Diender et al., 2015). This indicates differences in the CO metabolism, the enzymes involved and the ways of energy conservation within this group. Moreover, not all acetogens produce only acetate as the sole end-product. Organisms such as *E. limosum* and *C. autoethanogenum* also produce butyrate or ethanol, respectively, next to acetate (Genthner and Bryant, 1982; Abrini et al., 1994; Köpke et al., 2011a; Jeong et al., 2015). But non-photosynthetic carbon fixation is often ATP/energy limited. For sure, H_2 and CO have both been targeted as ideal electron sources for the production of biofuel by anaerobic acetogens (Köpke et al., 2011a; Schiel-Bengelsdorf and Dürre, 2012) but the product spectrum is limited due to limited energy availability of acetogens on gases (Bertsch and Müller, 2015b; Katsyv and Müller, 2020). These energy-limitations become apparent during growth on H_2 + CO_2, where minor amounts of the compound of interest are produced along with major amounts of acetic acid. Stoichiometric and energetic analyses of the WLP to produce bulk chemicals make it more clear: For the autotrophic production of bulk chemicals and biofuels like acetate and ethanol, the WLP shows the highest potential acetate (23.6 mol/100 mol H_2) and ethanol yield (16.0 mol EtOH/100 mol H_2) using H_2 as electron donor compared to other non-photosynthetic, non-sulfur pathways (Fast and Papoutsakis, 2012). But for higher, energetically expensive C-compounds like butanol, only a negligible butanol production (0.2 mol butanol/100 mol H_2) is predicted under autotrophic conditions, owing to ATP limitations (Fast and Papoutsakis, 2012). However, several examples were given in the literature where acetogenic bacteria produced butanol through native (Grethlein et al., 1991; Bruant et al., 2010) and engineered (Köpke et al., 2010) butanol pathways. But there is still future work to do to solve the energetic limitations to produce high-value products from syngas

using acetogenic bacteria. Unquestionable is the efficient production of lower C-compounds such as acetate and ethanol in high amounts from carbon dioxide and hydrogen and/or CO by using acetogenic bacteria as biocatalysts.

2.5. Formate bioeconomy

As mentioned before, formate is an intermediate in the WLP of acetogenic bacteria which is produced by formate dehydrogenases *via* CO_2 reduction. The formate bioeconomy and its popularity is rapidly growing since formate directly addresses major challenges in the field of energy storage and (bio)-chemical production (Enthaler et al., 2010; Yishai et al., 2016). Formate is well-known as bulk-chemical (Loges et al., 2010), but is further considered as liquid organic hydrogen carrier (LOHC) since formate alleviates the technical difficulties regarding the handling and transport of hydrogen gas (Enthaler, 2008; Preuster et al., 2017b). The ways to produce formate can be diverse (Fig. 6) and include chemical as well as biological ways of electrochemical reduction, photoreduction, hydration and hydrogenation of CO_2 (Yishai et al., 2016). Formate can also be produced by partial oxidation of biomass or oxidation of natural gas (Sorokin et al., 2010; Albert et al., 2014).

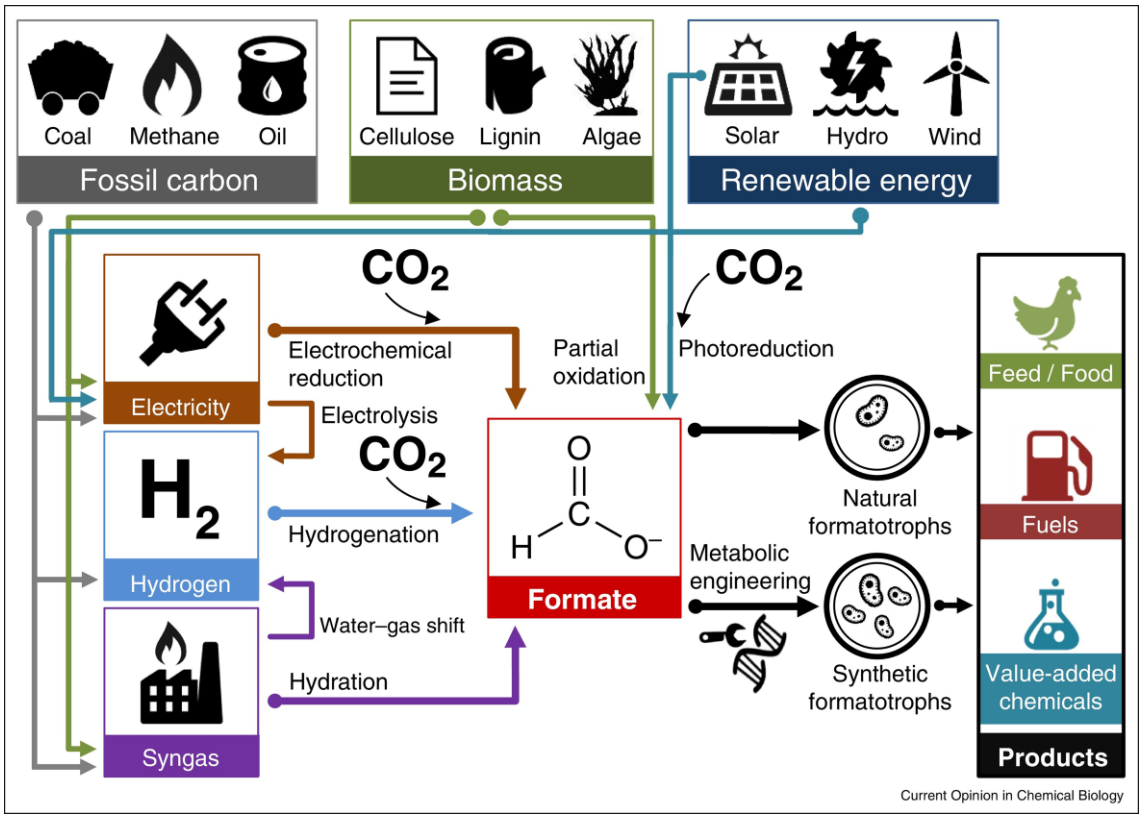

Fig. 6 The concept of the formate bioeconomy (Yishai et al., 2016). The versatile compound formate can be produced from different available sources *via* different biological/chemical routes. Due to the beneficial physicochemical and biological properties of the compound formate, it can be fed to natural or synthetic formatotrophic organisms to produce fuels, value-added chemicals and protein meal for animal consumption. Additional to the schematic representation, formate is considered as a liquid organic hydrogen carrier (LOHC) to store molecular hydrogen in a liquid, non-volatile and non-inflammable form. Moreover, formate can directly be used in direct formate fuel cells (DFFCs).

In the reaction of direct hydrogenation of CO_2, the hydrogen-lean molecule CO_2 is reduced with H_2 to formic acid/formate. But other hydrogenation products of CO_2 such as methanol, dimethyl ether (DME) or other hydrocarbons can also be formed *via* direct hydrogenation of CO_2 (Olah et al., 2009; Alvarez et al., 2017). However, since H_2 is directly bound to CO_2, the reaction is a feasible avenue for carbon recycling as well as hydrogen energy conversion and storage. Important to note, that the stored H_2 in form of formate can later be released in a dehydrogenation reaction to close the H_2 storage cycle (Mellmann et al., 2016; Preuster et al., 2017a).

The activation of CO_2 is often challenging, owing to the high thermodynamic stability and the poor electrophilic character of the CO_2 molecule (Ostapowicz et al., 2013). Many chemical catalysts (homogenous and heterogenous) have been described in the past years and several catalytic strategies have been employed to catalyze the direct hydrogenation of CO_2 to formate (Jessop et al., 2004; Wang

et al., 2015; Gunasekar et al., 2016; Mellmann et al., 2016). Many systems typically operate under very high pressures or temperatures, suffer from low turnover frequencies, need very expensive additives or ligands and mostly rely on the use of Ir (iridium)- and Ru (ruthenium)-based transition metal complexes in homogeneous catalytic systems (Klankermayer et al., 2016; Rohmann et al., 2016; Alvarez et al., 2017; Weilhard et al., 2021). Therefore, biological solutions apply using enzymes or whole cells as biocatalysts to catalyze the conversion of H_2 (or electrons) and CO_2 to formate (Schuchmann and Müller, 2013; Mourato et al., 2017; Roger et al., 2018; Schwarz et al., 2018; Chiranjeevi et al., 2019) (Moon et al., 2020; Schwarz and Müller, 2020).

The hydrogen content in formic acid (4.4 wt %) is not that high compared to other organic hydrogen storage materials such as methanol (hydrogen density 12.6 wt %) but formic acid is still an important LOHC and a highly attractive compound due to the additional employment as feedstock chemical, hydrogen source for fuel cells or its use as microbial carbon source (Wang et al., 2015; Cotton et al., 2019). Natural formatotrophic microorganisms are able to assimilate formate in their metabolism using either the Calvin cycle, the serine pathway or the Wood–Ljungdahl pathway for formate assimilation (Yishai et al., 2016; Cotton et al., 2019). Therefore, several acetogenic bacteria (i.e., *A. woodii*, *C. ljungdahlii* and *M. thermoacetica*) and methanogens can utilize the compound formate (*via* WLP) as sole energy and carbon source for growth (Drake et al., 2006; Moon et al., 2021). But also the facultative aerobic bacterium *C. necator* (*via* Calvin cycle) as well as the methylotrophic bacterium *Methylobacterium extorquens* AM1 (*via* Serin pathway) were shown to grown on formate naturally (Crowther et al., 2008; Grunwald et al., 2015). Formate can even be used as auxiliary substrate to support increased growth and product yields for multiple microorganisms under various conditions (Babel, 2009). Here, the C1 compound can serve as electron donor which provides reducing power and energy for CO_2 fixation and microbial bioproduction. This is owed to the low reduction potential of the CO_2/formate couple (E_0' = −420 mV), allowing a direct reduction of the main cellular electron carriers (Claassens et al., 2018). Based on the physicochemical and biological properties of formate, the compound fulfills different key characteristics as one-carbon compound electron carrier: formate 1) has a low reduction potential, 2) shows sufficient solubility to ensure efficient mass transfer, 3) can be consumed

by biotechnologically relevant microorganisms, 4) allows a safe handling (i.e., no flammability) and 5) can be applied in low-cost productive bioreactors (Claassens et al., 2018). Therefore, formate can be seen as one of the most promising electron donors for microbial CO_2 fixation and bioproduction aside from H_2 and CO (Claassens et al., 2018). But formate can not only be used as growth substrate and electron donor, it can even be directly used in direct formic acid fuel cells (DFAFCs) to generate energy (Yu and Pickup, 2008; An and Chen, 2016). The use of formate in DFAFCs or the use of H_2 in so far more developed H_2 fuel cells, results in the release of CO_2 or water, respectively. The previous captured CO_2 can then be reused for the next H_2 storage cycle. If the applied H_2 is produced from renewable energy sources (e.g., solar-, wind-, hydro- or geothermal power) by water-splitting and not from “traditional routes” such as steam reforming and partial oxidation of coal, oil and natural gas, no CO_2 is liberated as byproduct and no net CO_2 is generated in the H_2 cycle (Dufour et al., 2009). But for such a sustainable economy, the electricity prices of renewably produced energy have to be much more competitive to the low price of H_2 which is produced by traditional routes. The production of “green H_2” *via* commercially available electrolysis systems would result in costs of about 2−3 \$/kg H_2 (at 0.05 \$/kWh electricity cost) (Dincer, 2012; Tremel et al., 2015), whereas the current industrial production of H_2 from conventional fossil sources results in H_2 costs of lower than 1 \$/kg H_2 (Holladay et al., 2009; Acar and Dincer, 2014). As a result, 40% of the produced H_2 comes from natural gas, 30% from heavy oil, 18% from coal and only 4% are related to electrolysis and 1% to biomass (Sinha and Pandey, 2011). However, the process of direct hydrogenation of CO_2 to formate is one alternative route to photo- and electrochemical CO_2 reduction. The reaction harbors a great promise for large-scale and sustainable production of the versatile compound formate, thus allowing to contribute to a future, sustainable formate-bio economy.

2.6. Aim of this thesis

The group of acetogenic bacteria has gained more and more biotechnological interest due to their metabolic feature to convert H_2 and CO_2 and/or CO *via* the WLP into value-added products. An interest with the distinct aim to combine CO_2-emitting industrial technologies with CO_2-converting biological systems. The discovery of a soluble and highly efficient hydrogen-dependent CO_2 reductase (HDCR) in the two acetogenic bacteria *A. woodii* and *T. kivui* opened the route to use these microorganisms as biocatalysts for the direct hydrogenation of CO_2 to formate, especially since appropriate chemical catalysts are lacking. The investigated reaction does not only capture CO_2, it further allows the storage of H_2 in the liquid organic hydrogen carrier formate (CCS) and the further usage of formate as feedstock for biotechnological applications (CCU).

The overall aim of this thesis was to investigate the potential of the two acetogenic bacteria *A. woodii* and *T. kivui* in hydrogen storage and carbon capture with formate as the final product. Therefore, first of all, a whole-cell system should be established for the thermophilic acetogen *T. kivui* to have a thermophilic and mesophilic (*A. woodii*) whole-cell production platform to produce formate from H_2 and CO_2. After the implementation and characterization of the hydrogen-dependent CO_2 reduction to formate using whole cells of *T. kivui*, the HDCR-based whole-cell system should be further investigated for the ability to convert syngas (H_2, CO_2 and CO) into the desired product formate. The conversion of CO alone into the bulk chemicals formate and acetate should be also addressed for *A. woodii* and *T. kivui* cells. Since both organisms are so far the only identified acetogens harboring an HDCR complex and belonging to the different classes of ‘Rnf’- and ‘Ech-acetogens’, CO utilization should be studied in greater detail with mutants of both organisms.

Since this thesis puts emphasis on the direct hydrogenation of CO_2 to formate, the technical practicability of using acetogenic bacteria as future biocatalysts should be proven. The final goal was to establish a bioreactor application to demonstrate the upscaling feasibility of the designed whole-cell system and to gain further insights into process properties for H_2-dependet CO_2 reduction and *vice versa* under controlled reaction conditions.

3. General discussion

3.1. Enzyme-based hydrogenation of CO_2 to formate

Diverse routes are available to catalyze the reduction of CO_2 to the versatile compound formate. One of these routes comprises the direct hydrogenation of CO_2. Here, different enzymes are known from bacteria which directly use molecular H_2 for the reduction of CO_2 to formate, such as the well-known membrane bound formate hydrogenlyase (FHL) complex from *E. coli* (McDowall et al., 2014). Formate hydrogenlyase activity has also been found in other microbial species, including *Klebsiella pneumoniae* (Steuber et al., 1999), *Rhodospirillum rubrum* (Schön and Voelskow, 1976), *Salmonella typhimurium* (Chippaux et al., 1977) and many others. However, the FHL complex of *E. coli* is the most studied example. Enzymes which also catalyze the direct hydrogenation of CO_2 to formate include the electron-bifurcating multi-subunit complex of *C. autoethanogenum* (Wang et al., 2013b), the electron-bifurcating hydrogenase-formate dehydrogenase complex of *E. callanderi* KIST612 (Dietrich et al., 2021) as well as the H_2-dependent CO_2 reductase (HDCR) of *A. woodii* and *T. kivui* (Schuchmann and Müller, 2013; Schwarz et al., 2018).

Already in 1931, Stephenson and Stickland discovered the decomposition of formate into H_2 and CO_2 by whole cells of *E. coli* (Stephenson and Stickland, 1931, 1932), and the supposed enzyme system was named formate hydrogenlyase (FHL). As indicated by the name, the physiological role of the FHL complex in the metabolism of *E. coli* is the oxidation of formate produced during mixed-acid fermentation to avoid a critical acidification of the environment. The accumulation of extracellular formate as well as the drop in environmental pH, lead to an import of formate into the cell and induce the expression of genes encoding the FHL (*hycABCDEFGHI*) (Rossmann et al., 1991; Sawers, 2005; Pinske and Sargent, 2016). The understanding of the FHL physiology, expression, maturation and biochemistry was an integral part in *E. coli* research for over a century. Whole-cell experiments indicated the reversibility of the FHL reaction (Woods, 1936) but whether the enzyme complex catalyzes H_2-dependent CO_2 reduction to formate in particular could not be clarified without enzyme purification. Finally, the entire functional enzyme complex could be

purified by McDowall et al. in 2014 (McDowall et al., 2014). The purified FHL consists of 7 subunits, harboring two membrane anchored subunits (HycC/D) and 5 soluble subunits. Three of the soluble subunits (HycB/F/G) are iron-sulfur proteins, that, most likely, mediate the electron transfer from one catalytic subunit to the other. The remaining 2 soluble subunits comprise the catalytic subunits of [NiFe]-hydrogenase (HycE) and molybdenum-containing formate dehydrogenase (FdhF, known as formate dehydrogenase H; selenoenzyme), catalyzing the two reversible half reactions of proton reduction and formate oxidation (Fig. 7).

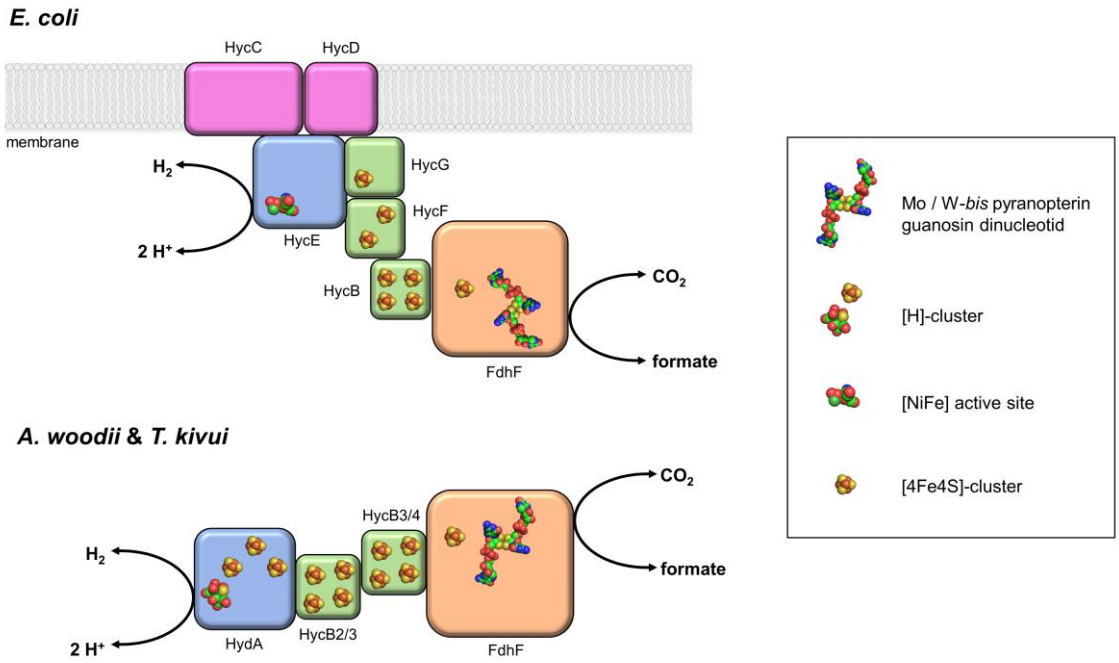

Fig. 7 Model of the formate hydrogenlyase complex (FHL) of *E. coli* and the hydrogen-dependent CO_2-reductase complex (HDCR) of *A. woodii* and *T. kivui*. *E. coli* FHL is membrane bound and harbors a [NiFe]-hydrogenase subunit for H_2 oxidation and H^+ reduction, respectively. In contrast, the HDCR from *A. woodii* and *T. kivui* is a soluble enzyme which harbors a catalytic [FeFe]-hydrogenase subunit. A catalytic formate dehydrogenase subunit as well as electron transferring subunits are present in both enzymes. The shown enzymes catalyze the reversible reduction of CO_2 to formate with molecular hydrogen as the electron donor.

The overall reaction is formate oxidation with the simultaneous evolution of H_2 and CO_2. Whether the FHL enzyme is coupled to energy conservation is controversially debated over years and is so far unknown (Trchounian and Gary Sawers, 2014; Pinske and Sargent, 2016). But undeniably is the strong bias towards formate oxidation of the FHL complex. The purified enzyme catalyzed formate oxidation (formate:H^+ oxidoreductase activity) with a specific activity of around 0.1 U/mg (TOF 1,800 h^{-1}). Protein film electrochemistry (PFE)

experiments of the FHL have even demonstrated the formation of H_2 at high H_2 partial pressures, showing an untypically high product inhibition constant for H_2 production in the group of [NiFe]-hydrogenases ($K_{i,app}^{H2}$ = 1.48 mM at pH 6, 37 °C and −558 mV vs. standard hydrogen electrode (SHE)). The K_m value for H_2 oxidation was determined the be 34 μM (at pH 6, 37 °C, and −107 mV vs. SHE) (McDowall et al., 2014). The K_m value for formate was determined to be 26 mM for the isolated FdhH subunit of the FHL complex when benzyl viologen was used as electron acceptor in the enzymatic assay (Axley and Grahame, 1991). Modern PFE experiments with *E. coli* FdhH identified a K_m value for formate in the μM range, indicating different sensitivities and limitations in the applied analytical methods (Robinson et al., 2017). The FHL complex also catalyzed the reverse reaction of H_2-dependent CO_2 reduction (H_2:CO_2 oxidoreductase activity), but the activity was only a fraction of the activity of formate oxidation with ~0.03 U/mg (TOF 550 h^{-1}) (McDowall et al., 2014). This is not surprising, since the physiological role of the FHL by modern-day *E. coli* is formate oxidation and not CO_2 reduction, owed to the metabolic trait of *E. coli*; the organism is unable to further utilize formate under anaerobic conditions.

In 2013 and 2021, an electron-bifurcating hydrogenase in complex with a formate dehydrogenase was identified in the acetogenic bacteria *C. autoethanogenum* and *E. callanderi* KIST612 (Wang et al., 2013b; Dietrich et al., 2021). These enzyme complexes were already summarized in the introduction part (see section 2.1) and differ from the FHL-like reaction due to the catalyzed multiple electron transfer reactions and FBEB *in vitro*. However, the counterpart of the FHL, namely the HDCR was also purified and characterized in the acetogenic group. Here, the HDCR was identified in the mesophilic and thermophilic bacterium *A. woodii* and *T. kivui* (Schuchmann and Müller, 2013; Schwarz et al., 2018) (Fig. 7). This enzyme has a much simpler architecture than the enzyme complex from *C. autoethanogenum*, and the enzyme is not involved in energetic coupling by electron bifurcation. Moreover, the HDCR is a cytoplasmic enzyme which is not involved in energy conservation and consists of only 4 subunits: 2 electron-transferring (HycB2/3, HycB3/4) and two catalytic subunits (FdhF, HydA). One catalytic subunit consists of a formate dehydrogenase (FdhF) which could either incorporate molybdenum (*A. woodii* HDCR) or tungsten (*T. kivui* HDCR) in the active site. Additionally, *A. woodii* harbors two isoenzymes of the

formate dehydrogenases, either containing selenocysteine (FdhF2) or cysteine (FdhF1) at the amino acid position 139 (Schuchmann and Müller, 2013). The second catalytic subunit of the HDCR is a hydrogenase subunit (HydA) which contains the conserved H-cluster, a characteristic for the group of [FeFe]-hydrogenases. This group of hydrogenases are typically biased towards proton reduction (H_2 production) compared to the group of [NiFe]-hydrogenases which favor the oxidation of H_2 (Fourmond et al., 2013; Lubitz et al., 2014). The purified *A. woodii* HDCR showed an K_m value for H_2 and formate of 0.125 and 1.0 mM, respectively, using methylviologen (MV) as artificial electron acceptor (Schuchmann and Müller, 2013). The K_m value for H_2 and formate of the *T. kivui* HDCR was determined to be 0.126 and 0.55 mM, respectively (Schwarz et al., 2018). PFE studies of the HDCR from *A. woodii* revealed a typical [FeFe]-hydrogenase phenotype with a strong bias towards proton reduction and an inhibition by CO and O_2 (Ceccaldi et al., 2017). The two types of [NiFe]- and [FeFe]-hydrogenases of the FHL and HDCR enzyme, respectively, can be inactivated by oxygen and CO. Carbon monoxide is a classic competitive inhibitor for hydrogenases but [NiFe]-hydrogenases tend to be more CO resistant than [FeFe]-hydrogenases (Goldet et al., 2009). Indeed, the FHL was much more tolerant towards CO inhibition than [FeFe]-hydrogenases. The CO inhibition constant K_i^{CO/H_2} was assessed by chronoamperometry experiments to be 8.2 ± 1.8 µM (at pH 6.0, 37 °C, 10% H_2 in Ar, −0.087 V vs. SHE). For the HDCR, the inhibition constant K_i^{CO} was determined to be 0.11 µM which is even multiple times smaller than reported values for other [FeFe]-hydrogenases (Ceccaldi et al., 2017). Interestingly, PFE studies revealed that the inhibition could be fully restored by removal of CO. Apparently, CO-binding to the H-cluster did not result in an irreversible damage of the oxidation state (H_{red}) of the H-cluster, which was shown in other CO inhibition studies for [FeFe]-hydrogenases before (Goldet et al., 2009; Baffert et al., 2011; Foster et al., 2012). Noteworthy, the HDCR from *T. kivui* also showed a substantial reversibility of CO-dependent inactivation in enzymatic electrosynthesis experiments (Ruth et al., 2021).

To date, the HDCRs were only purified from the two mentioned acetogenic bacteria, but *in-silico* analyses of annotated genome data indicate the presence of the corresponding HDCR gene cluster also outside the group of acetogenic bacteria (Schuchmann and Müller, 2013; Schwarz et al., 2018). Putative HDCR

gene clusters were identified in the genome of 25 organisms with multiple representatives of the genera *Paenibacillus*, *Clostridium* and *Desulfovibrio*. Since H_2 and formate are important electron shuttles in syntrophic communities (Schink, 2002; Dolfing et al., 2008; Morris et al., 2013) the flexible switch between formate and H_2 as electron carrier could be beneficial in many environments of syntrophic communities and could explain the diversity of enzymes involved.

As mentioned before, the FHL enzyme complex has a strong bias towards formate oxidation whereas the HDCR does not. The HDCR from *A. woodii* (H_2:CO_2 oxidoreductase activity of 10 U/mg) is more than 300 times faster in CO_2 reduction compared to the FHL activity. The *T. kivui* enzyme even shows a 30,000 times higher activity (H_2:CO_2 oxidoreductase activity of 900 U/mg). Since acetogenic bacteria can growth under lithotrophic conditions, a sufficient CO_2 reduction system is necessary to fix one CO_2 molecule in the methyl-branch of the WLP *via* formate dehydrogenases (CO_2 reductases). The produced compound is the intermediate formate. Reversibility of the enzyme complex is also required since *A. woodi and T. kivui* can growth with methanol or formate, respectively, as sole carbon and energy source (Kremp et al., 2018; Moon et al., 2021). In this scenario, the physiological function of the HDCR is formate oxidation to provide the necessary reducing equivalents for life. Therefore, the HDCRs catalyze both reaction directions (CO_2 reduction and formate oxidation) with almost equal kinetics and activities. The formate oxidation (formate:H^+ oxidoreductase activity) is catalyzed with 14 and 930 U/mg by the *A. woodii* and *T. kivui* enzyme, respectively (Schuchmann and Müller, 2013; Schwarz et al., 2018).

From a thermodynamic point of view, each reaction catalyzed by an enzyme is reversible. But in some cases, the equilibrium constant (K) can be that low or high that the state of the equilibrium is strongly based at the side of educts or products. Here, the necessary conditions to drive the “reversable reaction” can be far beyond the feasible conditions of a biological system, therefore termed as “irreversible”. Since the equilibrium constant of the HDCR-catalyzed reaction is close to one, the state of the equilibrium can be easily affected by pH, temperature and substrate/product concentrations (Amend and Shock, 2001). Under standard conditions, the H_2-dependent CO_2 reduction to formate is a

slightly endergonic reaction with a $\Delta G^{0'}$ of +3,5 kJ/mol. A change in reaction conditions by lowering the temperature or by increasing the pH to a more alkalic value would shift the thermodynamics in favor of CO_2 reduction. Here, the prevailing ΔG value would be more negative. This has to be kept in mind for biotechnological applications considering the two HDCR-catalyzed reactions. The applications of the HDCRs could be diverse and allow a wide process temperature (30 °C to 70 °C) due to the availability of a mesophilic and thermophilic enzyme. Moreover, the discovered HDCRs could be role models after structural elucidation to design optimized biocatalysts or even bioinspired chemical catalysts to utilize and reduce CO_2 in a more efficient manner in future. A detailed understanding of the structure and catalytic mechanisms is inevitable required to perform structure-based enzyme engineering. Pala et al. (2018) and Cakar et al. (2020) already performed enzyme engineering by active site mutations of the FDH enzyme of *Chaetomium thermophulum* (CtFDH) which resulted in an enhanced CO_2 reduction activity and an enhanced catalytic turnover rate (k_{cat}) compared to the wild type FDH. However, enzyme engineering of FDHs is still a topic in its infancy.

CO_2 reduction to formate can also be achieved using metal- (W or Mo) containing formate dehydrogenases as electroactive enzymes. Actual research comprises the development of electroenzymatic CO_2 refinery systems to produce formate with electrons derived from an electrode. The electrocatalytic interconversion of CO_2 and formate was demonstrated for various FDHs, covering the W-containing and Mo-containing FDH of *Syntrophobacter fumaroxidans* (SfFDH) and *E. coli* (EcFDH), respectively (Reda et al., 2008; Bassegoda et al., 2014). Both enzymes could be adsorbed onto the electrode surface and catalyzed the electrochemical reduction of CO_2 to formate. So far, many different electroenzymatic system were established to produce formate from CO_2 (Moon et al., 2020). In the different systems, the generated electrons can also be shuffled to the applied enzymes by using various artificial dyes or natural cofactors as electron mediators. However, since electrons are derived from an electrode and not *via* H_2 oxidation, the process is named as electrochemical CO_2 reduction and is beyond the topic of this thesis.

For biotechnological applications the previously described enzymes of FHL and HDCRs have the big advantage that they do not need any external cofactors as electron carriers and therefore no regeneration system is needed. Moreover, the HDCR can be seen as soluble catalysis-unit which could transform organisms into whole-cell factories for H_2 storage and CO_2 capture in future. This was recently shown for the industrial platform organism *E. coli*. Here, a functional HDCR enzyme complex could be heterologously produced in *E. coli* for the first time which enabled resting cells to capture and store H_2 and CO_2 in the form of formate (Leo et al., 2021). But to stay clear, the functional production of redox-active enzymes like formate dehydrogenases and hydrogenases require multiple accessory proteins and maturation enzymes (Lubitz et al., 2014; Maia et al., 2015) and different metabolic bottlenecks had to be addressed for the HDCR overproduction in *E. coli* (Leo et al., 2021). Nevertheless, both described enzymes of FHL and HDCR are promising candidates in CO_2 capture, H_2 storage as well as biohydrogen production and are part of ongoing research to establish a sustainable H_2/formate bioeconomy.

3.2. Whole-cell catalysis for H_2-dependet CO_2 reduction to formate

Another approach for CO_2 capture and H_2 storage is the use of whole cells as (bio-)catalysts instead of purified enzymes. This approach has different advantages since whole-cell catalysis avoids time and cost-intensive enzyme preparations, allows an economic upscaling (“economy of scale”) and could protect catalytic enzymes from potentially harmful surroundings (de Carvalho, 2017; Lin and Tao, 2017). Whole-cell catalysis can broadly be classified into two approaches: 1) biotransformation (biocatalysis) with resting cells and 2) fermentation bioprocesses. In the latter one, the desired products are directly synthesized in the fermentation growth broth along with metabolic intermediates and growth products. This could make downstream processing complicated and cost-intensive. Around 30–50% of the manufacturing costs of commodities are typically assigned to downstream processing aside of mostly substrate-related costs (National Academy of Sciences, 2009; Takors et al., 2018). In the second approach of biotransformation (biocatalysis), cell growth and production phase

are physically separated and resting cells are used to convert substrates to the desired product.

This thesis describes a biotechnological approach that uses resting cells of *T. kivui* as biocatalysts to catalyze the conversion of H_2 and CO_2 into formate (Fig. 8). Due to the remarkable catalytic activities of the thermostable HDCR, a whole-cell approach was established to catalyze the direct hydrogenation of CO_2 to formate at ambient pressure with resting cells.

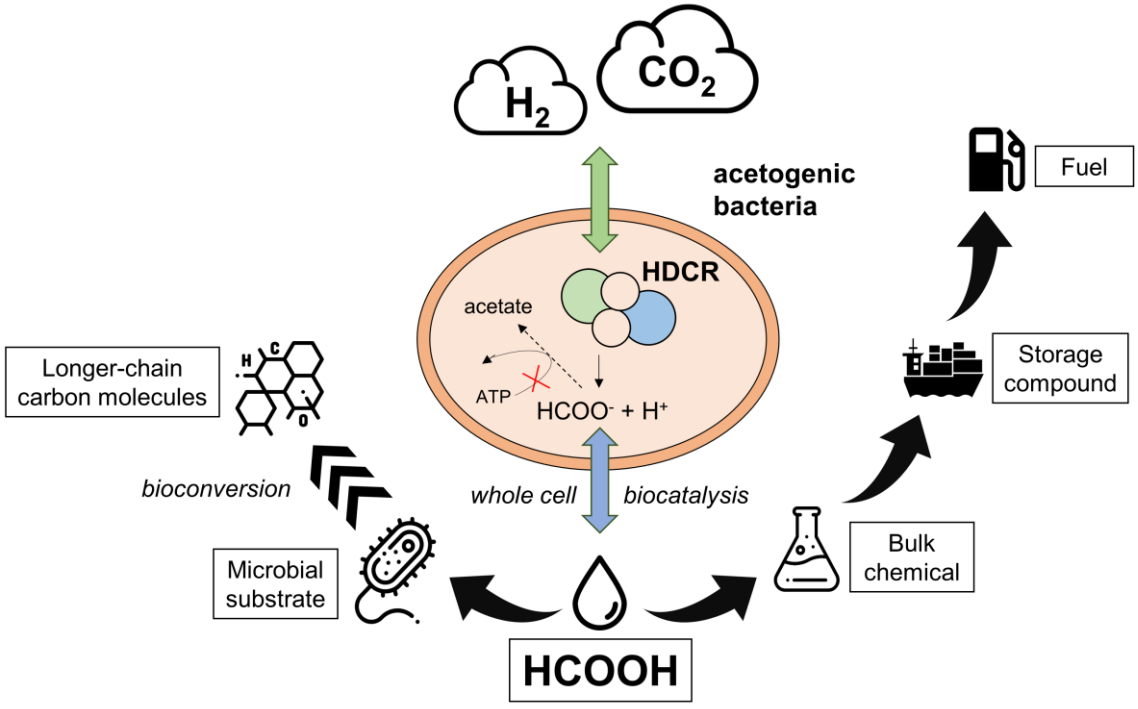

Fig. 8 Scheme of the HDCR-based whole-cell catalysis for the conversion of H_2 and CO_2 into formate (modified after Schwarz et al., 2021). By blocking the further conversion of formate to acetate in the metabolism of *T. kivui* and *A. woodii*, the intermediate compound formate becomes the dominant product. Formate is considered as liquid organic hydrogen carrier (LOHC) and can be used diversly. All icons were taken from freepik from flaticon.com.

Previously, a whole-cell system was already established for the HDCR-containing, mesophilic acetogen *A. woodii* (Schuchmann and Müller, 2013). A huge benefit of converting H_2 and CO_2 into formate, instead of producing acetate, is the multiple times higher reaction speed of formate formation due to the participation of only one (*via* HDCR) and not nine enzymes in the way of product formation. Moreover, the compound formate has different benefits in a H_2/formate bioeconomy as previously discussed. In general, formate is produced by many acetogens transiently during acetogenesis from H_2 + CO_2 (Peters et al., 1999).

But if the energy state of the cell is diminished, for example by uncoupling the primary bioenergetic to lower the cellular ATP content, the ATP-dependent further conversion of the intermediate formate is blocked. Without ATP, the N^{10}-formyl-THF synthetase can not bind the cofactor tetrahydrofolic acid (THF) to formate (Himes and Harmony, 1973; MacKenzie, 1984). As a result, no N^{10}-formyl-THF is formed and the subsequent reactions in the WLP to form acetate are interrupted. Therefore, formate accumulates and no acetate is formed. One way to diminish the intracellular ATP pool is the use of ionophores which destroy the electrochemical ion potential generated by the Rnf- or Ech-complex across the cytoplasmic membrane, thus making chemiosmotic ATP synthesis impossible. Another way is the disruption of the primary bioenergetic by limiting the coupling ion (H^+ or Na^+) or the direct inhibition of the membrane bound ATP synthase (Schuchmann and Müller, 2013; Schwarz and Müller, 2020). Using this metabolic understanding, the HDCR-based whole-cell catalysis was proven in several serum-bottle experiments, again, showing remarkable catalytic activities of the catalysts. The specific formate production rates of "uncoupled[3]" *A. woodii* and *T. kivui* cells were around 22 and 152 mmol g_{CDW}^{-1} h^{-1}, respectively (Schuchmann and Müller, 2013; Schwarz and Müller, 2020). The efficiency was almost 100% and only traces of the unwanted side product acetate (0.4 - 2.5 mM) was formed which is an undeniable benefit of using resting cells as biocatalysts in contrast to growing cells. As expected, resting cells which were "coupled", instead produced acetate from H_2 + CO_2 as the end product. Here, the specific acetate production rate of both organisms was much slower (roughly 15 mmol g_{CDW}^{-1} h^{-1}), owed to the participation of 8 additional enzymes in the conversion process which showed diverse catalytic rates (Andreesen et al., 1973; Ragsdale and Pierce, 2008; Wang et al., 2013b). *A. woodii* was the first autotrophic acetogen which has been described as genetically accessible (Strätz et al., 1994). Since then, the genetic tool box for acetogenic bacteria is constantly expanding and has made dramatic progress over the last few years (Bengelsdorf et al., 2018). Nowadays, the improvements enable genetic manipulations, metabolic engineering and synthetic biology of this bacterial group. This could also allow a genetic-based route to diminish acetate formation and to force

[3] ATP-limited, bioenergetically uncoupled cells will hereinafter be shortened as "uncoupled" in this thesis. In contrast, non-ATP limited cellular conditions are named as "coupled".

formate production in future. One possible and likely way would be the knock-out of the N^{10}-formyl-THF synthetase enzyme to prevent the further conversion of formate in the WLP. With modifications on a genetic level, the use of ionophores or uncoupling agents would become redundant. Nevertheless, keeping in mind that the redox-balance has to be maintained within the cell and the electron-flux has to be re-directed by implementing alternative routes other than the WLP. However, also some other organisms than *A. woodii* and *T. kivui* are known to produce formate from H_2 + CO_2. This has been demonstrated for whole cells of *E. coli* (Woods, 1936), the methanogenic archaeon *Methanobacterium formicicum* (Wu et al., 1993) the ”Knallgas“ bacterium *C. necator* (Klibanov et al., 1982) and the sulfate reducing bacterium *D. vulgaris* (da Silva et al., 2013). With the exception of *E. coli*, none of these organisms contain a membrane-bound FHL complex nor a soluble HDCR, and presumably multiple enzymes are involved and participate in the production of formate from H_2 and CO_2. Some of these organisms were already investigated to transform whole cells into efficient biocatalysts for the production of formate from H_2 and CO_2. For example, *E. coli* cells were modified by overexpressing different formate dehydrogenases from *C. carboxidivorans*, *Pyrococcus furiosus* and *Methanobacterium thermoformicicum* to turn this organism into a production platform for formate from H_2 and CO_2, the latter in form of bicarbonate (Alissandratos et al., 2014). The experiments were performed in two- or three-necked flasks at 37 °C, using 250 mM $NaHCO_3$ as CO_2 source and by applying a H_2 atmosphere or by sparging with H_2 gas. The highest obtained specific formate production rate of the recombinant JM109(DE3) *E. coli* cells overexpressing the *P. furiosus fdh* gene could be achieved with H_2 sparging and was calculated to be 0.25 mmol g_{CDW}^{-1} h^{-1}. A final formic acid concentration of 43 mM could be determined in the applied cell suspension experiment. Without H_2 sparging, only half of the specific rate and final formate concentration were reached. Noteworthy, the transformed *E. coli* cells were still reliant on one or more of the endogenous hydrogenases to obtain the required electrons for CO_2 reduction *via* H_2 oxidation. Recently, our group could demonstrate the heterologous production of a functional HDCR enzyme complex in *E. coli* (Leo et al., 2021). This transformed the organism into a whole-cell biocatalyst for hydrogen-driven CO_2 reduction to formate without the need of any external co-

factors or endogenous enzymes in the reaction process. Resting cells of the recombinant *E. coli* strain showed a specific formate production rate of 0.4 mmol g_{CDW}^{-1} h^{-1} in serum bottle experiments using a gas atmosphere of H_2 and CO_2 with additional 250 mM $KHCO_3$ and 5 mM formate was produced after 1 h. In contrast, the control strain was not able to convert H_2 and CO_2 to formate (Leo et al., 2021).

In another example, the sulfate-reducing bacteria of *D. vulgaris*, *D. alaskensis* and *D. desulfuricans* were investigated to produce formate from H_2 and CO_2 under sulfate-depleting conditions. Here, *D. desulfuricans* species showed the highest activity (~0.9 mmol g_{CDW}^{-1} h^{-1}) and 12 mM of formate was produced in serum bottle experiments at 37 °C and 1 bar overpressure (Mourato et al., 2017). It was postulated, that a cytoplasmic FDH (FdhAB) or a membrane-associated FDH (FdhABC) in addition to a periplasmic [FeFe]-hydrogenase (HydAB) are mainly involved in CO_2 hydrogenation under sulfate depleted conditions. The cellular electron mediator cytochrome c_3 is used to transfer the electrons from H_2 oxidation to the appropriate FDH center to reduce CO_2 (Mourato et al., 2017). An overview of different whole-cell catalysis experiments for hydrogen-dependent CO_2 reduction to formate is given in Tab. 1.

The different approaches clearly demonstrate the scientific interest to design whole cell-based biocatalysts that can transform H_2 and CO_2 into fromate with high product specificity and with reduced energy costs (i.e., ambient process temperature and low pressure).

Tab.1 Whole cell catalysis for hydrogen-dependent CO_2 reduction to formate by wild-type and recombinant strains in flasks experiments.

Organism	Reaction condition: temperature (°C)	Reaction condition: over-pressure (bar)	Mode	Biocatalyst	Na^+/K^+-bicarbonate (mM)	Specific formate production rate (mmol g_{CDW}^{-1} h^{-1})	Formate concentration (mM)	Reference
E. coli K-12 FTD89 (rec. strain[1])	37	~0.4	Closed-batch (Hungate-tubes)	Resting cells	no	~0.4	4.8 (after 20 h)	Roger et al., 2018
E. coli JM109 (rec. strain[2])	37	0	Closed-batch (flasks)	Resting cells	250	~0.1	20 (after 5 h)	Alissandratos et al., 2014
E. coli BL21(DE3) Δ*iscR* (rec. strain[3])	30	1	Closed-batch (flasks)	Resting cells	250	~0.4	5 (after 1 h)	Leo et al., 2021
D. desulfuricans (WT[4])	37	1	Closed-batch (flasks)	Growing cells under sulfate depleted conditions	no	~0.9	12 (after 240 h)	Mourato et al., 2017
A. woodii (WT[4])	30	1	Closed-batch (flasks)	Resting cells	no	~12	12 (after 0.4 h)	Schuchmann and Müller, 2013
A. woodii (WT[4])	30	1	Closed-batch (flasks)	Resting cells	300	~22	50 (after 1.5 h)	Schuchmann and Müller, 2013
T. kivui (WT[4])	60	1	Closed-batch (flasks)	Resting cells	300	~152	125 (after 1.5 h)	Schwarz and Müller, 2020

[1]*E. coli* K-12 FTD89 Δ*hyaB*, Δ*hybC*
[2]*E. coli* JM109(DE3) overexpressing *fdh* gen of ***Pyrococcus furiosus (fdh_Pyrfu)***
[3]*E. coli* BL21(DE3) Δ*iscR* overexpressing HDCR genes of *A. woodii* and maturation genes of *Shewanella. oneidensis* (pHDCR and pGXEF)
[4]WT, wild-type strain

3.3. Whole-cell catalysis for CO-based formate production

In addition, this thesis provides a whole-cell approach to convert syngas (H_2, CO_2 and CO) or CO alone into formate. *T. kivui* can grow on syngas and CO alone but the use of CO as sole carbon and electron source requires a stepwise adaptation of the organisms to increasing amounts of CO. Finally, up to 100% CO can be used as growth substrate (Weghoff and Müller, 2016). The requirement for CO adaptation was also reported for other acetogenic bacteria and methanogenic archaea such as *Butyribacterium methylotrophicum* (Lynd et al., 1982) and *Methanosarcina acetivorans*, respectively (Rother and Metcalf, 2004). The latter produced acetate and formate, rather than methane, as the major metabolic end products during growth on CO. The extent of CO utilization and CO tolerance can greatly vary between different carboxydotrophic organisms. The inhibiting effects of high CO partial pressures were shown for the acetogenic bacterium *Clostidium aceticum* (Mayer et al., 2018) whereas no substrate inhibition was observed in *C. carboxidivorans*. Here, increased CO partial pressures resulted in increased cell densities and ethanol formation (Hurst and Lewis, 2010). However, the mechanisms of CO utilization are still not fully understood for *T. kivui* and other acetogenic bacteria in detail (Diender et al., 2015; Weghoff and Müller, 2016).

In contrast to *T. kivui*, the model organisms *A. woodii* was not able to grow on CO alone but cells do grow on a gas mixture of H_2, CO_2 and CO (Bertsch and Müller, 2015a; Novak et al., 2021). The acetogenic bacterium can only co-metabolize CO when H_2 + CO_2 or formate are additional present as substrate (Bertsch and Müller, 2015a). However, resting cells of *A. woodii* are known to produce acetate from CO (Kerby et al., 1983; Diekert et al., 1986; Genthner and Bryant, 1987). Therefore, the previously established whole-cell systems of *A. woodii* and *T. kivui* were used to convert CO (or synthesis gas) into formate unlike to the typical product acetate. Again, CO_2 reduction to formate was exclusively based on the activity of the intracellular HDCR complex in the applied system. This assumption was proven by *A. woodii* and *T. kivui* mutants lacking the HDCR complex (Δ*hdcr*). Both mutant strains were neither able to produce formate nor acetate from CO, clearly demonstrating the essentiality of this enzyme complex in the WLP for CO_2 reduction. As described in section 2.4, the necessary electrons as well as the

CO_2 molecule itself have to be produced by CO oxidation *via* CO dehydrogenases. The electron acceptors could be diverse but the purified CODH of *A. woodii* and *M. thermoacetica* revealed the use of ferredoxin as electron acceptor (Ragsdale et al., 1983b; Ragsdale et al., 1983a). Since *T. kivui* harbors a monofunctional CO dehydrogenase (CooS) and the CODH subunit of the bifunctional CODH/ACS complex, the requirement of the monofunctional CO dehydrogenase in CO oxidation was investigated using a Δ*cooS* strain. Western-blot analysis revealed the presence of both enzymes in crude extracts, but CooS levels were highest in CO grown cells (Weghoff and Müller, 2016). Resting cells of *T. kivui* Δ*cooS* strain were still able to utilize CO due to the presence of the CODH/ACS complex but cells were not able to grow on CO anymore. The dispensability of monofunctional CO dehydrogenases in autotrophy was also shown by mutagenesis studies for *C. autoethanogenum* (Liew et al., 2016a). With the help of further genetic manipulations, two different CO utilization pathways could be assumed for the acetogenic bacteria *A. woodii* and *T. kivui* (Schwarz et al., 2020). Moreover, the CO-based formate production proceeded with highest rates so far reported (Rother and Metcalf, 2004; Henstra et al., 2007a; Mayer et al., 2018; Hwang et al., 2020). A direct comparison of the applied system with other organisms is rather difficult since CO-based formate production was mainly reported for growing cells in the literature. Formate formation was observed in growing cells of *M. acetivorans* where formate (~8 mM) was produced next to acetate (~10 mM) as major end product from CO oxidation. In contrast, formate accumulation occurred only transiently during growth of *Archaeoglobus fulgidus* and *C. aceticum* on CO (Mayer et al., 2018).

In general, CO inhibits growth of many strictly anaerobic microorganisms (Davidova et al., 1994; Sipma et al., 2006) and the CO molecule has an inhibitory effect on the active site of [FeFe] hydrogenases as well as [NiFe] hydrogenases (Lubitz et al., 2014). In both types of hydrogenases, the catalytically active site is buried inside the protein, therefore, CO (but also O_2 and the substrate H_2) has to enter the enzyme from the molecular surface *via* hydrophobic gas-access channels to reach the active center (Montet et al., 1997). With the help of X-ray crystallography and extended X-ray absorption fine structure (EXAFS) experiments, the binding of the extrinsic CO to the H_2 binding site was proven (Lemon and Peters, 1999; Mebs et al., 2018). This was confirmed by the crystal

structure of the CO-bound hydrogenase I of *C. pasteurianum* (Lemon and Peters, 1999). Like other hydrogenases, the hydrogenase subunit of the HDCR complex is sensitive to CO. But the formate dehydrogenase subunit still catalyzed formate oxidation or CO_2 reduction with artificial electron carriers or ferredoxin in the presence of CO (Schuchmann and Müller, 2013). But CO_2 reduction with ferredoxin was multiple times slower than H_2-dependent CO_2 reduction to formate. Since the HDCR complex exhibit a formate:ferredoxin and H_2:ferredoxin oxidoreductase activity, the use of reduced ferredoxin and/or genetic mutations in the CO-adapted strain of *T. kivui* are one likely assumption to explain the CO-based formate production with whole cells of *A. woodii* and *T. kivui*.

However, autotrophic growth on CO is directly coupled to H_2 evolution which requires the presence of CO-tolerant hydrogenases. Indeed, CO-tolerant and H_2-evolving hydrogenases have been identified in several organisms such as *Carboxydothermus hydrogenoformans* and *R. rubrum* (Fox et al., 1996; Soboh et al., 2002). Both organisms are able to grow on CO. Also the membrane-bound [NiFe]-hydrogenase from *R. eutropha* H16 was unaffected by carbon monoxide (Vincent et al., 2005). The inability to form a metal-CO bond at the active center is assumed to be the reason for non-CO inhibition. However, the exact mechanism to prevent CO inhibition is not fully understood and the effect of more distant residues that alter the structure of the active site pocket is one likely assumption.

3.4. Biotechnological upscaling

This thesis extends the biotechnological application of the designed whole-cell system of *A. woodii* and *T. kivui* by describing a batch process using a stirred-tank bioreactor (STR). The aim was the upscaling of the established whole-cell system and the target-oriented production of formate in a batch-operated STR with continuous gas supply of H_2 and CO_2. Noteworthy, the scale-up is a critical and important step in the biotech industry to bring innovative bioprocesses to commercialization (Delvigne et al., 2017). Viewed from an upscaling and technical perspective, acetogenic whole-cell conversion of H_2 and CO_2 into

acetate, but not to formate, was already shown for multiple types of bioreactor applications such as batch-operated stirred-tank bioreactors (Straub et al., 2014), stirred-tank bioreactors with a submerged microfiltration unit for full cell retention (Kantzow et al., 2015), packed-bed and trickle-bed biofilm reactors with immobilized cells (Riegler et al., 2019) and batch-operated stirred-tank bioreactors with increasing process pressure of the gaseous substrates (Kantzow and Weuster-Botz, 2016; Oswald et al., 2018). The target-oriented production of formate from H_2 and CO_2 was so far not reported in bioreactor experiments using acetogenic bacteria in particular. But increased formate formation was observed in high-pressure bioreactor experiments using *C. ljungdahlii* or *A. woodii* where the product spectrum changed with increasing partial pressure of the gaseous substrates (Peters et al., 1999; Kantzow and Weuster-Botz, 2016; Oswald et al., 2018). For *C. ljungdahlii*, a total pressure of 7 bar (53.3% H_2, 26.7% CO_2, 20% N_2 [v/v]) resulted in the production of 70 mM formate along with 13 mM acetate and 1.5 mM ethanol as co-products (Oswald et al., 2018). For *A. woodii*, an increased inlet hydrogen partial pressure from 0.4 up to 2.1 bar (total pressure of 3.5 bar) increased the final formate concentration from 8.7 mM to 159 mM and reduced the final acetate concentration by 50% (Kantzow and Weuster-Botz, 2016). Additional to an inhibition of acetate formation, an inhibition of growth was reported in both studies. These results are in accordance to earlier studies where same effects were observed for autotrophic cultivations of *A. woodii* and *Acetobacterium* BR-446 under increased hydrogen partial pressure as well as dissolved hydrogen concentration (Braun and Gottschalk, 1981; Morinaga and Kawada, 1990). But so far, an undeniable explanation is missing. Oswald and co-workers assumed that in *C. ljungdahlii* an increase in dissolved CO_2 concentration caused by an increase in substrate partial pressure could be responsible for the observed effects. CO_2 can freely diffuse through the cell membrane and dissociates in the cytoplasm into HCO_3^- and H^+, thus acidifying the intracellular pH. As one consequence the membrane potential is reduced and the ATP yield from the ATPase activity is decreased (Oswald et al., 2018). For *A. woodii* another assumption has been made since the primary bioenergetic and energy conservation is based on sodium ions and not on protons in this organism. Here, putative bottlenecks in the methyl branch of the WLP could be responsible for the fomate accumulation. A putative inhibition of enzymes of the central

carbon and energy metabolism by increased hydrogen concentrations is also conceivable (Kantzow and Weuster-Botz, 2016). An increase in partial pressure of hydrogen and carbon dioxide shifts the HDCR reaction towards direct hydrogenation of CO_2, thus making formate formation more favorable. Since the specific activities of enzymes following the HDCR reaction in the methyl branch are much lower, formate accumulates. Indeed, recombinant strains overexpressing either the genes for the THF-dependent enzymes in the methyl branch of the WLP or the genes of phosphotransacetylase and acetate kinase were finally able to produce more biomass and more acetate in the batch process and showed reduced final formate concentrations (Kantzow and Weuster-Botz, 2016). However, if the inhibition of biomass growth is related to an inhibitory effect of increased hydrogen partial pressures or increased dissolved carbon dioxide concentrations remains a topic of interest for further high-pressure experiments.

The bioreactor application provided in this thesis additionally demonstrates the great potential of acetogens in H_2 storage and CO_2 capture producing formate as the final product. The efficient conversion of H_2 and CO_2 into formate was shown for the first time in a batch-operated STR (Fig. 9) using resting cells of *A. woodii* and *T. kivui* (Schwarz et al., 2021).

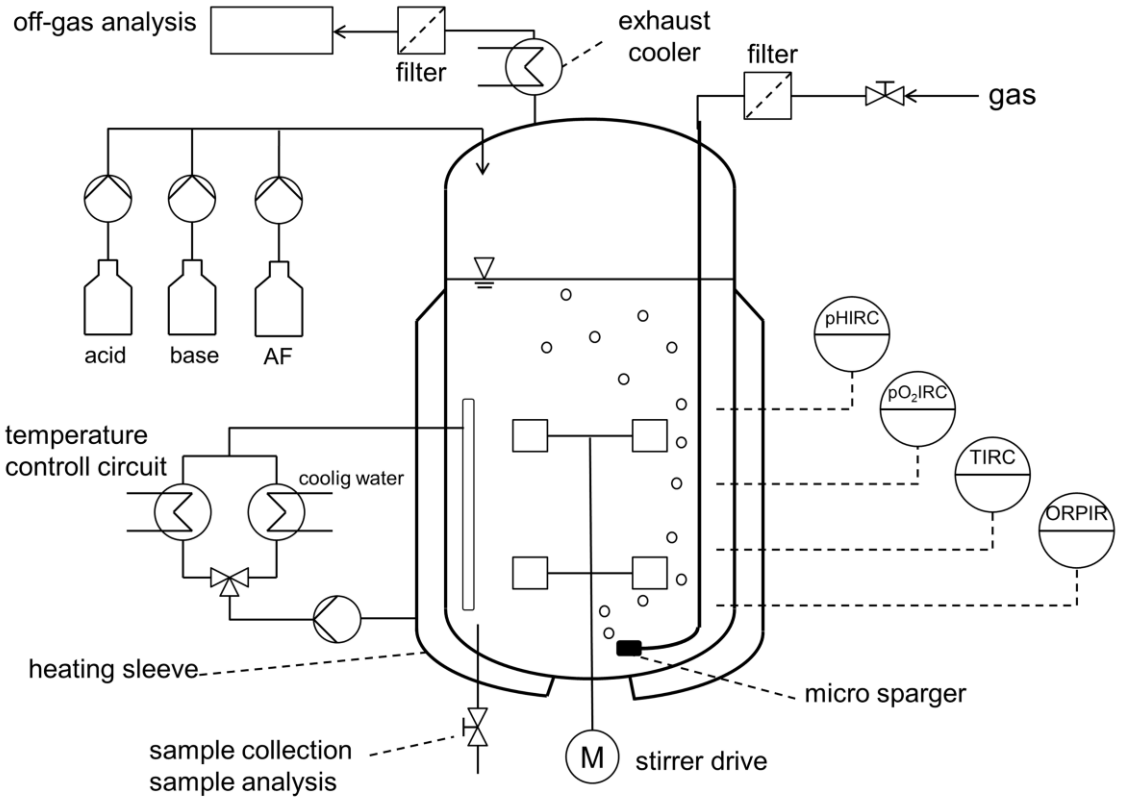

Fig. 9 Scheme of a fed-batch-operated stirred-tank bioreactor (STR) with continuous gas supply (Schwarz et al., 2021). Resting cells of *A. woodii* and *T. kivui* were used to convert H_2 and CO_2 to formate in a STR. pHIRC, pH indicator recording and control; pO_2IRC, pO_2 indicator recording and control; TIRC, temperature indicator recording and control; ORPIR, oxidation reduction potential indicator and recording; AF, antifoam.

The specific formate production rates could be increased in the bioreactor experiments compared to serum bottle experiments due to the better gas-liquid mass transfer and the pH-controlled conditions. *A. woodii* cells had a specific formate production rate of 42 mmol g^{-1} h^{-1} (18 mmol g_{CDW}^{-1} h^{-1}) and 73 mM formate could be produced under optimized conditions. Slightly reduced but comparable results were observed for *T. kivui* cells. Noteworthy, acetate was not produced overall which indicates an efficiency of 100% for the utilized CO_2 in the process. It has to be highlighted that the described rates were among the highest rates so far, which were reported in the literature for the process of hydrogen-dependent CO_2 reduction to formate using whole cells as biocatalysts (Schwarz et al., 2021). From these cell systems, only a few systems were applied in upscaling approaches using bioreactors. In a recent work, the previously described FHL enzyme complex of *E. coli* (see chapter 3.1) was demonstrated to efficiently operate in the reverse reaction as H_2-dependet CO_2 reductase under increased gas pressure (up to 10 bar). By using a highly pressurized bioreactor

system and a genetically modified *E. coli* K12 strain, approximately 500 mM formate could be produced from H_2 and CO_2 in the pH-controlled bioreactor after a time course of 23 h (Roger et al., 2018). Under the applied parameters (i.e., temperature of 37 °C, 10 bar pressure, controlled pH of 8.0) the formate production rate was 15 mmol g_{CDW}^{-1} h^{-1} (Roger et al., 2018). In the pressurized system the final formate concentration was roughly 7 times higher compared to the reported concentration of the applied bioreactor system in this thesis. This is not surprising, since an increase in partial pressure results in higher dissolved concentrations of the applied gases (H_2 and CO_2) which, therefore, allows the production of higher formate concentrations. Additionally, the higher substrate concentration affects the chemical equilibrium of the reaction, thus pushing the reaction towards formate formation. This effect becomes more clear by looking at the different rates in high pressure and ambient-pressure experiments using *E. coli* cells. The experiment conditions are not direct comparable, however, at 10 bar overpressure (in bioreactor experiments) the specific formate production rates were roughly 37 times higher compared to ambient pressure experiments in hungate tubes (Roger et al., 2018). To exploit the full potential of H_2-driven CO_2 reduction to formate by “uncoupled” *A. woodii* and *T. kivui* cells, the implementation of a highly pressurized (and pH-controlled) bioreactor system could be an interesting and promising approach in future. The application of highly pressurized bioreactor systems was shown for different bacteria and archaea before (Oswald et al., 2018; Roger et al., 2018; Pappenreiter et al., 2019).

In another work, Mourato and co-workers optimized formate production by using whole cells of *D. desulfuricans* in a developed column bioreactor for batch and continuous bioprocesses (Mourato et al., 2017). In the continuous mode, the bioreactor was sparged with a gas mixture of 80% H_2 and 20% CO_2 [v/v], the temperature was kept constant at 37 °C and a fed flow rate of 0.11 mL/min was applied for fresh medium (+20 mmol bicarbonate/day). Under these conditions, *D. desulfuricans* reached a specific formate production rate of 7 mmol g_{CDW}^{-1} h^{-1} and approximately 30 mM formate was produced after 64 h. A formate concentration of 45 mM was produced in the steady state in overall (Tab. 2).

Tab.2 Whole cell catalysis for hydrogen-dependent CO_2 reduction to formate by wild-type and recombinant strains in bioreactor experiments.

Organism	Reaction condition: temperature (°C)	Reaction condition: over-pressure (bar)	Mode	Biocatalyst	Na^+/K^+-bicarbonate (mM)	Specific formate production rate (mmol g_{CDW}^{-1} h^{-1})	Formate concentration (mM)	Reference
E. col K-12 RT1 (rec. strain[1])	37	10	Batch bioreactor	Resting cells	no	~15	500 (after 23h)	Roger et al., 2018
D. desulfuricans (WT[2])	37	0	Continuous bioreactor	Growing cells under sulfate depleted conditions	40 mM/day	~7	30 (after 64 h)	Mourato et al., 2017
D. desulfuricans (WT[2])	37	0	Batch bioreactor	Growing cells under sulfate depleted conditions	no	~5.5	12 (after 50 h)	Mourato et al., 2017
A. woodii (WT[2])	30	0	Batch bioreactor	Resting cells	no	~18	70 (after 30 h)	Schwarz et al., 2021

[1]*E. coli* K-12 RT1 Δ*hyaB*, Δ*hybC*, Δ*pflA*, Δ*fdhE*
[2]WT, wild-type strain

But also other biotechnological approaches were reported in the literature to catalyze the reduction of CO_2 to formate by using whole cells. These concepts are mainly based on the electrochemical conversion of CO_2 to formate which was shown for different organisms such as *M. extorquens* (Hwang et al., 2015) and *Shewanella oneidensis* (Le et al., 2018). Here, gaseous CO_2 is reduced to formate by electrons supplied from an electrode. Since these approaches use electricity as reducing power and the electrons are not derived from H_2 oxidation, the concept of electrochemical CO_2 reduction to formate by using whole cells will be not further discussed.

3.5. Formate bioconversion to longer-chain carbon molecules and formate oxidation to H_2

The formate-bio economy clearly shows the diversity in formate production and formate utilization. Independent of the strategy to produce formate, the soluble C1 compound formate can be used as substrate for natural or syntrophic formatotrophic organisms to produce longer-chain carbon molecules (Yishai et al., 2016). To address the need for renewably produced longer-chain carbon molecules, the concept of “two-stage bioconversion/fermentation” has been proposed as an appropriate solution. Here, the specialized metabolic traits of two different organisms can be combined to produce a product of interest by combining two different fermentation approaches i.e., combining an acetogenic fermentation with an aerobic fermentation (Hu et al., 2016). In such a setup, CO_2 and H_2 and/or CO can be feed to acetogens to produce short-chain bulk chemicals (i.e., acetate, formate, ethanol), which can then be fed to a second, separate bioreactor containing another microorganism (i.e., yeasts, other eukaryotes, bacteria) of interest (Fig. 10). This could allow the production of a vast number of chemicals entirely based on inorganic CO_2/CO. Even a two-step process in which biological and chemical steps are combined could be conceivable.

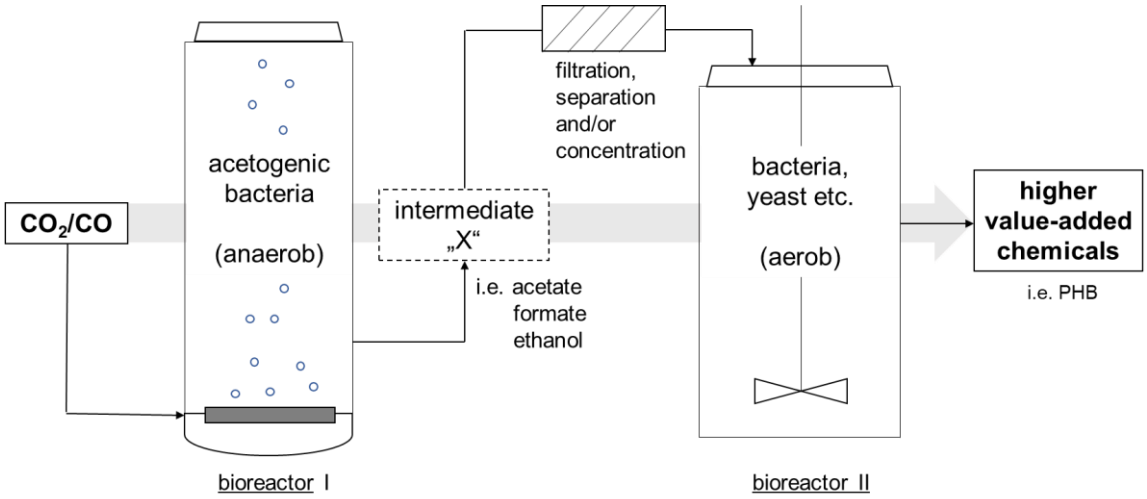

Fig. 10 Two-stage bioconversion for the production of higher value-added chemicals based on inorganic carbon. Acetogenic bacteria are used in bioreactor I to capture inorganic carbon and to produce compound „X“ (i.e., formate, acetate, ethanol). The compound from fermentation I (entitled as intermediate „X“) is then fed as substrate to a second bioreactor - interlinking bioreactor I with bioreactor II. The natural „X“-trophic or synthetic „X“-trophic microorganisms in bioreactor II possess the metabolic ability to produce higher value-added chemicals. PHB, poly-hydroxybutyrate.

The combination of autotrophic carbon fixation by acetogenic bacteria with modified acetotrophic or formatotrophic microorganisms in a second stage was already realized to produce longer-chain carbon molecules *via* two-stage fermentation (Hu et al., 2016; Hwang et al., 2020). In one example, CO_2 and CO/H_2 were initially converted to acetate in a bubble column bioreactor (anaerobic, first stage) using an evolved strain of *M. thermoacetica*. The produced acetate was subsequently converted to lipids by *Yarrowia lipolytica* in a second stage (aerobic, second stage) by using a stirred-tank bioreactor (Hu et al., 2016). In this stage, the engineered oleaginous yeast *Y. lipolytica* produced 18 g/L of C16-C18 triacylglycerides such as palmitate, palmitoleate, stearate, oleate and linoleate from the fed substrate acetate. In another example, the previously described HDCR-based whole-cell system (see chapter 3.3) to produce formate from CO was used in a two-stage bioconversion process (Hwang et al., 2020). In the first bioreactor, bioenergetically “uncoupled” *A. woodii* cells were used as whole-cell biocatalysts to exclusively convert CO into formate. The produced formate was then fed to a second bioreactor, where the engineered bacterium *M. extorquens* AM1 converted formate into poly-3-hydroxybutyrate (PHB) with a titer of 0.097 g/L (1.13 mM). PHB is a versatile biopolymer which is considered as an alternative to petroleum-based nondegradable plastics (Sagong et al., 2018). Once again, showing the promising strategy of using

acetogenic bacteria in a two-stage fermentation process to convert inorganic carbon (CO/CO_2) to a highly-valuable product. That formate can be regarded as a versatile feedstock was also shown for other native or synthetic formatotrophs. The natural formatotrophic bacterium *C. necator* was shown to produce higher alcohols (e.g., isobutanol and 3-methyl-1-butanol) from formate (Li et al., 2012). Furthermore, *Methylobacterium* sp. and genetically modified *E. coli* cells were already used to produce PHB and ethanol, respectively, from formate as substrate (Cho et al., 2016; Kim et al., 2019).

If formate is seen as LOHC, the stored and CO_2-bound hydrogen has to be released in a later formate oxidation reaction to close the H_2 storage cycle. Therefore, hydrogen production *via* microbial biotechnology is an active field of research which comprises three major categories: 1) biophotolysis of water, 2) photofermentation and 3) dark fermentation (Rosales-Colunga and Rodriguez, 2015). In the dark fermentation process, the organisms do not rely on the availability of light and can utilize a vast variety of carbon sources to break the substrates down into H_2 and most likely organic acids and alcohols. Since the process is technically much simpler, have higher production rates and do not need direct solar input, dark fermentative H_2 production seems to be more advantageous than photosynthetic hydrogen production and possesses a greater potential for practical applications (Das and Veziroglu, 2001; Rittmann and Herwig, 2012). Different microorganisms are known to oxidize formate with the concomitant evolution of H_2 and CO_2. As mentioned before, one of these organisms is *E. coli* which has become a workhorse for enhanced hydrogen production due to the FHL system. The hyperthermophilic archaeon *T. onnurineus* has a similar membrane-bound enzyme complex as the FHL of *E. coli* and the enzyme complex is involved in formate-driven H_2 production as well. The enhanced biohydrogen production from formate was already investigated in high cell density cultures of *T. onnurineus* and in a *T. onnurineus* strain with a mutated formate transporter caused by adaptive evolution of the organism (Bae et al., 2015; Jung et al., 2017). Formate conversion to hydrogen was mediated by the Fdh-Mrp-Mbh enzyme complex which consists of a formate dehydrogenase (Fdh) module, a membrane bound hydrogenase (Mbh) module and a multisubunit Na^+/H^+ antiporter (Mrp) module. So far, the entire enzyme complex could not be purified from *T. onnurineus* but the enzyme complex is

involved in chemiosmotic energy conservation (Kim et al., 2010; Lim et al., 2014; Mayer et al., 2015). The high growth temperature and putative prevailing environmental conditions (i.e., low H_2 concentrations) change the thermodynamics in favor of formate oxidation and allows *T. onnurineus* to grow by the oxidation of formate to H_2 + CO_2 (Kim et al., 2010). Growth of the sulfate-reducing bacterium *D. vulgaris* was also coupled to formate-driven H_2 production using a bioreactor with continuous gas sparging and without sulfate availability or syntrophic partners (Martins et al., 2015). Enough energy can be released in the formate oxidation reaction if the H_2 concentration is kept at a low level. In nature, this can be achieved by the coupling to H_2-consuming partner organisms which was demonstrated in a coculture of *Moorella* sp. strain AMP or *Desulfovibrio* sp. strain with a hydrogen-consuming methanogen (Dolfing et al., 2008).

The study of the formate metabolism in *A. woodii* and *T. kivui* is still in its infancy. But as mentioned before, both organisms harbor the HDCR complex which catalyzes CO_2 reduction and formate oxidation with almost the same rates. Therefore, a whole-cell system for formate-driven H_2 production was previously established for *A. woodii* cells in serum bottle scale (Kottenhahn et al., 2018). To take advantage of even higher catalytic rates, whole-cell biocatalysis using the thermophilic acetogen *T. kivui* is already under investigation in our research group. However, this thesis expands the application of the HDCR-based whole-cell system of *A. woodii* by demonstrating its application for formic acid-driven H_2 production in a fed-batch-operated stirred-tank bioreactor. By continuously feeding pure formic acid into the bioreactor more than 2.1 M formic acid was oxidized to H_2 over a process time of 185 h, showing a conversion efficiency of almost 100%. Due to the efficient reversibility of the HDCR enzyme, the HDCR-based whole-cell system can either be used for H_2 storage/CO_2 capturing or for “dark H_2 production”. Thereby, having one system for the two interesting and challenging reactions of 1) H_2-dependent CO_2 reduction to formate and 2) formate oxidation to H_2 and CO_2. This allows a wide field of applications considering the individually HDCR reactions or even in a combined process to store and release H_2 in and from formate (see section 5.1).

3.6. Future strategies

Based on the data obtained in this thesis there may be different strategies to further improve the applied system in future. One of these strategies covers the obstacle to further increase the final formate concentrations far above hundreds of mM in the process. As mentioned before, the equilibrium constant of the HDCR-catalyzed reaction is close to one. For that reason, the state of the equilibrium can easily be affected by pH, temperature and substrate/product concentrations (Amend and Shock, 2001). As shown before, an adjustment of the gas composition already increased the final formate concentration from 47 to 73 mM, mainly owed to the higher dissolved concentrations of the necessary substrates H_2 and CO_2 (Schwarz et al., 2021). Higher dissolved concentrations of the gaseous substrates are required to further increase the final formate concentrations. A proven method to avoid a low solubility of the applied gases in lithoautotrophic fermentations is by increasing the partial pressure of those gases in the gas phase (Abubackar et al., 2011). Of course, putative effects of higher partial pressure of the applied gases (i.e., H_2, CO or CO_2) on the growth behavior and product spectrum of the investigated organisms have to be kept in mind as mentioned before (see section 3.4). The production of 500 mM formate from H_2 and CO_2 was already demonstrated in a highly-pressurized bioreactor system (with 10 bar overpressure) using engineered resting cells of *E. coli* as biocatalyst (Roger et al., 2018). In contrast, under moderate reaction conditions with 0.4 bar overpressure only 4.8 mM of formate was produced from *E. coli* cells (Roger et al., 2018). Therefore, a pressurized (and pH-controlled) bioreactor system could be also an interesting approach to further increase the final formate concentration of the HDCR-based whole cell system.

Another and common approach to enhance gas-to-liquid mass transfer is by applying an increased power input. The increased bubble breakup as well as the increased interfacial area allow higher dissolved concentrations of the gases (Bredwell et al., 1999). However, in upscaling approaches the concept may not be economically feasible due to excessive costs for power supply. With regard to further upscaling of the demonstrated whole-cell system, a switch of the used bioreactor type would be one preferable way to reduce the high operating costs (by high power input) of a stirred-tank bioreactor. Costs have to be reduced in

future processes, since the produced product is the low-cost bulk chemical formate and not a high-value added product. Alternatives to stirred-tank bioreactors could be bubble-column and/or trickle-bed bioreactors. Both reactor types do not require mechanical agitation, thus lowering the energy consumption compared to STR (Bredwell et al., 1999). In general, both reactor types have an advantage of low operational and maintenance costs and bubble column bioreactors have been regarded as an attractive system for large-scale gas fermentation (Bredwell et al., 1999). However, each system has its own advantages and drawbacks that have to be considered prior to the application.

In case that higher formate concentrations are produced, a putative toxicity of the compound formate on the organism have to keep in mind. But the toxicity of formate differs between organisms and can be partly attributed to the reduction of the proton motive force due to a diffusion of the protonated acid across the cell membrane (Warnecke and Gill, 2005) or can be partly related to the reduced activity of present formate dehydrogenases (Yishai et al., 2016). An inhibition of respiratory cytochromes by formate is also possible (Nicholls, 1975). However, the sensitivity of organisms to formate can greatly vary and *A. woodii* cells were able to grow on formate concentrations up to 500 mM in batch cultivations (Moon et al., 2021). Recently, chemostat cultivations with a total feed of 200 mM formate were also demonstrated for *A. woodii* (Neuendorf et al., 2021). Since the used whole-cell system in this thesis is not reliant on growing cells, negative effects of higher formate concentrations could be less crucial here. In order to avoid the accumulation of high formate concentrations in highly-pressurized bioreactor systems, increased cell concentrations can be applied in continuous bioprocesses to increase the space-time yield as shown for gas fermentation (Peters et al., 1999; Kantzow et al., 2015). In a continuous bioprocess, new buffer can be continuously fed to the bioreactor and formate can be removed from the system for example *via* filtration through a permeable membrane which additionally allows cells retention. This circumvents the accumulation of high formate concentrations in the bioreactor broth with putative toxic effects on the applied cells. Future applications should also cover the genetic modification and metabolic engineering of the host organisms *A. woodii* and *T. kivui*. So far, a genetic system is available for both HDCR containing bacteria (Basen et al., 2018; Westphal et al., 2018). This paves the road to optimize whole-cell catalysis

on a genetic level. Since the addition of ionophores or antibiotic substances are not desirable in future demo or pilot scale approaches, the further conversion of H_2 and CO_2 to acetate has to be blocked *via* genetic modifications. Here, the knock-out of the formyl-THF synthetase genes would be one likely way to prevent the formation of acetate as unwanted side-product. Of course, also the knock-out of other genes coding for necessary enzymes in the methyl-branch of the WLP are conceivable opportunities to force formate accumulation from H_2 and CO_2. Also, the homologous or heterologous overproduction of the HDCR could be a promising way to further increase the activities of HDCR-based whole-cell catalysis. As mentioned before, the overproduction of a functional HDCR enzyme complex in the host organism *E. coli* was already demonstrated and enabled a deficient *E. coli* strain for the conversion of H_2 and CO_2 to formate (Leo et al., 2021). But not only H_2-dependent CO_2 reduction to formate can be addressed by genetic manipulations, moreover, formate-driven H_2 production can be part of optimization approaches in future. Different studies already demonstrated optimized H_2 production from formate using the host organisms *E. coli* and *T. onnurineous*. Here, an optimization of the formate transporter of *T. onnurineous* (Jung et al., 2017) or the overexpression of the genes coding for the FHL complex in *E. coli* (Yoshida et al., 2005) resulted in an increased H_2 production rate.

All the mentioned approaches demonstrate putative strategies to optimize the final product concentration, product specificity, specific activity, upscaling and economic viability of the established whole-cell system, thus, indicating the playground of future work.

3.7. Conclusion

The valorization of CO_2 is gaining more and more interest in the scientific and industrial communities. CO_2 is not regarded as a waste product anymore but is rather considered as an alternative carbon feedstock to transform the molecule into value-added products such as biofuels or biochemicals. Besides CO_2 sequestration strategies, also the H_2 economy attracts more and more attention due to the urgent need for alternative, renewable energy carriers. Obstacles which have to be addressed in both fields are the efficient reduction of CO_2 and the storage of renewably ("green") produced hydrogen. One reaction which addresses both topics is the direct hydrogenation of CO_2 into formate. The compound has favorable physicochemical properties and can be used diversely. In nature the redox reaction has been addressed to membrane-bound formate hydrogenlyase complexes which are widely distributed in the microbial world and whose participation in energy conservation is not fully resolved. But the diversity of nature was again proven by the discovery of a new, cytoplasmic enzyme complex which catalyzes the same reaction with multiple times higher reaction speed. This enzyme was called hydrogen-dependent CO_2 reductase (HDCR) and was found in the group of acetogenic bacteria. So far, the HDCR was experimentally analyzed only in *A. woodii* and *T. kivui* but available genome data of bacteria indicate the presence of HDCR-like gene clusters also outside the acetogenic group. Since the HDCRs show remarkable catalytic activities for the direct hydrogenation of CO_2 to formate as well as for the reverse reaction, the biotechnological application of these enzymes, especially in whole-cell catalysis, was the main focus of this thesis. Due to the established HDCR-based whole-cell system, formate could not only be produced from H_2 and CO_2 but also from synthesis gas (H_2, CO_2, CO) or CO alone. Moreover, the thesis extends the field of application by demonstrating a bioreactor application for the acetogenic conversion of H_2 and CO_2 into formic acid and *vice versa*, therefore killing two birds with one stone. The upscaling feasibility of the applied whole-cell system bears a greater potential for further biotechnological applications and might pave the road for a biological solution in H_2 storage and CO_2 capturing in future.

4. References

Abrini, J., Naveau, H. and Nyns, E.J. (1994) *Clostridium autoethanogenum*, sp. nov., an anaerobic bacterium that produces ethanol from carbon monoxide. Arch. Microbiol. **161**: 345-351.

Abubackar, H.N., Veiga, M.C. and Kennes, C. (2011) Biological conversion of carbon monoxide: rich syngas or waste gases to bioethanol. Biofuels Bioprod. Biorefin. **5**: 93-114.

Acar, C. and Dincer, I. (2014) Comparative assessment of hydrogen production methods from renewable and non-renewable sources. Int. J. Hydrog. Energy **39**: 1-12.

Ajanovic, A. (2011) Biofuels versus food production: Does biofuels production increase food prices? Energy **36**: 2070-2076.

Albert, J., Lüders, D., Bösmann, A., Guldi, D.M. and Wasserscheid, P. (2014) Spectroscopic and electrochemical characterization of heteropoly acids for their optimized application in selective biomass oxidation to formic acid. Green Chem. **16**: 226-237.

Alissandratos, A., Kim, H.K. and Easton, C.J. (2014) Formate production through carbon dioxide hydrogenation with recombinant whole cell biocatalysts. Bioresour. Technol. **164**: 7-11.

Allen, M.R., Frame, D.J., Huntingford, C., Jones, C.D., Lowe, J.A., Meinshausen, M. and Meinshausen, N. (2009) Warming caused by cumulative carbon emissions towards the trillionth tonne. Nature **458**: 1163-1166.

Alvarez, A., Bansode, A., Urakawa, A., Bavykina, A.V., Wezendonk, T.A., Makkee, M., Gascon, J. and Kapteijn, F. (2017) Challenges in the greener production of formates/formic acid, methanol, and DME by heterogeneously catalyzed CO_2 hydrogenation processes. Chem. Rev. **117**: 9804-9838.

Amao, Y. (2018) Formate dehydrogenase for CO_2 utilization and its application. J. CO2 Util. **26**: 623-641.

Amend, J.P. and Shock, E.L. (2001) Energetics of overall metabolic reactions of thermophilic and hyperthermophilic *Archaea* and *Bacteria*. FEMS Microbiol. Rev. **25**: 175-243.

An, L. and Chen, R. (2016) Direct formate fuel cells: A review. J. Power Sources **320**: 127-139.

Andreesen, J.R., Schaupp, A., Neurauter, C., Brown, A. and Ljungdahl, L.G. (1973) Fermentation of glucose, fructose, and xylose by *Clostridium thermoaceticum*: effect of metals on growth yield, enzymes, and the synthesis of acetate from CO_2. J. Bacteriol. **114**: 743-751.

Axley, M.J. and Grahame, D.A. (1991) Kinetics for formate dehydrogenase of *Escherichia coli* formate-hydrogenlyase. J. Biol. Chem. **266**: 13731-13736.

Axley, M.J., Böck, A. and Stadtman, T.C. (1991) Catalytic properties of an *Escherichia coli* formate dehydrogenase mutant in which sulfur replaces selenium. Proc. Natl. Acad. Sci. U.S.A. **88**: 8450-8454.

Babel, W. (2009) The auxiliary substrate concept: From simple considerations to heuristically valuable knowledge. Eng. Life Sci. **9**: 285-290.

Bae, S.S., Lee, H.S., Jeon, J.H., Lee, J.H., Kang, S.G. and Kim, T.W. (2015) Enhancing bio-hydrogen production from sodium formate by hyperthermophilic archaeon, *Thermococcus onnurineus* NA1. Bioprocess Biosyst. Eng. **38**: 989-993.

Bae, S.S., Kim, Y.J., Yang, S.H., Lim, J.K., Jeon, J.H., Lee, H.S., Kang, S.G., Kim, S.J. and Lee, J.H. (2006) *Thermococcus onnurineus* sp nov., a hyperthermophilic archaeon isolated from a deep-sea hydrothermal vent area at the PACMANUS field. J. Microbiol. Biotechnol. **16**: 1826-1831.

Baffert, C., Bertini, L., Lautier, T., Greco, C., Sybirna, K., Ezanno, P., Etienne, E., Soucaille, P., Bertrand, P., Bottin, H., Meynial-Salles, I., De Gioia, L. and Leger, C. (2011) CO disrupts the reduced H-cluster of FeFe hydrogenase. A combined DFT and protein film voltammetry study. J. Am. Chem. Soc. **133**: 2096-2099.

Balnokin, Y.V. and Popova, L.G. (1994) The ATP-driven Na^+-pump in the plasma membrane of the marine unicellular alga, *Platymonas viridis*. FEBS Lett. **343**: 61-64.

Banerjee, A., Leang, C., Ueki, T., Nevin, K.P. and Lovley, D.R. (2014) Lactose-inducible system for metabolic engineering of *Clostridium ljungdahlii*. Appl. Environ. Microbiol. **80**: 2410-2416.

Banerjee, R. and Ragsdale, S.W. (2003) The many faces of vitamin B_{12}: catalysis by cobalamin-dependent enzymes. Annu. Rev. Biochem. **72**: 209-247.

Bar-Even, A. (2013) Does acetogenesis really require especially low reduction potential? Biochim. Biophys. Acta. **1827**: 395-400.

Barker, H.A. and Kamen, M.D. (1945) Carbon dioxide utilization in the synthesis of acetic acid by *Clostridium thermoaceticum*. Proc. Natl. Acad. Sci. U.S.A. **31**: 219-225.

Basen, M., Geiger, I., Henke, L. and Müller, V. (2018) A genetic system for the thermophilic acetogenic bacterium *Thermoanaerobacter kivui*. Appl. Environ. Microbiol. **84**: e02210-02217.

Bassegoda, A., Madden, C., Wakerley, D.W., Reisner, E. and Hirst, J. (2014) Reversible interconversion of CO_2 and formate by a molybdenum-containing formate dehydrogenase. J. Am. Chem. Soc. **136**: 15473-15476.

Beaty, P.S. and Ljungdahl, L.G. (1991) Growth of *Clostridium thermoaceticum* on methanol, ethanol or dimethylsulfoxide. Ann. Meet. Am. Soc. Microbiol. **Abstr. K-131**: 236.

Bender, G. and Ragsdale, C.W. (2011) Evidence that ferredoxin interfaces with an internal redox shuttle in acetyl-CoA synthase during reductive activation and catalysis. Biochemistry **50**: 276-286.

Bengelsdorf, F.R. and Dürre, P. (2017) Gas fermentation for commodity chemicals and fuels. Microb. Biotechnol. **10**: 1167-1170.

Bengelsdorf, F.R., Straub, M. and Dürre, P. (2013) Bacterial synthesis gas (syngas) fermentation. Environ. Technol. **34**: 1639-1651.

Bengelsdorf, F.R., Poehlein, A., Linder, S., Erz, C., Hummel, T., Hoffmeister, S., Daniel, R. and Dürre, P. (2016) Industrial acetogenic biocatalysts: A comparative metabolic and genomic analysis. Front. Microbiol. **7**: 1036.

Bengelsdorf, F.R., Beck, M.H., Erz, C., Hoffmeister, S., Karl, M.M., Riegler, P., Wirth, S., Poehlein, A., Weuster-Botz, D. and Dürre, P. (2018) Bacterial anaerobic synthesis gas (syngas) and $CO_2 + H_2$ fermentation. Adv. Appl. Microbiol. **103**: 143-221.

Bennett, B.D., Kimball, E.H., Gao, M., Osterhout, R., Van Dien, S.J. and Rabinowitz, J.D. (2009) Absolute metabolite concentrations and implied enzyme active site occupancy in *Escherichia coli*. Nat. Chem. Biol. **5**: 593-599.

Berg, I.A. (2011) Ecological aspects of the distribution of different autotrophic CO_2 fixation pathways. Appl. Environ. Microbiol. **77**: 1925-1936.

Berg, I.A., Kockelkorn, D., Buckel, W. and Fuchs, G. (2007) A 3-hydroxypropionate/4-hydroxybutyrate autotrophic carbon dioxide assimilation pathway in *Archaea*. Science **318**: 1782-1786.

Bertsch, J. and Müller, V. (2015a) CO metabolism in the acetogen *Acetobacterium woodii*. Appl. Environ. Microbiol. **81**: 5949-5956.

Bertsch, J. and Müller, V. (2015b) Bioenergetic constraints for conversion of syngas to biofuels in acetogenic bacteria. Biotechnol. Biofuels **8**: 210.

Bertsch, J., Parthasarathy, A., Buckel, W. and Müller, V. (2013) An electron-bifurcating caffeyl-CoA reductase. J. Biol. Chem. **288**: 11304-11311.

Biegel, E. and Müller, V. (2010) Bacterial Na^+-translocating ferredoxin:NAD^+ oxidoreductase. Proc. Natl. Acad. Sci. U.S.A. **107**: 18138-18142.

Biegel, E., Schmidt, S. and Müller, V. (2009) Genetic, immunological and biochemical evidence of a Rnf complex in the acetogen *Acetobacterium woodii*. Environ. Microbiol. **11**: 1438-1443.

Biegel, E., Schmidt, S., González, J.M. and Müller, V. (2011) Biochemistry, evolution and physiological function of the Rnf complex, a novel ion-motive electron transport complex in prokaryotes. Cell. Mol. Life Sci. **68**: 613-634.

Boll, M., Fuchs, G., Tilley, G., Armstrong, F.A. and Lowe, D.J. (2000) Unusual spectroscopic and electrochemical properties of the 2[4Fe-4S] ferredoxin of *Thauera aromatica*. Biochemistry **39**: 4929-4938.

Brandt, K. and Müller, V. (2015) Hybrid rotors in F_1F_o ATP synthases: subunit composition, distribution, and physiological significance. Biol. Chem. **396**: 1031-1042.

Braun, K. and Gottschalk, G. (1981) Effect of molecular hydrogen and carbon dioxide on chemo-organotrophic growth of *Acetobacterium woodii* and *Clostridium aceticum*. Arch. Microbiol. **128**: 294-298.

Bredwell, M.D., Srivastava, P. and Worden, R.M. (1999) Reactor design issues for synthesis-gas fermentations. Biotechnol. Prog. **15**: 834-844.

Brondino, C.D., Romao, M.J., Moura, I. and Moura, J.J.G. (2006) Molybdenum and tungsten enzymes: the xanthine oxidase family. Curr. Opin. Chem. Biol. **10**: 109-114.

Brondino, C.D., Passeggi, M.C.G., Caldeira, J., Almendra, M.J., Feio, M.J., Moura, J.J.G. and Moura, I. (2004) Incorporation of either molybdenum or tungsten into formate dehydrogenase from *Desulfovibrio alaskensis* NCIMB 13491; EPR assignment of the proximal iron-sulfur cluster to the pterin cofactor in formate dehydrogenases from sulfate-reducing bacteria. J. Biol. Inorg. Chem. **9**: 145-151.

Brown, T.R. and Brown, R.C. (2013) A review of cellulosic biofuel commercial-scale projects in the United States. Biofuels Bioprod. Biorefining **7**: 235-245.

Bruant, G., Levesque, M.J., Peter, C., Guiot, S.R. and Masson, L. (2010) Genomic analysis of carbon monoxide utilization and butanol production by *Clostridium carboxidivorans* strain P7. PLoS One **5**: e13033.

Brunold, T.C. (2004) Spectroscopic and computational insights into the geometric and electronic properties of the A-cluster of acetyl-coenzyme A synthase. J. Biol. Inorg. Chem. **9**: 533-541.

Buckel, W. and Thauer, R.K. (2013) Energy conservation *via* electron bifurcating ferredoxin reduction and proton/Na^+ translocating ferredoxin oxidation. Biochim. Biophys. Acta **1827**: 94-113.

Buckel, W. and Thauer, R.K. (2018a) Flavin-based electron bifurcation, ferredoxin, flavodoxin, and anaerobic respiration with protons (Ech) or NAD^+ (Rnf) as electron acceptors: a historical review. Front. Microbiol. **9**: 401.

Buckel, W. and Thauer, R.K. (2018b) Flavin-based electron bifurcation, a new mechanism of biological energy coupling. Chem. Rev. **118**: 3862-3886.

Cakar, M.M., Ruupunen, J., Mangas-Sanchez, J., Birmingham, W.R., Yildirim, D., Turunen, O., Turner, N.J., Valjakka, J. and Binay, B. (2020) Engineered formate dehydrogenase from *Chaetomium thermophilum*, a promising enzymatic solution for biotechnical CO_2 fixation. Biotechnol. Lett. **42**: 2251-2262.

Calvin, M. and Benson, A.A. (1948) The path of carbon in photosynthesis. Science **107**: 476-480.

Castillo, R., Oliva, M., Marti, S. and Moliner, V. (2008) A theoretical study of the catalytic mechanism of formate dehydrogenase. J. Phys. Chem. B. **112**: 10012-10022.

Ceccaldi, P., Schuchmann, K., Müller, V. and Elliott, S.J. (2017) The hydrogen dependent CO_2 reductase: the first completely CO tolerant FeFe-hydrogenase. Energy. Environm. Sci. **10**: 503-508.

Cheah, W.Y., Ling, T.C., Juan, J.C., Lee, D.J., Chang, J.S. and Show, P.L. (2016) Biorefineries of carbon dioxide: From carbon capture and storage (CCS) to bioenergies production. Bioresour. Technol. **215**: 346-356.

Chippaux, M., Pascal, M.C. and Casse, F. (1977) Formate hydrogenlyase system in *Salmonella typhimurium* LT2. Eur. J. Biochem. **72**: 149-155.

Chiranjeevi, P., Bulut, M., Breugelmans, T., Patil, S.A. and Pant, D. (2019) Current trends in enzymatic electrosynthesis for CO_2 reduction. Curr. Opin. Green Sustain. **16**: 65-70.

Cho, D.H., Jang, M.G. and Kim, Y.H. (2016) Formatotrophic production of poly-β-hydroxybutyric acid (PHB) from *Methylobacterium sp.* using formate as the sole carbon and energy source. Korean Chem. Eng. Res. **54**: 719-721.

Choe, H., Ha, J.M., Joo, J.C., Kim, H., Yoon, H.J., Kim, S., Son, S.H., Gengan, R.M., Jeon, S.T., Chang, R., Jung, K.D., Kim, Y.H. and Lee, H.H. (2015) Structural insights into the efficient CO_2-reducing activity of an NAD-dependent formate dehydrogenase from *Thiobacillus sp.* KNK65MA. Acta Crystallogr. D Biol. Crystallogr. **71**: 313-323.

Chowdhury, N.P., Mowafy, A.M., Demmer, J.K., Upadhyay, V., Koelzer, S., Jayamani, E., Kahnt, J., Hornung, M., Demmer, U., Ermler, U. and Buckel, W. (2014) Studies on the mechanism of electron bifurcation catalyzed by electron transferring flavoprotein (Etf) and butyryl-CoA dehydrogenase (Bcd) of *Acidaminococcus fermentans*. J. Biol. Chem. **289**: 5145-5157.

Claassens, N.J., Sanchez-Andrea, I., Sousa, D.Z. and Bar-Even, A. (2018) Towards sustainable feedstocks: A guide to electron donors for microbial carbon fixation. Curr. Opin. Biotechnol. **50**: 195-205.

Clark, J.E. and Ljungdahl, L.G. (1982) Purification and properties of 5,10-methenyltetrahydrofolate cyclohydrolase from *Clostridium formicoaceticum*. J. Biol. Chem. **257**: 3833-3836.

Clark, J.E. and Ljungdahl, L.G. (1984) Purification and properties of 5,10-methylenetetrahydrofolate reductase, an iron-sulfur flavoprotein from *Clostridium formicoaceticum*. J. Biol. Chem. **259**: 10845-10849.

Cotton, C.A., Edlich-Muth, C. and Bar-Even, A. (2018) Reinforcing carbon fixation: CO_2 reduction replacing and supporting carboxylation. Curr. Opin. Biotechnol. **49**: 49-56.

Cotton, C.A., Claassens, N.J., Benito-Vaquerizo, S. and Bar-Even, A. (2019) Renewable methanol and formate as microbial feedstocks. Curr. Opin. Biotechnol. **62**: 168-180.

Cox, P.M., Betts, R.A., Jones, C.D., Spall, S.A. and Totterdell, I.J. (2000) Acceleration of global warming due to carbon-cycle feedbacks in a coupled climate model. Nature **408**: 184-187.

Crowther, G.J., Kosaly, G. and Lidstrom, M.E. (2008) Formate as the main branch point for methylotrophic metabolism in *Methylobacterium extorquens* AM1. J. Bacteriol. **190**: 5057-5062.

da Silva, S.M., Voordouw, J., Leitao, C., Martins, M., Voordouw, G. and Pereira, I.A. (2013) Function of formate dehydrogenases in *Desulfovibrio vulgaris* Hildenborough energy metabolism. Microbiology **159**: 1760-1769.

Dangel, W., Schulz, H., Diekert, G., König, H. and Fuchs, G. (1987) Occurence of corrinoid-containing membrane proteins in anaerobic bacteria. Arch. Microbiol. **148**: 52-56.

Daniell, J., Köpke, M. and Simpson, S.D. (2012) Commercial biomass syngas fermentation. Energies **5**: 5372-5417.

Daniell, J., Nagaraju, S., Burton, F., Köpke, M. and Simpson, S.D. (2016) Low-carbon fuel and chemical production by anaerobic gas fermentation. Adv. Biochem. Eng. Biotechnol. **156**: 293-321.

Darnault, C., Volbeda, A., Kim, E.J., Legrand, P., Vernede, X., Lindahl, P.A. and Fontecilla-Camps, J.C. (2003) Ni-Zn-[Fe4-S4] and Ni-Ni-[Fe4-S4] clusters in closed and open subunits of acetyl-CoA synthase/carbon monoxide dehydrogenase. Nat. Struct. Biol. **10**: 271-279.

Das, D. and Veziroglu, T.N. (2001) Hydrogen production by biological processes: a survey of literature. Int. J. Hydrog. Energy **26**: 13-28.

Davidova, M.N., Tarasova, N.B., Mukhitova, F.K. and Karpilova, I.U. (1994) Carbon monoxide in metabolism of anaerobic bacteria. Can. J. Microbiol. **40**: 417-425.

de Carvalho, C.C. (2017) Whole cell biocatalysts: essential workers from Nature to the industry. Microb. Biotechnol. **10**: 250-263.

Delvigne, F., Takors, R., Mudde, R., van Gulik, W. and Noorman, H. (2017) Bioprocess scale-up/down as integrative enabling technology: from fluid mechanics to systems biology and beyond. Microb. Biotechnol. **10**: 1267-1274.

Diekert, G. and Wohlfarth, G. (1994a) Energetics of acetogenesis from C_1 units. In *Acetogenesis*. Drake, H.L. (ed). New York: Chapman and Hall, pp. 157-179.

Diekert, G. and Wohlfarth, G. (1994b) Metabolism of homoacetogens. Anton Leeuwenhoek Int. J. G. **66**: 209-221.

Diekert, G., Schrader, E. and Harder, W. (1986) Energetics of CO formation and CO oxidation in cell suspensions of *Acetobacterium woodii*. Arch. Microbiol. **144**: 386-392.

Diekert, G.B. and Thauer, R.K. (1978) Carbon monoxide oxidation by *Clostridium thermoaceticum* and *Clostridium formicoaceticum*. J. Bacteriol. **136**: 597-606.

Diender, M., Stams, A.J. and Sousa, D.Z. (2015) Pathways and bioenergetics of anaerobic carbon monoxide fermentation. Front. Microbiol. **6**: 1275.

Dietrich, H.M., Kremp, F., Öppinger, C., Ribaric, L. and Müller, V. (2021) Biochemistry of methanol-dependent acetogenesis in *Eubacterium callanderi* KIST612. Environ. Microbiol. **8**: 4505-4517

Dincer, I. (2012) Green methods for hydrogen production. Int. J. Hydrog. Energy **37**: 1954-1971.

Dobbek, H., Svetlitchnyi, V., Gremer, L., Huber, R. and Meyer, O. (2001) Crystal structure of a carbon monoxide dehydrogenase reveals a [Ni-4Fe-5S] cluster. Science **293**: 1281-1285.

Dolfing, J., Jiang, B., Henstra, A.M., Stams, A.J. and Plugge, C.M. (2008) Syntrophic growth on formate: a new microbial niche in anoxic environments. Appl. Environ. Microbiol. **74**: 6126-6131.

Dönig, J. and Müller, V. (2018) Alanine, a novel growth substrate for the acetogenic bacterium *Acetobacterium woodii*. Appl. Environ. Microbiol. **84**: e02023-02018.

Doukov, T.I., Iverson, T.M., Seravalli, J., Ragsdale, S.W. and Drennan, C.L. (2002) A Ni-Fe-Cu center in a bifunctional carbon monoxide dehydrogenase/acetyl-CoA synthase. Science **298**: 567-572.

Drake, H.L. (1982) Demonstration of hydrogenase in extracts of the homoacetate-fermenting bacterium *Clostridium thermoaceticum*. J. Bacteriol. **150**: 702-709.

Drake, H.L. (1994) Acetogenesis, acetogenic bacteria, and the acetyl-CoA pathway: past and current perspectives. In *Acetogenesis*. Drake, H.L. (ed). New York: Chapman and Hall, pp. 3–60.

Drake, H.L. and Daniel, S.L. (2004) Physiology of the thermophilic acetogen *Moorella thermoacetica*. Res. Microbiol. **155**: 869-883.

Drake, H.L., Küsel, K. and Matthies, C. (2006) Acetogenic Prokaryotes. In *The Prokaryotes*. Dworkin, M., Falkow, S., Rosenberg, E., Schleifer, K.-H., and Stackebrandt, E. (eds). New York: Springer, p. 373.

Drake, H.L., Gößner, A.S. and Daniel, S.L. (2008) Old acetogens, new light. Ann. N. Y. Acad. Sci. **1125**: 100-128.

Drake, H.L., Daniel, S., Küsel, K., Matthies, C., Kuhner, C. and Braus-Strohmeyer, S. (1997) Acetogenic bacteria: what are the *in situ* consequences of their diverse metabolic diversities? Biofactors **1**: 13-24.

Drennan, C.L., Heo, J., Sintchak, M.D., Schreiter, E. and Ludden, P.W. (2001) Life on carbon monoxide: X-ray structure of *Rhodospirillum rubrum* Ni-Fe-S carbon monoxide dehydrogenase. Proc. Natl. Acad. Sci. U.S.A. **98**: 11973-11978.

Dufour, J., Serrano, D.P., Galvez, J.L., Moreno, J. and Garcia, C. (2009) Life cycle assessment of processes for hydrogen production. Environmental feasibility and reduction of greenhouse gases emissions. Int. J. Hydrog. Energy **34**: 1370-1376.

Eichler, B. and Schink, B. (1984) Oxidation of primary aliphatic alcohols by *Acetobacterium carbinolicum* sp. nov., a homoacetogenic anaerobe. Arch. Microbiol. **140**: 147-152.

Enthaler, S. (2008) Carbon dioxide--the hydrogen-storage material of the future? ChemSusChem **1**: 801-804.

Enthaler, S., von Langermann, J. and Schmidt, T. (2010) Carbon dioxide and formic acid-the couple for environmental-friendly hydrogen storage? Energy Environ. Sci. **3**: 1207-1217.

Evans, M.C., Buchanan, B.B. and Arnon, D.I. (1966) A new ferredoxin-dependent carbon reduction cycle in a photosynthetic bacterium. Proc Natl Acad Sci U.S.A. **55**: 928-934.

Fargione, J., Hill, J., Tilman, D., Polasky, S. and Hawthorne, P. (2008) Land clearing and the biofuel carbon debt. Science **319**: 1235-1238.

Fast, A.G. and Papoutsakis, E.T. (2012) Stoichiometric and energetic analyses of non-photosynthetic CO_2-fixation pathways to support synthetic biology strategies for production of fuels and chemicals. Curr. Opin. Chem. Eng. **1**: 380-395.

Fischer, F., Lieske, R. and Winzler, K. (1932) Biologische Gasreaktionen. II. Über die Bildung von Essigsäure bei der biologischen Umsetzung von Kohlenoxyd und Kohlensäure zu Methan. Biochem. Z. **245**: 2-12.

Fontaine, F.E., Peterson, W.H., McCoy, E., Johnson, M.J. and Ritter, G.J. (1942) A new type of glucose fermentation by *Clostridium thermoaceticum*. J. Bacteriol. **43**: 701-715.

Foster, C.E., Kramer, T., Wait, A.F., Parkin, A., Jennings, D.P., Happe, T., McGrady, J.E. and Armstrong, F.A. (2012) Inhibition of [FeFe]-hydrogenases by formaldehyde and wider mechanistic implications for biohydrogen activation. J. Am. Chem. Soc. **134**: 7553-7557.

Fourmond, V., Baffert, C., Sybirna, K., Dementin, S., Abou-Hamdan, A., Meynial-Salles, I., Soucaille, P., Bottin, H. and Leger, C. (2013) The mechanism of inhibition by H_2 of H_2-evolution by hydrogenases. Chem. Commun. **49**: 6840-6842.

Fox, J.D., Kerby, R.L., Roberts, G.P. and Ludden, P.W. (1996) Characterization of the CO-induced, CO-tolerant hydrogenase from *Rhodospirillum rubrum* and the gene encoding the large subunit of the enzyme. J. Bacteriol. **178**: 1515-1524.

Fritz, M., Klyszejko, A.L., Morgner, N., Vonck, J., Brutschy, B., Müller, D.J., Meier, T. and Müller, V. (2008) An intermediate step in the evolution of ATPases: a hybrid F_1F_O rotor in a bacterial Na^+ F_1F_O ATP synthase. FEBS J. **275**: 1999-2007.

Fuchs, G. (2011) Alternative pathways of carbon dioxide fixation: Insights into the early evolution of life? Annu. Rev. Microbiol. **65**: 631-658.

Geddes, C.C., Nieves, I.U. and Ingram, L.O. (2011) Advances in ethanol production. Curr. Opin. Biotechnol. **22**: 312-319.

Genthner, B.R.S. and Bryant, M.P. (1982) Growth of *Eubacterium limosum* with carbon monoxide as the energy source. Appl. Environ. Microbiol. **43**: 70-74.

Genthner, B.R.S. and Bryant, M.P. (1987) Additional characteristics of one-carbon-compound utilization by *Eubacterium limosum* and *Acetobacterium woodii*. Appl. Environ. Microbiol. **53**: 471-476.

Goldet, G., Brandmayr, C., Stripp, S.T., Happe, T., Cavazza, C., Fontecilla-Camps, J.C. and Armstrong, F.A. (2009) Electrochemical kinetic investigations of the reactions of [FeFe]-hydrogenases with carbon monoxide and oxygen: comparing the importance of gas tunnels and active-site electronic/redox effects. J. Am. Chem. Soc. **131**: 14979-14989.

Grethlein, A.J., Worden, R.M., Jain, M.K. and Datta, R. (1991) Evidence for production of *n*-butanol from carbon monoxide by *Butyribacterium methylotrophicum*. J. Ferment. Bioeng. **72**: 58-60.

Grignard, B., Gennen, S., Jerome, C., Kleij, A.W. and Detrembleur, C. (2019) Advances in the use of CO_2 as a renewable feedstock for the synthesis of polymers. Chem. Soc. Rev. **48**: 4466-4514.

Grimaldi, S., Schoepp-Cothenet, B., Ceccaldi, P., Guigliarelli, B. and Magalon, A. (2013) The prokaryotic Mo/W-*bis* PGD enzymes family: A catalytic workhorse in bioenergetic. Biochim. Biophys. Acta Bioenerg. **1827**: 1048-1085.

Grunwald, S., Mottet, A., Grousseau, E., Plassmeier, J.K., Popovic, M.K., Uribelarrea, J.L., Gorret, N., Guillouet, S.E. and Sinskey, A. (2015) Kinetic and stoichiometric characterization of organoautotrophic growth of *Ralstonia eutropha* on formic acid in fed-batch and continuous cultures. Microb. Biotechnol. **8**: 155-163.

Gunasekar, G.H., Park, K., Jung, K.D. and Yoon, S. (2016) Recent developments in the catalytic hydrogenation of CO_2 to formic acid/formate using heterogeneous catalysts. Inorg. Chem. Front. **3**: 882-895.

Hammerschmidt, A., Boukis, N., Hauer, E., Galla, U., Dinjus, E., Hitzmann, B., Larsen, T. and Nygaard, S.D. (2011) Catalytic conversion of waste biomass by hydrothermal treatment. Fuel **90**: 555-562.

Hansen, J., Sato, M., Ruedy, R., Kharecha, P., Lacis, A., Miller, R., Nazarenko, L., Lo, K., Schmidt, G.A., Russell, G., Aleinov, I., Bauer, S., Baum, E., Cairns, B., Canuto, V., Chandler, M., Cheng, Y., Cohen, A., Del Genio, A., Faluvegi, G., Fleming, E., Friend, A., Hall, T., Jackman, C., Jonas, J., Kelley, M., Kiang, N.Y., Koch, D., Labow, G., Lerner, J., Menon, S., Novakov, T., Oinas, V., Perlwitz, J., Perlwitz, J., Rind, D., Romanou, A., Schmunk, R., Shindell, D., Stone, P., Sun, S., Streets, D., Tausnev, N., Thresher, D., Unger, N., Yao, M. and Zhang, S. (2007) Dangerous human-made interference with climate: a GISS modelE study. Atmos. Chem. Phys. **7**: 2287-2312.

Hedderich, R. and Forzi, L. (2005) Energy-converting [NiFe] hydrogenases: more than just H_2 activation. J. Mol. Microbiol. Biotechnol. **10**: 92-104.

Heise, R., Müller, V. and Gottschalk, G. (1989) Sodium dependence of acetate formation by the acetogenic bacterium *Acetobacterium woodii*. J. Bacteriol. **171**: 5473-5478.

Heise, R., Müller, V. and Gottschalk, G. (1992) Presence of a sodium-translocating ATPase in membrane vesicles of the homoacetogenic bacterium *Acetobacterium woodii*. Eur. J. Biochem. **206**: 553-557.

Henstra, A.M., Dijkema, C. and Stams, A.J. (2007a) *Archaeoglobus fulgidus* couples CO oxidation to sulfate reduction and acetogenesis with transient formate accumulation. Environ. Microbiol. **9**: 1836-1841.

Henstra, A.M., Sipma, J., Rinzema, A. and Stams, A.J. (2007b) Microbiology of synthesis gas fermentation for biofuel production. Curr. Opin. Biotechnol. **18**: 200-206.

Herter, S., Fuchs, G., Bacher, A. and Eisenreich, W. (2002) A bicyclic autotrophic CO_2 fixation pathway in *Chloroflexus aurantiacus*. J. Biol. Chem. **277**: 20277-20283.

Hess, V., Schuchmann, K. and Müller, V. (2013) The ferredoxin:NAD^+ oxidoreductase (Rnf) from the acetogen *Acetobacterium woodii* requires Na^+ and is reversibly coupled to the membrane potential. J. Biol. Chem. **288**: 31496-31502.

Hess, V., Poehlein, A., Weghoff, M.C., Daniel, R. and Müller, V. (2014) A genome-guided analysis of energy conservation in the thermophilic, cytochrome-free acetogenic bacterium *Thermoanaerobacter kivui*. BMC Genomics **15**: 1139.

Himes, R.H. and Harmony, J.A. (1973) Formyltetrahydrofolate synthetase. CRC Crit. Rev. Biochem. **1**: 501-535.

Holladay, J.D., Hu, J., King, D.L. and Wang, Y. (2009) An overview of hydrogen production technologies. Catal. Today **139**: 244-260.

Holo, H. (1989) *Chloroflexus aurantiacus* secretes 3-hydroxypropionate, a possible intermediate in the assimilation of CO_2 and acetate. Arch. Microbiol. **151**: 252-256.

Houghton, J.T., Meira Filho, L.G., Callander, B.A., Harris, N., Kattenberg, A. and Maskell, K. (1996) *Climate change 1995: The science of climate change*. Cambridge: Cambridge Univ. Press.

Hu, P., Chakraborty, S., Kumar, A., Woolston, B., Liu, H., Emerson, D. and Stephanopoulos, G. (2016) Integrated bioprocess for conversion of gaseous substrates to liquids. Proc. Natl. Acad. Sci. U.S.A. **113**: 3773-3778.

Hu, S.I., Pezacka, E. and Wood, H.G. (1984) Acetate synthesis from carbon monoxide by *Clostridium thermoaceticum*. Purification of the corrinoid protein. J. Biol. Chem. **259**: 8892-8897.

Huang, H., Wang, S., Moll, J. and Thauer, R.K. (2012) Electron bifurcation involved in the energy metabolism of the acetogenic bacterium *Moorella thermoacetica* growing on glucose or H_2 plus CO_2. J. Bacteriol. **194**: 3689-3699.

Hugenholtz, J. and Ljungdahl, L.G. (1990) Metabolism and energy generation in homoacetogenic clostridia. FEMS Microbiol. Rev. **87**: 383-389.

Hugenholtz, J., Ivey, D.M. and Ljungdahl, L.G. (1987) Carbon monoxide-driven electron transport in *Clostridium thermoautotrophicum* membranes. J. Bacteriol. **169**: 5845-5847.

Hurst, K.M. and Lewis, R.S. (2010) Carbon monoxide partial pressure effects on the metabolic process of syngas fermentation. Biochem. Eng. J. **48**: 159-165.

Hwang, H., Yeon, Y.J., Lee, S., Choe, H., Jang, M.G., Cho, D.H., Park, S. and Kim, Y.H. (2015) Electro-biocatalytic production of formate from carbon dioxide using an oxygen-stable whole cell biocatalyst. Bioresour. Technol. **185**: 35-39.

Hwang, H.W., Yoon, J., Min, K., Kim, M.-S., Kim, S.-J., Cho, D.H., Susila, H., Na, J.-G., Oh, M.-K. and Kim, Y.H. (2020) Two-stage bioconversion of carbon monoxide to biopolymers *via* formate as an intermediate. Chem. Eng. J. **389**: 124394.

Jeong, J., Bertsch, J., Hess, V., Choi, S., Choi, I.G., Chang, I.S. and Müller, V. (2015) Energy conservation model based on genomic and experimental analyses of a carbon monoxide-utilizing, butyrate-forming acetogen, *Eubacterium limosum* KIST612. Appl. Environ. Microbiol. **81**: 4782-4790.

Jessop, P.G., Joo, F. and Tai, C.C. (2004) Recent advances in the homogeneous hydrogenation of carbon dioxide. Coord. Chem. Rev. **248**: 2425-2442.

Jones, J.B. and Stadtman, T.C. (1981) Selenium-dependent and selenium-independent formate dehydrogenases of *Methanococcus vannielii* - Separation of the 2 forms and characterization of the purified selenium-independent form. J. Biol. Chem. **256**: 656-663.

Jones, S.W., Fast, A.G., Carlson, E.D., Wiedel, C.A., Au, J., Antoniewicz, M.R., Papoutsakis, E.T. and Tracy, B.P. (2016) CO_2 fixation by anaerobic non-photosynthetic mixotrophy for improved carbon conversion. Nat. Commun. **7**: 12800.

Jung, H.C., Lee, S.H., Lee, S.M., An, Y.J., Lee, J.H., Lee, H.S. and Kang, S.G. (2017) Adaptive evolution of a hyperthermophilic archaeon pinpoints a formate transporter as a critical factor for the growth enhancement on formate. Sci. Rep. **7**: 6124.

Kantzow, C. and Weuster-Botz, D. (2016) Effects of hydrogen partial pressure on autotrophic growth and product formation of *Acetobacterium woodii*. Bioprocess Biosyst. Eng. **39**: 1325-1330.

Kantzow, C., Mayer, A. and Weuster-Botz, D. (2015) Continuous gas fermentation by *Acetobacterium woodii* in a submerged membrane reactor with full cell retention. J. Biotechnol. **212**: 11-18.

Katsyv, A. and Müller, V. (2020) Overcoming energetic barriers in acetogenic C1 conversion. Front. Bioeng. Biotechnol. **8**: 621166.

Kerby, R., Niemczura, W. and Zeikus, J.G. (1983) Single-carbon catabolism in acetogens: Analysis of carbon flow in *Acetobacterium woodii* and *Butyribacterium methylotrophicum* by fermentation and ^{13}C nuclear magnetic resonance measurement. J. Bacteriol. **155**: 1208-1218.

Kim, S.J., Yoon, J., Im, D.K., Kim, Y.H. and Oh, M.K. (2019) Adaptively evolved *Escherichia coli* for improved ability of formate utilization as a carbon source in sugar-free conditions. Biotechnol. Biofuels **12**: 207.

Kim, Y.J., Lee, H.S., Kim, E.S., Bae, S.S., Lim, J.K., Matsumi, R., Lebedinsky, A.V., Sokolova, T.G., Kozhevnikova, D.A., Cha, S.S., Kim, S.J., Kwon, K.K., Imanaka, T., Atomi, H., Bonch-Osmolovskaya, E.A., Lee, J.H. and Kang, S.G. (2010) Formate-driven growth coupled with H_2 production. Nature **467**: 352-355.

Klankermayer, J., Wesselbaum, S., Beydoun, K. and Leitner, W. (2016) Selective catalytic synthesis using the combination of carbon dioxide and hydrogen: Catalytic chess at the interface of energy and chemistry. Angew. Chem. Int. Ed. Engl. **55**: 7296-7343.

Klibanov, A.M., Alberti, B.N. and Zale, S.E. (1982) Enzymatic synthesis of formic acid from H_2 and CO_2 and production of hydrogen from formic acid. Biotechnol. Bioeng. **24**: 25-36.

Köpke, M. and Simpson, S.D. (2020) Pollution to products: recycling of 'above ground' carbon by gas fermentation. Curr. Opin. Biotechnol. **65**: 180-189.

Köpke, M., Mihalcea, C., Bromley, J.C. and Simpson, S.D. (2011a) Fermentative production of ethanol from carbon monoxide. Curr. Opin. Biotechnol. **22**: 320-325.

Köpke, M., Mihalcea, C., Liew, F., Tizard, J.H., Ali, M.S., Conolly, J.J., Al-Sinawi, B. and Simpson, S.D. (2011b) 2,3-butanediol production by acetogenic bacteria, an alternative route to chemical synthesis, using industrial waste gas. Appl. Environ. Microbiol. **77**: 5467-5475.

Köpke, M., Held, C., Hujer, S., Liesegang, H., Wiezer, A., Wollherr, A., Ehrenreich, A., Liebl, W., Gottschalk, G. and Dürre, P. (2010) *Clostridium ljungdahlii* represents a microbial production platform based on syngas. Proc. Natl. Acad. Sci. U.S.A. **107**: 13087-13092.

Kottenhahn, P., Schuchmann, K. and Müller, V. (2018) Efficient whole cell biocatalyst for formate-based hydrogen production. Biotechnol. Biofuels **11**: 93.

Kremp, F., Poehlein, A., Daniel, R. and Müller, V. (2018) Methanol metabolism in the acetogenic bacterium *Acetobacterium woodii*. Environ. Microbiol. **20**: 4369–4384.

Kucharska, K., Rybarczyk, P., Holowacz, I., Lukajtis, R., Glinka, M. and Kaminski, M. (2018) Pretreatment of lignocellulosic materials as substrates for fermentation processes. Molecules **23**: 2937.

Kumar, M., Sundaram, S., Gnansounou, E., Larroche, C. and Thakur, I.S. (2018) Carbon dioxide capture, storage and production of biofuel and biomaterials by bacteria: A review. Bioresour. Technol. **247**: 1059-1068.

Latif, H., Zeidan, A.A., Nielsen, A.T. and Zengler, K. (2014) Trash to treasure: production of biofuels and commodity chemicals *via* syngas fermenting microorganisms. Curr. Opin. Biotechnol. **27**: 79-87.

Le, Q.A.T., Kim, H.G. and Kim, Y.H. (2018) Electrochemical synthesis of formic acid from CO_2 catalyzed by *Shewanella oneidensis* MR-1 whole-cell biocatalyst. Enzyme. Microb. Technol. **116**: 1-5.

Leang, C., Ueki, T., Nevin, K.P. and Lovley, D.R. (2013) A genetic system for *Clostridium ljungdahlii*: a chassis for autotrophic production of biocommodities and a model homoacetogen. Appl. Environ. Microbiol. **79**: 1102-1109.

Lechtenfeld, M., Heine, J., Sameith, J., Kremp, F. and Müller, V. (2018) Glycine betaine metabolism in the acetogenic bacterium *Acetobacterium woodii*. Environ. Microbiol. **20**: 4512-4525

Lemon, B.J. and Peters, J.W. (1999) Binding of exogenously added carbon monoxide at the active site of the iron-only hydrogenase (CpI) from *Clostridium pasteurianum*. Biochemistry **38**: 12969-12973.

Leo, F., Schwarz, F.M., Schuchmann, K. and Müller, V. (2021) Capture of carbon dioxide and hydrogen by engineered *Escherichia coli*: hydrogen-dependent CO_2 reduction to formate. Appl. Microbiol. Biotechnol. **105**: 5861-5872.

Leung, D.Y.C., Caramanna, G. and Maroto-Valer, M.M. (2014) An overview of current status of carbon dioxide capture and storage technologies. Renew. Sust. Energ. Rev. **39**: 426-443.

Li, H., Opgenorth, P.H., Wernick, D.G., Rogers, S., Wu, T.Y., Higashide, W., Malati, P., Huo, Y.X., Cho, K.M. and Liao, J.C. (2012) Integrated electromicrobial conversion of CO_2 to higher alcohols. Science **335**: 1596.

Liew, F., Henstra, A.M., Winzer, K., Köpke, M., Simpson, S.D. and Minton, N.P. (2016a) Insights into CO_2 fixation pathway of *Clostridium autoethanogenum* by targeted mutagenesis. mBio **7**: e00427-00416.

Liew, F., Martin, M.E., Tappel, R.C., Heijstra, B.D., Mihalcea, C. and Köpke, M. (2016b) Gas fermentation-a flexible platform for commercial scale production of low-carbon-fuels and chemicals from waste and renewable feedstocks. Front. Microbiol. **7**: 694.

Lim, J.K., Mayer, F., Kang, S.G. and Müller, V. (2014) Energy conservation by oxidation of formate to carbon dioxide and hydrogen *via* a sodium ion current in a hyperthermophilic archaeon. Proc. Natl. Acad. Sci. U.S.A. **111**: 11497-11502.

Lin, B. and Tao, Y. (2017) Whole-cell biocatalysts by design. Microb. Cell Fact. **16**: 106.

Liou, J.S., Balkwill, D.L., Drake, G.R. and Tanner, R.S. (2005) *Clostridium carboxidivorans* sp. nov., a solvent-producing Clostridium isolated from an agricultural settling lagoon, and reclassification of the acetogen *Clostridium scatologenes* strain SL1 as *Clostridium drakei* sp. nov. Int. J. Syst. Evol. Microbiol. **55**: 2085-2091.

Ljungdahl, L.G. (1986) The autotrophic pathway of acetate synthesis in acetogenic bacteria. Ann. Rev. Microbiol. **40**: 415-450.

Ljungdahl, L.G. (1994) The acetyl-CoA pathway and the chemiosmotic generation of ATP during acetogenesis. In *Acetogenesis*. Drake, H.L. (ed). New York: Chapman & Hall, pp. 63-87.

Loges, B., Boddien, A., Gärtner, F., Junge, H. and Beller, M. (2010) Catalytic generation of hydrogen from formic acid and its derivatives: Useful hydrogen storage materials. Top.Catal. **53**: 902-914.

Lorowitz, W.H. and Bryant, M.P. (1984) *Peptostreptococcus productus* strain that grows rapidly with CO as the energy source. Appl. Environ. Microbiol. **47**: 961-964.

Lubitz, W., Ogata, H., Rüdiger, O. and Reijerse, E. (2014) Hydrogenases. Chem. Rev. **114**: 4081-4148.

Lynd, L.H., Kerby, R. and Zeikus, J.G. (1982) Carbon monoxide metabolism of the methylotrophic acidogen *Butyribacterium methylotrophicum*. J. Bacteriol. **149**: 255-263.

MacKenzie, R.M. (1984) Biogenesis and interconversion of substituted tetrahydrofolates. In *Folates and pterins*. Blakley, R.L., and Benkovic, S.J. (eds). New York: John Wiley and Sons, Inc., pp. 256-306.

Maddipati, P., Atiyeh, H.K., Bellmer, D.D. and Huhnke, R.L. (2011) Ethanol production from syngas by *Clostridium* strain P11 using corn steep liquor as a nutrient replacement to yeast extract. Bioresour. Technol. **102**: 6494-6501.

Maia, L.B., Moura, J.J. and Moura, I. (2015) Molybdenum and tungsten-dependent formate dehydrogenases. J. Biol. Inorg. Chem. **20**: 287-309.

Maia, L.B., Moura, I. and Moura, J.J.G. (2017) Molybdenum and tungsten-containing formate dehydrogenases: Aiming to inspire a catalyst for carbon dioxide utilization. Inorg. Chim. Acta **455**: 350-363.

Martin, W. and Russell, M.J. (2007) On the origin of biochemistry at an alkaline hydrothermal vent. Philos. Trans. R. Soc. Lond. B. Biol. Sci. **362**: 1887-1925.

Martin, W.F., Sousa, F.L. and Lane, N. (2014) Evolution. Energy at life's origin. Science **344**: 1092-1093.

Martins, M., Mourato, C. and Pereira, I.A. (2015) *Desulfovibrio vulgaris* growth coupled to formate-driven H_2 production. Environ. Sci. Technol. **49**: 14655-14662.

Matthies, D., Zhou, W., Klyszejko, A.L., Anselmi, C., Yildiz, O., Brandt, K., Müller, V., Faraldo-Gomez, J.D. and Meier, T. (2014) High-resolution structure and mechanism of an F/V-hybrid rotor ring in a Na^+-coupled ATP synthase. Nat. Commun. **5**: 5286.

Mayer, A., Schädler, T., Trunz, S., Stelzer, T. and Weuster-Botz, D. (2018) Carbon monoxide conversion with *Clostridium aceticum*. Biotechnol. Bioeng. **115**: 2740-2750.

Mayer, F., Lim, J.K., Langer, J.D., Kang, S.G. and Müller, V. (2015) Na^+ transport by the A_1A_O-ATP synthase purified from *Thermococcus onnurineus* and reconstituted into liposomes. J. Biol. Chem. **290**: 6994-7002.

Maynard, E.L. and Lindahl, P.A. (1999) Evidence of a molecular tunnel connecting the active sites for CO_2 reduction and acetyl-CoA synthesis in acetyl-CoA synthase from *Clostridium thermoaceticum*. J. Am. Chem. Soc. **121**: 9221-9222.

McDowall, J.S., Murphy, B.J., Haumann, M., Palmer, T., Armstrong, F.A. and Sargent, F. (2014) Bacterial formate hydrogenlyase complex. Proc. Natl. Acad. Sci. U.S.A. **111**: E3948-E3956.

Mebs, S., Kositzki, R., Duan, J., Kertess, L., Senger, M., Wittkamp, F., Apfel, U.P., Happe, T., Stripp, S.T., Winkler, M. and Haumann, M. (2018) Hydrogen and oxygen trapping at the H-cluster of [FeFe]-hydrogenase revealed by site-selective spectroscopy and QM/MM calculations. Biochim. Biophys. Acta Bioenerg. **1859**: 28-41.

Meier, T., Ferguson, S.A., Cook, G.M., Dimroth, P. and Vonck, J. (2006) Structural investigations of the membrane-embedded rotor ring of the F-ATPase from *Clostridium paradoxum*. J. Bacteriol. **188**: 7759-7764.

Meier, T., Krah, A., Bond, P.J., Pogoryelov, D., Diederichs, K. and Faraldo-Gómez, J.D. (2009) Complete ion-coordination structure in the rotor ring of Na^+-dependent F-ATP synthases. J. Mol. Biol. **391**: 498-507.

Meinshausen, M., Meinshausen, N., Hare, W., Raper, S.C., Frieler, K., Knutti, R., Frame, D.J. and Allen, M.R. (2009) Greenhouse-gas emission targets for limiting global warming to 2 °C. Nature **458**: 1158-1162.

Melillo, J.M., Reilly, J.M., Kicklighter, D.W., Gurgel, A.C., Cronin, T.W., Paltsev, S., Felzer, B.S., Wang, X., Sokolov, A.P. and Schlosser, C.A. (2009) Indirect emissions from biofuels: how important? Science **326**: 1397-1399.

Mellmann, D., Sponholz, P., Junge, H. and Beller, M. (2016) Formic acid as a hydrogen storage material - development of homogeneous catalysts for selective hydrogen release. Chem. Soc. Rev. **45**: 3954-3988.

Meyer, O. and Schlegel, H.G. (1983) Biology of aerobic carbon monoxide-oxidizing bacteria. Annu. Rev. Microbiol. **37**: 277-310.

Mock, J., Wang, S., Huang, H., Kahnt, J. and Thauer, R.K. (2014) Evidence for a hexaheteromeric methylenetetrahydrofolate reductase in *Moorella thermoacetica*. J. Bacteriol. **196**: 3303-3314.

Molino, A., Larocca, V., Chianese, S. and Musmarra, D. (2018) Biofuels production by biomass gasification: A review. Energies **11**: 811.

Montet, Y., Amara, P., Volbeda, A., Vernede, X., Hatchikian, E.C., Field, M.J., Frey, M. and FontecillaCamps, J.C. (1997) Gas access to the active site of Ni-Fe hydrogenases probed by X-ray crystallography and molecular dynamics. Nat. Struct. Biol. **4**: 523-526.

Moon, J., Dönig, J., Kramer, S., Poehlein, A., Daniel, R. and Müller, V. (2021) Formate metabolism in the acetogenic bacterium *Acetobacterium woodii*. Environ. Microbiol. **23**: 4214-4227

Moon, M., Park, G.W., Lee, J.P., Lee, J.S. and Min, K. (2020) Recent progress in formate dehydrogenase (FDH) as a non-photosynthetic CO_2 utilizing enzyme: A short review. J. CO2 Util. **42**: 101353.

Moore, M.R., O'Brien, W.E. and Ljungdahl, L.G. (1974) Purification and characterization of nicotinamide adenine dinucleotide-dependent methylenetetrahydrofolate dehydrogenase from *Clostridium formicoaceticum*. J. Biol. Chem. **249**: 5250-5253.

Morinaga, T. and Kawada, N. (1990) The production of acetic acid from carbon dioxide and hydrogen by an anaerobic bacterium. J. Biotechnol. **14**: 187-194.

Morris, B.E., Henneberger, R., Huber, H. and Moissl-Eichinger, C. (2013) Microbial syntrophy: interaction for the common good. FEMS Microbiol. Rev. **37**: 384-406.

Mourato, C., Martins, M., da Silva, S.M. and Pereira, I.A.C. (2017) A continuous system for biocatalytic hydrogenation of CO_2 to formate. Bioresour. Technol. **235**: 149-156.

Müller, V. (2003) Energy conservation in acetogenic bacteria. Appl. Environ. Microbiol. **69**: 6345-6353.

Müller, V. (2019) New horizons in acetogenic conversion of one-carbon substrates and biological hydrogen storage. Trends Biotechnol. **37**: 1344-1354.

Müller, V., Aufurth, S. and Rahlfs, S. (2001) The Na^+ cycle in *Acetobacterium woodii*: identification and characterization of a Na^+-translocating F_1F_O-ATPase with a mixed oligomer of 8 and 16 kDa proteolipids. Biochim. Biophys. Acta **1505**: 108-120.

Müller, V., Chowdhury, N.P. and Basen, M. (2018) Electron bifurcation: A long-hidden energy-coupling mechanism. Annu. Rev. Microbiol. **72**: 331-353.

Murphy, R., Woods, J., Black, M. and McManus, M. (2011) Global developments in the competition for land from biofuels. Food Policy **36**: 52-61.

Naik, S.N., Goud, V.V., Rout, P.K. and Dalai, A.K. (2010) Production of first and second generation biofuels: A comprehensive review. Renew. Sust. Energ. Rev. **14**: 578-597.

Najafpour, G.D. and Younesi, H. (2006) Ethanol and acetate synthesis from waste gas using batch culture of *Clostridium ljungdahlii*. Enzyme Microb. Technol. **38**: 223-228.

National Academy of Sciences, National Academy of Engineering, and National Research Council (2009) *Liquid transportation fuels from coal and biomass: Technological status, costs, and environmental impacts*. Washington, DC: The National Academies Press.

Naylor, R.L., Liska, A.J., Burke, M.B., Falcon, W.P., Gaskell, J.C., Rozelle, S.D. and Cassman, K.G. (2007) The ripple effect: Biofuels, food security, and the environment. Environ. Sci. Policy Sustain. Dev. **49**: 30-43.

Neuendorf, C.S., Vignolle, G.A., Derntl, C., Tomin, T., Novak, K., Mach, R.L., Birner-Grunberger, R. and Pflugl, S. (2021) A quantitative metabolic analysis reveals *Acetobacterium woodii* as a flexible and robust host for formate-based bioproduction. Metab. Eng. **68**: 68-85.

Nicholls, P. (1975) Formate as an inhibitor of cytochrome c oxidase. Biochem. Biophys. Res. Commun. **67**: 610-616.

Novak, K., Neuendorf, C.S., Kofler, I., Kieberger, N., Klamt, S. and Pflügl S. (2021) Blending industrial blast furnace gas with H_2 enables *Acetobacterium woodii* to efficiently co-utilize CO, CO_2 and H_2. Bioresour. Technol. **323**: 124573

O'Brien, J.M., Wolkin, R.H., Moench, T.T., Morgan, J.B. and Zeikus, J.G. (1984) Association of hydrogen metabolism with unitrophic or mixotrophic growth of *Methanosarcina barkeri* on carbon monoxide. J. Bacteriol. **158**: 373-375.

Oehler, D., Poehlein, A., Leimbach, A., Müller, N., Daniel, R., Gottschalk, G. and Schink, B. (2012) Genome-guided analysis of physiological and morphological traits of the fermentative acetate oxidizer *Thermacetogenium phaeum*. BMC Genomics **13**: 723.

Olah, G.A., Goeppert, A. and Prakash, G.K. (2009) Chemical recycling of carbon dioxide to methanol and dimethyl ether: from greenhouse gas to renewable, environmentally carbon neutral fuels and synthetic hydrocarbons. J. Org. Chem. **74**: 487-498.

Ostapowicz, T.G., Schmitz, M., Krystof, M., Klankermayer, J. and Leitner, W. (2013) Carbon dioxide as a C_1 building block for the formation of carboxylic acids by formal catalytic hydrocarboxylation. Angew. Chem. Int. Ed. Engl. **52**: 12119-12123.

Oswald, F., Stoll, I.K., Zwick, M., Herbig, S., Sauer, J., Boukis, N. and Neumann, A. (2018) Formic acid formation by *Clostridium ljungdahlii* at elevated pressures of carbon dioxide and hydrogen. Front. Bioeng. Biotechnol. **6**: 6.

Padella, M., O'Connell, A. and Prussi, M. (2019) What is still limiting the deployment of cellulosic ethanol? Analysis of the current status of the sector. Appl. Sci. **9**: 4523.

Pala, U., Yelmazer, B., Corbacioglu, M., Ruupunen, J., Valjakka, J., Turunen, O. and Binay, B. (2018) Functional effects of active site mutations in NAD^+-dependent formate dehydrogenases on transformation of hydrogen carbonate to formate. Protein Eng. Des. Sel. **31**: 327-335.

Pappenreiter, P.A., Zwirtmayr, S., Mauerhofer, L.M., Rittmann, S.K.R. and Paulik, C. (2019) Development of a simultaneous bioreactor system for characterization of gas production kinetics of methanogenic archaea at high pressure. Eng. Life Sci. **19**: 537-544.

Park, C.K. and Horton, N.C. (2019) Structures, functions, and mechanisms of filament forming enzymes: a renaissance of enzyme filamentation. Biophys. Rev. **11**: 927-994.

Pearson, P.N. and Palmer, M.R. (2000) Atmospheric carbon dioxide concentrations over the past 60 million years. Nature **406**: 695-699.

Peters, V., Janssen, P.H. and Conrad, R. (1999) Transient production of formate during chemolithotrophic growth of anaerobic microorganisms on hydrogen. Curr. Microbiol. **38**: 285-289.

Pezacka, E. and Wood, H.G. (1984a) Role of carbon monoxide dehydrogenase in the autotrophic pathway used by acetogenic bacteria. Proc. Natl. Acad. Sci. U.S.A. **81**: 6261-6265.

Pezacka, E. and Wood, H.G. (1984b) The synthesis of acetyl-CoA by *Clostridium thermoaceticum* from carbon dioxide, hydrogen, coenzyme A and methyltetrahydrofolate. Arch. Microbiol. **137**: 63-69.

Pierce, E., Xie, G., Barabote, R.D., Saunders, E., Han, C.S., Detter, J.C., Richardson, P., Brettin, T.S., Das, A., Ljungdahl, L.G. and Ragsdale, S.W. (2008) The complete genome sequence of *Moorella thermoacetica* (f. *Clostridium thermoaceticum*). Environ. Microbiol. **10**: 2550-2573.

Pinske, C. and Sargent, F. (2016) Exploring the directionality of *Escherichia coli* formate hydrogenlyase: a membrane-bound enzyme capable of fixing carbon dioxide to organic acid. Microbiologyopen **5**: 721-737.

Poehlein, A., Schmidt, S., Kaster, A.-K., Goenrich, M., Vollmers, J., Thürmer, A., Bertsch, J., Schuchmann, K., Voigt, B., Hecker, M., Daniel, R., Thauer, R.K., Gottschalk, G. and Müller, V. (2012) An ancient pathway combining carbon dioxide fixation with the generation and utilization of a sodium ion gradient for ATP synthesis. PLoS One **7**: e33439.

Preuster, P., Alekseev, A. and Wasserscheid, P. (2017a) Hydrogen storage technologies for future energy systems. Annu. Rev. Chem. Biomol. Eng. **8**: 445-471.

Preuster, P., Papp, C. and Wasserscheid, P. (2017b) Liquid organic hydrogen carriers (LOHCs): Toward a hydrogen-free hydrogen economy. Acc. Chem. Res. **50**: 74-85.

Ragsdale, S.W. (1991) Enzymology of the acetyl-CoA pathway of autotrophic CO_2 fixation. Crit. Rev. Biochem. Mol. Biol. **26**: 261-300.

Ragsdale, S.W. (2003) Pyruvate ferredoxin oxidoreductase and its radical intermediate. Chem. Rev. **103**: 2333-2346.

Ragsdale, S.W. (2004) Life with carbon monoxide. Crit. Rev. Biochem. Mol. Biol. **39**: 165-195

Ragsdale, S.W. (2008) Enzymology of the Wood-Ljungdahl pathway of acetogenesis. Ann. N. Y. Acad. Sci. **1125**: 129-136.

Ragsdale, S.W. and Ljungdahl, L.G. (1984) Purification and properties of NAD-dependent 5,10-methylenetetrahydrofolate dehydrogenase from *Acetobacterium woodii*. J. Biol. Chem. **259**: 3499-3503.

Ragsdale, S.W. and Wood, H.G. (1985) Acetate biosynthesis by acetogenic bacteria. Evidence that carbon monoxide dehydrogenase is the condensing enzyme that catalyzes the final steps in the synthesis. J. Biol. Chem. **260**: 3970-3977.

Ragsdale, S.W. and Pierce, E. (2008) Acetogenesis and the Wood-Ljungdahl pathway of CO_2 fixation. Biochim. Biophys. Acta **1784**: 1873-1898.

Ragsdale, S.W., Ljungdahl, L.G. and DerVartanian, D.V. (1983a) Isolation of carbon monoxide dehydrogenase from *Acetobacterium woodii* and comparison of its properties with those of the *Clostridium thermoaceticum* enzyme. J. Bacteriol. **155**: 1224-1237.

Ragsdale, S.W., Lindahl, P.A. and Münck, E. (1987) Mössbauer, EPR, and optical studies of the corrinoid/iron-sulfur protein involved in the synthesis of acetyl-coenzyme A by *Clostridium thermoaceticum.* J. Biol. Chem. **26**: 1489-1497.

Ragsdale, S.W., Clark, J.E., Ljungdahl, L.G., Lundie, L.L. and Drake, H.L. (1983b) Properties of purified carbon monoxide dehydrogenase from *Clostridium thermoaceticum*, a nickel, iron-sulfur protein. J. Biol. Chem. **258**: 2364-2369.

Rahlfs, S., Aufurth, S. and Müller, V. (1999) The Na^+-F_1F_O-ATPase operon from *Acetobacterium woodii*. Operon structure and presence of multiple copies of *atpE* which encode proteolipids of 8- and 18-kDa. J. Biol. Chem. **274**: 33999-34004.

Ramanathan, V. and Feng, Y. (2008) On avoiding dangerous anthropogenic interference with the climate system: formidable challenges ahead. Proc. Natl. Acad. Sci. U.S.A. **105**: 14245-14250.

Reda, T., Plugge, C.M., Abram, N.J. and Hirst, J. (2008) Reversible interconversion of carbon dioxide and formate by an electroactive enzyme. Proc. Natl. Acad. Sci. U.S.A. **105**: 10654-10658.

Riegler, P., Bieringer, E., Chrusciel, T., Stärz, M., Löwe, H. and Weuster-Botz, D. (2019) Continuous conversion of CO_2/H_2 with *Clostridium aceticum* in biofilm reactors. Bioresour. Technol. **291**: 121760.

Rittmann, S. and Herwig, C. (2012) A comprehensive and quantitative review of dark fermentative biohydrogen production. Microb. Cell Fact. **11**: 115.

Robinson, W.E., Bassegoda, A., Reisner, E. and Hirst, J. (2017) Oxidation-state-dependent binding properties of the active site in a Mo-containing formate dehydrogenase. J. Am. Chem. Soc. **139**: 9927-9936.

Roger, M., Brown, F., Gabrielli, W. and Sargent, F. (2018) Efficient hydrogen-dependent carbon dioxide reduction by *Escherichia coli*. Curr. Biol. **28**: 140-145.

Rohmann, K., Kothe, J., Haenel, M.W., Englert, U., Hölscher, M. and Leitner, W. (2016) Hydrogenation of CO_2 to formic acid with a highly active ruthenium ccriphos complex in DMSO and DMSO/water. Angew. Chem. Int. Ed. Engl. **55**: 8966-8969.

Rokni, M. (2015) Thermodynamic analyses of municipal solid waste gasification plant integrated with solid oxide fuel cell and stirling hybrid system. Int. J. Hydrogen Energy **40**: 7855-7869.

Rosales-Colunga, L.M. and Rodriguez, A.D. (2015) *Escherichia coli* and its application to biohydrogen production. Rev. Environ. Sci. Biotechnol. **14**: 123-135.

Rossmann, R., Sawers, G. and Böck, A. (1991) Mechanism of regulation of the formate-hydrogenlyase pathway by oxygen, nitrate, and pH: definition of the formate regulon. Mol. Microbiol. **5**: 2807-2814.

Rother, M. and Metcalf, W.W. (2004) Anaerobic growth of *Methanosarcina acetivorans* C2A on carbon monoxide: an unusual way of life for a methanogenic archaeon. Proc. Natl. Acad. Sci. U.S.A. **101**: 16929-16934.

Ruth, J.C., Schwarz, F.M., Müller, V. and Spormann, A.M. (2021) Enzymatic hydrogen electrosynthesis at enhanced current density using a redox polymer. Catalysts **11**: 1197.

Sagong, H.Y., Son, H.F., Choi, S.Y., Lee, S.Y. and Kim, K.J. (2018) Structural insights into polyhydroxyalkanoates biosynthesis. Trends. Biochem. Sci. **43**: 790-805.

Sánchez-Andrea, I., Guedes, I.A., Hornung, B., Boeren, S., Lawson, C.E., Sousa, D.Z., Bar-Even, A., Claassens, N.J. and Stams, A.J.M. (2020) The reductive glycine pathway allows autotrophic growth of *Desulfovibrio desulfuricans*. Nat. Commun. **11**: 5090.

Sarmiento, J.L. and Gruber, N. (2002) Sinks for anthropogenic carbon. Phys. Today **55**: 30-36.

Sawers, R.G. (2005) Formate and its role in hydrogen production in *Escherichia coli*. Biochem. Soc. Trans. **33**: 42-46.

Schauder, R., Preuss, A., Jetten, M. and Fuchs, G. (1988) Oxidative and reductive acetyl-CoA carbon monoxide dehydrogenase pathway in *Desulfobacterium autotrophicum* Arch. Microbiol. **151**: 84-89.

Schaupp, A. and Ljungdahl, L.G. (1974) Purification and properties of acetate kinase from *Clostridium thermoaceticum*. Arch. Microbiol. **100**: 121-129.

Scherer, P.A. and Thauer, R.K. (1978) Purification and properties of reduced ferredoxin: CO_2 oxidoreductase from *Clostridium pasteurianum*, a molybdenum iron-sulfur-protein. Eur. J. Biochem. **85**: 125-135.

Schiel-Bengelsdorf, B. and Dürre, P. (2012) Pathway engineering and synthetic biology using acetogens. FEBS Lett. **586**: 2191-2198.

Schink, B. (2002) Synergistic interactions in the microbial world. Antonie van Leeuwenhoek **81**: 257-261.

Schlager, S., Dumitru, L.M., Haberbauer, M., Fuchsbauer, A., Neugebauer, H., Hiemetsberger, D., Wagner, A., Portenkirchner, E. and Sariciftci, N.S. (2016) Electrochemical reduction of carbon dioxide to methanol by direct injection of electrons into immobilized enzymes on a modified electrode. ChemSusChem. **9**: 631-635.

Schölmerich, M.C. and Müller, V. (2020) Energy-converting hydrogenases: The link between H_2 metabolism and energy conservation. Cell. Mol. Life Sci. **77**: 1461-1481.

Schölmerich, M.C. and Müller, V. (2019) Energy conservation by a hydrogenase-dependent chemiosmotic mechanism in an ancient metabolic pathway. Proc. Natl. Acad. Sci. U.S.A. **116**: 6329-6334.

Schön, G. and Voelskow, H. (1976) Pyruvate fermentation in *Rhodospirillum rubrum* and after transfer from aerobic to anaerobic conditions in the dark. Arch. Microbiol. **107**: 87-92.

Schuchmann, K. and Müller, V. (2012) A bacterial electron bifurcating hydrogenase. J. Biol. Chem. **287**: 31165–31171.

Schuchmann, K. and Müller, V. (2013) Direct and reversible hydrogenation of CO_2 to formate by a bacterial carbon dioxide reductase. Science **342**: 1382-1385.

Schuchmann, K. and Müller, V. (2014) Autotrophy at the thermodynamic limit of life: A model for energy conservation in acetogenic bacteria. Nat. Rev. Microbiol. **12**: 809-821.

Schuchmann, K. and Müller, V. (2016) Energetics and application of heterotrophy in acetogenic bacteria. Appl. Environ. Microbiol. **82**: 4056-4069.

Schuchmann, K., Vonck, J. and Müller, V. (2016) A bacterial hydrogen-dependent CO_2 reductase forms filamentous structures. FEBS J. **283**: 1311-1322.

Schuchmann, K., Schmidt, S., Martinez Lopez, A., Kaberline, C., Kuhns, M., Lorenzen, W., Bode, H.B., Joos, F. and Müller, V. (2015) Nonacetogenic growth of the acetogen *Acetobacterium woodii* on 1,2-propanediol. J. Bacteriol. **197**: 382-391.

Schut, G.J. and Adams, M.W. (2009) The iron-hydrogenase of *Thermotoga maritima* utilizes ferredoxin and NADH synergistically: a new perspective on anaerobic hydrogen production. J. Bacteriol. **191**: 4451-4457.

Schwarz, F.M. and Müller, V. (2020) Whole-cell biocatalysis for hydrogen storage and syngas conversion to formate using a thermophilic acetogen. Biotechnol. Biofuels **13**: 32.

Schwarz, F.M., Schuchmann, K. and Müller, V. (2018) Hydrogenation of CO_2 at ambient pressure catalyzed by a highly active thermostable biocatalyst. Biotechnol. Biofuels **11**: 237.

Schwarz, F.M., Oswald, F. and Müller, V. (2021) Acetogenic conversion of H_2 and CO_2 into formic acid and *vice versa* in a fed-batch-operated stirred-tank bioreactor. ACS Sustain. Chem. Eng. **9**: 6810-6820.

Schwarz, F.M., Ciurus, S., Jain, S., Baum, C., Wiechmann, A., Basen, M. and Müller, V. (2020) Revealing formate production from carbon monoxide in wild type and mutants of Rnf- and Ech-containing acetogens, *Acetobacterium woodii* and *Thermoanaerobacter kivui*. Microb. Biotechnol. **13**: 2044-2056.

Seravalli, J. and Ragsdale, S.W. (2000) Channeling of carbon monoxide during anaerobic carbon dioxide fixation. Biochemistry **39**: 1274-1277.

Seravalli, J., Kumar, M., Lu, W.P. and Ragsdale, S.W. (1997) Mechanism of carbon monoxide oxidation by the carbon monoxide dehydrogenase/acetyl-CoA synthase from *Clostridium thermoaceticum*: Kinetic characterization of the intermediates. Biochemistry **36**: 11241-11251.

Sinha, P. and Pandey, A. (2011) An evaluative report and challenges for fermentative biohydrogen production. Int. J. Hydrog. Energy **36**: 7460-7478.

Sipma, J., Henstra, A.M., Parshina, S.M., Lens, P.N., Lettinga, G. and Stams, A.J. (2006) Microbial CO conversions with applications in synthesis gas purification and bio-desulfurization. Crit. Rev. Biotechnol. **26**: 41-65.

Smith, E.T. and Feinberg, B.A. (1990) Redox properties of several bacterial ferredoxins using square-wave voltammetry. J. Biol. Chem. **265**: 14371-14376.

Smith, E.T., Bennett, D.W. and Feinberg, B.A. (1991) Redox properties of 2[4Fe-4S] ferredoxins. Anal. Chim. Acta **251**: 27-33.

Soboh, B., Linder, D. and Hedderich, R. (2002) Purification and catalytic properties of a CO-oxidizing:H_2-evolving enzyme complex from *Carboxydothermus hydrogenoformans*. Eur. J. Biochem. **269**: 5712-5721.

Solomon, S., Plattner, G.K., Knutti, R. and Friedlingstein, P. (2009) Irreversible climate change due to carbon dioxide emissions. Proc. Natl. Acad. Sci. U.S.A **106**: 1704-1709.

Sorokin, A.B., Kudrik, E.V., Alvarez, L.X., Afanasiev, P., Millet, J.M.M. and Bouchu, D. (2010) Oxidation of methane and ethylene in water at ambient conditions. Catal. Today **157**: 149-154.

Spormann, A.M. and Thauer, R.K. (1988) Anaerobic acetate oxidation to CO_2 by *Desulfotomaculum acetoxidans* - demonstration of enzymes required for the operation of an oxidative acetyl-CoA/carbon monoxide dehydrogenase pathway. Arch. Microbiol. **150**: 374-380.

Stephenson, M. and Stickland, L.H. (1931) Hydrogenase: a bacterial enzyme activating molecular hydrogen: The properties of the enzyme. Biochem. J. **25**: 205-214.

Stephenson, M. and Stickland, L.H. (1932) Hydrogenlyases: Bacterial enzymes liberating molecular hydrogen. Biochem. J. **26**: 712-724.

Steuber, J., Krebs, W., Bott, M. and Dimroth, P. (1999) A membrane-bound $NAD(P)^+$-reducing hydrogenase provides reduced pyridine nucleotides during citrate fermentation by *Klebsiella pneumoniae*. J. Bacteriol. **181**: 241-245.

Strätz, M., Sauer, U., Kuhn, A. and Dürre, P. (1994) Plasmid transfer into the homoacetogen *Acetobacterium woodii* by electroporation and conjugation. Appl. Environ. Microbiol. **60**: 1033-1037.

Straub, M., Demler, M., Weuster-Botz, D. and Dürre, P. (2014) Selective enhancement of autotrophic acetate production with genetically modified *Acetobacterium woodii*. J. Biotechnol. **178**: 67-72.

Stupperich, E., Hammel, K.E., Fuchs, G. and Thauer, R.K. (1983) Carbon monoxide fixation into the carboxyl group of acetyl coenzyme A during autotrophic growth of *Methanobacterium*. FEBS. Lett. **152**: 21-23.

Takors, R., Kopf, M., Mampel, J., Bluemke, W., Blombach, B., Eikmanns, B., Bengelsdorf, F.R., Weuster-Botz, D. and Dürre, P. (2018) Using gas mixtures of CO, CO_2 and H_2 as microbial substrates: the do's and don'ts of successful technology transfer from laboratory to production scale. Microb. Biotechnol. **11**: 606-625.

Tanner, R.S., Miller, L.M. and Yang, D. (1993) *Clostridium ljungdahlii* sp. nov., an acetogenic species in clostridial rRNA homology Group-I. Int. J. Syst. Bacteriol. **43**: 232-236.

Thamer, W., Cirpus, I., Hans, M., Pierik, A.J., Selmer, T., Bill, E., Linder, D. and Buckel, W. (2003) A two [4Fe-4S]-cluster-containing ferredoxin as an alternative electron donor for 2-hydroxyglutaryl-CoA dehydratase from *Acidaminococcus fermentans*. Arch. Microbiol. **179**: 197-204.

Thauer, R.K., Jungermann, K. and Decker, K. (1977) Energy conservation in chemotrophic anaerobic bacteria. Bacteriol. Rev. **41**: 100-180.

Thauer, R.K., Kaster, A.K., Seedorf, H., Buckel, W. and Hedderich, R. (2008) Methanogenic archaea: ecologically relevant differences in energy conservation. Nat. Rev. Microbiol. **6**: 579-591.

Tishkov, V.I. and Popov, V.O. (2006) Protein engineering of formate dehydrogenase. Biomol. Eng. **23**: 89-110.

Tishkov, V.I., Matorin, A.D., Rojkova, A.M., Fedorchuk, V.V., Savitsky, P.A., Dementieva, L.A., Lamzin, V.S., Mezentzev, A.V. and Popov, V.O. (1996) Site-directed mutagenesis of the formate dehydrogenase active centre: role of the His332-Gln313 pair in enzyme catalysis. FEBS Lett. **390**: 104-108.

Tracy, B.P., Jones, S.W., Fast, A.G., Indurthi, D.C. and Papoutsakis, E.T. (2012) Clostridia: the importance of their exceptional substrate and metabolite diversity for biofuel and biorefinery applications. Curr. Opin. Biotechnol. **23**: 364-381.

Trchounian, A. and Gary Sawers, R. (2014) Novel insights into the bioenergetics of mixed-acid fermentation: can hydrogen and proton cycles combine to help maintain a proton motive force. IUBMB Life **66**: 1-7.

Tremblay, P.L., Zhang, T., Dar, S.A., Leang, C. and Lovley, D.R. (2012) The Rnf complex of *Clostridium ljungdahlii* is a proton-translocating ferredoxin:NAD^+ oxidoreductase essential for autotrophic growth. MBio **4**: e00406-00412.

Tremel, A., Wasserscheid, P., Baldauf, M. and Hammer, T. (2015) Techno-economic analysis for the synthesis of liquid and gaseous fuels based on hydrogen production *via* electrolysis. Int. J. Hydrogen Energy **40**: 11457-11464.

Uyeda, K. and Rabinowitz, J.C. (1971) Pyruvate-ferredoxin oxidoreductase. 3. Purification and properties of the enzyme. J. Biol .Chem. **246**: 3111-3119.

van der Drift, A., van Doorn, J. and Vermeulen, J.W. (2001) Ten residual biomass fuels for circulating fluidized-bed gasification. Biomass Bioenergy **20**: 45-56.

Venkata Mohan, S., Modestra, J.A., Amulya, K., Butti, S.K. and Velvizhi, G. (2016) A circular bioeconomy with biobased products from CO_2 sequestration. Trends. Biotechnol. **34**: 506-519.

Vinals, C., Depiereux, E. and Feytmans, E. (1993) Prediction of structurally conserved regions of D-specific hydroxy acid dehydrogenases by multiple alignment with formate dehydrogenase. Biochem. Biophys. Res. Commun. **192**: 182-188.

Vincent, K.A., Cracknell, J.A., Lenz, O., Zebger, I., Friedrich, B. and Armstrong, F.A. (2005) Electrocatalytic hydrogen oxidation by an enzyme at high carbon monoxide or oxygen levels. Proc. Natl. Acad. Sci. U.S.A. **102**: 16951-16954.

Wächtershäuser, G. (2007) On the chemistry and evolution of the pioneer organism. Chem. Biodivers. **4**: 584-602.

Wang, S., Huang, H., Kahnt, J. and Thauer, R.K. (2013a) A reversible electron-bifurcating ferredoxin- and NAD-dependent [FeFe]-hydrogenase (HydABC) in *Moorella thermoacetica*. J. Bacteriol. **195**: 1267-1275.

Wang, S., Huang, H., Kahnt, J., Müller, A.P., Köpke, M. and Thauer, R.K. (2013b) NADP-specific electron-bifurcating [FeFe]-hydrogenase in a functional complex with formate dehydrogenase in *Clostridium autoethanogenum* grown on CO. J. Bacteriol. **195**: 4373-4386.

Wang, W.H., Himeda, Y., Muckerman, J.T., Manbeck, G.F. and Fujita, E. (2015) CO_2 hydrogenation to formate and methanol as an alternative to photo- and electrochemical CO_2 reduction. Chem. Rev. **115**: 12936-12973.

Warnecke, T. and Gill, R.T. (2005) Organic acid toxicity, tolerance, and production in *Escherichia coli* biorefining applications. Microb. Cell Fact. **4**: 25.

Weghoff, M.C. and Müller, V. (2016) CO metabolism in the thermophilic acetogen *Thermoanaerobacter kivui*. Appl. Environ. Microbiol. **82**: 2312-2319.

Weghoff, M.C., Bertsch, J. and Müller, V. (2015) A novel mode of lactate metabolism in strictly anaerobic bacteria. Environ. Microbiol. **17**: 670-677.

Weilhard, A., Argent, S.P. and Sans, V. (2021) Efficient carbon dioxide hydrogenation to formic acid with buffering ionic liquids. Nat. Commun. **12**: 231.

Westphal, L., Wiechmann, A., Baker, J., Minton, N.P. and Müller, V. (2018) The Rnf complex is an energy coupled transhydrogenase essential to reversibly link cellular NADH and ferredoxin pools in the acetogen *Acetobacterium woodii*. J. Bacteriol. **200**: e00357-00318.

Wohlfarth, G., Geerligs, G. and Diekert, G. (1990) Purification and properties of a NADH-dependent 5,10-methylenetetrahydrofolate reductase from *Peptostreptococcus productus*. Eur. J. Biochem. **192**: 411-417.

Wood, H.G. and Ljungdahl, L.G. (1991) Autotrophic character of the acetogenic bacteria. In *Variations in autotrophic life*. Shively, J.M., and Barton, L.L. (eds). San Diego: Academic press, pp. 201-250.

Wood, H.G., Ragsdale, S.W. and Pezacka, E. (1986) The acetyl-CoA pathway of autotrophic growth. FEMS Microbiol. Rev. **39**: 345-362.

Woods, D.D. (1936) Hydrogenlyases. IV. The synthesis of formic acid by bacteria. Biochem. J. **30**: 515-527.

Wu, W.M., Hickey, R.F., Jain, M.K. and Zeikus, J.G. (1993) Energetics and regulations of formate and hydrogen metabolism by *Methanobacterium formicicum*. Arch. Microbiol. **159**: 57-65.

Yamamoto, I., Saiki, T., Liu, S.M. and Ljungdahl, L.G. (1983) Purification and properties of NADP-dependent formate dehydrogenase from *Clostridium thermoaceticum*, a tungsten-selenium-iron protein. J. Biol. Chem. **258**: 1826-1832.

Yang, S.-T., Tang, I.-C. and Okos, M.R. (1987) Kinetics of homoacetic fermentation of lactate by *Clostridium formicoaceticum*. App. Environ. Microbiol. **53**: 823-827.

Yishai, O., Lindner, S.N., Gonzalez de la Cruz, J., Tenenboim, H. and Bar-Even, A. (2016) The formate bio-economy. Curr. Opin. Chem. Biol. **35**: 1-9.

Yoshida, A., Nishimura, T., Kawaguchi, H., Inui, M. and Yukawa, H. (2005) Enhanced hydrogen production from formic acid by formate hydrogen lyase-overexpressing *Escherichia coli* strains. Appl. Environ. Microbiol. **71**: 6762-6768.

Yu, X.W. and Pickup, P.G. (2008) Recent advances in direct formic acid fuel cells (DFAFC). J. Power Sources **182**: 124-132.

Zarzycki, J., Brecht, V., Müller, M. and Fuchs, G. (2009) Identifying the missing steps of the autotrophic 3-hydroxypropionate CO_2 fixation cycle in *Chloroflexus aurantiacus*. Proc Natl Acad Sci U.S.A. **106**: 21317-21322.

5. Additional results

5.1. Biological hydrogen storage and release through multiple cycles of reversible hydrogenation of CO_2 to formic acid in a single process unit

Schwarz, F.M., Oswald, F., Müller, V.

Status: unpublished

5.1.1. Introduction

Concerns about climate change and global warming have prompted research to replace fossil-fuel based energy carriers with the coincident need to maintain the world's energy demand (Veziroğlu and Şahın, 2008; Bockris, 2013; Singh et al., 2015). Here, molecular hydrogen has been considered as an attractive, alternative energy carrier which can be produced environmentally friendly and renewable. If the applied hydrogen is produced from renewable energy sources (i.e., solar-, wind-, hydro-, geothermal power) by water splitting and not *via* traditional routes such as steam reforming and partial oxidation of coal, oil and natural gas, no net CO_2 is generated in the production process (Holladay et al., 2009; Wang et al., 2014; Brandon and Kurban, 2017). Furthermore, hydrogen is a strong candidate for energy/electricity storage in an environment with excess supply of renewable energy. However, due to handling and storage concerns of the highly volatile H_2 gas, the catalytic process of direct hydrogenation of CO_2 has attracted more and more attention in recent years (Wang et al., 2011; Moret et al., 2014; Preuster et al., 2017). The process does not only allow hydrogen energy conversion and storage on a large scale, it further provides a feasible avenue for carbon dioxide capture and storage. The necessary CO_2 molecule can be derived from sources such as industrial flue gas but direct carbon capture and storage (CCS) technologies also enable CO_2 capture from air, a technology which still requires optimization and is intensively studied (Lackner et al., 2012; Sanz-Perez et al., 2016; Shi et al., 2020). The two gases H_2 and CO_2 can then safely be stored in the versatile compound formic acid/formate that is one likely product in the process of hydrogen-dependent CO_2 reduction (Enthaler et al.,

2010; Eppinger and Huang, 2017; Preuster et al., 2017). Formic acid does not only belong to the group of liquid organic hydrogen carriers (LOHCs), moreover, the compound fulfills the necessary requirements for a putative sustainable formate bioeconomy in future (Yishai et al., 2016). Chemical catalysts can facilitate the interconversion of H_2 and CO_2 to formic acid, however, mostly requiring noble metals and/or extreme conditions in the reaction process which make the conversion economically not viable (Enthaler et al., 2010; Hull et al., 2012; Appel et al., 2013). But aside from chemical catalysts, also biological solutions arise. Recently, a soluble, biotechnological interesting enzyme complex was identified in the obligate anaerobic group of acetogenic bacteria, named as hydrogen-dependent CO_2 reductase (HDCR) (Schuchmann and Müller, 2013; Schwarz et al., 2018). So far, the HDCRs were only purified from the mesophilic and thermophilic acetogenic bacterium *Acetobacterium woodii* and *Thermoanaerobacter kivui*, respectively, but bioinformatic analysis of available genome data indicates the presence of HDCR-like enzymes also outside of this bacterial group (Schuchmann and Müller, 2013; Schwarz et al., 2018). However, the known HDCR enzymes catalyze the direct hydrogenation of CO_2 to formic acid with remarkable catalytic rates, outcompeting chemical catalysts under comparable moderate reaction conditions (Müller, 2019). Noteworthy, the activity is fully reversible and can be affected by the substrate concentrations and prevailing reaction conditions, thus, facilitating the release of stored hydrogen in another catalytic dehydrogenation reaction to close the H_2 storage cycle. Interestingly, the two challenging reactions of hydrogen-dependent CO_2 reduction to formate as well as formate-driven H_2 production are catalyzed with almost identical catalytic rates (Schuchmann and Müller, 2013; Schwarz et al., 2018). To take advantage of using whole cells instead of the purified enzyme as biocatalysts, a HDCR-based whole-cell system was established in serum bottle and bioreactor scale, again, demonstrating the remarkable reversible nature of the HDCR-based system (Schuchmann and Müller, 2013; Kottenhahn et al., 2018; Schwarz and Müller, 2020; Schwarz et al., 2021). The system is based on the depletion of the cellular ATP content, therefore, blocking the ATP-dependent further conversion of formic acid to acetic acid in the Wood-Ljungdahl pathway (WLP) of these organisms. A more detailed explanation of the applied system

and the possibilities to uncouple the bioenergetics was already given in the literature (Schuchmann and Müller, 2013; Schwarz and Müller, 2020).

In this study, we describe and implement a new process design for biological hydrogen storage and release through multiple cycles of reversible hydrogenation of CO_2 to formic acid in a single bioreactor. Here, we make use of the good reversibility of the HDCR-based whole-cell system and demonstrate a plain and single bioprocess unit to store and release molecular hydrogen in and from formic acid. In such a future process, excess energy can be used to produce "green" H_2 by water splitting. The necessary renewable energy can be obtained, for example, from sunlight during daytime. H_2 and air-captured CO_2 can be further converted to the LOHC formic acid in a bioreactor under ambient pressure and temperature. Worthy to mention, the accumulated formic acid can later be re-oxidized in the same bioreactor to release the stored H_2 in times of power deficiencies. The emitted hydrogen-lean CO_2 molecule can be recycled and can later be used in another H_2 storage cycle (Fig. 1).

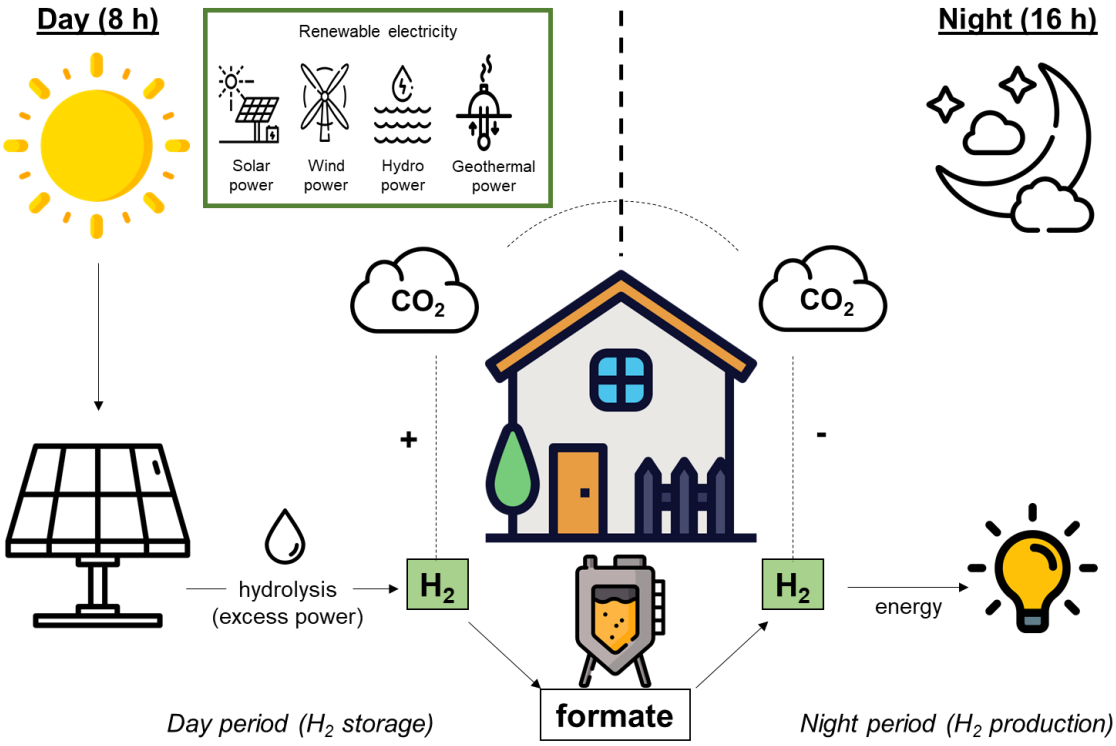

Fig. 1 Schematic cycle of future reversible H_2 storage *via* direct hydrogenation of CO_2 to formate using a single bioreactor. Excess energy generated from renewable sources can be used to produce H_2 by water splitting. Captured CO_2 and H_2 are then converted into the LOHC formate by whole-cell catalysis in a single process unit. The same bioreactor system and biocatalyst are used for overnight hydrogen release from the LOHC system. The produced H_2 can ensure off-grid power supply in energy-lean times and CO_2 can be recycled and re-used in another H_2 storage cycle. All icons were taken from freepik from flaticon.com.

The use of sunlight is just exemplary and, of course, different sources can be used to produce renewable electricity in dependence of the local conditions, therefore, making different scenarios more likely and more beneficial. In southern Germany, the average hours of sunshine during summer time are about 7-8 h and thus a day/night cycle of 8/16 h was assumed in the applied experiment. Of course, the field of applications for renewably produced formic acid is diverse since formic acid can be used as bulk chemical, microbial feedstock or can even be applied in direct formic acid fuel cells (DFAFC) (Aslama et al., 2012; Yishai et al., 2016; Kawanami et al., 2017). But here we want to focus on the ability of formic acid to serve as H_2 storage compound (Preuster et al., 2017). Therefore, the aim was to demonstrate the feasibility of reversible hydrogenation of CO_2 to formic acid in a single bioreactor by using our established whole-cell system from *A. woodii*. Moreover, the designed process unit can be considered as a future "bio-battery" for the reversible storage of electrons in form of H_2 in the versatile compound formic acid.

5.1.2. Materials and methods

Organism and cultivation

Acetobacterium woodii (DSM 1030) was cultivated at 30 °C under anoxic conditions in carbonate-buffered medium (Heise et al., 1989) using 1 L flasks (Müller-Krempel, Bülach, Switzerland) with 500 mL media or under anoxic conditions using 20 L flasks (Glasgerätebau Ochs; Bovenden-Lenglern, Germany). The medium was prepared under anoxic conditions as described before (Hungate, 1969; Bryant, 1972). Fructose (20 mM) was used as growth substrate for all cultivations and cell growth was followed by measuring the optical density at 600 nm with an UV/Vis spectrophotometer.

Preparation of resting cells and cell suspension experiments

Resting cells of *A. woodii* were prepared as described before (Schuchmann and Müller, 2013). The cells were washed and resuspended in K-phosphate buffer (50 mM K-phosphate, 20 mM KCl, 4 µM resazurin, 2 mM DTE, pH 7.0). The total cell protein concentration of the cell suspension was determined according to

Schmidt et al. (1963) and the prepared cells were directly used for the subsequent cell suspension experiments. To determine the conversion of H_2 + CO_2 into formate by resting cells of *A. woodii*, 120 mL serum bottles (Glasgerätebau Ochs GmbH, Bovenden-Lenglern, Germany) containing pre-warmed buffer (50 mM K-phosphate, 20 mM KCl, 4 µM resazurin, 2 mM DTE, pH 7.0) and a N_2 atmosphere were incubated with cell suspensions at the protein concentration stated. The final liquid volume in the serum flasks was 10 mL and the resting cells were incubated for at least 10 min at 30 °C prior to the start of the experiment. The reaction was started by changing the head space to a H_2 + CO_2 (80:20%, [v/v]) atmosphere with 1 bar overpressure. If necessary, the ionophore monensin sodium salt (dissolved in EtOH) was added prior to the reaction start and liquid samples were taken over the time to analyze the formation of acetic acid and formic acid.

Multiple cycles of reversible hydrogenation of CO_2 to formic acid in a single bioreactor

The bioreactor experiments were carried out in Biostat Aplus bench-top reactors from Sartorius (Melsungen, Germany) with a working volume of 1.5 L as described before (Schwarz et al., 2021). Each bioreactor was equipped with microsparger, baffles, two Rushton-impeller, pH-probe (Hamilton, Bonaduz, Switzerland), temperature probe and a redox potential probe (Hamilton, Bonaduz, Switzerland). The temperature of the buffer (50 mM K-phosphate, 20 mM KCl, 2 mM DTE, pH 7.0) was maintained at 30 °C, using a cooling finger and heating sleeve. The permitted pH-range of the bioreactor experiments was from pH 5.9 to 8.1 and was achieved by titration with H_3PO_4 (4 M) and NH_4OH (4 M). The gas flow rate was maintained during the “day/night cycles” at a constant value of 10 mL/min using a digital mass-flow controller (Bronkhorst High-Tech, Ruurlo, Netherlands). The supplied gas composition varied in the stoichiometry of H_2, CO_2 and N_2 in dependence of the catalytic cycle. During the “day period” (duration: 8 h; H_2 storage process) a gas composition of 45% H_2, 45% CO_2 and 10% N_2 [v/v] was used (Nippon Gases, Germany). During the “night period” (duration: 16 h; H_2 production process) a gas composition of 100% N_2 [v/v] was used. The gas switch was made manually without an interruption of the existing gas flow. The installed micro sparger ensured the formation of

microbubbles to enhance mass transfer between gaseous and aqueous phase (Bredwell and Worden, 1998). The headspace of the bioreactor was at atmospheric pressure and the gas-liquid mixing was achieved by using a stirrer set-up with two Rushton-impeller at 400 rpm. The bioreactor buffer was prepared under aerobic, non-sterile conditions and oxygen was removed by subsequent sparging with 45% H_2, 45% CO_2 and 10% N_2 [v/v]. After the achievement of anoxic conditions and CO_2 saturation in the liquid phase, 2 mM DTE and 30 µM monensin were supplemented as indicated. Whole-cell biocatalysis was started by adding *A. woodii* cell suspension to a final cell protein concentration of 1 mg/mL to the bioreactor. Samples (2 mL) were taken at defined time points for HPLC measurement as well as OD and protein determination. A single liquid sample of 3 mL reactor broth was taken and discarded prior to the bioreactor sampling to account for the dead volume of the sampling line. The samples were centrifuged (18,000 × g, 8 min, room temperature) to remove cells and the supernatant was frozen at −20 °C until further off-line analysis *via* HPLC.

Inhibitory effect of reactor buffer on fresh cell suspensions

Fresh cells suspensions of *A. woodii* were prepared as described in the section above. The reaction buffer for cell suspension experiments was obtained from the bioreactor approach. Therefore, 60 mL cell suspension of each bioreactor was transferred in a 120 mL anoxic serum bottle (Glasgerätebau Ochs GmbH, Bovenden-Lenglern, Germany) at the end of the fermentation process. Afterwards, buffer and cells were separated *via* centrifugation under anoxic conditions. The supernatant was taken as reaction buffer in the subsequent serum bottle experiment with a total cell protein concentration of 1 mg/mL of the freshly prepared *A. woodii* cells. The serum bottle experiments were performed as described above.

Analytical methods

The concentrations of formic acid and acetic acid were measured by high-performance liquid chromatography using a 1260 Infinity II LC System (Agilent Technologies, Santa Clara, CA, USA) as described before (Schwarz et al., 2020) or by using a commercially available formic acid and acetic acid determination kit (Boehringer Mannheim/R-Biopharm AG, Mannheim/Darmstadt, Germany)

following the instructions of the manufacturer. Bioreactor off-gas analysis was conducted *via* a Micro-GC (Inficon, Bad Ragaz, Switzerland) which was equipped with two measurement modules containing different analytical columns. The analytical conditions and columns were used as described before (Wiechmann et al., 2020). The total cell protein concentration of the prepared cell suspensions was determined according to Schmidt et al. (1963).

5.1.3. Results

Multiple cycles of reversible hydrogenation of CO_2 to formic acid in a single bioreactor

The reversible nature of the HDCR-based whole-cell system was previously described and the upscaling feasibility of the cell system into bioreactors was recently proven (Schuchmann and Müller, 2013; Kottenhahn et al., 2018; Schwarz and Müller, 2020; Schwarz et al., 2021). Building on the existing knowledge, we aimed to design a process for the biological hydrogen storage and release through multiple cycles of reversible hydrogenation of CO_2 to formic acid in a single bioreactor. Therefore, *A. woodii* was grown in 20 L complex medium with fructose to the end of the exponential growth phase and resting cells were prepared. The bioreactor contained 50 mM K-phosphate buffer at pH 7.0 with additional 15 µM of the uncoupler monensin. The tolerated pH range of 5.9 to 8.1 was ensured by titration of NH_4OH and H_3PO_4. The experiment was started by adding resting cells to a final cell protein concentration of 1 mg/mL to the bioreactor which was flushed with H_2, CO_2 and N_2. As expected, resting cells immediately started to produce formic acid from H_2 and CO_2 with a production rate of 5.4 (± 1.0) mmol g^{-1} h^{-1} (Fig. 2A).

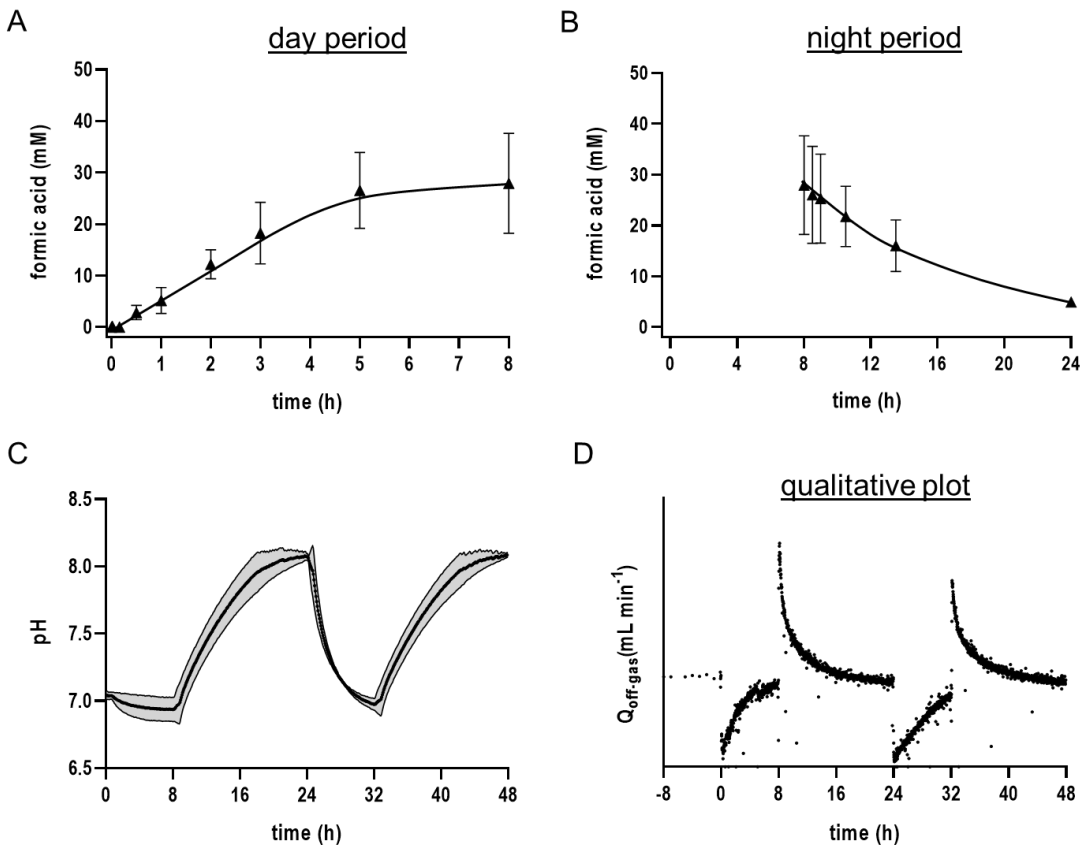

Fig. 2 Process development during day/night cycle for biological hydrogen storage and release in a single bioreactor. A) Formate production from H_2 and CO_2 during day period, B) formate oxidation during night period, C) corresponding pH course over two day/night cycles and D) qualitative off-gas graph over the first 48 h. Here, the shown data is from one representative experiment out of three independent replicates. All other data points are mean ± SD, N = 3.

During the “day-period” of 8 h, 28 mM formic acid were produced *via* direct hydrogenation of CO_2. Then, the gas composition was switched to 100% N_2 in the “night period” to release the stored H_2 from formic acid. By sparging with 100% N_2 the chemical equilibrium was pushed towards hydrogen formation from formate and the *A. woodii* cells started to re-oxidize the produced formic acid from the reactor-broth (Fig. 2B). The formic acid oxidation proceeded with a specific rate of 2.3 (± 0.6) mmol g^{-1} h^{-1}. During the 16 h “night period”, the formic acid concentration decreased from initial 28 mM to 4.9 mM. The formic acid-driven gas production in the “night period” as well as the H_2-dependent CO_2 reduction in the “day-period” could also be observed in the off-gas flow rate. Here, only a qualitative plot and not a quantitative plot with exact quantities of the gas components can be shown for the off-gas. This is owed to the used bioreactor set-up since a 1.5 L headspace was applied in the bioreactor to allow potential foaming. Additionally, a low gas-flow rate of 10 mL/min was applied to reduce gas

wasting and gas dilution during H_2 production. The applied set-up allowed a diffusive back mixing of the head space additional to a prolonged mean retention time of the gases which distorted the data for quantitative analysis. Nevertheless, the qualitative plot clearly showed that the off-gas flow was reduced during the day period due to H_2 and CO_2 consumption. In contrast, more gas was released from the bioreactor in the night period due to formic acid-driven H_2 and CO_2 production (Fig. 2C). The effect of alternating gas mixtures, mainly based on varying CO_2 concentrations, could also be seen in the pH profile (Fig. 2D). Prior to cell supplementation, CO_2 saturation was achieved in the liquid phase in the bioreactor. Therefore, the initial pH drop was mainly based on the production of formic acid from H_2 and CO_2. After the gas composition was switched to 100% N_2, formic acid was re-oxidized and dissolved H_2 as well as CO_2 were flushed out of the reactor. The pH value shifted to more alkalic conditions. In a new cycle of H_2 storage, dissolving CO_2 concentrations as well as formic acid production relocates the pH value to a more neutral state. Since the process enabled the reversible storage and release of H_2, the bioreactor application was continued. Over the first 96 h (4 day/night cycles) the reaction kinetics of formate formation and formate oxidation were monitored (Fig. 3A).

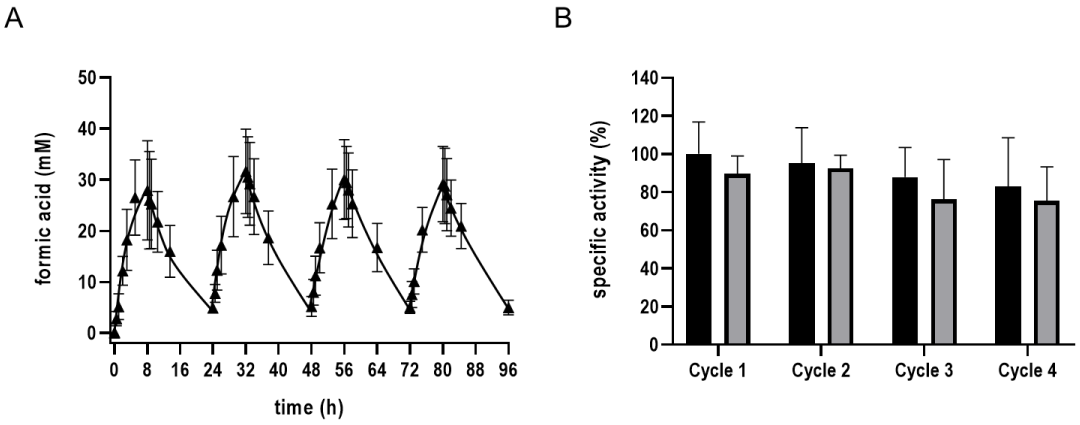

Fig. 3 Multiple cycles of reversible hydrogenation of CO_2 to formic acid in a single process unit. A) Formic acid formation and formic acid oxidation over 4 day/night cycles in the first 96 h of process time and B) the corresponding specific activity of formic acid production (black bars) and formic acid oxidation (grey bars). 100% of the activity corresponds to a formic acid production rate of 5.4 mmol g^{-1} h^{-1}. The formic acid oxidation rate of 100% is similar to 2.3 mmol g^{-1} h^{-1}. All data points are mean ± SD, N = 3.

The specific activity of both reactions was determined for repeating cycles and indicates a constant conversion efficiency over the time (Fig. 3B). After 4 cycles, 83 and 75% of the initial formic acid formation and formic acid oxidation rate,

respectively, were present. Therefore, the system was kept running over 2 weeks which corresponds to 15 day/night-cycles or 360 h process time. The amount of produced formic acid per day-period decreased with increasing process time (Fig. 4A).

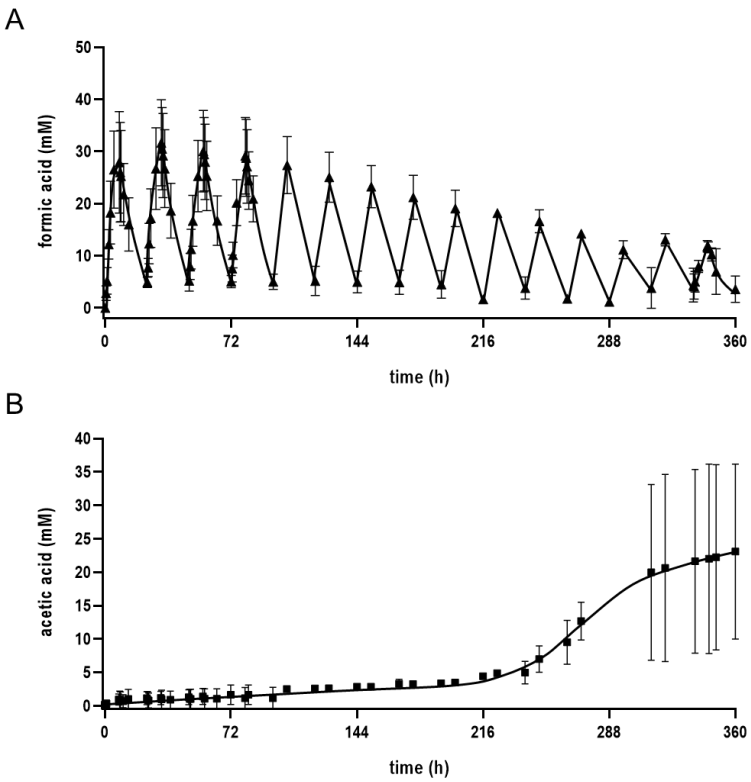

Fig. 4 Long-term application of reversible hydrogenation of CO_2 to formic acid in a single process unit. Shown are A) 15 formic acid formation/oxidation cycles of the entire process (360 h) and B) corresponding side-product formation profile of acetic acid. All data points are mean ± SD, N = 3.

At the same time, acetic acid formation increased (Fig. 4B). The unwanted side product acetic acid was only produced in traces (around 2 mM) during the first 96 h of fermentation but increased up to 23 mM at the end (t_{360} h). In the last day/night cycle 20% of the initial formic acid formation and formic acid oxidation rate was still present. In sum 330 (± 85) mM formic acid was produced and oxidized by direct hydrogenation of CO_2 within 15 day/night cycles in a single bioreactor. The corresponding pH profile, optical density and total cell protein concentration were also monitored (Fig. 5).

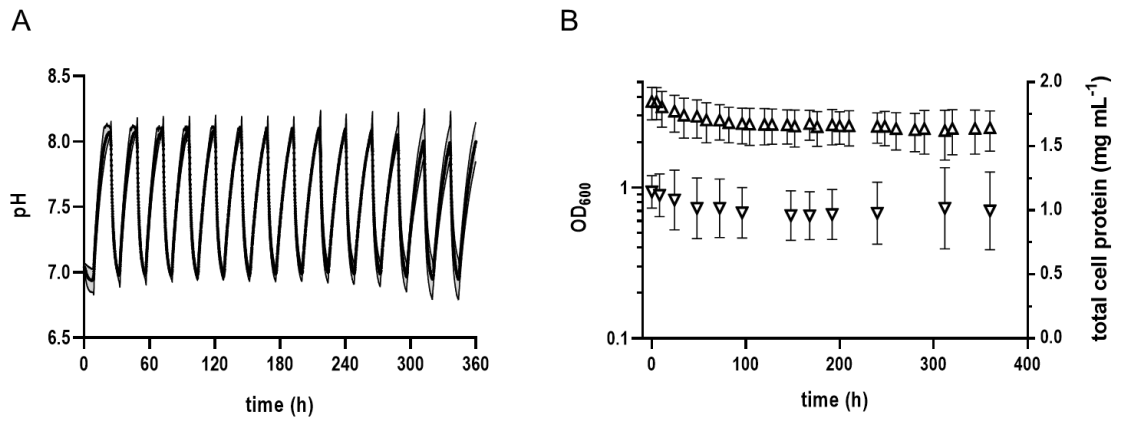

Fig. 5 pH and optical density profile. A) pH and B) optical density (OD_{600}) as well as total cell protein concentration are monitored over the entire bioreactor application (360 h). Empty triangles up, optical density at 600 nm; empty triangles down, total cell protein concentration. All data points are mean ± SD, N = 3.

Here, the optical density decreased slightly at the beginning of the experiments and stayed constant for the rest of the application. As expected, the total cell protein concentration behaved similar to the optical density. Noteworthy, 87% of the initial cell concentration remains after 2 weeks of application, indicating a solid robustness of the *A. woodii* cell system under the given conditions. Moreover, the chosen bioreactor set-up required only 25 mM of phosphoric acid and even no base was needed in the entire process.

However, the observed decrease in formic acid formation seemed to be directly connected to an increase in acetic acid formation which is not preferable in the process of H_2 storage and H_2 release. Since acetic acid is only produced from H_2 and CO_2 if the energy state of resting cells is not fully diminished, a putative loss of efficacy of the used ionophor monensin was assumed over the time. To counter whole-cell based production of acetic acid from H_2 and CO_2, monensin was repetitively added every 72 h to the bioreactor broth. In this approach, the entire bioreactor set-up and the process parameters (gas flow, stirrer speed, gas composition, duration of day/night cycling etc.) were equal to the previous experiment with the exception of repetitive monensin addition. Here, the behavior of the bioreactor process was comparable to the previously shown process and the data will therefore not be shown in greater detail. An overview of the entire process with product formation of formic acid/acidic acid is shown in Fig. 6.

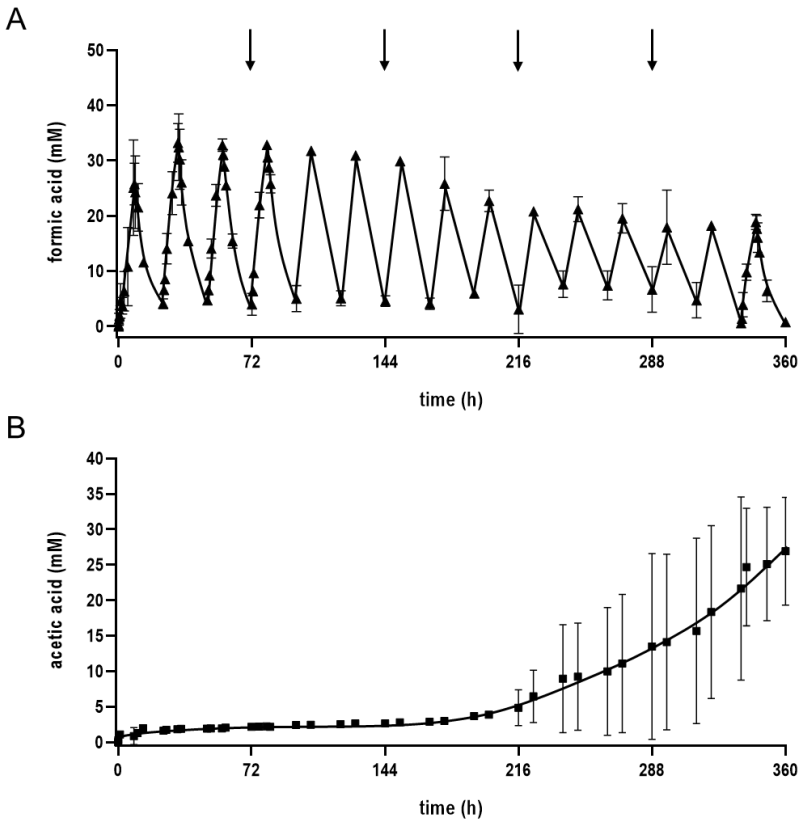

Fig. 6 Long-term application of reversible hydrogenation of CO_2 to formic acid in a single process unit with repetitive monensin supply. Shown are A) 15 formic acid formation/oxidation cycles of the entire process (360 h) and B) corresponding side-product formation profile of acetic acid. Black arrows indicate the repetitive addition of monensin (15 µM) to the bioreactor. All data points are mean ± SD, N = 3.

Again, formic acid formation was constant for the first 4 day/night cycles, but decreased afterwards whereas acetic acid formation increased. To check whether the bioreactor buffer has still an uncoupling ability due to the presence of sufficient amounts of active monensin, some bioreactor broth was taken at the end of the process to check for its uncoupling ability. Therefore, *A. woodii* cells were removed from the bioreactor broth and the recovered cell-free bioreactor buffer was used for another cell suspension experiment with freshly prepared *A. woodii* cells. No additional monensin was added to the cell-free bioreactor buffer to check its ability to uncouple fresh cells and to force formic acid production. Indeed, the cell-free bioreactor buffer was able to uncouple *A. woodii* cells which showed a specific formic acid production rate of 29.1 mmol g^{-1} h^{-1} (data not shown). The control experiment with new buffer and added monensin (15 µM) showed a specific activity of 18.8 mmol g^{-1} h^{-1}. This clearly shows that the ionophore monensin is still active in the bioreactor broth after 360 h of process

time and that other reasons seem to be responsible for the reactivation of the *A. woodii* cell metabolism.

5.1.4. Discussion

In this study, we investigated the biological hydrogen storage and release in a single bioreactor using *A. woodii* cells as biocatalysts. We demonstrated multiple cycles of reversible hydrogenation of CO_2 to formic acid by applying our established HDCR-based whole-cell system in a single process unit. So far, previous studies only analyzed the HDCR-catalyzed reactions of H_2-dependent CO_2 reduction and formate-driven H_2 production separately. The presented approach of H_2 storage and release in a single stirred-tank bioreactor takes advantage of the good reversibility of the entire HDCR system, outcompeting other enzyme-based whole-cell systems which mostly show a strong bias towards one of the mentioned reactions. This was also observed for the formate hydrogenlyase (FHL) system of *Escherichia coli* (McDowall et al., 2014; Pinske and Sargent, 2016). The organism is well-known for its good ability in dark fermentative H_2 production as well as formate-driven H_2 production due to the high FHL activity. But harsh reaction conditions are needed to efficiently drive H_2-dependent CO_2 reduction to formic acid by the same enzyme (Roger et al., 2018). However, the HDCR enzyme catalyzes the conversion of H_2 and CO_2 to formic acid and *vice versa* with almost identical kinetics and activities. Since the equilibrium constant for H_2-dependent CO_2 reduction to formic acid is close to one, minor changes in substrate/product concentrations, pH and temperature can influence the chemical equilibrium. The effect was demonstrated in this study by varying substrate concentrations. Here, varying gas compositions affected the formation or degradation of formic acid in the bioreactor. Obviously, the observed rates for both reactions were multiple times lower than previously reported rates (Schwarz et al., 2021), mainly owed to reaction limitations (i.e., substrate limitations) in the bioreactor process. We decided to use a realistic and reduced gas flow rate to reduce the gas waste stream and to avoid an excessive dilution of the produced H_2. Additionally, it has to keep in mind that a change in gas flow rates has an effect on the change in pH values due to the contribution of CO_2. Of

course, in a more applied process, the non-captured H_2 and CO_2 (in the day-period) can be recycled and can be fed back into the bioreactor. Additionally, produced H_2 (in the night-period) can be separated from CO_2 by existing methods for gas separation (Galizia et al., 2017; Tong and Sekizkardes, 2021). As mentioned before, the necessary H_2 and CO_2 molecules can be obtained *via* different routes. In one of these scenarios, H_2 is produced from renewable energy sources by water-splitting and CO_2 is captured from air *via* CCS technologies. But alternatively, captured and stored CO_2 in form of bicarbonate can also be used as CO_2 source in the applied whole-cell system in future. Previously, it was shown that resting cells of *A. woodii* convert $KHCO_3$ and H_2 into formic acid (Schuchmann and Müller, 2013). This conversion is possible due to the presence of a fast and soluble carbonic anhydrase enzyme which catalyzes the interconversion of bicarbonate in CO_2 and H_2O. *A. woodii* cells even showed the highest carbonic anhydrase activity of different investigated acetogens (Braus-Stromeyer et al., 1997). In such an approach, the necessary bicarbonate can be obtained from a process called carbon capture and storage by mineral carbonation (CCSM). In this route of CO_2 sequestration, CO_2 is stored in the form of bicarbonate by carbonation of carbonate minerals (Lackner, 2002; Sanna et al., 2012). However, the demonstrated bioreactor set-up in this study allowed multiple cycles of reversible hydrogenation of CO_2 to formic acid. Interestingly, the uncoupling effect of monensin on *A. woodii* cells could not be maintained over the whole process time. In general, monensin is an antibiotic substance which was isolated from *Streptomyces cinnamonensis* (Haney and Hoehn, 1967). The substance works as a carboxylic ion-selective ionophore (especially Na^+/H^+ antiporter) which facilitates electroneutral, monovalent ion transport across the cell membrane. Therefore, the substance interferes with the ion gradient needed to drive ATP synthesis. Since *A. woodii* cells started to produce acetic acid from H_2 and CO_2 in the late phase of fermentation, Na^+-dependent energy conservation seemed not to be impaired anymore by added monensin. But the loss of function of monensin could be experimentally excluded. The activity of freshly prepared *A. woodii* cells uncoupled by the bioreactor buffer had more than 100% of the control activity. The even higher formic acid production rate is mainly based on the fact that the re-used bioreactor buffer had a more alkalic pH (pH 7.94) which favors formic acid production as shown before (Schwarz and Müller,

2020). However, acetic acid formation leads to the assumption that *A. woodii* cells may adapt to the antibiotic substance. Monensin is a common antibiotic substance given to dairy cows in the United States to increase milk production efficiency or to treat coccidiosis which is a parasitic infection. It is also administered to cattle and/or pigs for growth promotion (Chapman et al., 2010; Wong, 2019). In general, Gram-positive bacteria are considered to be more sensitive to monensin than Gram-negative bacteria. But monensin adaptation is not a new phenomenon. Pure culture studies of three isolated cattle rumen bacteria have been demonstrated to exhibit a long lag phase prior to growth in the presence of monensin (Simjee et al., 2012). The three investigated Gram-positive bacteria *Enterococcus faecium*, *Enterococcus faecalis* and *Clostridium perfringens* developed monensin resistance through altered cell wall characteristics, showing a thickening of the cell wall or the extracellular polysaccharide (glycocalyx) layer. Similarly, the Gram-positive, amino acid fermenting bacterium *Clostridium aminophilum* could be adapted to monensin (Rychlik and Russell, 2002). It was even shown that adapted cultures can subsequently grow in even higher concentrations of monensin (Morehead and Dawson, 1992; Callaway and Russell, 1999). Putative responsible genes for ionophore resistance in ruminal bacteria have not been identified yet and the exact mechanisms of monensin resistance are still not well understood. In the context of acetogenic bacteria, different ionophores as well as monensin were used for decoupling experiments to study bacterial bioenergetics and ion growth dependencies, but rarely is known about acetogenic adaptation (Heise et al., 1989; Daniel et al., 1990; Mayer and Weuster-Botz, 2017). Also, the effect of monensin on the anaerobic digesters microbiome composition and function is part of current research but does not allow an overall and strong statement with regard to the acetogenic community and their adaptation. Another assumption for acetic acid formation could be the contamination of the bioreactor broth with a further autotrophic, acetic acid forming organism due to non-sterile conditions. Since buffer was used and no increase in optical density as well as total cell protein concentration could be observed, the assumption is more unlikely. Moreover, the microscopic control was inconspicuous. However, for further perspectives, genetic modifications could be a promising and sufficient way to avoid the addition of putative unwanted, environmentally unfriendly and cost-

intensive substances (i.e., chemical ionophores, antibiotics) as well as to prevent unwanted side-product formation such as acetic acid in the bioreactor process. Since the entire catalysis of reversible H_2 storage and release relies on the activity of the HDCR enzyme, a gene knock-out of the participating enzymes in the WLP could prevent the further conversion of formic acid to acetic acid. Here, the knock-out of the formyl-THF synthetase gene would be one likely and obvious way. In summary, we could prove the feasibility of reversible hydrogenation of CO_2 to formic acid in a single bioreactor by using our established whole-cell system from *A. woodii*. Here, the stored and captured H_2 and CO_2 during the day period could be released in the night period by the same biocatalyst and the same process unit. As far as we know, it is the first time that a bio-based system allows multiple cycles of reversible hydrogenation of CO_2 to formic acid in a single bioreactor. However, the unique presented process design combines two chemically challenging reactions which are an integral part of a future hydrogen economy to combat global warming and to solve the renewable energy demand of the growing world population.

5.1.5. References

Appel, A.M., Bercaw, J.E., Bocarsly, A.B., Dobbek, H., DuBois, D.L., Dupuis, M., Ferry, J.G., Fujita, E., Hille, R., Kenis, P.J., Kerfeld, C.A., Morris, R.H., Peden, C.H., Portis, A.R., Ragsdale, S.W., Rauchfuss, T.B., Reek, J.N., Seefeldt, L.C., Thauer, R.K. and Waldrop, G.L. (2013) Frontiers, opportunities, and challenges in biochemical and chemical catalysis of CO_2 fixation. Chem. Rev. **113**: 6621-6658.

Aslama, N.M., Masdara, M.S., Kamarudina, S.K. and Dauda, W.R.W. (2012) Overview on direct formic acid fuel cells (DFAFCs) as an energy sources. APCBEE Procedia **3**: 33-39.

Bockris, J.O.M. (2013) The hydrogen economy: Its history. Int. J. Hydrogen Energy **38**: 2579-2588.

Brandon, N.P. and Kurban, Z. (2017) Clean energy and the hydrogen economy. Philos. Trans. Royal Soc. A **375**: 20160400.

Braus-Stromeyer, S.A., Schnappauf, G., Braus, G.H., Gössner, A.S. and Drake, H.L. (1997) Carbonic anhydrase in *Acetobacterium woodii* and other acetogenic bacteria. J. Bacteriol. **179**: 7197-7200.

Bredwell, M.D. and Worden, R.M. (1998) Mass-transfer properties of microbubbles. 1. Experimental studies. Biotechnol. Prog. **14**: 31-38.

Bryant, M.P. (1972) Commentary on the Hungate technique for culture of anaerobic bacteria. Am. J. Clin. Nutr. **25**: 1324-1328.

Callaway, T.R. and Russell, J.B. (1999) Selection of a highly monensin-resistant *Prevotella bryantii* subpopulation with altered outer membrane characteristics. Appl. Environ. Microbiol. **65**: 4753-4759.

Chapman, H.D., Jeffers, T.K. and Williams, R.B. (2010) Forty years of monensin for the control of coccidiosis in poultry. Poult. Sci. **89**: 1788-1801.

Daniel, S.L., Hsu, T., Dean, S.I. and Drake, H.L. (1990) Characterization of the H_2-dependent and CO-dependent chemolithotrophic potentials of the acetogens *Clostridium thermoaceticum* and *Acetogenium kivui*. J. Bacteriol. **172**: 4464-4471.

Enthaler, S., von Langermann, J. and Schmidt, T. (2010) Carbon dioxide and formic acid-the couple for environmental-friendly hydrogen storage? Energy Environ. Sci. **3**: 1207-1217.

Eppinger, J. and Huang, K.W. (2017) Formic acid as a hydrogen energy carrier. ACS Energy Lett. **2**: 188-195.

Galizia, M., Chi, W.S., Smith, Z.P., Merkel, T.C., Baker, R.W. and Freeman, B.D. (2017) 50th anniversary perspective: polymers and mixed matrix membranes for gas and vapor separation: a review and prospective opportunities. Macromolecules **50**: 7809-7843.

Haney, M.E., Jr. and Hoehn, M.M. (1967) Monensin, a new biologically active compound. I. Discovery and isolation. Antimicrob. Agents Chemother. **7**: 349-352.

Heise, R., Müller, V. and Gottschalk, G. (1989) Sodium dependence of acetate formation by the acetogenic bacterium *Acetobacterium woodii*. J. Bacteriol. **171**: 5473-5478.

Holladay, J.D., Hu, J., King, D.L. and Wang, Y. (2009) An overview of hydrogen production technologies. Catal. Today **139**: 244-260.

Hull, J.F., Himeda, Y., Wang, W.H., Hashiguchi, B., Periana, R., Szalda, D.J., Muckerman, J.T. and Fujita, E. (2012) Reversible hydrogen storage using CO_2 and a proton-switchable iridium catalyst in aqueous media under mild temperatures and pressures. Nat. Chem. **4**: 383-388.

Hungate, R.E. (1969) A roll tube method for cultivation of strict anaerobes. In *Methods in Microbiology*. Norris, J.R., and Ribbons, D.W. (eds). New York and London: Academic Press, pp. 117-132.

Kawanami, H., Himeda, Y. and Laurenczy, G. (2017) Formic acid as a hydrogen carrier for fuel cells toward a sustainable energy system. Adv. Inorg. Chem. **70**: 395-427.

Kottenhahn, P., Schuchmann, K. and Müller, V. (2018) Efficient whole cell biocatalyst for formate-based hydrogen production. Biotechnol. Biofuels **11**: 93.

Lackner, K.S. (2002) Carbonate chemistry for sequestering fossil carbon. Annu. Rev. Energy Environ. **27**: 193-232.

Lackner, K.S., Brennan, S., Matter, J.M., Park, A.H., Wright, A. and van der Zwaan, B. (2012) The urgency of the development of CO_2 capture from ambient air. Proc. Natl. Acad. Sci. U.S.A. **109**: 13156-13162.

Mayer, A. and Weuster-Botz, D. (2017) Reaction engineering analysis of the autotrophic energy metabolism of *Clostridium aceticum*. FEMS Microbiol. Lett. **364**: 1-8.

McDowall, J.S., Murphy, B.J., Haumann, M., Palmer, T., Armstrong, F.A. and Sargent, F. (2014) Bacterial formate hydrogenlyase complex. Proc. Natl. Acad. Sci. U.S.A. **111**: E3948-E3956.

Morehead, M.C. and Dawson, K.A. (1992) Some growth and metabolic characteristics of monensin-sensitive and monensin-resistant strains of *Prevotella* (Bacteroides) *ruminicola*. Appl. Environ. Microbiol. **58**: 1617-1623.

Moret, S., Dyson, P.J. and Laurenczy, G. (2014) Direct synthesis of formic acid from carbon dioxide by hydrogenation in acidic media. Nat. Commun. **5**: 4017.

Müller, V. (2019) New horizons in acetogenic conversion of one-carbon substrates and biological hydrogen storage. Trends Biotechnol. **37**: 1344-1354.

Pinske, C. and Sargent, F. (2016) Exploring the directionality of *Escherichia coli* formate hydrogenlyase: a membrane-bound enzyme capable of fixing carbon dioxide to organic acid. Microbiologyopen **5**: 721-737.

Preuster, P., Papp, C. and Wasserscheid, P. (2017) Liquid organic hydrogen carriers (LOHCs): Toward a hydrogen-free hydrogen economy. Acc. Chem. Res. **50**: 74-85.

Roger, M., Brown, F., Gabrielli, W. and Sargent, F. (2018) Efficient hydrogen-dependent carbon dioxide reduction by *Escherichia coli*. Curr. Biol. **28**: 140-145.

Rychlik, J.L. and Russell, J.B. (2002) The adaptation and resistance of *Clostridium aminophilum* F to the butyrivibriocin-like substance of *Butyrivibrio fibrisolvens* JL5 and monensin. FEMS Microbiol. Lett. **209**: 93-98.

Sanna, A., Hall, M.R. and Maroto-Valer, M. (2012) Post-processing pathways in carbon capture and storage by mineral carbonation (CCSM) towards the introduction of carbon neutral materials. Energy Environ. Sci. **5**: 7781-7796.

Sanz-Perez, E.S., Murdock, C.R., Didas, S.A. and Jones, C.W. (2016) Direct capture of CO_2 from ambient air. Chem. Rev. **116**: 11840-11876.

Schmidt, K., Liaaen-Jensen, S. and Schlegel, H.G. (1963) Die Carotinoide der *Thiorhodaceae*. Arch. Mikrobiol. **46**: 117-126.

Schuchmann, K. and Müller, V. (2013) Direct and reversible hydrogenation of CO_2 to formate by a bacterial carbon dioxide reductase. Science **342**: 1382-1385.

Schwarz, F.M. and Müller, V. (2020) Whole-cell biocatalysis for hydrogen storage and syngas conversion to formate using a thermophilic acetogen. Biotechnol. Biofuels **13**: 32.

Schwarz, F.M., Schuchmann, K. and Müller, V. (2018) Hydrogenation of CO_2 at ambient pressure catalyzed by a highly active thermostable biocatalyst. Biotechnol. Biofuels **11**: 237.

Schwarz, F.M., Oswald, F. and Müller, V. (2021) Acetogenic conversion of H_2 and CO_2 into formic acid and *vice versa* in a fed-batch-operated stirred-tank bioreactor. ACS Sustain. Chem. Eng. **9**: 6810-6820.

Schwarz, F.M., Ciurus, S., Jain, S., Baum, C., Wiechmann, A., Basen, M. and Müller, V. (2020) Revealing formate production from carbon monoxide in wild type and mutants of Rnf- and Ech-containing acetogens, *Acetobacterium woodii* and *Thermoanaerobacter kivui*. Microb. Biotechnol. **13**: 2044-2056.

Shi, X., Xiao, H., Azarabadi, H., Song, J., Wu, X., Chen, X. and Lackner, K.S. (2020) Sorbents for the direct capture of CO_2 from ambient air. Angew. Chem. Int. Ed. Engl. **59**: 6984-7006.

Simjee, S., Heffron, A.L., Pridmore, A. and Shryock, T.R. (2012) Reversible monensin adaptation in *Enterococcus faecium*, *Enterococcus faecalis* and *Clostridium perfringens* of cattle origin: potential impact on human food safety. J. Antimicrob. Chemother. **67**: 2388-2395.

Singh, S., Jain, S., Venkateswaran, P., Tiwari, A.K., Nouni, M.R., Pandey, J.K. and Goel, S. (2015) Hydrogen: A sustainable fuel for future of the transport sector. Renew. Sustain. Energy Rev. **51**: 623-633.

Tong, Z. and Sekizkardes, A.K. (2021) Recent developments in high-performance membranes for CO_2 separation. Membranes **11**: 156.

Veziroğlu, T.N. and Şahın, S. (2008) 21st Century's energy: Hydrogen energy system. Energy Convers. Manag. **49**: 1820−1831.

Wang, M., Wang, Z., Gong, X. and Guo, Z. (2014) The intensification technologies to water electrolysis for hydrogen production–A review. Renew. Sustain. Energy Rev. **29**: 573-588.

Wang, W., Wang, S., Ma, X. and Gong, J. (2011) Recent advances in catalytic hydrogenation of carbon dioxide. Chem. Soc. Rev. **40**: 3703-3727.

Wiechmann, A., Ciurus, S., Oswald, F., Seiler, V.N. and Müller, V. (2020) It does not always take two to tango: "Syntrophy" *via* hydrogen cycling in one bacterial cell. ISME J. **14**: 1561-1570.

Wong, A. (2019) Unknown risk on the farm: does agricultural use of ionophores contribute to the burden of antimicrobial resistance? mSphere **4**: e00433-00419.

Yishai, O., Lindner, S.N., Gonzalez de la Cruz, J., Tenenboim, H. and Bar-Even, A. (2016) The formate bio-economy. Curr. Opin. Chem. Biol. **35**: 1-9.

6. Publications

Research articles

6.1 **Schwarz, F.M.** and Müller, V. (2020) Whole-cell biocatalysis for hydrogen storage and syngas conversion to formate using a thermophilic acetogen. Biotechnol. Biofuels 13: 32.

6.2 **Schwarz, F.M.**, Ciurus, S., Jain, S., Baum, C., Wiechmann, A., Basen, M. and Müller, V. (2020) Revealing formate production from carbon monoxide in wild type and mutants of Rnf- and Ech-containing acetogens, *Acetobacterium woodii* and *Thermoanaerobacter kivui*. Microb. Biotechnol. 13: 2044-2056.

6.3 **Schwarz, F.M.**, Oswald, F. and Müller, V. (2021) Acetogenic conversion of H_2 and CO_2 into formic acid and *vice versa* in a fed-batch operated stirred tank bioreactor. ACS Sustain. Chem. Eng. 9: 6810-6820.

6.1. Whole-cell biocatalysis for hydrogen storage and syngas conversion to formate using a thermophilic acetogen

Declaration of author contributions to the publication / manuscript (title):

Whole-cell biocatalysis for hydrogen storage and syngas conversion to formate using a thermophilic acetogen

Status: published, 2020

Journal: Biotechnology for Biofuels

Contributing authors: Fabian M. Schwarz (F.M.S.) and Volker Müller (V.M.)

What are the contributions of the doctoral candidate and his co-authors?

(1) Concept and design

Doctoral candidate F.M.S.:	50%
Co-author V.M.:	50%

(2) Conducting tests and experiments

Doctoral candidate F.M.S.:	Performed all experiments

(3) Compilation of data sets and figures

Doctoral candidate F.M.S.:	Compiled all figures and data sets

(4) Analysis and interpretation of data

Doctoral candidate F.M.S.:	Analyzed and interpreted all data
Co-author V.M.:	Analyzed and interpreted all data

(5) Drafting of manuscript

Doctoral candidate F.M.S.:	50%
Co-author V.M.:	50%

Schwarz and Müller *Biotechnol Biofuels* (2020) 13:32
https://doi.org/10.1186/s13068-020-1670-x

Biotechnology for Biofuels

RESEARCH Open Access

Whole-cell biocatalysis for hydrogen storage and syngas conversion to formate using a thermophilic acetogen

Fabian M. Schwarz and Volker Müller*

Abstract

Background: In times of global climate change, the conversion and capturing of inorganic CO_2 have gained increased attention because of its great potential as sustainable feedstock in the production of biofuels and biochemicals. CO_2 is not only the substrate for the production of value-added chemicals in CO_2-based bioprocesses, it can also be directly hydrated to formic acid, a so-called liquid organic hydrogen carrier (LOHC), by chemical and biological catalysts. Recently, a new group of enzymes were discovered in the two acetogenic bacteria *Acetobacterium woodii* and *Thermoanaerobacter kivui* which catalyze the direct hydrogenation of CO_2 to formic acid with exceptional high rates, the hydrogen-dependent CO_2 reductases (HDCRs). Since these enzymes are promising biocatalysts for the capturing of CO_2 and the storage of molecular hydrogen in form of formic acid, we designed a whole-cell approach for *T. kivui* to take advantage of using whole cells from a thermophilic organism as H_2/CO_2 storage platform. Additionally, *T. kivui* cells were used as microbial cell factories for the production of formic acid from syngas.

Results: This study demonstrates the efficient whole-cell biocatalysis for the conversion of $H_2 + CO_2$ to formic acid in the presence of bicarbonate by *T. kivui*. Interestingly, the addition of $KHCO_3$ not only stimulated formate formation dramatically but it also completely abolished unwanted side product formation (acetate) under these conditions and bicarbonate was shown to inhibit the membrane-bound ATP synthase. Cell suspensions reached specific formate production rates of 234 mmol $g_{protein}^{-1}$ h^{-1} (152 mmol g_{CDW}^{-1} h^{-1}), the highest rates ever reported in closed-batch conditions. The volumetric formate production rate was 270 mmol L^{-1} h^{-1} at 4 mg mL^{-1}. Additionally, this study is the first demonstration that syngas can be converted exclusively to formate using an acetogenic bacterium and high titers up to 130 mM of formate were reached.

Conclusions: The thermophilic acetogenic bacterium *T. kivui* is an efficient biocatalyst which makes this organism a promising candidate for future biotechnological applications in hydrogen storage, CO_2 capturing and syngas conversion to formate.

Keywords: Carbon capture, Syngas, Whole-cell biocatalysis, Closed-batch fermentation, Hydrogen-dependent CO_2 reductase, Formate dehydrogenase, Hydrogenase, Thermophiles, *Thermoanaerobacter kivui*

Background

Carbon dioxide and syngas are considered as "renewable options" in biotechnological applications, especially in times of global climate change and gradual increase of atmospheric CO_2 [1, 2]. Among the organisms able to reduce CO_2, strictly anaerobic, acetogenic bacteria have gained much attraction in recent years [3–5] because

*Correspondence: vmueller@bio.uni-frankfurt.de
Molecular Microbiology & Bioenergetics, Institute of Molecular Biosciences, Johann Wolfgang Goethe University, Max-von-Laue-Str. 9, 60438 Frankfurt am Main, Germany

they can use H_2 and CO as reductant for CO_2 reduction. The use of acetogenic bacteria to produce ethanol from syngas (H_2, CO, CO_2) is already realized on an industrial scale [6, 7]. The first step in acetogenic CO_2 reduction is the reduction of CO_2 to formic acid (Fig. 1). Acetogens are phylogenetically very diverse and employ different enzymes for this reaction [8, 9]. Typically, they have NADP- or ferredoxin-dependent formate dehydrogenases [10–12], whereas *Acetobacterium woodii* and *Thermoanaerobacter kivui* have a different enzyme, a hydrogen-dependent CO_2 reductase (HDCR) [13, 14]. This enzyme has a formate dehydrogenase module and a [FeFe]-hydrogenase module that are connected by two small FeS-containing proteins. In contrast to formate dehydrogenases, these enzymes can use molecular hydrogen directly as reductant for CO_2, without the need for external soluble cofactors. Interestingly, the enzyme also accepts electrons from CO (via ferredoxin) [14], making it a catalyst for the conversion of syngas to formic acid. The HDCR not only reduces CO_2 with remarkable catalytic activities but also oxidizes H_2 and, thus, can be used to kill two birds with one stone [14, 15]. Apart from CO_2 reduction, it can be used to store hydrogen gas in a liquid, non-toxic product, formic acid or its base, formate, a so-called liquid organic hydrogen carrier (LOHC) [16, 17]. The equilibrium constant for the conversion of $CO_2 + H_2$ to formic acid is close to one and, therefore, it is an ideal biocatalyst for the storage of H_2. All other enzymes known, including the membrane-bound formate hydrogen lyase of *Escherichia coli* have a strong bias towards formate oxidation and reduce CO_2 only under harsh conditions with low activities [18, 19].

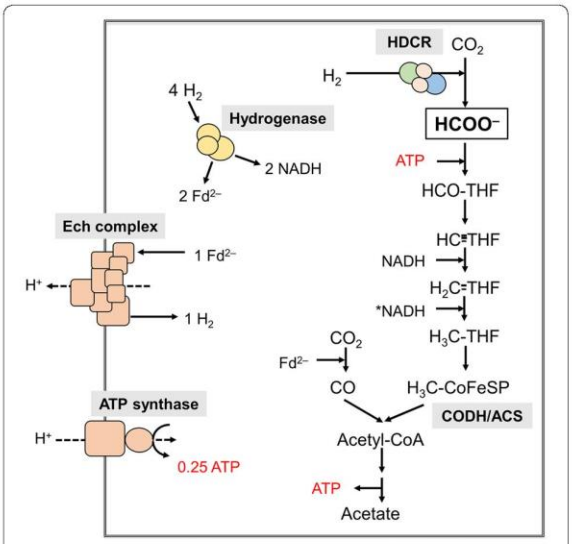

Fig. 1 Model of the biochemistry and bioenergetics of acetogenesis from $H_2 + CO_2$ in *T. kivui*. The bioenergetics and biochemistry of acetogenesis from $H_2 + CO_2$ by *T. kivui* are shown. CODH/ACS, CO dehydrogenase/acetyl-CoA synthase; Ech, energy-conserving hydrogenase; HDCR, hydrogen-dependent CO_2 reductase; hydrogenase, electron bifurcation hydrogenase; THF, tetrahydrofolic acid; HCO-THF, formyl-THF; HC-THF, methenyl-THF; H_2C-THF, methylene-THF; H_3C-THF, methyl-THF; CoFeSP, corrinoid iron–sulfur protein; Fd^{2-}, reduced ferredoxin; * reduction of methylene-THF might occur using an electron donor with a similar redox potential as NADH

Our isolated HDCR from *A. woodii* and *T. kivui* require strictly anoxic conditions which makes an application rather difficult. Using *A. woodii*, we have overcome this problem by establishing an efficient whole-cell system to convert $H_2 + CO_2$ to formic acid and vice versa [14, 15]. This system makes use of the ATP-dependent further conversion of formate in acetogens (Fig. 1). By lowering the cellular ATP content, formate is no longer reduced to acetate and stoichiometrically produced from $H_2 + CO_2$. However, *A. woodii* cannot grow on syngas or CO [20, 21] and resting cells produced only little formate from syngas and high amounts of acetate were still produced as unwanted side product [14]. In contrast, the HDCR containing thermophile *T. kivui* can grow in mineral medium on CO or syngas [22, 23]. Therefore, we started out to analyze hydrogenation of CO_2 in a whole-cell system of *T. kivui* with the aim to increase productivity (due to its thermophilic nature) and to establish an efficient whole-cell biocatalyst for hydrogen storage and formate production from syngas.

Results

Formate production by *T. kivui* cells

To analyze the potential use of whole cells of *T. kivui* as microbial cell factories for the efficient conversion of $H_2 + CO_2$ to formate, the organism was grown in complex medium with pyruvate as substrate and resting cells were prepared. As expected, the addition of $H_2 + CO_2$ to the cell suspension resulted in the production of acetate as the major end product with a specific acetate production rate of 19 mmol $g_{protein}^{-1}\ h^{-1}$ (12 mmol $g_{CDW}^{-1}\ h^{-1}$) (Fig. 2a). Formate was only produced in low amounts at the beginning of the experiment and was consumed afterwards. This is expected since formate is an intermediate in the WLP. As seen before with *A. woodii*, formate accumulation requires inhibition of further formate metabolism [14]. This can be achieved by reducing the energy status of the cell (Fig. 1). Hence, formate can no longer be activated due to a lack of ATP. One possibility to uncouple the energy metabolism of cells is by using ionophores. Depending on the ionophores used, there was a variation in the formate/acetate ratio after incubation with $H_2 + CO_2$ as substrate (Fig. 2b). In contrast to *A. woodii*, whose energy metabolism is strictly Na^+

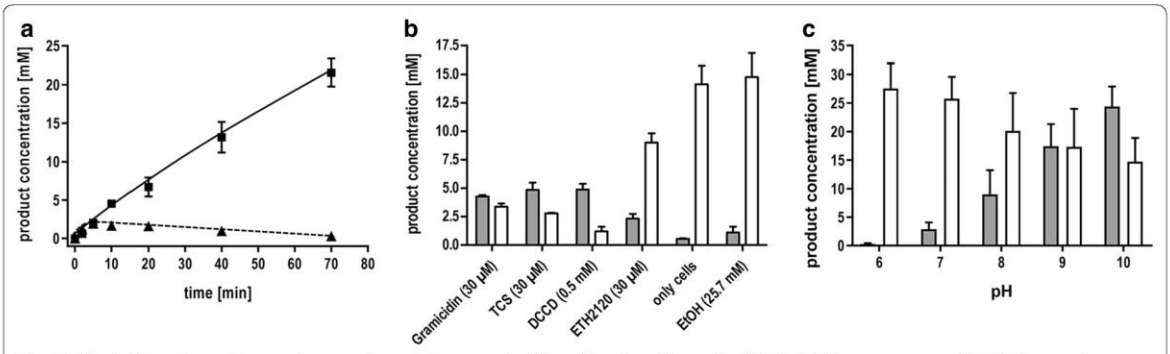

Fig. 2 Effect of ionophores/uncoupling agents and pH on product formation by resting cells of *T. kivui*. Cells were grown with 0.1 M pyruvate, harvested in the end-exponential growth phase and suspended in buffer (50 mM Imidazole, 20 mM KCl, 20 mM $MgSO_4$, 2 mM DTE, 4 µM Resazurin, pH 7.0 or 25 mM MES, 25 mM MOPS, 25 mM HEPES, 25 mM EPPS, 25 mM CHES, 20 mM KCl, 20 mM $MgSO_4$, 2 mM DTE, 4 µM Resazurin, pH as indicated) to a final concentration of 1 mg/mL. **a** Cells were incubated without or **b** with ionophores/uncoupling agents or (**c**) at the corresponding pH for 10 min at 60 °C. The experiment was started by replacing the gas phase with $H_2 + CO_2$ (80:20%, 2×10^5 Pa) and the product formation was determined after 40 (**b**) or 90 min (**c**). Squares and white bars, acetic acid; triangles and grey bars, formic acid

dependent [24, 25], the Na^+ ionophore ETH2120 had almost no effect on product formation in *T. kivui* and the dominant compound was acetate. 9.1 mM acetate was produced but only 2.3 mM formate. This is consistent with previous experiments and the assumption that H^+ instead of Na^+ is used as the coupling ion for the primary bioenergetics in *T. kivui* [26, 27]. Thus, a more favorable formate to acetate ratio of 1.7 was achieved using the protonophore 3,3,4,5-tetrachlorosalicylanilide (TCS). A four times higher formate yield was detected using the ATPase inhibitor *N,N′*-dicyclohexylcarbodiimide (DCCD). Since acetate was still produced, the membrane potential seemed to be not fully diminished by the ionophores used in this study.

Interestingly, a change in pH had a dramatic effect on the product yields (Fig. 2c). At pH 6.0, there was no formate produced, but formate production increased with increasing pH. At the same time, acetate production decreased, but to a lesser extent. This led to an inversion of the formate/acetate ratio from 0.01 at pH 6.0 to 1.7 at pH 10.

For further experiments, we added bicarbonate to resting cells to increase the available amount of CO_2 in solution and to achieve higher formate yields. At 50 mM bicarbonate, the acetate formation rate was slightly increased by 24% and, more important, the transient formation of formate was also increased by 319% (Fig. 3). At 300 mM bicarbonate acetate formation was completely abolished and formate production was drastically stimulated: The formate production rate was 220 mmol $g^{-1}_{protein}$ h^{-1} (143 mmol g^{-1}_{CDW} h^{-1}) and the final formate concentration reached 126 mM after 90 min.

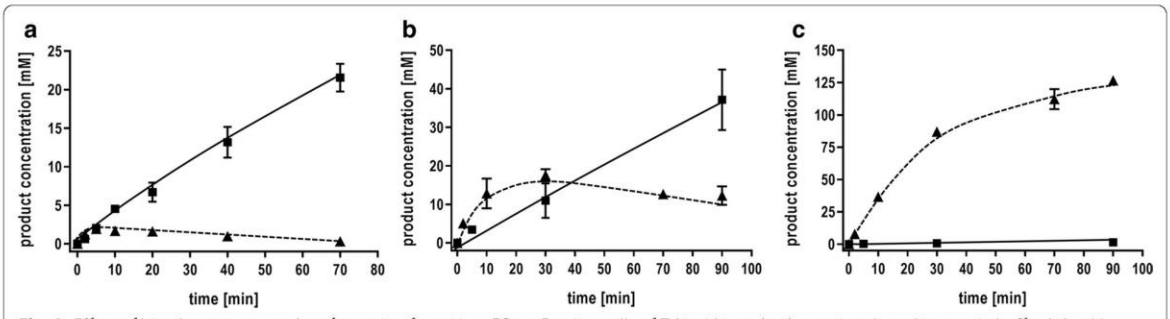

Fig. 3 Effect of bicarbonate on product formation from $H_2 + CO_2$. **a** Resting cells of *T. kivui* (1 mg/mL) were incubated in anoxic buffer (50 mM Imidazole, 20 mM KCl, 20 mM $MgSO_4$, 2 mM DTE, 4 µM resazurin, pH 7.0) with $H_2 + CO_2$ (80:20%, 2×10^5 Pa). **b** 50 mM or **c** 300 mM $KHCO_3$ were added to the cell suspensions before the experiment was started by replacing the gas phase. Squares, acetic acid; triangles, formic acid

Inhibitory effect of bicarbonate on ATP synthesis

To analyze the effect of bicarbonate on the energy metabolism of *T. kivui* in detail, the cellular ATP content of resting cells was measured in the presence or absence of bicarbonate (Fig. 4a). Therefore, cells were incubated in buffer with H_2+CO_2 as substrate, increasing bicarbonate concentrations were added and the ATP content was measured over time. As seen in Fig. 4a, the ATP content dropped immediately to zero if 300 mM bicarbonate was present in the cell suspensions. At 50 mM bicarbonate, there was also a decrease in the intracellular ATP content, but only by 62%. Next, we investigated the effect of bicarbonate on the activity of the membrane-bound ATPase in *T. kivui* (Fig. 4b). After the preparation of membranes, ATP hydrolysis was measured in the presence or absence of bicarbonate. Indeed, ATP hydrolysis as catalyzed by membranes (138 mU/mg) was inhibited by 81% by 300 mM $NaHCO_3$. The same was observed with $KHCO_3$. Additionally, we examined the ability of ATP synthesis by cell suspensions of *T. kivui* with an artificial ΔpH over the membrane as driving force (Additional file 1: Figure S1). In this experiment, resting cells were incubated in the presence or absence of 300 mM $KHCO_3$ and then HCl was added to induce a ΔpH across the membrane. At a ΔpH of 6, ATP was synthesized to 3.2 nmol $mg^{-1}_{protein}$. In contrast, when cells were incubated with 300 mM $KHCO_3$, ATP was only synthesized to 1.1 nmol $mg^{-1}_{protein}$. In accordance with the ATP hydrolysis experiments, only 34% of the ATP was synthesized in the presence of bicarbonate. Overall, these experiments could be interpreted to mean that the ATP synthase is inhibited by bicarbonate.

A possible pH effect by the addition of bicarbonate to the cell suspension was excluded. Therefore, the pH was adjusted in the control experiments with KOH to the same pH as in cell suspensions with additional 300 mM bicarbonate. The change in pH from 7.0 to 8.2 by the addition of KOH did not result in the same formate production. Only 14 mM of formate was formed after 90 min (data not shown).

Characterization of hydrogen-dependent CO_2 reduction by whole cells

After the discovery that bicarbonate completely inhibits further downstream processing of formate, formate production from H_2+CO_2 was studied in detail in the presence of 300 mM $KHCO_3$. The cells showed highest specific formate production rates of 220 mmol $g^{-1}_{protein}$ h^{-1} (143 mmol g^{-1}_{CDW} h^{-1}) at a temperature of 60 °C (Fig. 5a). Nevertheless, even at moderate reaction temperature of 30 °C, there was still a catalytic activity of 58 mmol $g^{-1}_{protein}$ h^{-1} (38 mmol g^{-1}_{CDW} h^{-1}). Moreover, an increase of the specific formate production rate up to 234 mmol $g^{-1}_{protein}$ h^{-1} (152 mmol g^{-1}_{CDW} h^{-1}) was observed at a cell concentration of 0.5 mg mL^{-1} (Fig. 5b). Increasing cell densities resulted in a linear increase of the volumetric formate production rates up to 270 mmol L^{-1} h^{-1} at 4 mg mL^{-1}. Simultaneously, the specific rates decreased.

Thermoanaerobacter kivui is a promising organism for industrial applications, since it can grow on syngas/CO in mineral medium without the requirement for

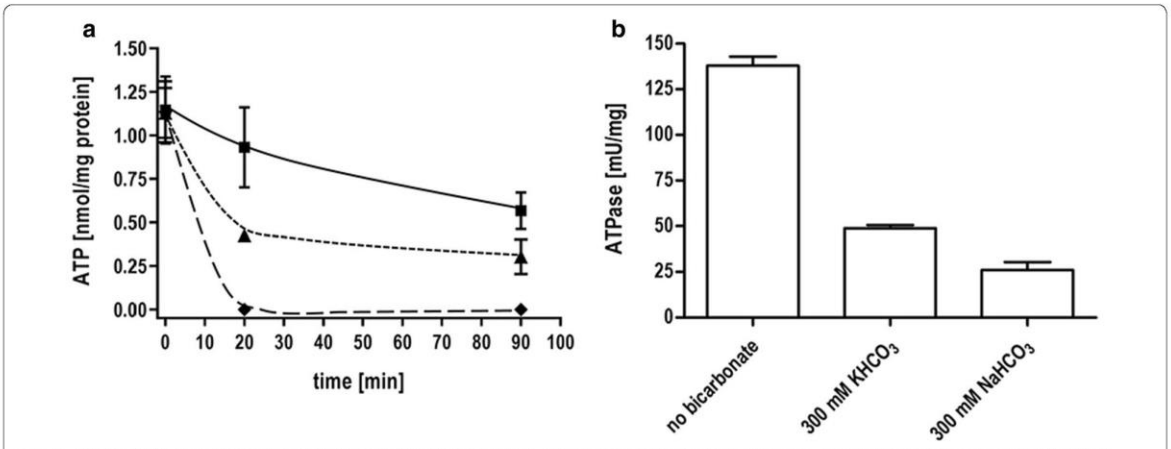

Fig. 4 Effect of bicarbonate on the ATP content of resting cells and ATP hydrolysis catalyzed by membranes of *T. kivui*. **a** Resting cells of *T. kivui* (1 mg/mL) were incubated in anoxic buffer (50 mM Imidazole, 20 mM KCl, 20 mM $MgSO_4$, 2 mM DTE, 4 µM Resazurin, pH 7,0) with H_2+CO_2 (80:20%, 2×10^5 Pa) in the absence or presence of $KHCO_3$ and the ATP content of cells were determined. Squares, without bicarbonate; triangles, 50 mM $KHCO_3$; diamonds, 300 mM $KHCO_3$. **b** Membranes from *T. kivui* were incubated for 3 min in the presence (300 mM $KHCO_3$ or 300 mM $NaHCO_3$) or absence of bicarbonate in buffer (100 mM Tris/HCl, 20 mM $MgSO_4$, 20 mM KCl, pH 7.0) and the ATP hydrolysis of membranes was determined

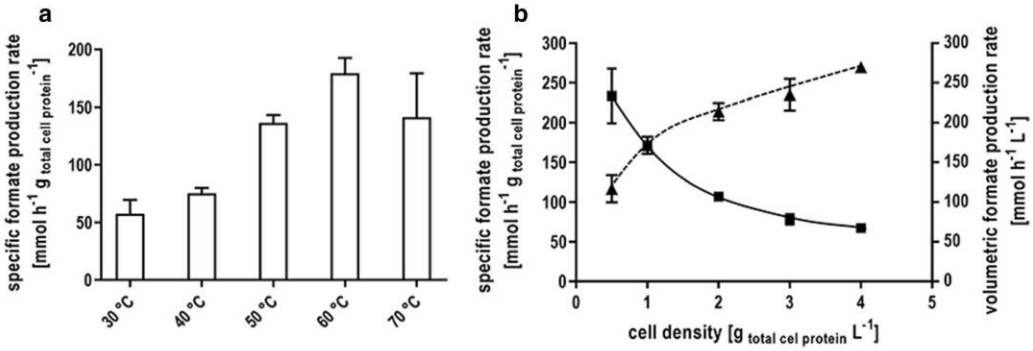

Fig. 5 Characterization of hydrogen-dependent CO_2 reduction by whole cells of *T. kivui*. **a** Resting cells of *T. kivui* (1 mg/mL) were incubated in anoxic buffer (50 mM Imidazole, 20 mM KCl, 20 mM $MgSO_4$, 2 mM DTE, 4 µM Resazurin, pH 7.0) with H_2+CO_2 (80:20%, 2×10^5 Pa) in the presence of 300 mM $KHCO_3$. Shown is the temperature profile for formate production by whole cells at the temperature indicated. **b** The influence of the cell density on formate production by resting cells was determined by applying a final concentration of 0.5–4 mg mL^{-1} in anoxic serum bottles at a temperature of 60 °C. 300 mM $KHCO_3$ was added to the cell suspension and the experiments were started by replacing the gas phase with H_2+CO_2 (80:20%, 2×10^5 Pa). The initial formate production rates (squares) and the volumetric production rates (triangle) were plotted against the cell density used in the experiment

yeast extract and additional vitamins [22, 28]. Therefore, we investigated the specific formate production rate of resting cells that were grown on mineral medium with pyruvate or glucose as growth substrate (Additional file 1: Figure S2). No differences in the specific formate production rates were observed if the complex medium was replaced by defined mineral medium in the cultivation process. Glucose-grown cells (in mineral medium) showed a slight decrease of 33% in the specific formate production rate compared to pyruvate grown cells.

Syngas conversion to formate

Syngas is an increasingly considered "green" option for the production of chemicals and biofuels [1] and *T. kivui* was already shown to grow on CO or syngas [22]. To analyze whether syngas is converted to formate, cells were grown on 50% CO and cell suspensions were prepared. A syngas mixture of H_2 (26%), CO_2 (11%) and CO (63%) was used as substrate. The gas consumption in the head space of the serum bottles was monitored by gas chromatography. In the absence of bicarbonate, resting cells converted syngas to acetate (Fig. 6a, b). Notably, the CO concentration decreased by 99 mM. At the same time, H_2 and CO_2 increased by only 26 and 74 mM, indicating that CO and H_2 were used as reductant for CO_2. If additional bicarbonate was added to the cell suspension, the product spectrum changed and mainly formate was produced in high titers up to 130 mM (Fig. 6c, d). The specific formate production rate was 8 mmol $g^{-1}_{protein}$ h^{-1} (5 mmol g^{-1}_{CDW} h^{-1}). CO was almost completely used up but the hydrogen level remained almost the same. This indicates that H_2 is not oxidized in the presence of CO and an alternative electron donor seems to be used for the reduction of CO_2 to formate. Additionally, a clear increase in the CO_2 concentration was detectable, provoked by the interconversion of HCO_3^- to CO_2. This is the first demonstration that syngas can be converted exclusively to formate by an acetogenic bacterium. *T. kivui* cells which were not adapted on CO, instead grown heterotrophic with pyruvate as substrate, showed only a little formation of acetate and almost no formate was produced in the presence of bicarbonate.

Formate production in closed-batch fermentation

Next, we wanted to establish a production platform for formate in closed-batch fermentation (Fig. 7). Here, *T. kivui* cells were grown in defined mineral medium with 28 mM glucose as substrate ($t_D = 3.2$ h) to an optical density of ~0.3. Then, bicarbonate, H_2+CO_2 or a combination of both were added. The addition of bicarbonate led to an immediate growth arrest and stop of acetate formation. By adding H_2+CO_2, the optical density did not increase but cells produced more acetate. Formate was not produced overall. Now, when bicarbonate and H_2+CO_2 were added, growth as well as acetate formation was completely abolished, but cells started to produce formate. The specific rate of formate production was 96 mmol $g^{-1}_{protein}$ h^{-1} (62 mmol g^{-1}_{CDW} h^{-1}). Finally, up to 50 mM formate was produced in the cultivation broth.

Discussion

Resting cells of *T. kivui* were proven in this study as highly efficient whole-cell biocatalysts for the direct hydrogenation of CO_2 to formate with remarkable catalytic

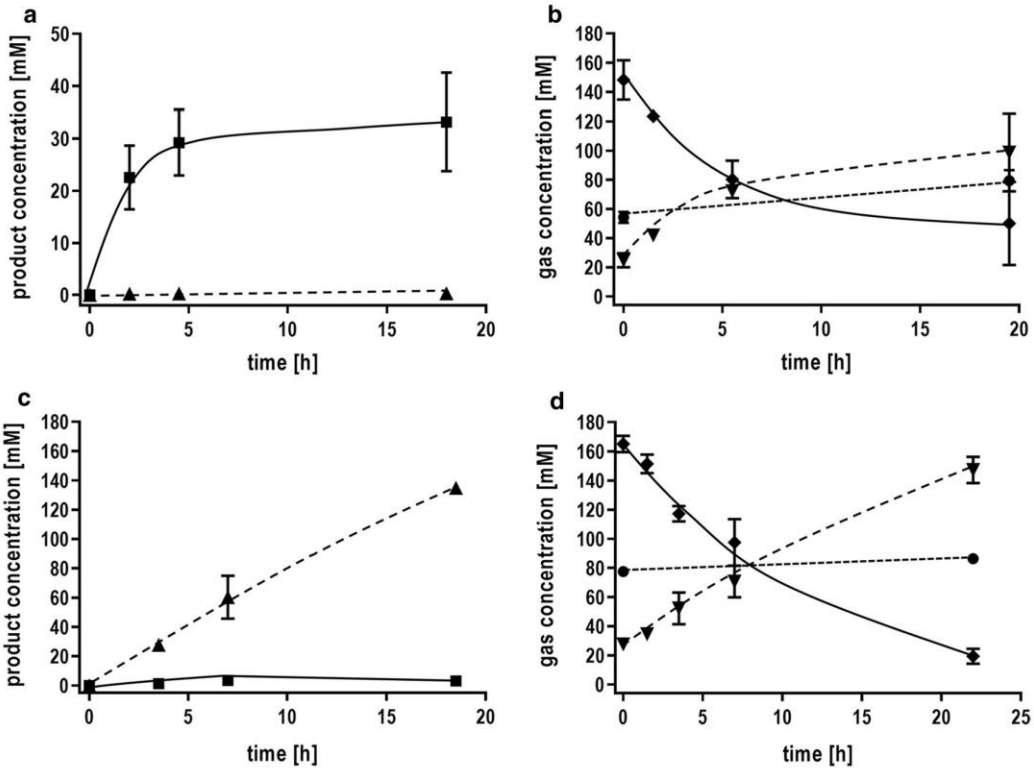

Fig. 6 Formate production from syngas using whole cells of *T. kivui*. Cells were grown on 50% CO in complex medium, harvested in the end-exponential growth phase and suspended in buffer (50 mM Imidazole, 20 mM KCl, 20 mM $MgSO_4$, 2 mM DTE, 4 µM Resazurin, pH 7,0) to a final concentration of 1 mg/mL in anoxic serum bottles. The experiment was started by replacing the gas phase with a mixture of H_2+CO_2+CO (26:11:63%, 2×10^5 Pa) **a**, **b** in the absence of bicarbonate and **c**, **d** in the presence of 300 mM $KHCO_3$. The product formation in liquid (**a**), **c** and the gas consumption in the head space (**b**, **d**) is shown over time. Squares, acetic acid; triangles, formic acid; diamonds, CO; triangles down, CO_2; circles, H_2

activities. In addition, we showed the first whole-cell approach for the exclusive conversion of syngas to formate using an acetogenic bacterium. The recently identified hydrogen-dependent CO_2 reductase (HDCR) [13] is the key enzyme in whole cell of *T. kivui* used as microbial cell factories for hydrogen storage, CO_2 capturing and syngas conversion to formate.

Since the K value for Eq. 1

$$H_2 + CO_2 \Leftrightarrow HCOO^- + H^+ \qquad \Delta G^{0'} = 3.5\ \mathrm{kJmol}^{-1} \tag{1}$$

is close to one, the chemical equilibrium can be easily controlled by small variations in pH, pressure and substrate/product concentrations. High concentrations of formate will favor the backwards reaction. An alkaline environment serves as proton scavenger and therefore pulls the reaction to the product side. The favored formate formation from H_2+CO_2 in a more alkaline environment was also observed in a whole-cell system for hydrogen-dependent CO_2 reduction based on *E. coli* [29]. By the addition of bicarbonate to resting cells, the available amount of CO_2 in solution was increased and the reaction was pushed towards product formation. Since formate dehydrogenases of the Mo/W-bis PGD family are known to use only CO_2 and not bicarbonate as substrate [12], we inspected the genome of *T. kivui* to identify a putative carbonic anhydrase (CA) which catalyzes the rapid interconversion of HCO_3^- and CO_2, and found one gene annotated as putative carbonic anhydrase/acetyltransferase (TKV_c11400). Consistent with this, cell extracts of *T. kivui* had specific CA activity of 0.17 U/mg [30].

Bicarbonate was identified here as an inhibitor of ATP synthesis. The inhibition of bacterial F_1F_0 ATP synthases by bicarbonate is not a common feature, but the effect was already described in literature [31, 32]. The effect of different anions like sulfite, azide and bicarbonate on the ATPase activity of membrane-bound F_1F_0 is known

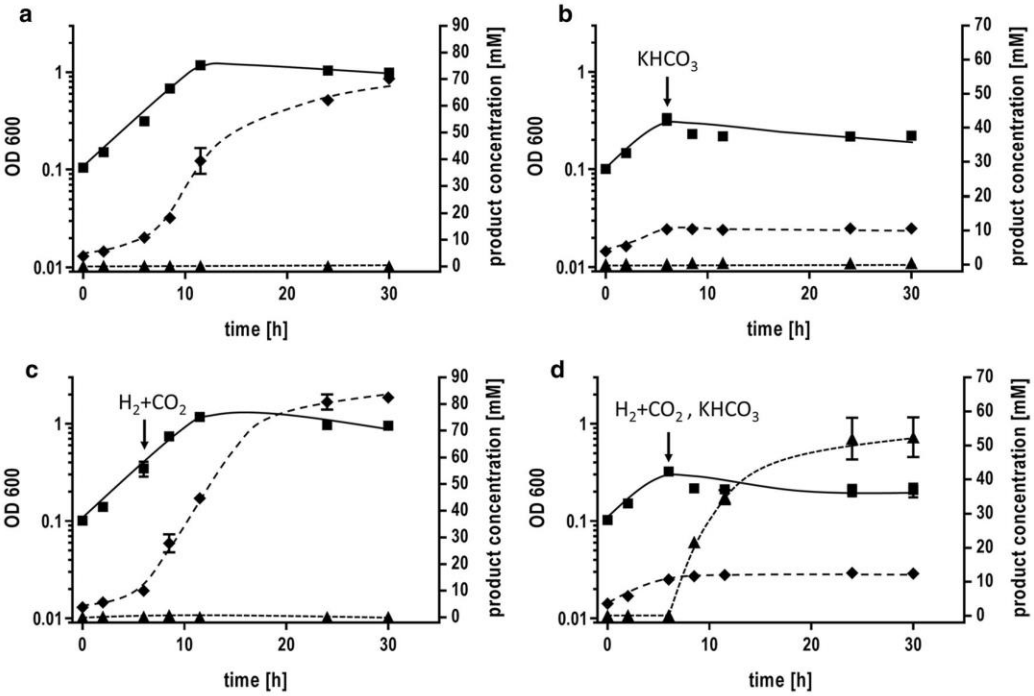

Fig. 7 Closed-batch fermentation for hydrogen-dependent CO_2 reduction to formic acid. **a** *T. kivui* was grown on 28 mM glucose in a defined mineral medium in a shaking water bath at 66 °C. At the time point indicated **b** 300 mM $KHCO_3$, **c** H_2+CO_2 (80:20%, 2×10^5 Pa) or **d** H_2+CO_2 (80:20%, 2×10^5 Pa) + 300 mM $KHCO_3$ were added to the growing culture. The optical density of the culture was between 0.3 and 0.4. Squares, OD_{600}; diamonds, acetic acid; triangles, formic acid

for decades but a detailed understanding of the mechanism of action of the activating anions is still missing and a matter of controversy [33–36]. In our study potassium bicarbonate could be replaced by sodium bicarbonate, indeed indicating an inhibitory effect of the anion HCO_3^-. Lodeyro et al. concluded in their study [32] that the anion bicarbonate competes with the binding of ADP to a low-affinity binding site instead of binding to a P_i site in the F_1 subunit. They postulated that ATP hydrolysis and inhibition of ATP synthesis was affected by bicarbonate by modulating the relative affinities of the catalytic site for ATP and ADP. Since anions like bicarbonate and acid were shown to bind to different sites on the mitochondrial F_1 subunit, further studies for the direct identification of the HCO_3^- binding site on the F_1F_0 ATP synthase of *T. kivui* have to be done. Purification and characterization of this enzyme could help to finally elucidate the mechanism and site of action of bicarbonate.

Whole-cell biocatalysis for the production of formate from the greenhouse gas CO_2 and the energy carrier H_2 was also observed in other biological systems [14, 29, 37]. Besides the acetogenic bacteria *A. woodii* and *T. kivui*, the well-known model organism *E. coli* was also used as a cell factory for the hydrogenation of CO_2 [29]. The key enzyme in *E. coli* to catalyze H_2+CO_2 conversion to formate is the membrane-bound formate hydrogen lyase (FHL) complex [18, 38]. But this enzyme is designed by nature to produce H_2 and CO_2 from formate under fermentative conditions and therefore, the catalytic rates for formate formation are pretty low and harsh conditions are required for the reaction. In a pH-controlled and highly pressurized reactor system (up to 10 bar overpressure), the specific formate production rates were 15 mmol g_{CDW}^{-1} h^{-1} [29]. This is only a small fraction of the activity of whole cells from *T. kivui* at moderate conditions of 30 or 60 °C with one bar overpressure. Here, the cells showed specific formate production rates of 58 mmol $g_{protein}^{-1}$ h^{-1} (38 mmol g_{CDW}^{-1} h^{-1}) and 220 mmol $g_{protein}^{-1}$ h^{-1} (143 mmol g_{CDW}^{-1} h^{-1}), respectively, qualifying *T. kivui* for applications at high and moderate reaction temperatures. Nevertheless, the thermophilic acetogenic bacterium *T. kivui* showed the highest specific formate production rates of 234 mmol $g_{protein}^{-1}$ h^{-1} (152 mmol g_{CDW}^{-1} h^{-1}) ever reported in biological systems (Table 1).

Furthermore, the volumetric formate production rates of 270 mmol L^{-1} h^{-1} at cell concentrations of 4 mg mL^{-1}

Table 1 Whole-cell biocatalysis for hydrogen-dependent CO_2 reduction to formate in closed-batch conditions

Organism	Reaction condition: temperature (°C)	Reaction condition: overpressure (MPa)	Mode	Specific formate production rate (mmol g_{CDW}^{-1} h^{-1})	Refs.
E. coli (WT)	37	10	Closed-batch bioreactor[a]	~15	[29]
E. coli (rec. strain[b])	37	–	Closed-batch (flasks)	~0.1	[37]
Desulfovibrio desulfuricans (WT)	37	1	Closed-batch (flasks)	~0.7	[39]
A. woodii (WT)	30	1	Closed-batch (flasks)	~22	[14]
T. kivui (WT)	30	1	Closed-batch (flasks)	~38	This study
	60	1	Closed-batch (flasks)	~152	This study

WT wild-type strain

[a] pH-controlled

[b] Rec. strain, recombinant *E. coli* strain JM109(DE3) overexpressing FDH of *Pyrococcus furiosus* (*FDH*_Pyrfu)

is not an insignificant economical factor: implementing high cell densities in a later fermentation process is considered to be one of the most effective ways for enhancing the productivity [40]. Efficient cell recycling and cell retention systems with optimized conditions for the accumulation of high cell densities up to 200 g/L were already implemented in bioprocesses [41–43].

The fermentation of syngas into biofuels and biochemicals using acetogenic bacteria has attracted more and more interest over the last few years and some acetogens were already implemented in this process [44–47]. Since the syngas composition depends strongly on the kind of gasifier and the kind and condition of the feedstock used, there is no "universal" composition of syngas. But it was already shown that *T. kivui* can be adapted to a carboxydotrophic lifestyle by a stepwise adaptation on increasing CO concentrations, up to 100% CO [22]. A detailed understanding of the CO metabolism in *T. kivui* is still missing. Since CO is a potent inhibitor of the active site of [FeFe]-hydrogenases [48–50], the HDCR hydrogenase subunit should be inactive and no formate should be formed. The inhibitory effect of CO on the HDCR hydrogenase activity of *A. woodii* was already described [14]. However, reduced ferredoxin can serve as an alternative electron donor for the reduction of CO_2 to formate in in vitro studies. This correlates with the finding that H_2 was not utilized by *T. kivui* in the previous syngas experiment if CO was present but formate was still produced. Therefore, the two annotated CO dehydrogenases genes in the genome of *T. kivui* could play a key role in the oxidation of CO to CO_2 with simultaneous reduction of ferredoxin, which is subsequently used by the HDCR for a ferredoxin-driven CO_2 reduction to formate.

In this study, we showed the feasibility of two approaches for the efficient conversion of H_2+CO_2 to formate: whole-cell biocatalysis and closed-batch bioprocess/fermentation. But the production rates as well as the finally produced formate concentration differed between the two approaches. The reasons could be diverse and are probably linked to pH, buffer capacity, feedback inhibition, etc. The applicability of growing cells as microbial cell factories has to be proven in further fermentation studies. Nevertheless, the addition of bicarbonate and H_2+CO_2 can switch the growing culture to the production of formate instead of acetate. The gases H_2+CO_2 can also serve in the first phase as growth substrate till the production phase is initiated. In this production phase, H_2+CO_2 act as reactants for the efficient production of formate. Whether the minimized cost-intensive and time-consuming work flow in a closed-batch fermentation can rebalance the increasing downstream costs due to the accumulation of unwanted metabolic side products (e.g., acetate) in the fermentation broth during the growth phase has to be considered and individually calculated.

Conclusion

This work demonstrates an efficient whole-cell approach for the production of formate from H_2+CO_2 or syngas using the thermophilic acetogen *T. kivui*. Bicarbonate seems to be an efficient inhibitor of the ATP synthase of this organism, thus preventing further downstream conversion of formate to acetate, resulting in high titers of the desired end product. *T. kivui* catalyzed the hydrogen-dependent CO_2 reduction with remarkable catalytic activities at elevated and ambient temperatures. Its thermophilic nature and the autotrophic growth properties on mineral medium qualify this organism for future fermentation approaches to address the process on a larger scale and to investigate the stability of the whole-cell system.

Methods

Organism and cultivation

Thermoanaerobacter kivui LKT-1 (DSM 2030) was cultivated at 66 °C under anaerobic conditions in complex and defined mineral medium [22]. Media were prepared under anoxic conditions as described before [51, 52]. Glucose (28 mM), pyruvate (100 mM) or CO (50% CO, 40% N_2 and 10% CO_2 [v/v] at 2×10^5 Pa) were used as growth substrate. Cell were cultivated in 1-L flasks (Müller-Krempel, Bülach, Switzerland) containing 500 mL or 200 mL medium in the case of autotrophic cultivation. Growth was determined by measuring the optical density at 600 nm with an UV/Vis spectrophotometer.

Preparation of resting cells and cell suspension experiments

For the preparation of resting cells, *T. kivui* was cultivated in 1-L flasks (Müller-Krempel, Bülach, Switzerland) in the above-mentioned growth media to the late exponential growth phase. Glucose- and fructose-grown cells were harvested at an OD_{600} of 1.7–2.0, CO-grown cells were harvested at OD_{600} of 0.6. The culture was centrifuged under anoxic conditions at 11,500 g and 4 °C for 10 min and was washed twice in imidazole puffer (50 mM imidazole–HCl, 20 mM $MgSO_4$, 20 mM KCl, 2 mM DTE, 4 µM resazurin, pH 7.0). Afterwards, the cells were resuspended, if not otherwise stated, in the same buffer to a protein concentration of 1 mg/mL and kept in gas-tight Hungate tubes. All preparation steps were performed under strictly anoxic conditions at room temperature in an anaerobic chamber (Coy Laboratory Products, Grass Lake, MI) as described [53]. The protein concentration of the cell suspension was determined according to [54] and the cells were directly used for the subsequent cell suspension experiments.

To determine the conversion of $H_2 + CO_2$ in cell suspension experiments, the 120-mL serum flasks (Glasgerätebau Ochs GmbH, Bovenden-Lenglern, Germany) contained pre-warmed buffer under a N_2 atmosphere, incubated with cell suspensions for 10 min at 60 °C. Subsequently, bicarbonate ($KHCO_3$ or $NaHCO_3$) was added and the gas phase of the serum flasks was changed to 2×10^5 Pa $H_2 + CO_2$ (80:20 [v/v]). When syngas was the substrate, the reaction was started by replacing the head space of the serum flasks with a gas composition of 26% H_2 + 11% CO_2 + 63% CO [v/v] at 2×10^5 Pa. Ionophores and uncoupling agents such as 3,3,4,5-tetrachlorosalicylanilide (TCS, dissolved in EtOH), *N,N,N′,N′*-tetracyclohexyl-1,2-phenylenedioxydiacetamide (ETH2120, dissolved in EtOH), gramicidin (dissolved in EtOH) and *N,N′*-dicyclohexylcarbodiimide (DCCD, dissolved in EtOH) were added 10 min prior to the reaction start. The serum flasks contained a final volume of 10 mL buffer in all the experiments. Samples were taken and ATP [55], acetate, formate, H_2, CO_2 and CO were determined as described before [13, 22].

Preparation of membranes and measurement of ATP hydrolysis activity

Cells were grown in 500 mL complex medium in 1-L flasks (Glasgerätebau Ochs, Bovenden-Lenglern, Germany) with 100 mM pyruvate as carbon source to an optical density at 600 nm of 1.7–2.0. The cells were harvested under toxic conditions at 11,500*g* for 10 min at 4 °C, were washed twice in buffer A (50 mM imidazole–HCl, 20 mM $MgSO_4$, 20 mM KCl, pH 7.0) and membranes were prepared as described before [26]. The protein concentration was determined as described [56] and the membranes were directly used to measure ATP hydrolysis.

For the determination of the ATP hydrolysis, membranes (200 µg) were resuspended in buffer B (100 mM Tris/HCl, 20 mM $MgSO_4$, 20 mM KCl, pH 7.0) to a final volume of 1200 µL and incubated at 60 °C for 3 min in the presence or absence of 300 mM $KHCO_3$. After addition of 2.5 mM Na_2ATP, samples (200 µL) were taken at defined time points and the ATP content was determined as described [55].

Closed-batch fermentation

Thermoanaerobacter kivui was grown at 66 °C in 50 mL mineral medium in 120 mL serum flasks (Glasgerätebau Ochs GmbH, Bovenden-Lenglern, Germany) with 28 mM glucose as growth substrate and a gas phase of $N_2 + CO_2$ (80:20 [v/v]). At OD_{600} 0.3–0.4 the growing cells were switched into the formate production phase by addition of 300 mM $KHCO_3$ and by changing the gas phase to a $H_2 + CO_2$ (80:20% [v/v]) atmosphere. Samples for the product determination were taken with a syringe.

Determination of cell dry weight

For cell dry weight determination of *T. kivui*, three independent cultures were grown in complex medium with 0.1 M pyruvate as growth substrate. At three different optical densities in the exponential growth phase the culture was harvested (4150*g*, 30 min, 4 °C) in technical triplicates (3×50 mL). Afterwards, the cell pellet was frozen in liquid N_2 and dried by lyophilisation over 24 h. The dried samples were weighted and the cell dry weight (CDW) was calculated to 0.379 mg/mL at OD_{600} of 1.

Supplementary information

Supplementary information accompanies this paper at https://doi.org/10.1186/s13068-020-1670-x.

Additional file 1: Figure S1. ATP synthesis by cell suspensions of *T. kivui* driven by an artificial ΔpH. Cells were grown with 0.1 M pyruvate, harvested in the end-exponential growth phase and suspended in buffer (50 mM Imidazole, 20 mM KCl, 20 mM $MgSO_4$, 2 mM DTE, 4 µM Resazurin, pH 7.0). Cell suspensions (1 mg/mL) were incubated with and without $KHCO_3$ for 10 min in buffer (25 mM Tris/HCl, 20 mM $MgCl_2$, pH 9.0) at 60 °C. At the time point indicated (arrow), HCl was added to the cell suspensions. Shown are data from one representative experiment out of two independent replicates. Squares, without $KHCO_3$; triangles, 300 mM $KHCO_3$.

Additional file 2: Figure S2. Specific formate production rates of resting cells from *T. kivui* grown on mineral medium. Cells were grown with 28 mM glucose or 0.1 M pyruvate in a defined mineral or complex medium, harvested in the end-exponential growth phase and suspended in buffer (50 mM Imidazole, 20 mM KCl, 20 mM $MgSO_4$, 2 mM DTE, 4 µM Resazurin, pH 7.0) to a final concentration of 1 mg/mL in anoxic serum bottles. The bottles were incubated in a shaking water bath for 10 min at 60 °C with additional 300 mM $KHCO_3$. The experiment was started by replacing the gas phase with $H_2 + CO_2$ (80:20%, 2×10^5 Pa). *MM* mineral medium, *CM* complex medium.

Abbreviations

LOHC: Liquid organic hydrogen carrier; HDCR: Hydrogen-dependent CO_2 reductase; *A. woodii*: *Acetobacterium woodii*; *T. kivui*: *Thermoanaerobacter kivui*; CDW: Cell dry weight; FHL: Formate hydrogen lyase; *E. coli*: *Escherichia coli*; ETH2120: *N,N,N′,N′*-Tetracyclohexyl-1,2-phenylenedioxydiacetamide; TCS: 3,3,4,5-Tetrachlorosalicylanilide; DCCD: *N,N′*-Dicyclohexylcarbodiimide; MES: 2-Morpholin-4-ylethanesulfonic acid; MOPS: 3-Morpholinopropane-1-sulfonic acid; HEPES: 2-[4-(2-Hydroxyethyl)piperazin-1-yl]ethanesulfonic acid; EPPS: 4-(2-Hydroxyethyl)piperazine-1-propanesulfonic acid; CHES: 2-(Cyclohexylamino)ethanesulfonic acid; Tris: 2-Amino-2-(hydroxymethyl)propane-1,3-diol; DTE: Dithioerythritol; HCO_3^-: Bicarbonate; t_D: Doubling time; *K*: Equilibrium constant; $\Delta G^{0'}$: Gibbs energy; Mo/W-bis PGD: Molybdenum/tungsten-bis pyranopterin guanosine dinucleotide; CA: Carbonic anhydrase; UV/Vis: Ultraviolet/visible; OD: Optical density.

Authors' contributions

VM designed and supervised the research, analyzed the data and wrote the manuscript. FMS designed the research, performed the experiments, analyzed the data and wrote the manuscript. Both authors read and approved the final manuscript.

Funding

This project has received funding from the European Research Council (ERC) under the European Union's Horizon 2020 research and innovation programme (Grant Agreement No 741791).

Availability of data and materials

All data generated or analyzed during this study are included in this published article.

Ethics approval and consent to participate

Not applicable.

Consent for publication

Not applicable.

Competing interests

The authors declare that they have no competing interests.

Received: 9 November 2019 Accepted: 28 January 2020
Published online: 28 February 2020

References

1. Munasinghe PC, Khanal SK. Biomass-derived syngas fermentation into biofuels: opportunities and challenges. Bioresour Technol. 2010;101:5013–22.
2. Mondal M, Goswami S, Ghosh A, Oinam G, Tiwari ON, Das P, Gayen K, Mandal MK, Halder GN. Production of biodiesel from microalgae through biological carbon capture: a review. 3 Biotech. 2017;7:99.
3. Bengelsdorf FR, Poehlein A, Linder S, Erz C, Hummel T, Hoffmeister S, Daniel R, Dürre P. Industrial acetogenic biocatalysts: a comparative metabolic and genomic analysis. Front Microbiol. 2016;7:1036.
4. Nevin KP, Hensley SA, Franks AE, Summers ZM, Ou J, Woodard TL, Snoeyenbos-West OL, Lovley DR. Electrosynthesis of organic compounds from carbon dioxide is catalyzed by a diversity of acetogenic microorganisms. Appl Environ Microbiol. 2011;77:2882–6.
5. Müller V. New horizons in acetogenic conversion of one-carbon substrates and biological hydrogen storage. Trends Biotechnol. 2019;37:1344–54.
6. Bengelsdorf FR, Straub M, Dürre P. Bacterial synthesis gas (syngas) fermentation. Environ Technol. 2013;34:1639–51.
7. Daniell J, Köpke M, Simpson SD. Commercial biomass syngas fermentation. Energies. 2012;5:5372–417.
8. Drake HL. Acetogenesis, acetogenic bacteria, and the acetyl-CoA pathway: past and current perspectives. In: Drake HL, editor. Acetogenesis. New York: Chapman and Hall; 1994. p. 3–60.
9. Müller V, Inkamp F, Rauwolf A, Küsel K, Drake HL. Molecular and cellular biology of acetogenic bacteria. In: Nakano M, Zuber P, editors. Strict and facultative anaerobes Medical and environmental aspects. Norfolk: Horizon Scientific Press; 2004. p. 251–81.
10. Wang S, Huang H, Kahnt J, Mueller AP, Köpke M, Thauer RK. NADP-specific electron-bifurcating [FeFe]-hydrogenase in a functional complex with formate dehydrogenase in *Clostridium autoethanogenum* grown on CO. J Bacteriol. 2013;195:4373–86.
11. Yamamoto I, Saiki T, Liu SM, Ljungdahl LG. Purification and properties of NADP-dependent formate dehydrogenase from *Clostridium thermoaceticum*, a tungsten-selenium-iron protein. J Biol Chem. 1983;258:1826–32.
12. Maia LB, Moura JJ, Moura I. Molybdenum and tungsten-dependent formate dehydrogenases. J Biol Inorg Chem. 2015;20:287–309.
13. Schwarz FM, Schuchmann K, Müller V. Hydrogenation of CO_2 at ambient pressure catalyzed by a highly active thermostable biocatalyst. Biotechnol Biofuels. 2018;11:237.
14. Schuchmann K, Müller V. Direct and reversible hydrogenation of CO_2 to formate by a bacterial carbon dioxide reductase. Science. 2013;342:1382–5.
15. Kottenhahn P, Schuchmann K, Müller V. Efficient whole cell biocatalyst for formate-based hydrogen production. Biotechnol Biofuels. 2018;11:93.
16. Preuster P, Papp C, Wasserscheid P. Liquid organic hydrogen carriers (LOHCs): toward a hydrogen-free hydrogen economy. Acc Chem Res. 2017;50:74–85.
17. Enthaler S, von Langermann J, Schmidt T. Carbon dioxide and formic acid-the couple for environmental-friendly hydrogen storage? Energy Environ Sci. 2010;3:1207–17.
18. McDowall JS, Murphy BJ, Haumann M, Palmer T, Armstrong FA, Sargent F. Bacterial formate hydrogenlyase complex. Proc Natl Acad Sci USA. 2014;111:E3948–56.
19. Pinske C, Sargent F. Exploring the directionality of *Escherichia coli* formate hydrogenlyase: a membrane-bound enzyme capable of fixing carbon dioxide to organic acid. Microbiologyopen. 2016;5:721–37.
20. Bertsch J, Müller V. CO metabolism in the acetogen *Acetobacterium woodii*. Appl Environ Microbiol. 2015;81:5949–56.
21. Bertsch J, Müller V. Bioenergetic constraints for conversion of syngas to biofuels in acetogenic bacteria. Biotechnol Biofuels. 2015;8:210.
22. Weghoff MC, Müller V. CO metabolism in the thermophilic acetogen *Thermoanaerobacter kivui*. Appl Environ Microbiol. 2016;82:2312–9.
23. Schölmerich MC, Müller V. Energy conservation by a hydrogenase-dependent chemiosmotic mechanism in an ancient metabolic pathway. Proc Natl Acad Sci USA. 2019;116:6329–34.
24. Biegel E, Müller V. Bacterial Na^+-translocating ferredoxin:NAD^+ oxidoreductase. Proc Natl Acad Sci USA. 2010;107:18138–42.
25. Müller V, Aufurth S, Rahlfs S. The Na^+ cycle in *Acetobacterium woodii*: identification and characterization of a Na^+-translocating F_1F_O-ATPase with

a mixed oligomer of 8 and 16 kDa proteolipids. Biochim Biophys Acta. 2001;1505:108–20.
26. Hess V, Poehlein A, Weghoff MC, Daniel R, Müller V. A genome-guided analysis of energy conservation in the thermophilic, cytochrome-free acetogenic bacterium *Thermoanaerobacter kivui*. BMC Genomics. 2014;15:1139.
27. Yang H, Drake HL. Differential effects of sodium on hydrogen- and glucose-dependent growth of the acetogenic bacterium *Acetogenium kivui*. Appl Environ Microbiol. 1990;56:81–6.
28. Leigh JA, Mayer F, Wolfe RS. *Acetogenium kivui*, a new thermophilic hydrogen-oxidizing, acetogenic bacterium. Arch Microbiol. 1981;129:275–80.
29. Roger M, Brown F, Gabrielli W, Sargent F. Efficient hydrogen-dependent carbon dioxide reduction by *Escherichia coli*. Curr Biol. 2018;28:140–5.
30. Braus-Stromeyer SA, Schnappauf G, Braus GH, Gössner AS, Drake HL. Carbonic anhydrase in *Acetobacterium woodii* and other acetogenic bacteria. J Bacteriol. 1997;179:7197–200.
31. Das A, Ljungdahl LG. *Clostridium pasteurianum* F_1F_O ATP synthase: operon, composition, and some properties. J Bacteriol. 2003;185:5527–35.
32. Lodeyro AF, Calcaterra NB, Roveri OA. Inhibition of steady-state mitochondrial ATP synthesis by bicarbonate, an activating anion of ATP hydrolysis. Biochim Biophys Acta. 2001;1506:236–43.
33. Ebel RE, Lardy HA. Stimulation of rat liver mitochondrial adenosine triphosphatase by anions. J Biol Chem. 1975;250:191–6.
34. Recktenwald E, Hess B. Allosteric influence of anions on mitochondrial ATPase of yeast. FEBS Lett. 1977;76:25–8.
35. Du ZY, Boyer PD. On the mechanism of sulfite activation of chloroplast thylakoid ATPase and the relation of ADP tightly bound at a catalytic site to the binding change mechanism. Biochemistry. 1990;29:402–7.
36. Hartog AF, Edel CM, Braham J, Muijsers AO, Berden JA. FSBA modifies both α- and β-subunits of F1 specifically and can be bound together with AXP at the same alpha-subunit. Biochim Biophys Acta. 1997;1318:107–22.
37. Alissandratos A, Kim HK, Easton CJ. Formate production through carbon dioxide hydrogenation with recombinant whole cell biocatalysts. Bioresour Technol. 2014;164:7–11.
38. Stephenson M, Stickland LH. Hydrogenlyases: bacterial enzymes liberating molecular hydrogen. Biochem J. 1932;26:712–24.
39. Mourato C, Martins M, da Silva SM, Pereira IAC. A continuous system for biocatalytic hydrogenation of CO_2 to formate. Bioresour Technol. 2017;235:149–56.
40. Lin B, Tao Y. Whole-cell biocatalysts by design. Microb Cell Fact. 2017;16:106.
41. Mauerhofer LM, Pappenreiter P, Paulik C, Seifert AH, Bernacchi S, Rittmann SKR. Methods for quantification of growth and productivity in anaerobic microbiology and biotechnology. Folia Microbiol. 2019;64:321–60.
42. Richter K, Nottelmann S. An empiric steady state model of lactate production in continuous fermentation with total cell retention. Eng Life Sci. 2004;4:426–32.
43. Okabe M, Oda A, Park YS, Noguchi K, Okamoto T, Mitsui S. Continuous beer fermentation by high cell-density culture of bottom brewer's yeast. J Ferment Bioeng. 1994;77:41–5.
44. Henstra AM, Sipma J, Rinzema A, Stams AJ. Microbiology of synthesis gas fermentation for biofuel production. Curr Opin Biotechnol. 2007;18:200–6.
45. Liew F, Martin ME, Tappel RC, Heijstra BD, Mihalcea C, Köpke M. Gas fermentation-a flexible platform for commercial scale production of low-carbon-fuels and chemicals from waste and renewable feedstocks. Front Microbiol. 2016;7:694.
46. Liew F, Henstra AM, Köpke M, Winzer K, Simpson SD, Minton NP. Metabolic engineering of *Clostridium autoethanogenum* for selective alcohol production. Metab Eng. 2017;40:104–14.
47. Köpke M, Held C, Hujer S, Liesegang H, Wiezer A, Wollherr A, Ehrenreich A, Liebl W, Gottschalk G, Dürre P. *Clostridium ljungdahlii* represents a microbial production platform based on syngas. Proc Natl Acad Sci USA. 2010;107:13087–92.
48. Lubitz W, Ogata H, Rudiger O, Reijerse E. Hydrogenases. Chem Rev. 2014;114:4081–148.
49. Goldet G, Brandmayr C, Stripp ST, Happe T, Cavazza C, Fontecilla-Camps JC, Armstrong FA. Electrochemical kinetic investigations of the reactions of [FeFe]-hydrogenases with carbon monoxide and oxygen: comparing the importance of gas tunnels and active-site electronic/redox effects. J Am Chem Soc. 2009;131:14979–89.
50. Baffert C, Bertini L, Lautier T, Greco C, Sybirna K, Ezanno P, Etienne E, Soucaille P, Bertrand P, Bottin H, et al. CO disrupts the reduced H-cluster of FeFe hydrogenase. A combined DFT and protein film voltammetry study. J Am Chem Soc. 2011;133:2096–9.
51. Bryant MP. Commentary on the Hungate technique for culture of anaerobic bacteria. The American journal of clinical nutrition. 1972;25:1324–8.
52. Hungate RE. A roll tube method for cultivation of strict anaerobes. In: Norris JR, Ribbons DW, editors. Methods in microbiology, vol. 3b. New York and London: Academic Press; 1969. p. 117–32.
53. Heise R, Müller V, Gottschalk G. Presence of a sodium-translocating ATPase in membrane vesicles of the homoacetogenic bacterium *Acetobacterium woodii*. Eur J Biochem. 1992;206:553–7.
54. Schmidt K, Liaaen-Jensen S, Schlegel HG. Die Carotinoide der Thiorhodaceae. Arch Mikrobiol. 1963;46:117–26.
55. Kimmich GA, Randles J, Brand JS. Assay of picomole amounts of ATP, ADP and AMP using the luciferase enzyme system. Anal Biochem. 1975;69:187–206.
56. Lowry OH, Rosebrough NJ, Farr AL, Randall RJ. Protein measurement with the Folin-phenol reagent. J Biol Chem. 1951;193:265–75.

Publisher's Note

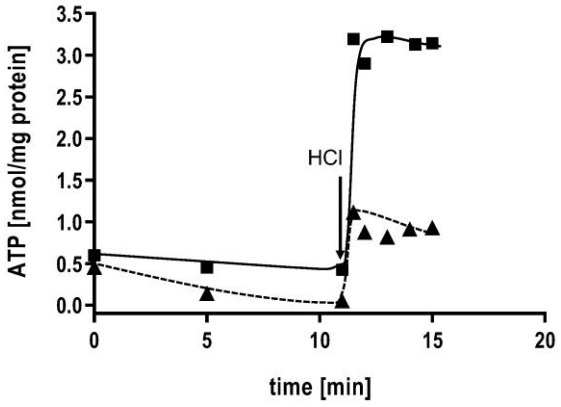

Additional file 1: Figure S1. ATP synthesis by cell suspensions of *T.kivui* driven by an artificial ΔpH. Cells were grown with 0.1 M pyruvate, harvested in the end-exponential growth phase and suspended in buffer (50 mM Imidazole, 20 mM KCl, 20 mM $MgSO_4$, 2 mM DTE, 4 µM Resazurin, pH 7.0). Cell suspensions (1 mg/mL) were incubated with and without $KHCO_3$ for 10 min in buffer (25 mM Tris/HCl, 20 mM $MgCl_2$, pH 9.0) at 60 °C. At the time point indicated (arrow), HCl was added to the cell suspensions. Shown are data from one representative experiment out of two independent replicates. Squares, without $KHCO_3$; triangles, 300 mM $KHCO_3$.

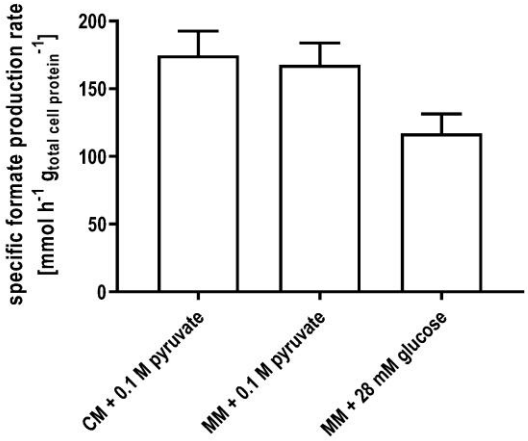

Additional file 2: Figure S2. Specific formate production rates of resting cells from *T. kivui* grown on mineral medium. Cells were grown with 28 mM glucose or 0.1 M pyruvate in a defined mineral or complex medium, harvested in the end-exponential growth phase and suspended in buffer (50 mM Imidazole, 20 mM KCl, 20 mM $MgSO_4$, 2 mM DTE, 4 µM Resazurin, pH 7.0) to a final concentration of 1 mg/mL in anoxic serum bottles. The bottles were incubated in a shaking water bath for 10 min at 60 °C with additional 300 mM $KHCO_3$. The experiment was started by replacing the gas phase with H_2 + CO_2 (80:20%, 2 × 105 Pa). *MM* mineral medium, *CM* complex medium.

6.2. Revealing formate production from carbon monoxide in wild type and mutants of Rnf- and Ech-containing acetogens, *Acetobacterium woodii* and *Thermoanaerobacter kivui*

Declaration of author contributions to the publication / manuscript (title):

Revealing formate production from carbon monoxide in wild type and mutants of Rnf- and Ech-containing acetogens, *Acetobacterium woodii* and *Thermoanaerobacter kivui*

Status: published, 2020

Journal: Microbial Biotechnology

Contributing authors: Fabian M. Schwarz (F.M.S.), Sara Ciurus (S.C.), Surbhi Jain (S.C.), Christoph Baum (C.B.), Anja Wiechmann (A.W.), Mirko Basen (M.B.) and Volker Müller (V.M.)

What are the contributions of the doctoral candidate and his co-authors?

(1) Concept and design

Doctoral candidate F.M.S.: 30%

Co-author S.C.: 10%

Co-author V.M.: 60%

(2) Conducting tests and experiments

Doctoral candidate F.M.S.: Performed all experiments with the organism *Thermoanaerobacter kivui* and its mutants.

Co-author S.C.: Performed all experiments with the organism *Acetobacterium woodii* and its mutants.

Co-author S.J.: Generated and provided the mutant strains *T. kivui* Δ*hdcr* and *T. kivui* Δ*cooS*

Co-author C.B.: Generated and provided the mutant strain *T. kivui* Δ*ech2*

Co-author A.W.: Generated and provided the mutant strains *A. woodii* Δ*rnf* and *A. woodii* Δ*hydBA*

(3) Compilation of data sets and figures

Doctoral candidate F.M.S.: Compiled the figures and data sets for Fig. 1C/D, Fig. 2, Fig. 3, Fig. 4, Fig. 5 and Fig. 8

Co-author S.C.: Compiled the figures and data sets for Fig. 1A/B, Fig. 6, Fig. 7, Table 1 and the Additional Files S1-S3

(4) Analysis and interpretation of data

Doctoral candidate F.M.S.: Analyzed and interpreted all data

Co-author S.C.: Analyzed and interpreted the data for the *A. woodii* experiments

Co-author V.M.: Analyzed and interpreted all data

(5) Drafting of manuscript

Doctoral candidate F.M.S.: 40%

Co-author V.M.: 60%

microbial biotechnology

Open Access

Revealing formate production from carbon monoxide in wild type and mutants of Rnf- and Ech-containing acetogens, *Acetobacterium woodii* and *Thermoanaerobacter kivui*

Fabian M. Schwarz,[1] Sarah Ciurus,[1] Surbhi Jain,[1] Christoph Baum,[2] Anja Wiechmann,[1] Mirko Basen[2] and Volker Müller[1*]

[1]*Molecular Microbiology and Bioenergetics, Institute of Molecular Biosciences, Johann Wolfgang Goethe University, Frankfurt am Main, Germany.*

[2]*Microbiology, Institute of Biological Sciences, University Rostock, Rostock, Germany.*

Summary

Acetogenic bacteria have gained much attraction in recent years as they can produce different biofuels and biochemicals from H_2 plus CO_2 or even CO alone, therefore opening a promising alternative route for the production of biofuels from renewable sources compared to existing sugar-based routes. However, CO metabolism still raises questions concerning the biochemistry and bioenergetics in many acetogens. In this study, we focused on the two acetogenic bacteria *Acetobacterium woodii* and *Thermoanaerobacter kivui* which, so far, are the only identified acetogens harbouring a H_2-dependent CO_2 reductase and furthermore belong to different classes of 'Rnf'- and 'Ech-acetogens'. Both strains catalysed the conversion of CO into the bulk chemical acetate and formate. Formate production was stimulated by uncoupling the energy metabolism from the Wood–Ljungdahl pathway, and specific rates of 1.44 and 1.34 mmol g^{-1} h^{-1} for *A. woodii* Δ*rnf* and *T. kivui* wild type were reached. The demonstrated CO-based formate production rates are, to the best of our knowledge, among the highest rates ever reported. Using mutants of Δ*hdcr*, Δ*cooS*, Δ*hydBA*, Δ*rnf* and Δ*ech2* with deficiencies in key enzyme activities of the central metabolism enabled us to postulate two different CO utilization pathways in these two model organisms.

Received 2 July, 2020; revised 18 August, 2020; accepted 19 August, 2020.
*For correspondence. E-mail vmueller@bio.uni-frankfurt.de; Tel: (+49) 69 79829507; Fax (+49) 69 79829306.
Microbial Biotechnology (2020) **13**(6), 2044–2056
doi:10.1111/1751-7915.13663
Funding information
This project has received funding from the European Research Council (ERC) under the European Union's Horizon 2020 research and innovation programme (grant agreement no 741791).

Introduction

Most bulk chemicals are still based on fossil fuels, such as crude oil and natural gas. But in times of global climate change and the fear of dwindling resources, the development of sustainable biological methods for the production of industrially relevant chemicals is urgently needed. Historically, biotechnological production plants for chemicals were based on sugar (i.e. sugarcane, corn and wheat) (Naik *et al.*, 2010) and there is a broad range of processes for the production of different compounds from different sources by different organisms (Wendisch, 2014). However, the processes have in common that they also produce CO_2 and that they compete with the food industry for the same feedstock (Fargione *et al.*, 2008; Ajanovic, 2011). Second-generation biofuels are based on lignocellulose (Naik *et al.*, 2010; Kucharska *et al.*, 2018), but, again, the process is not CO_2 neutral and due to technical and non-technical barriers most projects of this kind were put on hold (Padella *et al.*, 2019). Third-generation biofuels are based on carbon oxides as feedstock and instead of producing CO_2 gas fermentation captures and stores CO_2 in the form of value-added chemicals (Munasinghe and Khanal, 2010; Dürre and Eikmanns, 2015; Liew *et al.*, 2016b; Bengelsdorf and Dürre, 2017). One available CO_2 source is synthesis gas (syngas) which mainly consists of H_2, CO_2 and CO. Syngas can be obtained from industrial exhaust gases, such as steel mill off-gas (Köpke *et al.*, 2011) or by gasification of biomass and waste streams, such as sewage sludge and municipal waste (Hammerschmidt *et al.*, 2011; Rokni, 2015).

Many microbes are known to convert syngas into chemicals (Henstra *et al.*, 2007b; Bengelsdorf *et al.*, 2013; Bengelsdorf *et al.*, 2018). Among those are the acetogenic bacteria that grow autotrophically by converting H_2 + CO_2 to acetate according to Eq. 1:

$$4H_2 + 2CO_2 \leftrightarrow CH_3COO^- + H^+ + 2H_2O \quad \Delta G'_0 = -95\,kJ/mol \quad (1)$$

Some are also able to produce ethanol in addition to acetate (Najafpour and Younesi, 2006; Maddipati *et al.*, 2011; Bertsch and Müller, 2015a). Many acetogens can also grow on carbon monoxide according to Eq. 2:

$$4CO + 2H_2O \leftrightarrow CH_3COO^- + H^+ + 2CO_2 \quad \Delta G'_0 = -165.6\,kJ/mol \quad (2)$$

CO is first oxidized to CO_2 which is subsequently reduced to acetate with electrons derived from CO oxidation (Diekert and Thauer, 1978; Diender *et al.*, 2015). The production of acetate and ethanol from syngas requires a linear pathway of CO_2 reduction that has two branches, the Wood–Ljungdahl pathway (WLP; Drake, 1994; Ragsdale, 2008; Schuchmann and Müller, 2016). In the methyl branch, one molecule of CO_2 is first reduced to formate, then bound at the expense of ATP hydrolysis to the cofactor tetrahydrofolic acid (THF) and reduced in a THF-bound form to a methyl group. In the second branch, the carbonyl branch, a second molecule of carbon dioxide, is reduced by the enzyme CO dehydrogenase/acetyl-CoA synthase (CODH/ACS) to enzyme-bound CO which is then combined with the methyl group and coenzyme A on the CODH/ACS to acetyl-CoA. Acetyl-CoA is then converted *via* acetyl phosphate to acetate generating one ATP (Diekert and Wohlfarth, 1994). Although the ATP yield by substrate level phosphorylation is zero, the bacteria grow by this conversion, due to additional ATP generation by a chemiosmotic mechanism that involves an energized membrane for ATP synthesis (Müller, 2003; Poehlein *et al.*, 2012; Schuchmann and Müller, 2014). The respiratory enzymes present in acetogens are either the Rnf or the Ech complex (Biegel and Müller, 2010; Schölmerich and Müller, 2019). Therefore, acetogens can bioenergetically be classified in 'Rnf-' and 'Ech-acetogens' (Schuchmann and Müller, 2014). The translocated ions by these complexes (and the ATP synthase) could either be Na^+ or H^+. In *A. woodii,* the Rnf complex translocates Na^+ and the Ech complex of *T. kivui* translocates H^+, whereas the Rnf complex of *Clostridium ljungdahlii* most likely pumps H^+ (Tremblay *et al.*, 2012). However, acetogens grow at the thermodynamic limit of life and only a fraction of an ATP is made per turnover (Müller, 2015; Spahn *et al.*, 2015; Müller and Hess, 2017).

Acetyl-CoA (or acetate) can be converted to ethanol, and some acetogens like *Clostridium autoethanogenum* are used industrially to produce ethanol from syngas (Bengelsdorf *et al.*, 2013; Takors *et al.*, 2018; Köpke and Simpson, 2020). Some acetogens naturally produce minor amounts of butyrate or lactate (Liou *et al.*, 2005; Köpke *et al.*, 2011; Jeong *et al.*, 2015). However, with the advent of genetic tools in acetogens metabolic engineering is now possible leading to many new products like acetone, butanol, 3-hydroxybutyrate and isopropanol (Köpke *et al.*, 2010; Banerjee *et al.*, 2014; Bengelsdorf *et al.*, 2016; Bengelsdorf and Dürre, 2017). Since acetogens are energy-limited during growth on $H_2 + CO_2$, minor amounts of the compound of interest are produced along with major amounts of acetic acid. With CO as electron source, the energetics are much better and the selectivity is increased (Bertsch and Müller, 2015a).

Formic acid is produced by many acetogens transiently during acetogenesis from $H_2 + CO_2$ (Peters *et al.*, 1999). Formate is an interesting product since it can be further converted by acetogens or other formatotrophic organisms into higher value-added chemicals (Harris *et al.*, 2007; Cotton *et al.*, 2019; Hwang *et al.*, 2020). Recently, we discovered a novel class of formate dehydrogenases in the acetogens *Acetobacterium woodii* and *Thermoanaerobacter kivui*, namely a hydrogen-dependent CO_2 reductase (HDCR) (Schuchmann and Müller, 2013; Schwarz *et al.*, 2018). In contrast to classical formate dehydrogenases, HDCR directly uses H_2 as reductant for CO_2 reduction for formate. HDCR has a formate dehydrogenase module and a hydrogenase module that are most likely connected by two small FeS centre-containing electron transfer proteins. HDCR from *A. woodii* and *T. kivui* has extraordinary high rates of CO_2 hydrogenation, and they are 30- and 1200-times faster than any chemical catalyst (Müller, 2019). Industrially produced hydrogen often contains traces of CO that are tolerated by the enzyme. Indeed, the HDCR purified from *A. woodii* was shown to convert CO in the presence of purified CO dehydrogenase and purified ferredoxin (Schuchmann and Müller, 2013), which may be of physiological and industrial significance. Since the HDCR is oxygen sensitive, a whole cell system for both species was established to capture and store CO_2 and hydrogen in the form of formic acid (Schuchmann and Müller, 2013; Schwarz and Müller, 2020). Since the equilibrium constant for the reaction is close to one, the direction of the reaction can be determined by the concentration of the reactants and, thus, formate oxidation to CO_2 and H_2 is also possible (Kottenhahn *et al.*, 2018). Indeed, both the forward and backward reactions proceed with the highest rates ever found in biological systems (Müller, 2019). Interestingly, the purified HDCR from *A. woodii* can produce formate from CO in the presence of the CODH enzyme of *A. woodii* (Schuchmann and Müller, 2013) and recently we have also shown that whole cells of *T. kivui* convert syngas with high rates into formic acid. Notably, CO was consumed during this process and converted to formate (Schwarz and Müller, 2020). Here, we have built on this existing knowledge to analyse formate production from CO in the presence or

absence of Na^+ and bicarbonate ions. Additional mutagenesis studies should help to give a more detailed understanding of CO-based formate production in the metabolism of *A. woodii* and *T. kivui*.

Results

Whole cell biocatalysis for CO-dependent acetate and formate production

Experiments with A.woodii *wild type. Acetobacterium woodii* does not grow on CO alone, but resting cells are known to produce acetate from CO (Kerby *et al.*, 1983; Diekert *et al.*, 1986; Genthner and Bryant, 1987; Bertsch and Müller, 2015b). Indeed, we observed in this study that cells pre-grown on fructose produced acetate from CO as electron and carbon source, albeit in small amounts. Under an atmosphere of 20% CO, 0.53 mM acetate was formed after 48 h compared to 42 mM acetate from $H_2 + CO_2$ (Fig. 1A). Chemiosmotic energy conservation in *A. woodii* requires the presence of Na^+ since the respiratory enzyme, the ferredoxin:NAD^+ oxidoreductase (Rnf complex), requires Na^+ for activity and translocates Na^+ across the membrane thereby establishing a Na^+ gradient for ATP synthesis (Fritz and Müller, 2007; Biegel and Müller, 2010). In the absence of Na^+, cells are no longer able to synthesize net ATP and, in general, no acetate is produced. When Na^+ was omitted in resting cells of *A. woodii* using CO as substrate, little acetate was formed (0.7 mM) but formate (3.4 mM) was now the dominant product; the specific rate of formate production was 0.2 mmol g^{-1} h^{-1} (Fig. 1B).

Experiments with T. kivui *wild type.* Resting cells of *T. kivui* grown on glucose produced acetate from CO with a rate of 0.43 mmol g^{-1} h^{-1} (Fig. 1C), but no formate. However, when the energy metabolism was uncoupled from the WLP by bicarbonate (Schwarz and Müller, 2020), acetate was no longer produced but formate instead (~0.16 mmol g^{-1} h^{-1}), up to 2 mM in average (Fig. 1D). By mechanisms that are still not understood, *T. kivui* can be adapted to grow on CO as sole carbon and energy source after several rounds of transfer in media containing increasing amounts of CO (Weghoff and Müller, 2016). When cells were pre-grown on CO (50%), rates of acetate and formate production from CO were dramatically increased (Fig. 2). The specific acetate production rate in the energetically coupled cells was 3.27 mmol g^{-1} h^{-1}, and the specific formate production rate in the energetically uncoupled cells increased by a factor of 8 to 1.34 mmol g^{-1} h^{-1}. CO was completely consumed in both cases, and CO consumption was much faster in the energetically coupled, acetate-forming cells compared to the uncoupled, formate-producing cells. Under both conditions, hydrogen production was observed, but the uncoupled, formate-producing cells produced twice as much of molecular hydrogen.

CO conversion to formate by T. kivui *at elevated CO concentrations*

Next, we tested higher concentrations of 50 and 100% CO as substrate for the production of formate (Fig. 3A). The highest specific formate production rates (1.34 mmol g^{-1} h^{-1}) and formate titres (46 mM) were reached using 20% CO. With 50% and 100% CO, formate production rates of only 0.24 and 0.22 mmol g^{-1} h^{-1} and formate titres of only 6.8 mM and 4.7 mM were reached. Clearly, increasing CO concentrations resulted in a reduction of formate production. Only H_2 production had its peak at 50% CO (Fig. 3B).

Analysis of CO conversion by mutants

Experiments with T. kivui *mutants.* To get a deeper look into the enzymes involved in formate production from CO, mutants of *T. kivui* were analysed. The generation and physiological characterization of the Δ*cooS* (TKV_c08080) and Δ*ech2* (TKV_c19680-TKV_c19750) mutants of *T. kivui* which are lacking the monofunctional CO dehydrogenase (CooS) or energy-conserving hydrogenase (Ech2) will be described elsewhere; the HDCR deletion mutant (Jain *et al.*, 2020) as well as the genetic system (Basen *et al.*, 2018) has recently been described in detail. All mutants were generated in the *pyrE*-deficient uracil-auxotrophic strain *T. kivui* TKV002, which is a direct daughter strain of *T. kivui* DSM2030, and the generation of all *T. kivui* mutants in this study was based on the same, previously reported genetic system (Basen *et al.*, 2018). The Δ*cooS* mutant was generated from a CO-adapted strain whereas the two other mutants were generated in a glucose-adapted strain. In this study, all three mutants were grown in complex medium with 28 mM glucose, and the Δ*hdcr* strain with additional 50 mM formate as electron acceptor (Jain *et al.*, 2020). Resting cells were then prepared from exponentially grown cultures to analyse their ability for CO (20%) conversion to acetate or formate. As expected, the Δ*hdcr* strain (TKV_c19960-TKV_c19990) was neither able to produce acetate nor formate from CO, underlining the essentiality of the HDCR complex in the WLP (Fig. 4). The loss of product formation is consistent with a loss of CO consumption (data not shown). Only small amounts of H_2 (5 mM) were produced (Fig. 5). *T. kivui* has two sets of genes each encoding a membrane-bound, energy-conserving hydrogenase (Ech) that catalyses reduction of protons to

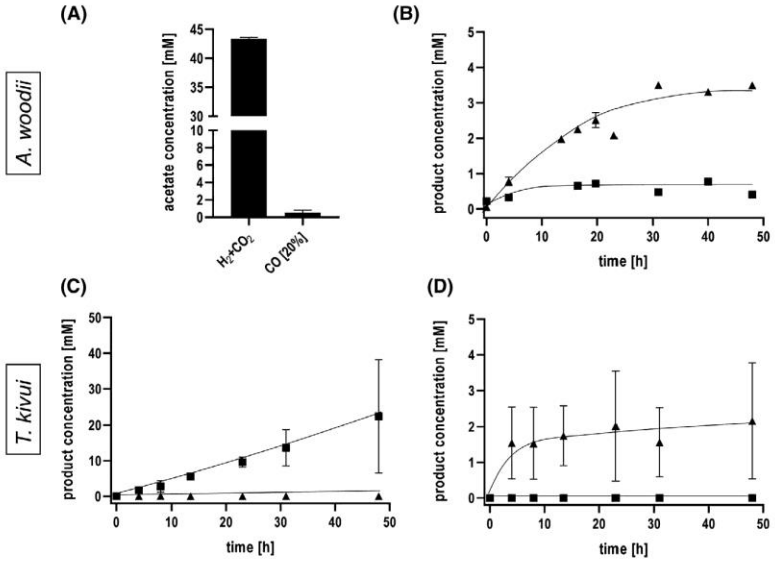

Fig. 1. Conversion of CO to formate and acetate by whole cells of *A. woodii* and *T. kivui*. Upper panel (A and B): Cells of *A. woodii* were grown on 20 mM fructose to the late exponential growth phase. The harvested and washed cells were resuspended in buffer A (200 mM imidazole, 20 mM $MgSO_4$, 20 mM KCl, 2 mM DTE, 4 μM resazurin, pH 9.0) to a final protein concentration of 2 mg ml^{-1} in anoxic serum bottles. For the $H_2 + CO_2$ experiments, a protein concentration of 1 mg ml^{-1} in buffer B (50 mM imidazole, 20 mM $MgSO_4$, 20 mM KCl, 2 mM DTE, 4 μM resazurin, pH 7.0) was used. The cells were incubated with 20% CO (80% N_2 as makeup gas) or $H_2 + CO_2$ (80:20% [v/v]) at 2×10^5 Pa in a shaking water bath at 30 °C. (A) CO and $H_2 + CO_2$ conversion to acetate in the presence of 20 mM NaCl after 48 h and (B) CO conversion to formate in the absence of NaCl over the time. Lower panel (C and D): Cells of *T. kivui* (pre-grown on sugar) were grown on 28 mM glucose to the late exponential growth phase. The harvested and washed cells were resuspended in buffer (50 mM imidazole, 20 mM $MgSO_4$, 20 mM KCl, 2 mM DTE, 4 μM resazurin, pH 7.0) to a final protein concentration of 1 mg ml^{-1} in anoxic serum bottles. The cells were incubated with 20% CO (80% N_2 as makeup gas) at 2×10^5 Pa in a shaking water bath at 60 °C. CO conversion to (C) acetate in the absence of $KHCO_3$ and (D) formate in the presence of 300 mM $KHCO_3$. Triangles up, formate; squares, acetate. Shown are data from two biological replicates. All data points are mean ± SD, $N = 2$.

H_2 with electrons derived from reduced ferredoxin (Schölmerich and Müller, 2019). The Δ*ech2* strain was no longer able to produce acetate from 20% CO (Fig. 4), and the H_2 production dramatically decreased by 80% to 3 mM H_2 (Fig. 5). Furthermore, only traces of formate (0.3 mM) were produced in uncoupled cells and no H_2 production was observed overall (Figs 4 and 5). These experiments clearly demonstrate a vital function of Ech2 in electron flow from CO to the WLP.

Interestingly, resting cells of the mutant lacking the *cooS* genes were still able to consume CO and to produce acetate. Here, the specific acetate formation rates even increased by a factor of 1.5 to 4.9 mmol g^{-1} h^{-1}. 20% CO was completely used up after 23 h, and 8.7 mM H_2 was produced. When CO-adapted cells of the wild-type strain were incubated under uncoupled conditions with CO, formate production was increased dramatically from 2 mM to 45 mM as previously described (Fig. 2B). When the *cooS* gene was deleted, formate production from CO was nearly abolished. Uncoupled cells of the Δ*cooS* mutant produced 2 mM formate like the wild type, and only 5.4 mM H_2 evolution was observed within 48 h (Figs 4 and 5).

Experiments with A. woodii *mutants.* For *A. woodii*, we analysed three mutants in which the HDCR gene cluster (Awo_c08190-Awo_c08260), the Rnf gene cluster (Awo_c22060-Awo_c22010) coding for the Na^+-dependent membrane-bound respiratory enzyme and the HydBA gene cluster (Awo_c26980-Awo_c26970) coding for the soluble electron-bifurcating hydrogenase were deleted. The latter two mutants and the used genetic system have been described in detail (Westphal *et al.*, 2018; Wiechmann *et al.*, 2020), and the generation of the HDCR mutant was based on the previously reported genetic system. The generation and characterization of the HDCR mutant will be described elsewhere.

First and as a control, we tested the effect of gene deletions on product formation from $H_2 + CO_2$ (Fig. S1). As expected, the wild type produced high amounts of acetate from $H_2 + CO_2$ only in the presence of Na^+ and formate production increased in the absence of Na^+. Since the Rnf complex is directly involved in the bioenergetics of *A. woodii* by generating an electrochemical Na^+-ion gradient, the dramatic difference in acetate production as a function of Na^+ was revoked in the Δ*rnf* mutant. The amount of produced formate stayed the

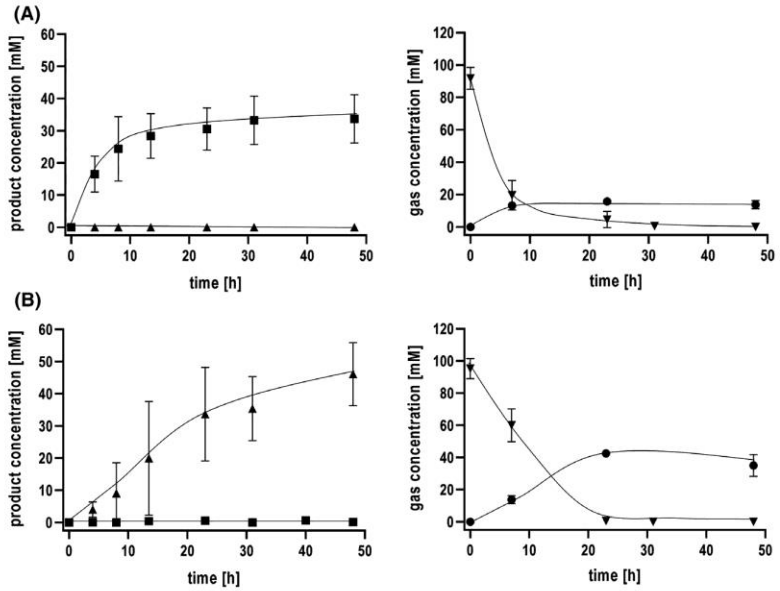

Fig. 2. CO-dependent acetate and formate production by CO-adapted cells of *T. kivui*. The experiments were performed as described before. Cells of *T. kivui* adapted on 50% CO were supplemented with 20% CO (80% N_2 as makeup gas) at 2×10^5 Pa as substrate. (A) Production of acetate with the corresponding gas consumption/production and (B) CO conversion to formate in the presence of 300 mM $KHCO_3$ with the corresponding gas consumption/production. Triangles up, formate; squares, acetate; triangles down, CO; circles, H_2. Shown are data from two biological replicates. All data points are mean ± SD, $N = 2$.

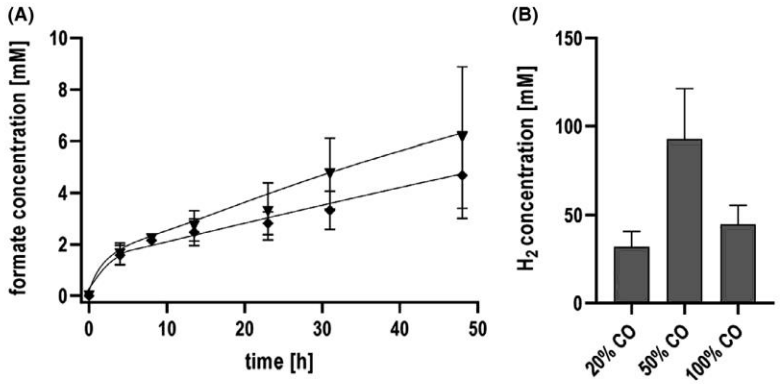

Fig. 3. CO conversion to formate under increased CO concentrations. The experiments were performed with cells of *T. kivui* adapted on 50% CO using 300 mM $KHCO_3$. (A) Production of formate from 50% (triangles down) and 100% (diamonds) CO. (B) Corresponding H_2 production on different CO concentrations. Shown are data from two biological replicates. All data points are mean ± SD, $N = 2$.

same. The hydrogenase is essential for growth on $H_2 + CO_2$ (Wiechmann *et al.*, 2020), and accordingly no acetate was formed; formate production increased slightly.

The Δ*hdcr* mutant was again no longer able to produce acetate or formate from CO, and CO utilization was not observed (data not shown). The wild type of *A. woodii* produced only little formate from CO in the presence (2.9 mM formate) or absence (3.4 mM formate) of Na^+ (Fig. 6A). As seen before (Schuchmann and Müller, 2013), the addition of bicarbonate dramatically stimulated formate production by the HDCR in the wild-type strain but also in the two mutant strains Δ*hydBA* and Δ*rnf* (Fig. 6). The addition of bicarbonate under Na^+ limiting conditions increased the specific formate production rate in the wild-type strain by a factor of 4.1. Cell suspension experiments without additional bicarbonate in the reaction buffer will hereinafter be called 'under CO_2-limiting

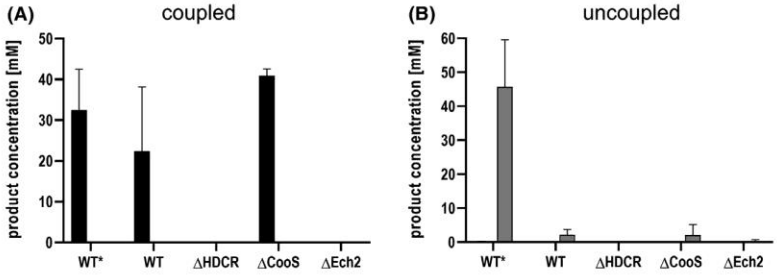

Fig. 4. Effect of gene deletions on acetate and formate production by resting cells of *T. kivui*. Cells of *T. kivui* wild type (WT), Δ*hdcr*, Δ*cooS* and Δ*ech2* were grown on 28 mM glucose. Δ*hdrc* had additional 50 mM formate as growth substrate. For the experiments, the cells were incubated with 20% CO (80% N_2 as makeup gas) at 2×10^5 Pa and the product formation was investigated in (A) coupled or (B) uncoupled cells (additional 300 mM $KHCO_3$). WT*, wild-type strain adapted on 50% CO; WT, non-CO-adapted wild-type strain pre-grown on glucose; Δ*hdcr*, deletion of the hydrogen-dependent CO_2 reductase; Δ*cooS*, deletion of the monofunctional CO dehydrogenase; Δ*ech2*, deletion of the membrane-bound energy-conserving hydrogenase. Black bars, acetate; grey bars, formate. Shown are data from two biological replicates. All data points are mean ± SD, $N = 2$.

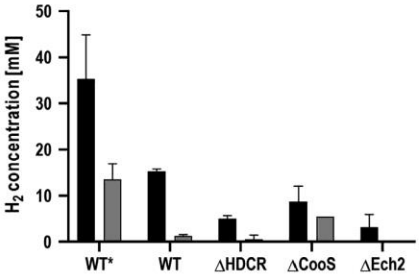

Fig. 5. Effect of gene deletions on H_2 production by resting cells of *T. kivui*. Resting cells of *T. kivui* wild type (WT), CO-adapted wild type (WT*), Δ*hdcr*, Δ*cooS* and Δ*ech2* were prepared as described before. H_2 production was monitored during the cell suspension experiments using 20% CO (80% N_2 as makeup gas) at 2×10^5 Pa as substrate. Black bars, H_2 production of coupled cells; grey bars, H_2 production of uncoupled cells. Shown are data from two biological replicates. All data points are mean ± SD, $N = 2$.

conditions'. Independent of the presence or absence of Na^+ ions and/ or bicarbonate, wild-type cells of *A. woodii* produced only traces of acetate (Fig. 6A). The Δ*rnf* mutant showed a slight increase (38%) in formate production compared to the wild-type strain under CO_2-limiting conditions. Amounts of acetate produced were still low but a little higher as in the wild type (Fig. 6B). Interestingly, in the absence of Na^+ and under CO_2-limiting conditions the Δ*hydBA* mutants showed the clearest increase in formate production from CO with rates of 0.48 mmol g^{-1} h^{-1}. Here, the final formate titre increased dramatically, reaching 13.3 mM formate after 48 h. This corresponds to an increase in formate by 300% compared to the wild-type strain (Fig. 6C). In addition to formate, 6.72 mM of acetate was produced as a side product in the mutant strains of Δ*hydBA*, which is roughly 10 times higher compared to the wild type (0.65 mM).

In the wild-type strain, the rate of formate production increased by 310% to 0.78 mmol g^{-1} h^{-1} and the final titre increased by 610 % to 24.2 mM in the presence of bicarbonate (Fig. S2). This is 82% more compared to the Δ*hydBA* and 390% more to the Δ*rnf* mutants under CO_2-limiting conditions. Although formate production in the Δh*ydBA* was already higher than in the wild type in the absence of bicarbonate, addition of bicarbonate stimulated formate formation even more. In the presence of 300 mM bicarbonate, the Δ*rnf* mutant showed the highest formate production rate of 1.22 mmol g^{-1} h^{-1} and reached the highest final formate titre of 34.5 mM after 48 h. The Δ*hydBA* mutant reached equal dimensions of formate titres (24.8 mM) and a similar range in production rates (0.55 mmol g^{-1} h^{-1}) compared to the wild type. The amount of acetate produced in all three strains, wild type, Δ*hydBA* and Δ*rnf*, was analysed to be 0.9, 3.11 and 1.5 mM, respectively. A summary of the specific formate production rates in the absence or presence of bicarbonate and/or Na^+ using the mutants or wild-type strain is shown in Table 1.

CO consumption and formate production by A. woodii ΔhydBA

CO utilization and formate formation were further analysed in detail in the presence of bicarbonate and under Na^+ limiting conditions using the Δ*hydBA* mutant. The cell suspension converted 20% CO to 24.8 mM formate with a formate production rate of 0.55 mmol g^{-1} h^{-1}. In addition, 3.81 mM of acetate was produced (Fig. 7A). Simultaneously, 39 mM of CO was consumed (Fig. 7B). CO concentrations up to 100% were tolerated without significant loss of formate production activities (Fig. S3).

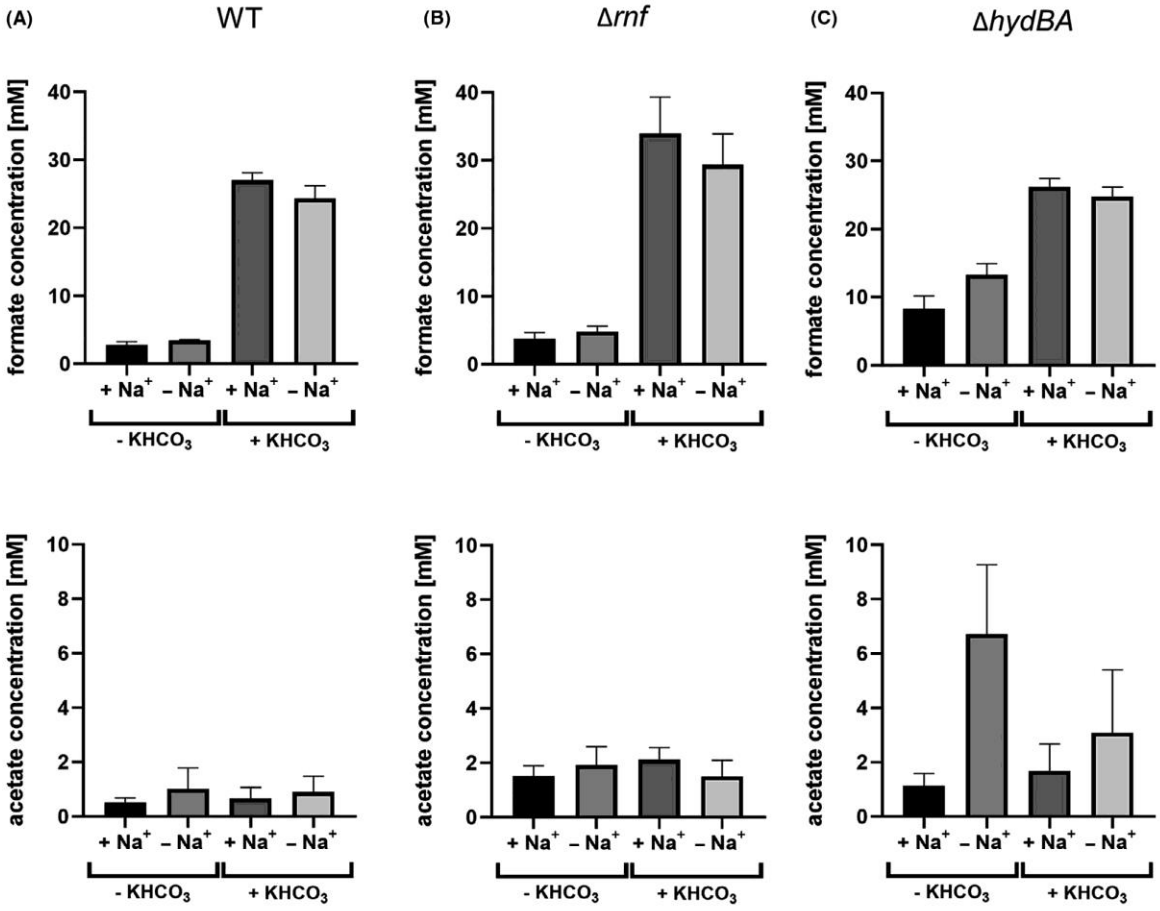

Fig. 6. Effect of gene deletions on product formation from 20% CO by whole cells of *A. woodii*. Resting cells of *A. woodii* WT, Δ*rnf* or Δ*hydBA* were prepared as described before. Formate and acetate production was determined after 48 h in the cell suspension experiments with 20% CO (80% N_2 as makeup gas) at 2×10^5 Pa as substrate using (A) *A. woodii* WT, (B) Δ*rnf* or (C) Δ*hydBA*. $+Na^+$, additional 20 mM NaCl, $+KHCO_3$, additional 300 mM $KHCO_3$; $-Na^+$, no NaCl was added; $-KHCO_3$, no $KHCO_3$ was added. Shown are data from two biological replicates. All data points are mean ± SD, $N = 2$.

Table 1. Rates of formate production from CO by wild type and mutants of *A. woodii*. An atmosphere of 20% CO was used; makeup gas was N_2. Shown are data from two biological replicates. All data points are mean (± SD, $N = 2$).

	Specific formate production rates [mmol g^{-1} h^{-1}]			
	Without 300 mM $KHCO_3$		Additional 300 mM $KHCO_3$	
	$+Na^+$	Without Na^+	$+Na^+$	Without Na^+
Wild type	0.17 (± 0.03)	0.19 (± 0.02)	0.68 (± 0.07)	0.78 (± 0.13)
Δ*rnf*	0.35 (± 0.18)	0.48 (± 0.27)	1.44 (± 0.14)	1.22 (± 0.16)
Δ*hydBA*	0.35 (± 0.02)	0.39 (± 0.05)	0.94 (± 0.17)	0.55 (± 0.07)

$+Na^+$, additional 20 mM of NaCl was used in the reaction buffer.

Discussion

CO utilization pathway in T. kivui

The two acetogenic bacteria *A. woodii* and *T. kivui* were shown in this study to work as whole cell biocatalysts for the conversion of the toxic gas CO either to acetate or to formate, the latter with rates which are so far the highest in the literature (Rother and Metcalf, 2004; Henstra *et al.*, 2007a; Mayer *et al.*, 2018; Hwang *et al.*, 2020). This allows the production of two interesting bulk chemicals from the highly abundant and toxic industrial gas CO as initial substrate. Noteworthy, production of formate goes along with little side products, that is high selectivity. In contrast to other CO utilizers such as *C. autoethanogenum*, product formation is thus more

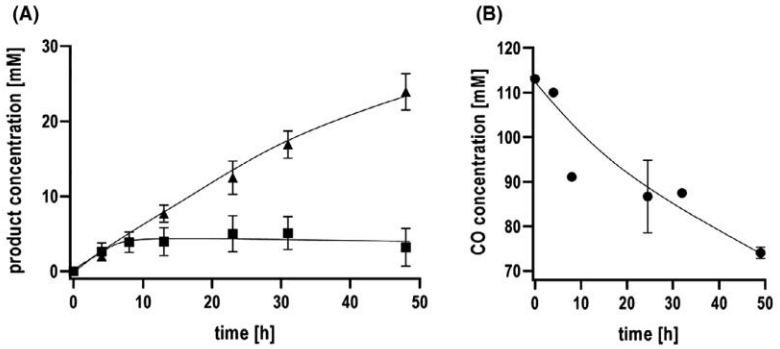

Fig. 7. Formate production from CO by *A. woodii* Δ*hydBA*. Cell suspensions in 200 mM imidazole, 20 mM $MgSO_4$, 20 mM KCl, 2mM DTE, 4 μM resazurin, pH 7.0 without an additional source of Na^+. Cells were incubated with 20% CO (80% N_2 as makeup gas) at 2×10^5 Pa and with additional 300 mM $KHCO_3$. (A) Formate (triangles up) and acetate (squares) production and corresponding (B) CO (circles) consumption. Shown are data from two biological replicates. All data points are mean ± SD, $N = 2$.

controllable. Furthermore, the mechanism responsible for the CO-based formate production was investigated in a closer look at using mutants with defects in key intracellular enzyme activities.

The key enzyme in anaerobic as well as aerobic microbial CO utilization is the carbon monoxide dehydrogenase (CODH). This enzyme catalyses the oxidation of CO to CO_2 and protons/electrons (Eq. 3).

$$1CO + 1H_2O \Leftrightarrow 1CO_2 + 2H^+ + 2e^- \quad (3)$$

The electron acceptors are diverse and in the two acetogenic bacteria *A. woodii* and *Moorella thermoacetica* the CODH was purified and shown to use ferredoxin as electron acceptor (Ragsdale *et al.*, 1983). The same can be assumed for *T. kivui*. However, there are two CO dehydrogenases present in *T. kivui*, the monofunctional CODH (CooS) and the bifunctional CODH/ACS (Hess *et al.*, 2014). Deletion of *cooS* did not reduce but stimulated acetate formation compared to the wild type, leading to the conclusion that the CODH/ACS alone is able to oxidize CO and to catalyse acetate formation from CO. The dispensability of the monofunctional CO dehydrogenases in autotrophy was also shown in mutagenesis studies for *C. autoethanogenum* (Liew *et al.*, 2016a). In the uncoupled system of *T. kivui* that does not allow for acetate synthesis, the wild type produced only little formate. However, the CO-adapted strain produced much more formate and deletion of *cooS* almost abolished formate production. This is consistent with the hypothesis that CooS is essential for CO-coupled formate production in CO-adapted cells. The ferredoxin reduced by CooS is then oxidized by Ech2, as evident from the complete loss of formate and acetate production and dramatic reduction in production of molecular hydrogen in the Δ*ech2* mutant. The HDCR uses H_2 as preferred reductant, but can also use reduced ferredoxin as reductant, albeit with ~ 95% less activity. Since a Δ*ech2* mutant does no longer produce formate or acetate, it has to be concluded that the HDCR *in vivo* requires H_2 that cannot be replaced by reduced ferredoxin. The same has been observed very recently for the HDCR from *A. woodii in vivo* (Wiechmann *et al.*, 2020). Last, a Δ*hdcr* mutant does not produce formate. In sum, these data are consistent with the following pathway of formate production from CO: CO is oxidized to CO_2 by CODH/ACS or CooS; the former dominates in non-CO-adapted cells, the latter in CO-adapted cells. CO oxidation is coupled to reduction of ferredoxin which is oxidized by Ech2 to produce molecular hydrogen. CO_2 is then reduced by the HDCR with electrons derived from H_2 to formate (Fig. 8A).

CO utilization pathway in A. woodii

In *A. woodii* the situation is not as clear. CO is oxidized either by CooS (Awo_c19050) or CODH/ACS thereby reducing ferredoxin. Reduced ferredoxin is then reoxidized by the Rnf complex to reduce NAD^+. NADH and Fd^{2-} are then used by the electron-bifurcating hydrogenase to reduce protons to molecular hydrogen, which can drive CO_2 reduction to formate via the HDCR. But since resting cells of the Δ*rnf* mutant as well as the wild-type strain under Na^+ limiting conditions are still able to produce acetate from $H_2 + CO_2$ (Fig. S1), we have to assume that residual ATP pools enable the cells to produce small amounts of acetate (Westphal *et al.*, 2018) without the need for an electrochemical Na^+ gradient. Furthermore, the HDCR seems to be able to use reduced ferredoxin as an alternative electron donor for the reduction of CO_2 to formate, especially in resting cells of *A. woodii*. As previously mentioned, the use of reduced ferredoxin as reductant was already shown for

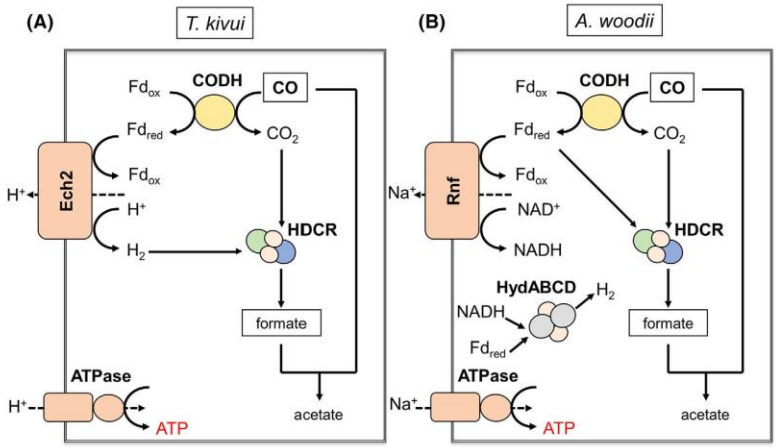

Fig. 8. Schematic model of the CO utilization pathway in the two acetogenic bacteria *T. kivui* and *A. woodii*. CODH, CO dehydrogenase; HDCR, Hydrogen-dependent CO_2 reductase; Ech, Energy-conserving hydrogenase complex; Rnf, Rhodobacter nitrogen fixation complex; HydABCD, Electron-bifurcating hydrogenase; Fd_{red}, reduced ferredoxin; Fd_{ox}, oxidized ferredoxin.

the purified HDCR in *in vitro* experiments (Schuchmann and Müller, 2013). This is not in contradiction to the postulated hydrogen cycling mechanism in *A. woodii* where hydrogen is directly used as reductant for CO_2 reduction in growing cells of *A. woodii* (Wiechmann *et al.*, 2020). The use of reduced ferredoxin (Fd^{2-}) from the HDCR could also explain the increasing amounts of formate produced in the Δ*hydBA* and Δ*rnf* mutant, since in each mutant only one Fd^{2-} consuming module is active, thus increasing the electron-pressure in form of reduced ferredoxin towards the HDCR, resulting in increased formate titres. In the case of Δ*hydBA*, a putative electron-loss by the electron-bifurcating, hydrogen-producing hydrogenase is not possible and could, therefore, result in even higher formate titres. Hydrogen evolution could not be observed in any strain tested. This is not surprising since until now, hydrogen evolution and hydrogen cycling could only be observed for cultures of *A. woodii* which were cultivated in a stirred-tank bioreactor (Wiechmann *et al.*, 2020). Unfortunately, the production of 6.72 mM acetate in the Δ*hydBA* mutant strain under CO_2- and Na^+-limiting conditions cannot be resolved in this study and remains uncertain. Based on the metabolic and enzymatic knowledge to date, an additional enzyme for the conversion of reduced ferredoxin to NADH seems to be necessary to explain the production of acetate from CO under the given conditions. Nevertheless, in sum the data allow to postulate the following pathway of formate production from CO in resting cells of *A. woodii*: CO is oxidized to CO_2 by CODH/ACS or CooS, generating reduced ferredoxin. Ferredoxin can then either be used by the Rnf complex, the electron-bifurcating hydrogenase or the HDCR complex, the latter one involved in ferredoxin-based CO_2 reduction to formate (Fig. 8B). Depending of the electron-pressure (as Fd^{2-}), the HDCR catalysed formate production, especially the specific formate formation rates as well as formate titres, could differ.

Bicarbonate stimulates formate production in A. woodii

All three strains tested, wild type, Δ*hydBA* and Δ*rnf* of *A. woodii*, have in common that additional bicarbonate dramatically stimulated formate formation. The addition of bicarbonate leads to a fast interconversion of bicarbonate and CO_2 by the carbonic anhydrase of resting cells (Braus-Stromeyer *et al.*, 1997), thus increasing the available amount of substrate (CO_2) for the HDCR reaction. Since the equilibrium constant of the hydrogen-dependent CO_2 reduction is close to one, the state of the chemical equilibrium can be easily affected. As seen for *T. kivui* (Schwarz and Müller, 2020), bicarbonate could also potentially influence enzymes in the WLP or enzymes involved in energy conservation/ATP generation that inhibit the further conversion of formate to acetate and thereby stimulating the HDCR catalysed Fd^{2-}-dependent CO_2 reduction to formate through higher substrate availability of CO_2.

At the end, we can sum up that mutagenesis studies in *A. woodii* and *T. kivui* revealed a difference in the electron donor (Fd^{2-} or H_2) as well as in the electron flow for CO-based formate production in resting cells of these organisms. Not only the mutations but also the presence/absence of Na^+ and bicarbonate ions affected the specific formate production rates as well as final formate/acetate titres.

Experimental procedures

Organism and cultivation

Thermoanaerobacter kivui LKT-1 (DSM 2030) and its mutants Δ*hdcr*, Δ*ech2* and Δ*cooS* were cultivated at 66 °C under anoxic conditions in complex medium (Weghoff and Müller, 2016) using 1-l flasks (Müller-Krempel, Bülach, Switzerland). The flasks contained 500 ml media for heterotrophic cultivation and 200 ml media for autotrophic cultivation to increase the gas-to-liquid ratio. Media were prepared under anoxic conditions as described before (Hungate, 1969; Bryant, 1972). Glucose (28 mM) or CO (50% CO, 40% N_2 and 10% CO_2 [v/v] at 2×10^5 Pa) were used as substrate. For the cultivation of *T. kivui* Δ*hdcr,* additional 50 mM formate was used. *Acetobacterium woodii* (DSM 1030) and its mutants Δ*hydBA*, Δ*hdcr* and Δ*rnf* were cultivated at 30 °C under anoxic conditions in carbonate-buffered medium (Heise *et al*., 1989). The medium was prepared as described before (Hungate, 1969; Bryant, 1972). Fructose (20 mM) was used as growth substrate for all cultivations, and additional 50 mg l^{-1} uracil was added to the *pyrE* deletion mutants. The growth media of *A. woodii* Δ*hdcr* and Δ*hydBA* were supplemented with additional 40 mM formate. Growth was followed by measuring the optical density at 600 nm with an UV/Vis spectrophotometer.

Preparation of resting cells and cell suspension experiments

Preparation of resting cells was performed under strictly anoxic conditions in an anaerobic chamber (Coy Laboratory Products, Grass Lake, MI, USA) as described (Heise *et al*., 1992). Cells of *A. woodii* and *T. kivui* were cultivated in 1-l flasks (Müller-Krempel, Bülach, Switzerland) to the late exponential growth phase and were harvested by centrifugation at 11500 *g* at 4 °C for 10 min. Afterwards, the cells were washed twice in imidazole buffer (50 mM imidazole, 20 mM $MgSO_4$, 20 mM KCl, 4 μM resazurin, 2 mM DTE, pH 7.0). If not otherwise stated, *T. kivui* cells were resuspended in the same imidazole buffer to a final protein concentration of 1 mg/ml. Cells of *A. woodii* were resuspended in 200 mM imidazole buffer (200 mM imidazole, 20 mM $MgSO_4$, 20 mM KCl, 4 μM resazurin, 2 mM DTE, pH 9.0) to a final protein concentration of 2 mg ml^{-1}. The cell suspensions were transferred to gas-tight Hungate tubes and were directly used for the subsequent cell suspension experiments. The protein concentration of the cell suspension was determined according to (Schmidt *et al*., 1963).

For determining the conversion of CO in cell suspension experiments of *A. woodii* and *T. kivui*, 60 ml serum bottles (Glasgerätebau Ochs GmbH, Bovenden-Lenglern, Germany) with N_2 atmosphere were filled with imidazole buffer (50 mM imidazole, 20 mM $MgSO_4$, 20 mM KCl, 4 μM resazurin, 2 mM DTE, pH 7.0 or 200 mM imidazole, 20 mM $MgSO_4$, 20 mM KCl, 4 μM resazurin, 2 mM DTE, pH 9.0) and the head space was changed to 20% CO (80% N_2 as makeup gas), 50% CO (50% N_2 as makeup gas) and 100% CO with 1 bar overpressure in total. The serum flasks contained a final liquid volume of 5 ml. The serum flasks were pre-warmed for at least 10 min at 30 °C or at 60 °C for cells of *A. woodii* and *T. kivui*, respectively. If necessary, bicarbonate was added prior to the reaction start. The reaction was started by adding the cell suspension and samples were taken at defined time points.

For acetogenesis from $H_2 + CO_2$ by *A. woodii*, cells were cultivated and harvested as described above. Cell suspensions in imidazole buffer (50 mM imidazole, 20 mM $MgSO_4$, 20 mM KCl, 4 μM resazurin, 2 mM DTE, pH 7.0) containing additional 20 mM NaCl or no additional NaCl were incubated in 120 ml serum bottles (Glasgerätebau Ochs GmbH, Bovenden-Lenglern, Germany) filled with a final volume of 10 ml. A cell concentration corresponding to 1 mg total cell protein per ml and a gas atmosphere of $H_2 + CO_2$ (80:20%, [v/v]) at 1 bar overpressure were used.

Analytical methods

The concentrations of acetate and formate were measured by high-performance liquid chromatography (1260 Infinity II LC System) equipped with 1260 Infinity II Quaternary Pump, 1260 Infinity II Vialsampler, 1260 Infinity II Multicolumn Thermostat, 1260 Infinity II Diode Array Detector and 1260 Infinity II Refractive Index Detector (Agilent Technologies, Santa Clara, CA, USA). For sample preparation, cells were spun down by centrifugation at 18 000 *g* for 10 min and the supernatant was filtered via syringe filters (4 mm Millex-LH Syringe Filters; Merck KGaA, Darmstadt, Germany) into a 400 μl flat bottom glass insert (Agilent Technologies, Santa Clara, CA, USA) of the HPLC vial. A Hi-Plex H 300 × 7.7 mm column with its precolumn Hi-Plex H Guard 50 × 7.7 mm (Agilent Technologies, Santa Clara, CA, USA) was used for separation. Filtered and degassed sulphuric acid (5 mM) was used as eluent at a flow rate of 0.6 ml min^{-1}. The vial sampler and the oven were kept at 5 °C and 55 °C, respectively. The sample (5 μl) was injected by the auto-sampler and analysed with a refractive index detector at 55 °C and a diode array detector operating in the range of 200 to 220 nm. The reference cell of the refractive index detector was purged with the eluent prior to analysis. The run time of the sample analysis was 30 min. CO and H_2 were determined as

described before (Weghoff and Müller, 2016; Schwarz *et al.*, 2018).

Acknowledgements

The support of our work from the European Research Council (ERC) under the European Union's Horizon 2020 research and innovation programme (grant agreement no 741791) is gratefully acknowledged. Open access funding enabled and organized by Projekt DEAL.

Conflict of interest

The authors declare that they have no competing interests.

Author contributions

V.M. designed and supervised the research, analysed the data and wrote the manuscript. F.M.S. designed and supervised the research, performed the experiments, analysed the data and wrote the manuscript. M.B. supervised the research of C.B. S.C. performed the experiments and analysed the data. S.J., A.W. and C.B. generated the mutant strains.

References

Ajanovic, A. (2011) Biofuels versus food production: Does biofuels production increase food prices? *Energy* **36:** 2070–2076.

Banerjee, A., Leang, C., Ueki, T., Nevin, K.P., and Lovley, D.R. (2014) Lactose-inducible system for metabolic engineering of *Clostridium ljungdahlii*. *Appl Environ Microbiol* **80:** 2410–2416.

Basen, M., Geiger, I., Henke, L., and Müller, V. (2018) A genetic system for the thermophilic acetogenic bacterium *Thermoanaerobacter kivui*. *Appl Environ Microbiol* **84:** e02210-02217.

Bengelsdorf, F.R., Beck, M.H., Erz, C., Hoffmeister, S., Karl, M.M., Riegler, P., *et al.* (2018) Bacterial anaerobic synthesis gas (syngas) and CO_2+H_2 Fermentation. *Adv Appl Microbiol* **103:** 143–221.

Bengelsdorf, F.R., and Dürre, P. (2017) Gas fermentation for commodity chemicals and fuels. *Microb Biotechnol* **10:** 1167–1170.

Bengelsdorf, F.R., Poehlein, A., Linder, S., Erz, C., Hummel, T., Hoffmeister, S., *et al.* (2016) Industrial acetogenic biocatalysts: A comparative metabolic and genomic analysis. *Front Microbiol* **7:** 1036.

Bengelsdorf, F.R., Straub, M., and Dürre, P. (2013) Bacterial synthesis gas (syngas) fermentation. *Environ Technol* **34:** 1639–1651.

Bertsch, J., and Müller, V. (2015) Bioenergetic constraints for conversion of syngas to biofuels in acetogenic bacteria. *Biotechnol Biofuels* **8:** 210.

Bertsch, J., and Müller, V. (2015) CO metabolism in the acetogen *Acetobacterium woodii*. *Appl Environ Microbiol* **81:** 5949–5956.

Biegel, E., and Müller, V. (2010) Bacterial Na^+-translocating ferredoxin:NAD^+ oxidoreductase. *Proc Natl Acad Sci USA* **107:** 18138–18142.

Braus-Stromeyer, S.A., Schnappauf, G., Braus, G.H., Gössner, A.S., and Drake, H.L. (1997) Carbonic anhydrase in *Acetobacterium woodii* and other acetogenic bacteria. *J Bacteriol* **179:** 7197–7200.

Bryant, M.P. (1972) Commentary on the Hungate technique for culture of anaerobic bacteria. *Am J Clin Nutr* **25:** 1324–1328.

Cotton, C.A., Claassens, N.J., Benito-Vaquerizo, S., and Bar-Even, A. (2019) Renewable methanol and formate as microbial feedstocks. *Curr Opin Biotechnol* **62:** 168–180.

Diekert, G., Schrader, E., and Harder, W. (1986) Energetics of CO formation and CO oxidation in cell suspensions of *Acetobacterium woodii*. *Arch Microbiol* **144:** 386–392.

Diekert, G.B., and Thauer, R.K. (1978) Carbon monoxide oxidation by *Clostridium thermoaceticum* and *Clostridium formicoaceticum*. *J Bacteriol* **136:** 597–606.

Diekert, G., and Wohlfarth, G. (1994) Metabolism of homoacetogens. *Anton Leeuwenhoek Int J G* **66:** 209–221.

Diender, M., Stams, A.J., and Sousa, D.Z. (2015) Pathways and bioenergetics of anaerobic carbon monoxide fermentation. *Front Microbiol* **6:** 1275.

Drake, H.L. (1994) Acetogenesis, acetogenic bacteria, and the acetyl-CoA pathway: past and current perspectives. In *Acetogenesis*. Drake, H.L. (ed). New York, NY, USA: Chapman and Hall, pp. 3–60.

Dürre, P., and Eikmanns, B.J. (2015) C1-carbon sources for chemical and fuel production by microbial gas fermentation. *Curr Opin Biotechnol* **35:** 63–72.

Fargione, J., Hill, J., Tilman, D., Polasky, S., and Hawthorne, P. (2008) Land clearing and the biofuel carbon debt. *Science* **319:** 1235–1238.

Fritz, M., and Müller, V. (2007) An intermediate step in the evolution of ATPases - the F_1F_O-ATPase from *Acetobacterium woodii* contains F-type and V-type rotor subunits and is capable of ATP synthesis. *FEBS J* **274:** 3421–3428.

Genthner, B.R.S., and Bryant, M.P. (1987) Additional characteristics of one-carbon-compound utilization by *Eubacterium limosum* and *Acetobacterium woodii*. *Appl Environ Microbiol* **53:** 471–476.

Hammerschmidt, A., Boukis, N., Hauer, E., Galla, U., Dinjus, E., Hitzmann, B., *et al.* (2011) Catalytic conversion of waste biomass by hydrothermal treatment. *Fuel* **90:** 555–562.

Harris, D.M., van der Krogt, Z.A., van Gulik, W.M., van Dijken, J.P., and Pronk, J.T. (2007) Formate as an auxiliary substrate for glucose-limited cultivation of *Penicillium chrysogenum*: impact on penicillin G production and biomass yield. *Appl Environ Microbiol* **73:** 5020–5025.

Heise, R., Müller, V., and Gottschalk, G. (1989) Sodium dependence of acetate formation by the acetogenic bacterium *Acetobacterium woodii*. *J Bacteriol* **171:** 5473–5478.

Heise, R., Müller, V., and Gottschalk, G. (1992) Presence of a sodium-translocating ATPase in membrane vesicles of the homoacetogenic bacterium *Acetobacterium woodii*. *Eur J Biochem* **206:** 553–557.

Henstra, A.M., Dijkema, C., and Stams, A.J. (2007) *Archaeoglobus fulgidus* couples CO oxidation to sulfate reduction and acetogenesis with transient formate accumulation. *Environ Microbiol* **9:** 1836–1841.

Henstra, A.M., Sipma, J., Rinzema, A., and Stams, A.J. (2007) Microbiology of synthesis gas fermentation for biofuel production. *Curr Opin Biotechnol* **18:** 200–206.

Hess, V., Poehlein, A., Weghoff, M.C., Daniel, R., and Müller, V. (2014) A genome-guided analysis of energy conservation in the thermophilic, cytochrome-free acetogenic bacterium *Thermoanaerobacter kivui*. *BMC Genom* **15:** 1139.

Hungate, R.E. (1969) A roll tube method for cultivation of strict anaerobes. In *Methods in Microbiology*. Norris, J.R., and Ribbons, D.W. (eds). New York, NY, USA and London, UK: Academic Press, pp. 117–132.

Hwang, H.W., Yoon, J., Min, K., Kim, M.-S., Kim, S.-J., Cho, D.H., *et al.* (2020) Two-stage bioconversion of carbon monoxide to biopolymers via formate as an intermediate. *Chem Eng J* **389:** 124394.

Jain, S., Dietrich, H.M., Müller, V., and Basen, M. (2020) Formate is required for growth of the thermophilic acetogenic bacterium *Thermoanaerobacter kivui* lacking hydrogen-dependent carbon dioxide reductase (HDCR). *Front Microbiol* **11:** 59.

Jeong, J., Bertsch, J., Hess, V., Choi, S., Choi, I.G., Chang, I.S., and Müller, V. (2015) Energy conservation model based on genomic and experimental analyses of a carbon monoxide-utilizing, butyrate-forming acetogen, *Eubacterium limosum* KIST612. *Appl Environ Microbiol* **81:** 4782–4790.

Kerby, R., Niemczura, W., and Zeikus, J.G. (1983) Single-carbon catabolism in acetogens: Analysis of carbon flow in *Acetobacterium woodii* and *Butyribacterium methylotrophicum* by fermentation and ^{13}C nuclear magnetic resonance measurement. *J Bacteriol* **155:** 1208–1218.

Köpke, M., Held, C., Hujer, S., Liesegang, H., Wiezer, A., Wollherr, A., *et al.* (2010) *Clostridium ljungdahlii* represents a microbial production platform based on syngas. *Proc Natl Acad Sci USA* **107:** 13087–13092.

Köpke, M., Mihalcea, C., Liew, F., Tizard, J.H., Ali, M.S., Conolly, J.J., *et al.* (2011) 2,3-butanediol production by acetogenic bacteria, an alternative route to chemical synthesis, using industrial waste gas. *Appl Environ Microbiol* **77:** 5467–5475.

Köpke, M., and Simpson, S.D. (2020) Pollution to products: recycling of 'above ground' carbon by gas fermentation. *Curr Opin Biotechnol* **65:** 180–189.

Kottenhahn, P., Schuchmann, K., and Müller, V. (2018) Efficient whole cell biocatalyst for formate-based hydrogen production. *Biotechnol Biofuels* **11:** 93.

Kucharska, K., Rybarczyk, P., Holowacz, I., Lukajtis, R., Glinka, M., and Kaminski, M. (2018) Pretreatment of lignocellulosic materials as substrates for fermentation processes. *Molecules* **23:** 2937.

Liew, F., Henstra, A.M., Winzer, K., Köpke, M., Simpson, S.D., and Minton, N.P. (2016) Insights into CO_2 fixation pathway of *Clostridium autoethanogenum* by targeted mutagenesis. *MBio* **7:** e00427-00416.

Liew, F., Martin, M.E., Tappel, R.C., Heijstra, B.D., Mihalcea, C., and Köpke, M. (2016) Gas fermentation-a flexible platform for commercial scale production of low-carbon-fuels and chemicals from waste and renewable feedstocks. *Front Microbiol* **7:** 694.

Liou, J.S., Balkwill, D.L., Drake, G.R., and Tanner, R.S. (2005) *Clostridium carboxidivorans* sp. nov., a solvent-producing Clostridium isolated from an agricultural settling lagoon, and reclassification of the acetogen *Clostridium scatologenes* strain SL1 as *Clostridium drakei* sp. nov. *Int J Syst Evol Microbiol* **55:** 2085–2091.

Maddipati, P., Atiyeh, H.K., Bellmer, D.D., and Huhnke, R.L. (2011) Ethanol production from syngas by *Clostridium* strain P11 using corn steep liquor as a nutrient replacement to yeast extract. *Bioresour Technol* **102:** 6494–6501.

Mayer, A., Schädler, T., Trunz, S., Stelzer, T., and Weuster-Botz, D. (2018) Carbon monoxide conversion with *Clostridium aceticum*. *Biotechnol Bioeng* **115:** 2740–2750.

Müller, V. (2003) Energy conservation in acetogenic bacteria. *Appl Environ Microbiol* **69:** 6345–6353.

Müller, V. (2015) Microbial life at the thermodynamic limit: how much energy is required to sustain life. *Environ Microbiol Rep* **7:** 31–32.

Müller, V. (2019) New horizons in acetogenic conversion of one-carbon substrates and biological hydrogen storage. *Trends Biotechnol* **37:** 1344–1354.

Müller, V., and Hess, V. (2017) The minimum biological energy quantum. *Front Microbiol* **8:** 2019.

Munasinghe, P.C., and Khanal, S.K. (2010) Biomass-derived syngas fermentation into biofuels: Opportunities and challenges. *Bioresour Technol* **101:** 5013–5022.

Naik, S.N., Goud, V.V., Rout, P.K., and Dalai, A.K. (2010) Production of first and second generation biofuels: a comprehensive review. *Renew Sust Energ Rev* **14:** 578–597.

Najafpour, G.D., and Younesi, H. (2006) Ethanol and acetate synthesis from waste gas using batch culture of *Clostridium ljungdahlii*. *Enzyme Microb Technol* **38:** 223–228.

Padella, M., O'Connell, A., and Prussi, M. (2019) What is still limiting the deployment of cellulosic ethanol? Analysis of the current status of the sector. *Appl Sci* **9:** 4523.

Peters, V., Janssen, P.H., and Conrad, R. (1999) Transient production of formate during chemolithotrophic growth of anaerobic microorganisms on hydrogen. *Curr Microbiol* **38:** 285–289.

Poehlein, A., Schmidt, S., Kaster, A.-K., Goenrich, M., Vollmers, J., Thürmer, A., *et al.* (2012) An ancient pathway combining carbon dioxide fixation with the generation and utilization of a sodium ion gradient for ATP synthesis. *PLoS One* **7:** e33439.

Ragsdale, S.W. (2008) Enzymology of the Wood-Ljungdahl pathway of acetogenesis. *Ann N Y Acad Sci* **1125:** 129–136.

Ragsdale, S.W., Ljungdahl, L.G., and DerVartanian, D.V. (1983) Isolation of carbon monoxide dehydrogenase from *Acetobacterium woodii* and comparison of its properties with those of the *Clostridium thermoaceticum* enzyme. *J Bacteriol* **155:** 1224–1237.

Rokni, M. (2015) Thermodynamic analyses of municipal solid waste gasification plant integrated with solid oxide fuel cell and stirling hybrid system. *Int J Hydrogen Energy* **40:** 7855–7869.

Rother, M., and Metcalf, W.W. (2004) Anaerobic growth of *Methanosarcina acetivorans* C2A on carbon monoxide: an unusual way of life for a methanogenic archaeon. *Proc Natl Acad Sci USA* **101:** 16929–16934.

Schmidt, K., Liaaen-Jensen, S., and Schlegel, H.G. (1963) Die Carotinoide der Thiorhodaceae. *Arch Mikrobiol* **46:** 117–126.

Schölmerich, M.C., and Müller, V. (2019) Energy conservation by a hydrogenase-dependent chemiosmotic mechanism in an ancient metabolic pathway. *Proc Natl Acad Sci USA* **116:** 6329–6334.

Schuchmann, K., and Müller, V. (2013) Direct and reversible hydrogenation of CO_2 to formate by a bacterial carbon dioxide reductase. *Science* **342:** 1382–1385.

Schuchmann, K., and Müller, V. (2014) Autotrophy at the thermodynamic limit of life: A model for energy conservation in acetogenic bacteria. *Nat Rev Microbiol* **12:** 809–821.

Schuchmann, K., and Müller, V. (2016) Energetics and application of heterotrophy in acetogenic bacteria. *Appl Environ Microbiol* **82:** 4056–4069.

Schwarz, F.M., and Müller, V. (2020) Whole-cell biocatalysis for hydrogen storage and syngas conversion to formate using a thermophilic acetogen. *Biotechnol Biofuels* **13:** 32.

Schwarz, F.M., Schuchmann, K., and Müller, V. (2018) Hydrogenation of CO_2 at ambient pressure catalyzed by a highly active thermostable biocatalyst. *Biotechnol Biofuels* **11:** 237.

Spahn, S., Brandt, K., and Müller, V. (2015) A low phosphorylation potential in the acetogen *Acetobacterium woodii* reflects its lifestyle at the thermodynamic edge of life. *Arch Microbiol* **197:** 745–751.

Takors, R., Kopf, M., Mampel, J., Bluemke, W., Blombach, B., Eikmanns, B., *et al.* (2018) Using gas mixtures of CO, CO_2 and H_2 as microbial substrates: the do's and don'ts of successful technology transfer from laboratory to production scale. *Microb Biotechnol* **11:** 606–625.

Tremblay, P.L., Zhang, T., Dar, S.A., Leang, C., and Lovley, D.R. (2012) The Rnf complex of *Clostridium ljungdahlii* is a proton-translocating ferredoxin:NAD^+ oxidoreductase essential for autotrophic growth. *MBio* **4:** e00406-00412.

Weghoff, M.C., and Müller, V. (2016) CO metabolism in the thermophilic acetogen *Thermoanaerobacter kivui*. *Appl Environ Microbiol* **82:** 2312–2319.

Wendisch, V.F. (2014) Microbial production of amino acids and derived chemicals: synthetic biology approaches to strain development. *Curr Opin Biotechnol* **30:** 51–58.

Westphal, L., Wiechmann, A., Baker, J., Minton, N.P., and Müller, V. (2018) The Rnf complex is an energy coupled transhydrogenase essential to reversibly link cellular NADH and ferredoxin pools in the acetogen *Acetobacterium woodii*. *J Bacteriol* **200:** e00357-00318.

Wiechmann, A., Ciurus, S., Oswald, F., Seiler, V.N., and Müller, V. (2020) It does not always take two to tango: "Syntrophy" via hydrogen cycling in one bacterial cell. *ISME J* **14:** 1561–1570.

Supporting information

Additional supporting information may be found online in the Supporting Information section at the end of the article.

Fig. S1. Effect of gene deletions on product formation from H_2 + CO_2 by whole-cells of *Acetobacterium woodii* in the presence or absence of Na^+.

Fig. S2. Stimulation of formate production by increasing concentrations of bicarbonate.

Fig. S3. Influence of various CO concentrations on formate production using resting cells of *A. woodii* ΔhydBA.

SUPPORTING INFORMATION

Revealing formate production from carbon monoxide in wild type and mutants of Rnf- and Ech-containing acetogens, *Acetobacterium woodii* and *Thermoanaerobacter kivui*

Fabian M. Schwarz[1], Sarah Ciurus[1], Surbhi Jain[1], Christoph Baum[2], Anja Wiechmann[1], Mirko Basen[2], Volker Müller[1]*

[1]Molecular Microbiology & Bioenergetics, Institute of Molecular Biosciences, Johann Wolfgang Goethe University, Frankfurt am Main, Germany

[2]Microbiology, Institute of Biological Sciences, University Rostock, Rostock, Germany

*Mailing address: Max-von-Laue-Str. 9, 60438 Frankfurt, Germany. Phone +49-6979829507. Fax +49-69-79829306. E-mail: vmueller@bio.uni-frankfurt.de

Additional file S1

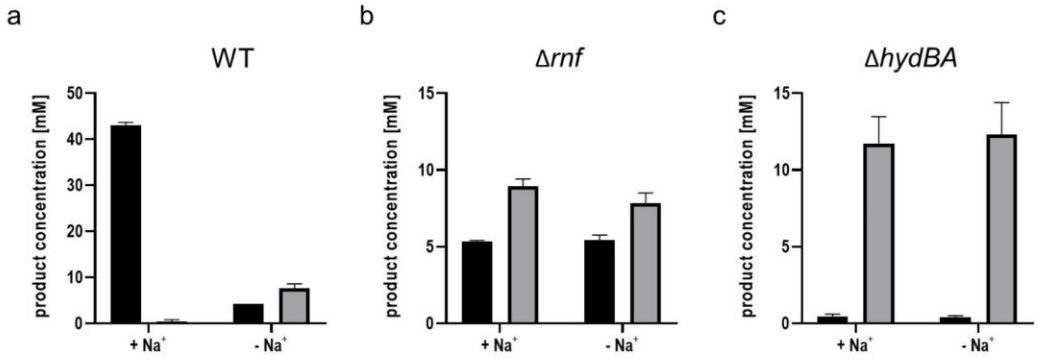

Figure S1. Effect of gene deletions on product formation from H_2 + CO_2 by whole-cells of *A. woodii* in the presence or absence of Na^+. Resting cells of *A. woodii* WT, Δ*rnf* or Δ*hydBA* were prepared as described before in buffer B (50 mM imidazole, 20 mM $MgSO_4$, 20 mM KCl, 2mM DTE, 4 μM resazurin, pH 7.0). Formate (grey bars) and acetate (black bars) production was determined after 48 h in cell suspension experiments with H_2 + CO_2 (80:20% [v/v]) at 2 x 10^5 Pa as substrate using **(a)** *A. woodii* WT, **(b)** Δ*rnf* or **(c)** Δ*hydBA*. +Na^+, additional 20 mM NaCl in the reaction buffer; -Na^+, no additional NaCl. Shown are data from two biological replicates. All data points are mean ± SD, N=2.

Additional file S2

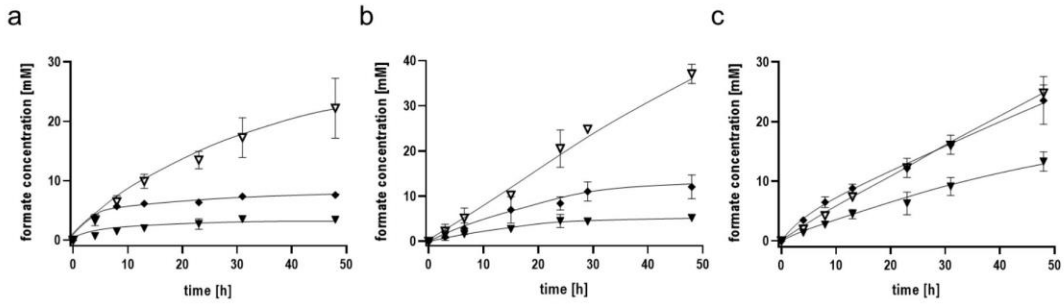

Figure S2. Stimulation of formate production by increasing concentrations of bicarbonate. Resting cells of **(a)** *A. woodii* wildtype, **(b)** Δ*rnf* and **(c)** Δ*hydBA* were incubated with additional 0 mM (triangles down), 50 mM (diamonds) and 300 mM (open triangles down) $KHCO_3$ in the buffer. The experiment was performed in the absence of Na^+ and by using 20% CO (80% N_2 as makeup gas) at 2 x 10^5 Pa as substrate. Shown are data from two biological replicates. All data points are mean ± SD, N=2.

Additional file S3

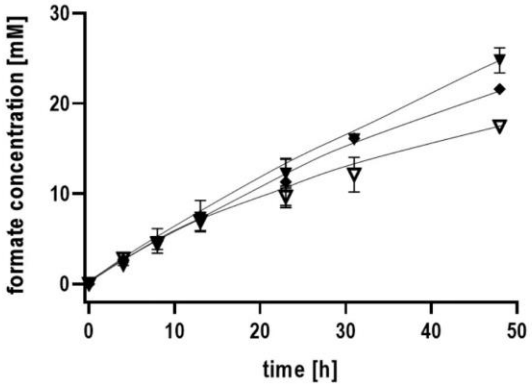

Figure S3. Influence of various CO concentrations on formate production using resting cells of *A. woodii* Δ*hydBA*. Cells were resuspended in buffer (200 mM imidazole, 20 mM $MgSO_4$, 20 mM KCl, 2mM DTE, 4 μM resazurin, pH 7.0) and were incubated with 20% (triangles down), 50% (diamonds) and 100% (open triangles down) CO as substrate. N_2 was used as makeup gas. The experiments were performed with additional 300 mM $KHCO_3$ and in the absence of Na^+. Shown are data from two biological replicates. All data points are mean ± SD, N=2.

6.3. Acetogenic conversion of H_2 and CO_2 into formic acid and *vice versa* in a fed-batch operated stirred tank bioreactor

Declaration of author contributions to the publication / manuscript (title):

Acetogenic conversion of H_2 and CO_2 into formic acid and *vice versa* in a fed-batch operated stirred tank bioreactor

Status: published, 2021

Journal: ACS Sustainable Chemistry and Engineering

Contributing authors: Fabian M. Schwarz (F.M.S.), Florian Oswald (F.O.) and Volker Müller (V.M.)

What are the contributions of the doctoral candidate and his co-authors?

(1) Concept and design

Doctoral candidate F.M.S.: 50%

Co-author F.O.: 20%

Co-author V.M.: 30%

(2) Conducting tests and experiments

Doctoral candidate F.M.S.: Performed all experiments

Co-author F.O.: Supervised the fermentation

(3) Compilation of data sets and figures

Doctoral candidate F.M.S.: Compiled all figures and data sets

(4) Analysis and interpretation of data

Doctoral candidate F.M.S.: Analyzed and interpreted all data

Co-author V.M.: Analyzed and interpreted all data

(5) Drafting of manuscript

Doctoral candidate F.M.S.: 60%

Co-author V.M.: 40%

ACS Sustainable Chemistry & Engineering

pubs.acs.org/journal/ascecg Research Article

Acetogenic Conversion of H_2 and CO_2 into Formic Acid and *Vice Versa* in a Fed-Batch-Operated Stirred-Tank Bioreactor

Fabian M. Schwarz, Florian Oswald, and Volker Müller*

Cite This: *ACS Sustainable Chem. Eng.* 2021, 9, 6810–6820 Read Online

ACCESS | Metrics & More | Article Recommendations | Supporting Information

ABSTRACT: Currently one of the biggest challenges for society is to combat global warming which requires the implementation of CO_2 mitigation strategies as well as strategies to replace fossil-fuel-based energy carriers. Since formic acid is considered as a liquid organic hydrogen carrier which directly addresses major challenges in the field of energy storage and (bio)chemical production, the formate bioeconomy and its popularity are rapidly growing. In this study, we describe a biological route for the storage of H_2 and the capturing of CO_2 in the compound formic acid using acetogenic bacteria as catalysts. The biocatalysis was proven in batch-operated stirred-tank bioreactors, demonstrating the technical feasibility of upscaling of the established whole-cell system. The process showed an efficiency of 100% for CO_2 conversion, and formic acid production proceeded with a specific rate of 48.3 mmol g^{-1} h^{-1}. Notably, no other products were coproduced in the process. The reverse reaction, H_2 production from formic acid, was also possible with a qH_2 of 27.6 mmol g^{-1} h^{-1}. The determined turnover frequency and turnover number underline the potential of acetogenic bacteria as biocatalysts for the two challenging reactions of CO_2 hydrogenation and H_2 evolution from formic acid.

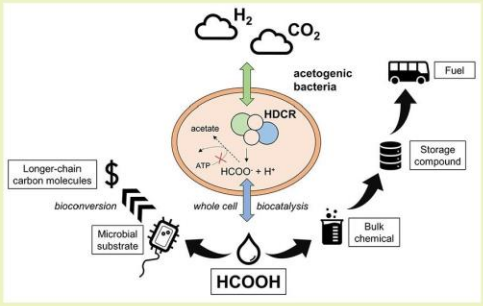

KEYWORDS: *Carbon capture, Hydrogen-storage, Whole-cell biocatalysis, Acetogenic bacteria, Fermentation, Bioreactor, Hydrogenation of CO_2, Hydrogen-dependent CO_2 reductase*

INTRODUCTION

In recent years, an increasing focus toward the sustainable production of biofuels and biochemicals has emerged. The issue of climate change and the possibility of dwindling resources demonstrate the urgency to develop alternative, sustainable routes within the field of energy generation and chemical production which are not based on fossil fuels. The worldwide strategic goal to reduce CO_2 emissions needs processes to prevent non-necessary CO_2 emissions as well as production technologies for the direct incorporation and capturing of inorganic carbon.[1,2] A special group of anaerobic bacteria, called acetogenic bacteria, are able to reduce CO_2 with H_2 or CO as the sole reductant and have therefore gained much attraction in recent years.[3,4] Chemical building blocks like acetate, butanol, butyrate, and 2,3-butanediol are formed under lithotrophic conditions by this group of bacteria,[5−8] and production of ethanol from the cost-effective and abundant substrate synthesis gas or syngas (H_2, CO, CO_2) is already realized on an industrial scale.[9−11] The metabolic pathway which enables acetogenic bacteria to use the gases H_2, CO_2, and/or CO as the sole energy and carbon source is the so-called Wood−Ljungdahl pathway (WLP). In this unique, two-branched linear pathway, two molecules of CO_2 are reduced to one molecule of acetyl-CoA.[12−14] The further conversion of acetyl-CoA to other natural products is diverse and differs within the group of acetogenic bacteria, but acetic acid is a common, major end product. In acetogenic bacteria, the WLP is hooked up to an electron transport chain providing energy for growth.[15−17] A detailed review of acetogenic bacteria and their metabolic features is given by Drake et al. (2008),[14] Ragsdale (2008),[13] and Schuchmann and Müller (2016).[18]

Interestingly, the two acetogenic bacteria *Acetobacterium woodii* and *Thermoanaerobacter kivui* harbor a special enzyme complex which catalyzes the fixation of one CO_2 molecule in the WLP via direct hydrogenation to formic acid.[19,20] These enzymes consist of a formate dehydrogenase module and an [FeFe]-hydrogenase module that are most likely connected by two small FeS-cluster-containing proteins. Since they use molecular hydrogen as a direct electron donor for the reduction of CO_2 to formic acid, they were named hydrogen-dependent CO_2 reductases (HDCRs). HDCR genes are also found in other species.[19,20] Both HDCRs were purified and characterized and showed the highest CO_2 reduction rates

Received: February 15, 2021
Revised: April 22, 2021
Published: May 4, 2021

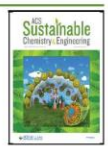

https://doi.org/10.1021/acssuschemeng.1c01062
ACS Sustainable Chem. Eng. 2021, 9, 6810−6820

ever reported for a biological system; moreover, they are orders of magnitude more efficient than any known chemical catalyst so far.[21] Not only CO_2 reduction but also formate oxidation to H_2 and CO_2 was catalyzed with remarkable catalytic activities. Based on their outstanding catalytic properties and biotechnological importance, whole-cell approaches were already established to take advantage of whole cells instead of the purified enzyme to convert H_2 + CO_2 to formic acid and *vice versa*.[19,22,23] This system is based on the turn-off of the ATP-dependent further conversion of formic acid to acetic acid. By lowering the cellular ATP content of these organism, the ATP-dependent further conversion of formic acid is blocked, and formic acid is no longer reduced to acetic acid in the WLP. This ATP reduction can be achieved either by using ionophores that destroy the electrochemical ion potential across the cytoplasmic membrane thus making chemiosmotic ATP synthesis impossible, by limiting the coupling ion, or by direct inhibition of the ATP synthase.[19,22] Apart from CO_2 capturing and formation of an industrial bulk chemical, formic acid is further considered as a storage compound for H_2 in a liquid, nontoxic form, therefore called a liquid-organic hydrogen carrier (LOHC).[24,25] Formate can even be used as a fuel in "direct formate fuel cells" (DFFCs).[26] Besides, the produced formic acid can be fed to different natural or syntrophic formatotrophic organisms to produce value-added compounds.[27−30] Interlinking anaerobic acid production with aerobic production of malic acid[31] or diesel fuels[32] has been demonstrated using acetic acid as an intermediate carbon source.

So far, conversion of hydrogen and carbon dioxide to acetic acid has been demonstrated for different acetogenic bacteria in bioreactor applications. The process of hydrogenotrophic acetic acid production by acetogens was investigated in batch-operated stirred-tank bioreactors,[33] packed-bed and trickle-bed biofilm reactors with immobilized cells,[34] standard stirred-tank bioreactors with a customized submerged microfiltration unit for full cell retention under continuous gas supply,[35] and controlled batch-operated stirred-tank bioreactors with increasing process pressure of the gaseous substrates.[36,37] In the latter application, an increase of the total system pressure (up to 7 bar) resulted in a shift of the product spectrum from mainly acetic acid and ethanol to 82.7% formic acid, 15.6% acetic acid, and 1.7% ethanol, as catalyzed by *Clostridium ljungdahlii*.[36]

So far, the experiments described above for the reversible conversion of hydrogen and carbon dioxide to formic acid have only been demonstrated in small-scale serum bottles without process control. To further characterize, optimize, and scale up the reaction, we set up a bioreactor under fully controlled reaction conditions (i.e., temperature, pH, gas feed rates). The aim was the successful demonstration of the target-oriented production of formic acid in a batch-operated stirred-tank bioreactor with a continuous gas supply of H_2 and CO_2. The upscaling approach should demonstrate the technical feasibility of our whole-cell system, underlining the great potential of a new biotechnological route in hydrogen storage and CO_2 capturing using acetogenic bacteria.

MATERIALS AND METHODS

Organism and Cultivation. *Thermoanaerobacter kivui* (DSM 2030) was cultivated at 66 °C under anoxic conditions in complex medium[38] using 1 L flasks (Müller-Krempel, Bülach, Switzerland) with 500 mL of media. Media was prepared under anoxic conditions as described before.[39,40] Pyruvate (100 mM) was used as a substrate. *Acetobacterium woodii* (DSM 1030) was cultivated at 30 °C under anoxic conditions in carbonate-buffered medium[41] using 1 L flasks with 500 mL of media. The medium was prepared as described before.[39,40] Fructose (20 mM) was used as a growth substrate for all cultivations. Growth was followed by measuring the optical density at 600 nm with a UV/vis spectrophotometer.

Preparation of Cell-Free Extracts. For the preparation of cell-free extracts of *A. woodii* and *T. kivui*, all preparation steps were performed under strictly anoxic conditions using an anaerobic chamber (Coy Laboratory Products, Grass Lake, MI) as described.[42] Cell-free extracts were prepared as described before[20] by harvesting and washing the cells with buffer A (25 mM Tris/HCl, 20 mM $MgSO_4$, 20% glycerin [v/v], pH 7.5). The cell-free extract was immediately used for the measurement of formate formation from H_2 and CO_2 (H_2:CO_2 oxidoreductase activity) as described below. Therefore, 120 mL serum bottles (Glasgerätebau Ochs GmbH, Bovenden-Lenglern, Germany) were filled with buffer B (100 mM HEPES/NaOH, 20 mM $MgSO_4$, 4 μM resazurin, 2 mM DTE, pH 7.0) and incubated at 30 or 60 °C, and the gas atmosphere was changed to H_2 + CO_2 (80:20%, [v/v]) with 1 bar overpressure. The serum flasks contained a final liquid volume of 2 mL after starting the experiment by adding cell-free extracts to a final protein concentration of 0.5 mg/mL. For analysis purposes, samples (100 μL) were taken over time.

Preparation of Resting Cells and Cell Suspension Experiments. Resting cells of *A. woodii* and *T. kivui* were prepared as described before.[22] The cells were washed and resuspended in imidazole buffer (50 mM imidazole, 20 mM $MgSO_4$, 20 mM KCl, 4 μM resazurin, 2 mM DTE, pH 7.0) or the appropriate reaction buffer used in the resting cell experiment. Resting cells were directly used for the subsequent experiments, and the protein concentration of the cell suspension was determined according to Schmidt (1963).[43] To determine the conversion of H_2 + CO_2 into formate by resting cells of *A. woodii* and *T. kivui*, 120 mL serum bottles (Glasgerätebau Ochs GmbH, Bovenden-Lenglern, Germany) containing prewarmed buffer (50 mM imidazole, 20 mM $MgSO_4$, 20 mM KCl, 4 μM resazurin, 2 mM DTE, pH 7.0; 50 mM Tris, 20 mM $MgSO_4$, 20 mM KCl, 4 μM resazurin, 2 mM DTE, pH 7.5; 50 mM K-phosphate, 20 mM KCl, 4 μM resazurin, 2 mM DTE, pH 7.0) under a N_2 atmosphere were incubated with cell suspensions at the protein concentration stated. The serum flasks contained a final liquid volume of 10 mL, and the cells were incubated for at least 10 min at 30 or 60 °C for cells of *A. woodii* and *T. kivui*, respectively. The reaction was started by changing the head space to H_2 + CO_2 (80:20%, [v/v]) with 1 bar overpressure. If necessary, ionophores and uncoupling agents such as *N,N,N′,N′*-tetracyclohexyl-1,2-phenylenedioxydiacetamide (ETH2120, dissolved in EtOH), monensin sodium salt (dissolved in EtOH), 20 mM NaCl, as well as 300 mM bicarbonate were added prior to the start of the reaction. Samples were taken over time to analyze the formation of acetic acid and formic acid.

Storage Stability of Cells. Resting cells, prepared as mentioned above, were resuspended in imidazole buffer (50 mM imidazole, 20 mM $MgSO_4$, 20 mM KCl, 4 μM resazurin, 2 mM DTE, pH 7.0) and were transferred into gastight Hungate tubes. Cell suspensions were stored at 4 °C up to their use in serum bottle experiments as stated before. In all experiments, the above-mentioned imidazole buffer and a gas atmosphere of H_2 + CO_2 (80:20%, [v/v]) with 1 bar overpressure were used. In the case of *A. woodii*, bioenergetically "coupled" cells contained additional 20 mM NaCl compared to "uncoupled" cells where additional 30 μM ETH2120 was present as an uncoupler. To "uncouple" *T. kivui* cells, additional 300 mM of bicarbonate was used in the experiment. *A. woodii* and *T. kivui* were investigated on their ability to produce acetic acid ("coupled") and formic acid ("uncoupled") from H_2 and CO_2 over several days of storage.

Bioreactor Application: Formic Acid Production from H_2 and CO_2. Fermentations were carried out in Biostat Aplus benchtop reactors from Sartorius (Melsungen, Germany) with a working volume of 2 L. Each bioreactor was equipped with a temperature

https://doi.org/10.1021/acssuschemeng.1c01062
ACS Sustainable Chem. Eng. 2021, 9, 6810−6820

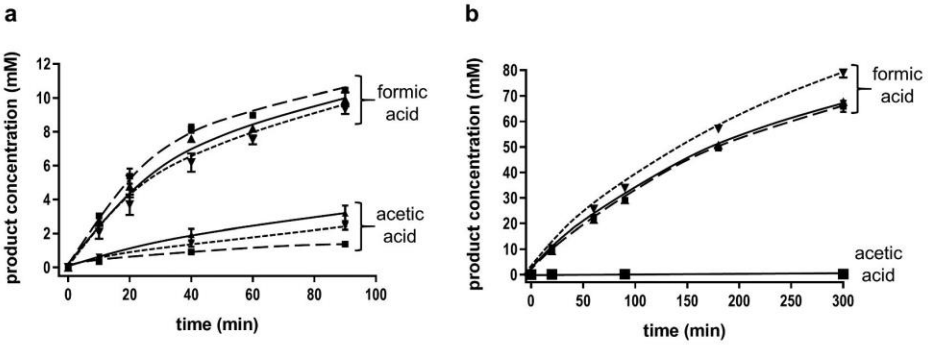

Figure 1. Effect of different ways to reduce the cellular energy charge on acetic acid and formic acid formation from H_2 and CO_2 by resting cells of *A. woodii*. Resting cells (1 mg/mL) were prepared in resuspension buffer (50 mM imidazole, 20 mM KCl, 20 mM $MgSO_4$, 20 mM NaCl, 2 mM DTE, 4 μM resazurin, pH 7.0) under an atmosphere of H_2 + CO_2 (80:20% [v/v], 2 × 105 kPa) in the presence of 30 μM ETH2120 (▲), 30 μM monensin (▼), or no additional NaCl (■). The buffers contained no additional bicarbonate (a) or 300 mM $KHCO_3$ (b). Formic acid and acetic acid were determined as described in the Materials and Methods section. All data points are mean ± SD, N = 2.

probe, a microsparger, baffles, two Rushton-impellers, a pH-probe (Hamilton, Bonaduz, Switzerland), and a redox potential probe (Hamilton, Bonaduz, Switzerland). The temperature of the buffer (50 mM imidazole, 20 mM $MgSO_4$, 20 mM KCl, 20 mM NaCl, 2 mM DTE, pH 7.0; or 50 mM K-phosphate, 20 mM KCl, 20 mM NaCl, 2 mM DTE, pH 7.0) was maintained at 30 and 60 °C for *A. woodii* and *T. kivui*, respectively, using a cooling finger and heating sleeve. The pH value was kept constant at 7.0 by titration with NaOH. The gas flow rate was maintained at a value of 25 mL/min using a digital mass-flow controller (Bronkhorst High-Tech, Ruurlo, Netherlands). The supplied gas composition varied in the stoichiometry of H_2 and CO_2 and was either 70% H_2, 20% CO_2, and 10% N_2 or 45% H_2, 45% CO_2, and 10% N_2 [v/v] (Air Liquide, France). The installed microsparger ensured the formation of microbubbles to enhance mass transfer between the gaseous and aqueous phase.[44] The headspace of the bioreactor was at atmospheric pressure. Gas−liquid mixing was achieved by using a stirrer set up with two Rushton-impellers at 800 rpm. Buffers were prepared under aerobic, nonsterile conditions, and oxygen was removed by subsequent sparging with the above-mentioned gas composition. After anoxic conditions and CO_2 saturation in the liquid phase were achieved, 2 mM DTE and 30 μM monensin or 300 mM $KHCO_3$ were supplemented as indicated. In low Na^+ bioreactor approaches, additional NaCl (20 mM) in the buffer as well as uncoupling agents were omitted. Whole-cell biocatalysis was started by adding the cell suspension to a final cell protein concentration of 1 mg/mL to the bioreactor. Bioreactor samples (2 mL) were taken at defined time points for the HPLC measurement as well as OD and protein determination.[43] Prior to sampling, a single liquid sample of 3 mL of reactor broth was taken and discarded to account for the dead volume of the sampling line. The samples were centrifuged (18 000*g*, 10 min, room temperature) to remove cells, and the supernatant was frozen at −20 °C until further off-line analysis via HPLC. All bioreactor experiments were performed in triplicates.

Bioreactor Application: H_2 Production from Formic Acid. For formic-acid-driven H_2 production, the general bioreactor setup was used as described above. Additionally, a foam electrode (Infors-HT) was installed to prevent excessive foaming in the bioreactor. Antifoam A (Sigma-Aldrich, Germany) was used as an antifoaming agent. The process parameters were adjusted to a gas flow rate of 50 mL/min of 100% N_2 to remove the produced H_2 in the liquid, and the stirrer speed was adjusted to 400 rpm. To prevent a dramatic pH drop at the initial addition of pure formic acid to the bioreactor, the buffer concentration was increased (500 mM K-phosphate, 20 mM KCl, 20 mM NaCl, 2 mM DTE, pH 7.0). Monensin (30 μM) was used as an uncoupling agent. The reaction was started by the addition of formic acid (150 mM) to the bioreactor, containing the cell suspension with a final cell protein concentration of 1 mg/mL. The experiment can generally be divided into two different phases: In the first phase, the experiment was started with the one-time addition of formic acid (150 mM), and the pH value was not controlled (named as Batch 1). After 3.5 h of process time, the second phase was started, and the pH control as well as substrate concentration were maintained at a constant level by feeding formic acid over the pH pump into the bioreactor (named as Fed-Batch 2). Thereby, the pH value was kept constant at pH 6.2, and the formic acid concentration remained at 150 mM over the whole process time. Samples for analytical purposes and OD measurements were taken as described in the previous section.

Analytical Methods. The concentrations of acetic acid and formic acid were measured by high-performance liquid chromatography (1260 Infinity II LC System) equipped with a quaternary pump, vial sampler, multicolumn thermostat, diode array detector, and refractive index detector (Agilent Technologies, Santa Clara, CA) as described before[45] or by using a commercially available formic acid and acetic acid kit (Boehringer Mannheim/R-Biopharm AG, Mannheim/Darmstadt, Germany) following the instructions of the manufacturer. Off-gas analysis was conducted via a Micro-GC instrument (Inficon, Bad Ragaz, Switzerland) equipped with two measurement modules and the applied analytical conditions as described before.[46]

Cell Recycling after Fermentation. At the end of the fermentation period, about 60 mL of cell suspension of each bioreactor was transferred in a 120 mL anoxic serum bottle (Glasgerätebau Ochs GmbH, Bovenden-Lenglern, Germany). Afterward, the cells were harvested and washed twice with fresh buffer (same as used in the bioreactor application), and a cell concentration of 1 mg/mL was used in the subsequent serum bottle experiment. The serum bottle experiments were done as described above.

Chemicals. All chemicals were supplied by Sigma-Aldrich (St. Louis, MO) and Carl Roth GmbH & Co KG (Karlsruhe, Germany). All premixed gases for cell suspension experiments and bioreactor applications were purchased from Air Liquide (Paris, France). Pure gases such as N_2 (purity of 5.0) were purchased from Nippon Gases Europe (Düsseldorf, Germany).

RESULTS

Optimization of Formic Acid Production from H_2 and CO_2. The uncoupler used previously to stimulate formic acid formation from H_2 and CO_2 was the sodium-ionophore ETH2120[19] which is rather cost-intensive. As an alternative, we analyzed the effect of monensin, an antibiotic that catalyzes Na^+/H^+ antiport, or the omission of the coupling ion Na^+ (Figure 1a). As observed before,[19] ETH2120 stimulated formic acid production and repressed acetic acid formation; 52 times

https://doi.org/10.1021/acssuschemeng.1c01062
ACS Sustainable Chem. Eng. 2021, 9, 6810−6820

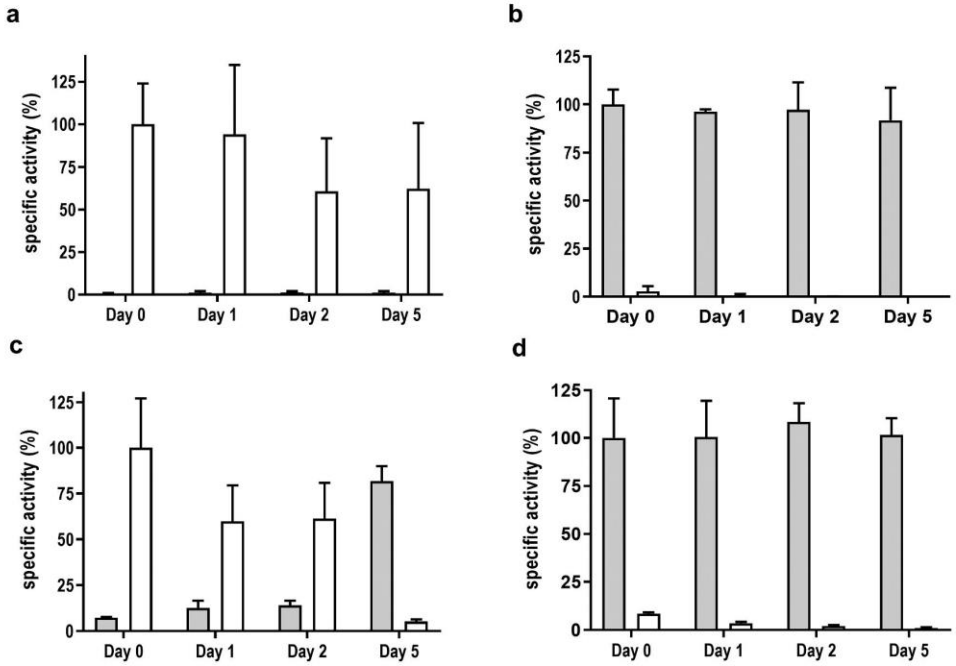

Figure 2. Catalytic viability of resting cells from *A. woodii* and *T. kivui*. Resting cells were prepared in buffer containing 50 mM imidazole, 20 mM KCl, 20 mM $MgSO_4$, 2 mM DTE, 4 μM resazurin, pH 7.0. The cell suspension was stored over several days at 4 °C. At the time points indicated, cells (1 mg/mL) were incubated in anoxic serum bottles without (a, c) or with (b, d) ionophores/uncoupling agents under a gas atmosphere of H_2 + CO_2 (80:20% [v/v], 2 × 105 kPa), and the specific production rates of acetic acid (white bars) and formic acid (gray bars) were determined. In the case of *T. kivui* (a, b) and *A. woodii* (c, d), 100% of the activity corresponds to a formic acid production rate of 22 and 215 mmol g^{-1} h^{-1} for *A. woodii* and *T. kivui*, respectively. The acetic acid production rate of 100% is similar to 16 and 30 mmol g^{-1} h^{-1} for *A. woodii* and *T. kivui*, respectively. All data points are mean ± SD, $N = 2$.

more formic acid and 16 times less acetic acid were produced compared to conditions without the uncoupler. The same stimulation of formic acid production and inhibition of acetic acid production were seen in cell suspensions of *A. woodii* that contained monensin or that lacked additional NaCl. When 300 mM potassium bicarbonate was added, formic acid production was stimulated to ~30 mmol g^{-1} h^{-1} (12.9 mmol g_{CDW}^{-1} h^{-1}), and acetic acid production was almost completely inhibited (0.2 mM acetic acid) (Figure 1b), as observed before.[19] These experiments indicate that the omission of NaCl could be the easiest and most cost-efficient way to achieve maximal formic acid production in bioreactor experiments. Imidazole could be substituted by Tris or phosphate, alternative low-priced buffer systems (Figure S1).

Growth-Phase-Dependent Conversion Activity of H_2 and CO_2 into Formic Acid by the HDCR. A previous study has shown that the formate dehydrogenase (Fdh) activity in cell-free extracts of the thermophilic acetogenic bacterium *Moorella thermoacetica* was dramatically affected by the growth phase; Fdh activity was maximal in the early exponential growth phase but decreased to almost zero in the late exponential growth phase and slightly increased again to a marginal activity of ~7% in the stationary phase.[47] Therefore, we determined a possible growth-phase dependence of the HDCR conversion rate in cell-free extracts of *A. woodii* and *T. kivui*. H_2:CO_2 oxidoreductase activity was also growth-phase-dependent for both organisms. In *T. kivui*, activity was maximal with 2.1 U/mg in the early exponential growth phase and decreased by 33% to 1.4 U/mg in the late exponential growth phase and stayed at that level through the early stationary phase. In contrast, the HDCR-based conversion rate of H_2 and CO_2 to formic acid by *A. woodii* increased from 0.1 to 0.5 U/mg by an increase in OD from 0.13 to 2.5 (Figure S2). Therefore, cells for the bioreactor experiments were grown to the end of the exponential growth phase with an OD of around 1.8−2.0.

Storage Stability of Resting Cells. To address the viability of cells over time, resting cells were prepared and tested for their ability to produce acetic acid and formic acid from H_2 and CO_2 over several days when stored at 4 °C in resuspension buffer (Figure 2). The formation of acetic acid was also determined to make sure that the cell integrity was not impaired during storage. Acetic acid production by resting cells of *T. kivui* decreased over time with 62% residual activity after 5 days. The same trend was observed in *A. woodii*, but after 5 days, acetic acid production was only 5% of the initial activity. At the same time, formic acid production increased dramatically, showing that the energy status was reduced to a level that prevented further reduction of formic acid to acetic acid. When the energy level was reduced by uncoupling agents in *A. woodii* or by ATPase inhibitors in *T. kivui*,[19,22] acetic acid formation was blocked, and formic acid was produced instead. The specific formic acid productions were 22 mmol g^{-1} h^{-1} (9.5 mmol g_{CDW}^{-1} h^{-1}) and 215 mmol g^{-1} h^{-1} (135.5 mmol g_{CDW}^{-1} h^{-1}) for *A. woodii* and *T. kivui*, respectively.

https://doi.org/10.1021/acssuschemeng.1c01062
ACS Sustainable Chem. Eng. 2021, 9, 6810−6820

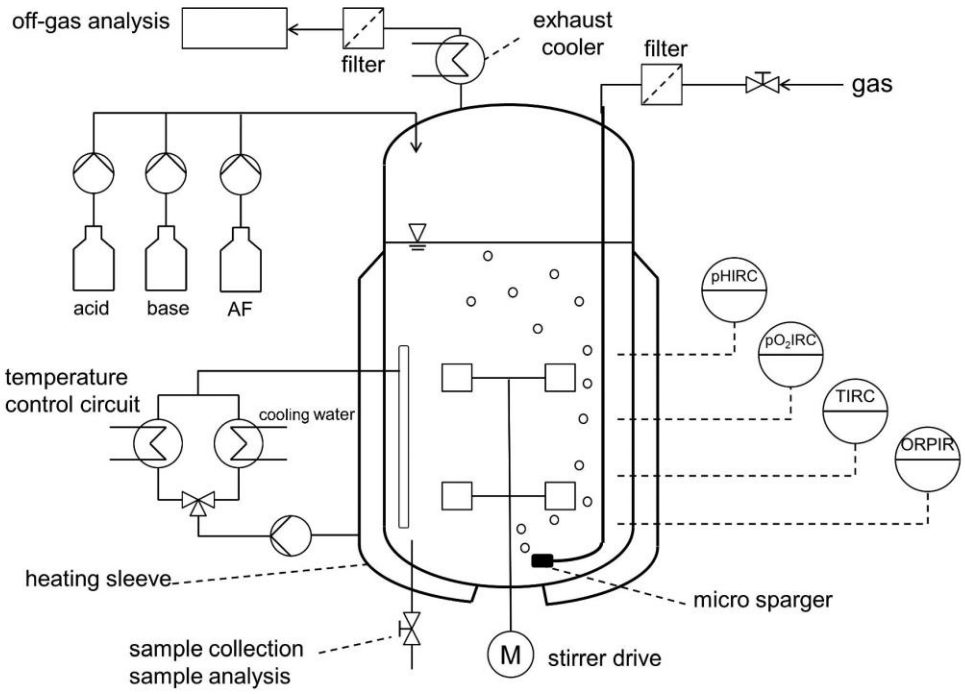

Figure 3. Scheme of a fed-batch-operated stirred-tank bioreactor with continuous gas supply. pHIRC, pH indicator recording and control; pO_2IRC, pO_2 indicator recording and control; TIRC, temperature indicator recording and control; ORPIR, oxidation reduction potential indicator and recording; AF, antifoam.

Interestingly, formic acid production rates remained at the initial high level over 5 days in both species.

Bioreactor Application for Whole-Cell Biocatalysis. Next, we analyzed formate production by resting cells of *A. woodii* and *T. kivui* in a batch-operated stirred-tank bioreactor with continuous gas supply (Figure 3). Therefore, the organisms were grown in 20 L of complex medium with the corresponding substrate to the end of the exponential growth phase, and resting cells were prepared. The bioreactor contained 50 mM imidazole buffer at pH 7.0 with additional 30 μM monensin; the pH value was kept constant at 7.0 by titration with NaOH. The reaction was started by adding resting cells to a final cell protein concentration of 1 mg/mL to the bioreactor. Formic acid formation started immediately after the addition of the cell suspension (Figure 4a), and the production proceeded with a rate of 48.3 mmol g^{-1} h^{-1} (20.8 mmol g_{CDW}^{-1} h^{-1}) which was 2.6 times faster than the rate observed in serum bottles (18.3 mmol g^{-1} h^{-1} or 7.9 mmol g_{CDW}^{-1} h^{-1}). Already after 25 min, a formic acid concentration of 19 mM was reached in the bioreactor which corresponds to 40% of the final formic acid concentration. The maximal formic acid concentration of 47 mM was reached after 21 h, and the formic acid concentration did not change further, even after 100 h of operation. At the same time, acetic acid production was very low with a maximal acetic acid concentration of 0.4 mM, giving a formic acid/acetic acid ratio of 47:0.4. This indicates the high specificity (99.2%) of the process toward the desired product formic acid. Notably, the optical density as well as the total cell protein stayed almost constant over the entire fermentation period (Figure 4b). Remarkably, during the first 20 min of the experiment, the supplied H_2 and CO_2 were completely converted into the product formic acid. When the formic acid production slowed down after 20 min of process time, the amount of H_2 and CO_2 in the off-gas stream likewise increased again (Figure 4c,d).

To analyze whether the plateau reached in the formic acid production is due to an inactivation of the cells, the cells were harvested after 100 h of fermentation, washed and resuspended in fresh buffer (50 mM imidazole, 20 mM $MgSO_4$, 20 mM KCl, 20 mM NaCl, 2 mM DTE, pH 7.0), and incubated in serum bottles with H_2 + CO_2 (80:20%) in the gas atmosphere at 1 bar overpressure. Monensin (30 μM) was added prior to the start of the reaction. Under these conditions, formic acid was produced with a rate of 69% of the fresh cell suspension (Figure S3). This clearly demonstrates that the maximal formic acid concentration in the bioreactor is not a function of cell viability but rather is limited by the equilibrium of the reaction.

With this knowledge, we set up a fed-batch-operated stirred-tank bioreactor using a less cost-intensive buffer system (50 mM K-phosphate, 20 mM KCl, 20 mM NaCl, 2 mM DTE, pH 7.0) and, most important, adjusted the gas composition to a stoichiometric ratio of 1:1 of H_2 and CO_2 (45% H_2:45% CO_2:10% N_2 [v:v]). Monensin was used for *A. woodii* cell suspensions whereas bicarbonate (300 mM) was used to "uncouple" *T. kivui* cells as shown before. The final formic acid concentration could indeed be further increased using the adjusted gas composition. *A. woodii* cells produced 62% more formic acid ending up with 73 mM formic acid in average (Figure 5). Acetic acid was not produced which indicates an efficiency of 100% for the utilized CO_2 in the process. The

https://doi.org/10.1021/acssuschemeng.1c01062
ACS Sustainable Chem. Eng. 2021, 9, 6810−6820

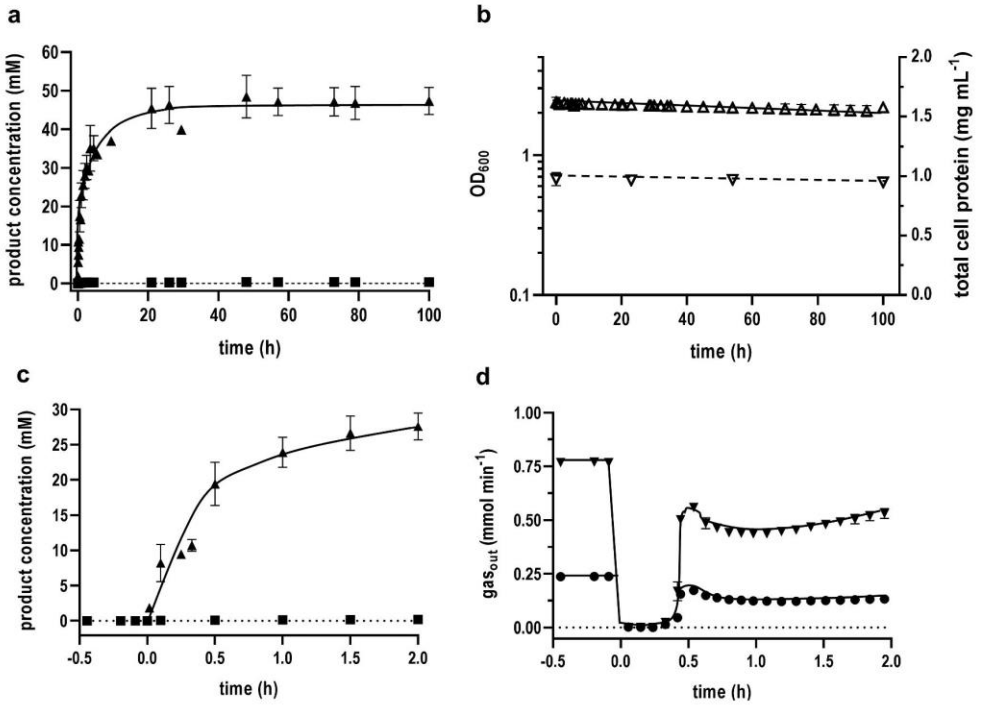

Figure 4. Bioreactor application for hydrogen-dependent CO_2 reduction to formic acid by *A. woodii*. Resting cells were transferred into the bioreactor to a final concentration of 1 mg/mL in buffer (50 mM imidazole, 20 mM KCl, 20 mM $MgSO_4$, 20 mM NaCl, 2 mM DTE, pH 7.0) containing additional 30 μM monensin. A continuous gas flow rate of 25 mL min^{-1} was applied, consisting of a gas mixture of 70% H_2, 20% CO_2, and 10% N_2 [v/v]. The reaction temperature was kept at 30 °C in the liquid phase; the stirrer speed was set at 800 rpm, and the pH was controlled with NaOH to be constant at 7.0. (a) The product formation is shown over the whole fermentation time. The optical density and total cell protein was measured during the whole process (b), and the initial section of product formation (c) and corresponding off-gas analysis (d) are highlighted. ▲, formic acid; ■, acetic acid; △, optical density at 600 nm; ▽, total cell protein; ▼, H_2; ●, CO_2. All data points are mean ± SD, N = 3.

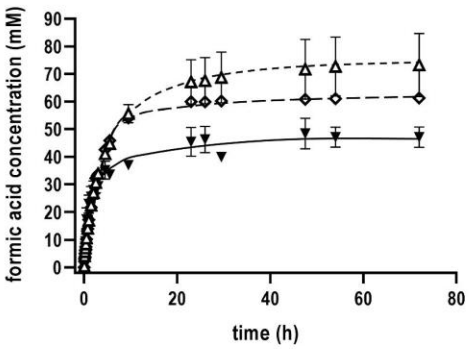

Figure 5. Change in product concentrations using adjusted gas compositions in a mesophilic (30 °C) and thermophilic (60 °C) bioreactor approach. The initial gas composition was changed from 70% H_2:20% CO_2:10% N_2 [v/v] (▼) to the optimized gas composition of 45% H_2:45% CO_2:10% N_2 [v/v] (△; ◇) to increase the final formic acid concentration. Shown is the product formation from H_2 and CO_2 by *A. woodii* (▼; △) and *T. kivui* (◇). All data points are mean ± SD, N = 3.

experiment was repeated by omitting monensin and omitting Na^+ in the bioreactor approach, keeping the remaining parameters (gas composition, buffer, flow rate, etc.) the same. Unfortunately, under these conditions, 55 mM formic acid along with 18 mM acetic acid were produced (data not shown). With *T. kivui* cells as biocatalysts, H_2 and CO_2 also ended up solely in formic acid. Here, the formic acid production rates (30 mmol g^{-1} h^{-1} or 19.2 mmol g_{CDW}^{-1} h^{-1}) were almost comparable to *A. woodii*, but the maximum achieved formic acid concentration was only 60 mM at the end of the fermentation (Figure 5).

Formic Acid Oxidation to H_2 and CO_2. Next, we analyzed the reverse reaction, formic acid oxidation to H_2 and CO_2. Therefore, pure formic acid was used (and not Na/K-formate) as a substrate to avoid salt accumulation in the reaction buffer, and the buffer concentration was increased to 500 mM K-phosphate at an optimal pH of 6.2. Preliminary serum bottle experiments clearly showed a decrease in the H_2 production rates (qH_2) from 71 mmol g^{-1} h^{-1} (30.5 mmol g_{CDW}^{-1} h^{-1}) to 37 mmol g^{-1} h^{-1} (15.9 mmol g_{CDW}^{-1} h^{-1}) by changing the buffer concentration and substrate (Table S1). However, the buffer concentration had to be increased since the addition of formic acid (200 mM) led to a strong acidification of 50 mM imidazole buffer up to pH 2.5 thus stopping the formic-acid-driven H_2 production in total.

Using these conditions, the turnover number (TON) was determined in the bioreactor. N_2 (100%) was used as an inert gas to remove the produced gases H_2 and CO_2, and monensin (30 μM) was used as an uncoupling agent. We divided the experiment into two sections, named as Batch 1 and Fed-Batch

https://doi.org/10.1021/acssuschemeng.1c01062
ACS Sustainable Chem. Eng. 2021, 9, 6810−6820

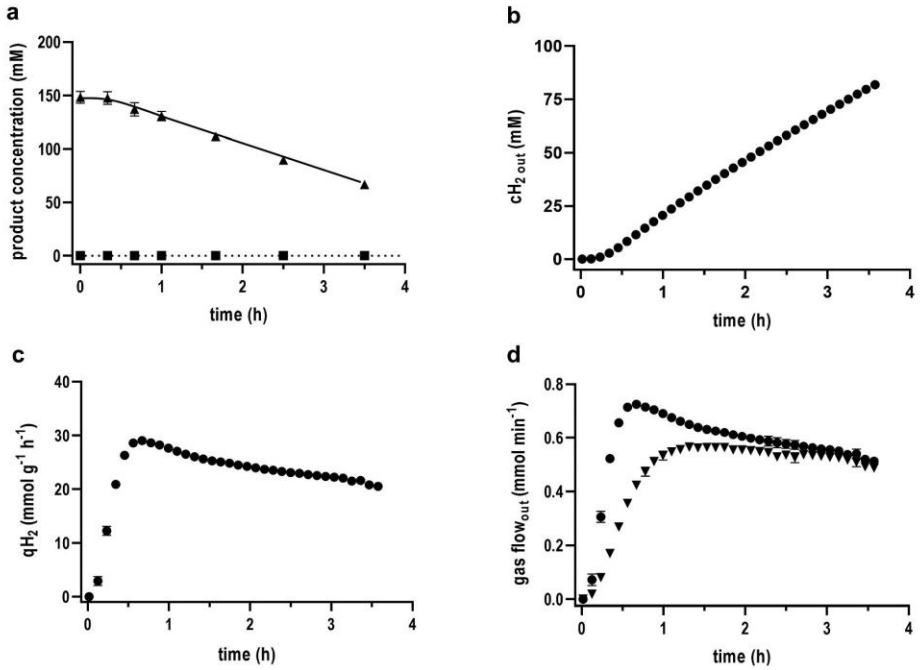

Figure 6. Bioreactor application for formic-acid-driven H_2 production using resting cells of *A. woodii* (Batch 1). Resting cells were transferred into the bioreactor at a final concentration of 1 mg/mL containing K-phosphate buffer (500 mM K-phosphate, 20 mM KCl, 20 mM NaCl, 2 mM DTE, pH 7.0). A continuous gas flow rate of 50 mL/min with 100% N_2 was applied. The reaction temperature was kept at 30 °C in the liquid phase, and the stirrer speed was set at 400 rpm. Monensin (30 μM) was added as an uncoupling agent. The reaction was started by adding 150 mM formic acid to the bioreactor. The formic acid consumption (a) and H_2 evolution (b) are shown over time. Additionally, the specific H_2 production rate (c) and the gas flow in the off-gas (d) are shown. ▲, formic acid; ■, acetic acid; ▼, CO_2; ●, H_2. All data points are mean ± SD, N = 3.

2. In Batch 1, the experiment was started by the one-time addition of 150 mM formic acid, and H_2 evolution and substrate consumption were monitored over time (Figure 6a,b). The one-time addition of 150 mM formic acid resulted in a drop of pH from pH 7 to 6.2, which subsequently increased steadily to pH 6.58 after 3.5 h of process time, due to the oxidation of formic acid. The H_2 production rate (qH_2) was calculated to be 27.6 mmol g^{-1} h^{-1} (11.9 mmol g_{CDW}^{-1} h^{-1}) which matches the corresponding formic acid consumption rate of 27.02 mmol g^{-1} h^{-1} (11.6 mmol g_{CDW}^{-1} h^{-1}). The rates are lower than reported previously,[23] but this is due to the use of formic acid and a higher buffer concentration. Acetic acid was not produced at all. The qH_2 decreased by 26% over the first 3.5 h of fermentation (Figure 6c). At the beginning of the experiment, the amount of CO_2 observed was lower than the amount of H_2 observed, but similar amounts were observed during the course of the experiment (Figure 6d). This observation is caused due to the higher solubility of CO_2 in the liquid phase compared to H_2, since both gases are produced in stoichiometric amounts in the catalyzed reaction. After 3.5 h of fermentation, the experiment was switched into the Fed-Batch 2 mode. Here, a continuous pH control with a set point of 6.2 was applied. Formic acid was used to titrate the pH, thereby keeping the substrate concentration and pH value at a constant level of 150 mM and pH 6.2, respectively (Figure 7a). The qH_2 and the optical cell density were monitored over the remaining 195 h of process time (Figure 7b,c). After 50 h of fermentation, 50% of the initial qH_2 remained which further decreased to 20% of the initial qH_2 after 168 h of process time. A strong decrease in qH_2 could be detected over the entire time period which seemed to be directly connected to the exponential decay of the optical density. When cells were recycled at the end of the fermentation, a qH_2 of only 4.3 mmol g^{-1} h^{-1} (1.8 mmol g_{CDW}^{-1} h^{-1}) was achieved, indicating an inactivation of the cells. Nevertheless, the total yield ($Y_{H_2/HCOOH}$) was 0.95 which means that 95% of the added formic acid ended up in H_2. In total, 2.12 M formic acid was oxidized in the Fed-Batch 2 phase.

For the calculation of the turnover number, we assumed that each bacterial cell acts as a catalyst for the above-mentioned reaction. A correlation between the total cell protein and the total cell count was implemented via cell counting. The results showed that a total cell protein concentration of 1 g/L correlated to 4×10^{12} cells per liter. With this correlation, the assumption that each bacterial cell is catalytically active, and the given qH_2 of 27.6 mmol g^{-1} h^{-1}, we first calculated the turnover frequency (TOF) of the catalyst which was 4.14×10^9 h^{-1}. Then, the half-life of the catalyst ($TON_{1/2}$) was calculated according to eq 1.[48]

$$\mathrm{TON} = \frac{\mathrm{TOF} \times t_{1/2}}{\ln(2)} \quad (1)$$

resulting in a TON of 2.99×10^{11}, meaning that one bacterial cell can catalyze 2.99×10^{11} conversions until its full inactivation in the process.

https://doi.org/10.1021/acssuschemeng.1c01062
ACS Sustainable Chem. Eng. 2021, 9, 6810−6820

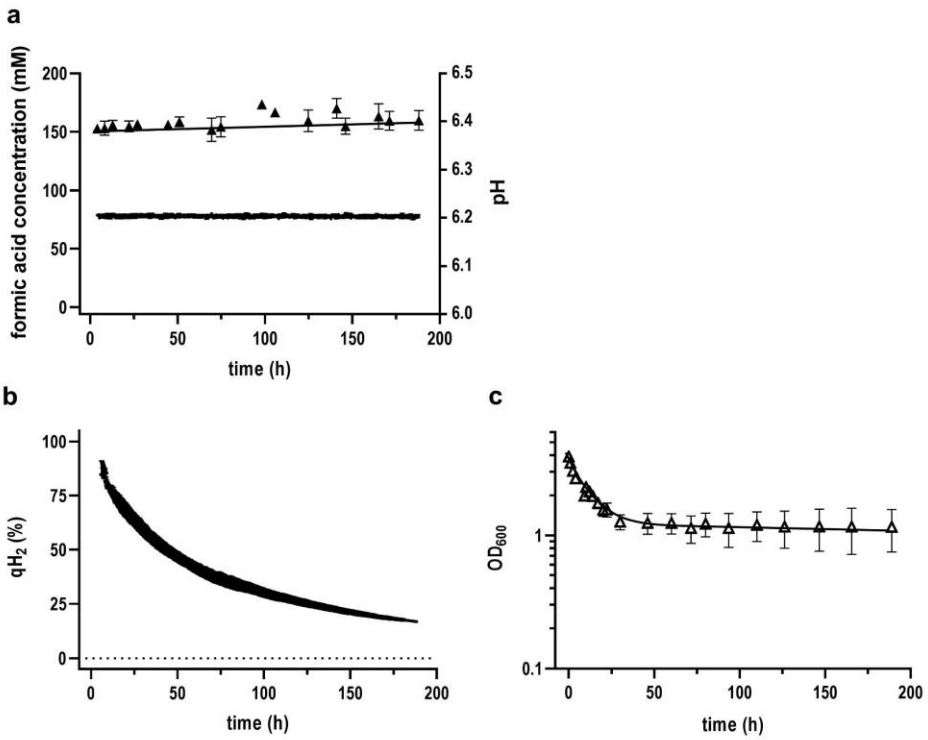

Figure 7. Bioreactor application for formic-acid-driven H_2 production using resting cells of *A. woodii* (Fed-Batch 2). After 3.5 h of process time, the pH and substrate concentration were kept constant at 6.2 by adding formic acid (substrate) to the bioreactor. (a) The formic acid concentration as well as the corresponding pH are shown. The qH_2 (b) as well as optical density (c) were calculated and monitored over the whole time period. The qH_2 of 100% is equal to 27.6 mmol g^{-1} h^{-1}. ▲, formic acid; —, pH; △, optical density at 600 nm; ●, H_2. All data points are mean ± SD, $N = 3$.

DISCUSSION

The two acetogenic bacteria *A. woodii* and *T. kivui* have been shown before to catalyze hydrogenation of carbon dioxide to formic acid with the highest rates ever reported.[21] These experiments were done without control of process parameters in serum bottles, and thus, there was a high potential for increasing yields and rates under controlled conditions. Furthermore, we aimed for lower process costs. Using these constraints, we developed a process under controlled conditions in a bioreactor in which the rates of CO_2 hydrogenation were increased by 160% in *A. woodii*, again showing the highest rates of the few reported bioreactor applications using whole cells as catalysts.[49,50] Not only the rates but also the final yields were increased by a factor of 6.6 compared to serum bottles. By using a whole-cell biocatalysis approach, we could achieve a high selectivity of 100% for the formation of formic acid from H_2 and CO_2, and we could prevent the accumulation of unwanted side products such as acetic acid. Because of economic and sustainable reasons, we changed the reaction buffer to K-phosphate, and we omitted Na^+ to avoid the need for monensin as an uncoupler. Here, *A. woodii* cells produced 55 mM formic acid along with 18 mM acetic acid as a side product in the bioreactor. Measurements of the Na^+ concentration in imidazole and K-phosphate buffer revealed the presence of 0.1 and 1.3 mM Na^+ in the two buffers, respectively. Since *A. woodii* cells require only a Na^+ concentration of around 0.7 mM to maintain the cellular bioenergetics for autotrophic growth,[41] Na^+ impurities in the K-phosphate buffer likely resulted in the coproduction of acetic acid next to formic acid. This is an important note for further bioreactor applications to choose the appropriate chemicals (i.e., buffer, pH correcting agents). If the use of uncoupling agents is undesired in the process, the use of highly Na^+-free chemicals is necessary to avoid acetic acid formation under Na^+ omitting conditions.

Interestingly, uncoupled *T. kivui* cells showed comparable catalytic rates in formic acid production as *A. woodii* cells, but the formic acid concentration was reduced to 60 mM. The lower product concentration is not surprising since the concentrations of dissolved gaseous compounds such as H_2 and CO_2 are strongly affected by the process temperature. An increase in the temperature from 30 to 60 °C lowers the dissolved concentration of H_2 by approximately 14%. This is in accordance to the observed decrease in the final formic acid concentration from 73 to 60 mM. More ambiguous are the catalytic rates of *T. kivui* cells since the purified enzyme is ~90 times faster than the *A. woodii* HDCR, and resting cells also showed a 7 times higher formic acid production rate compared to *A. woodii* cells in serum bottle experiments. The difference in the catalytic rates of serum bottle and bioreactor experiments could be related to the higher partial pressures in the serum bottles thus stimulating the reaction in *T. kivui*. An interesting approach to further investigate the promising potential of H_2-driven CO_2 reduction by whole cells of *A. woodii* and *T. kivui* would therefore be the implementation of a

https://doi.org/10.1021/acssuschemeng.1c01062
ACS Sustainable Chem. Eng. 2021, 9, 6810−6820

pressurized (and pH-controlled) bioreactor system as shown for different bacteria and archaea before.[36,50,51]

The reversibility of CO_2 hydrogenation could also be shown in our bioreactor experiments, a beneficial characteristic for a latter biotechnological application. Besides H_2 storage, the production of H_2 from formic acid was also shown, and *A. woodii* cells performed the conversion with a qH_2 of 28 mmol g^{-1} h^{-1}. Noteworthy, the $Y_{H_2/formic\text{-}acid}$ was close to one, indicating a conversion efficiency of almost 100%. However, a strong decrease in the optical density and the total cell count, respectively, was also monitored in the experiment. The reasons for this decrease could be diverse and are likely related to the strong buffer concentration, the use of formic acid as a substrate, and the slightly acidic pH conditions in the experiment. These are all factors which could affect and support proteolysis of resting cells.

The long-term application of formic-acid-driven H_2 production revealed an impressive turnover number (TON) and turnover frequency (TOF). In enzymatic catalysis, the TON (also known as total turnover number (TTN)) deals with the lifetime robustness of the catalyst whereas the TOF measures the instantaneous efficiency of the catalyst with units of $time^{-1}$. In general, the TOF is defined in enzyme catalysis as molecules reacting per active site per time. In our heterogeneous catalysis, a single bacterial cell was considered as a catalyst, keeping in mind that each bacterial cell harbors many active sites/HDCRs. However, the proportion of HDCR at the entire total cell protein is not known to further specify the value. As discussed before,[48] it is difficult to compare different fields of catalysis such as chemical catalysts with enzymes or even with whole cells. Many conditions must be taken into account, such as the substrate concentration, the reaction temperature, the solvent, the pH, cocatalysts, etc., hampering the comparison of different catalysts. Nevertheless, the high TON (2.99×10^{11}) and TOF (4.14×10^{9} h^{-1}) of our established whole-cell system indicate the great potential of a putative biological route for the direct hydrogenation of CO_2 to formic acid and *vice versa*, especially when many chemical solutions suffer from low TOF or TON, dependency on high pressure or temperature, or very expensive additives. The limit of a good TON depends on the application, but for industrial applications, a high turnover catalyst should have a TON ideally over 10^5, a dimension that is given for our biocatalyst. In summary, the study clearly demonstrates the up-scaling feasibility and efficiency of our established whole-cell system using acetogenic bacteria. The HDCR-containing organisms *A. woodii* and *T. kivui* are promising biocatalysts for the production of H_2 from formic acid as well as for the storage of molecular hydrogen and the capturing of inorganic CO_2 in formic acid, thus directly addressing major challenges in the field of energy storage and biochemical production.

CONCLUSION

In this study, we have proven the two acetogenic bacteria *A. woodii* and *T. kivui* as efficient biocatalysts for the direct hydrogenation of CO_2 to formic acid in a bioreactor application, catalyzing a challenging reaction for H_2 storage and CO_2 capture. The specific formic acid production rates were so far the highest rates reported for bioreactor-based whole-cell systems, and the process showed a high specificity, ending up with 100% of the desired product formic acid. Since the stored H_2 has to be released in a later dehydrogenation reaction to close a H_2 storage cycle, we also showed the reversibility of our established whole-cell system. Here, formic acid was oxidized in a fed-batch-operated stirred-tank bioreactor, and H_2 was produced. The bioreactor approach demonstrates the upscaling and technical feasibility of the applied whole-cell system and indicates the great potential of acetogenic bacteria to contribute to a future hydrogen and formate bioeconomy.

ASSOCIATED CONTENT

Supporting Information

The Supporting Information is available free of charge at https://pubs.acs.org/doi/10.1021/acssuschemeng.1c01062.

Buffer effect in whole-cell-based formic acid production of *A. woodii* and *T. kivui*; growth-phase-dependent conversion activity of H_2 and CO_2 into formic acid by the HDCR; cell recycling of bioreactor cells; buffer and substrate effect for formate and formic-acid-driven H_2 production using resting cells of *A. woodii* (PDF)

AUTHOR INFORMATION

Corresponding Author

Volker Müller − *Molecular Microbiology & Bioenergetics, Institute of Molecular Biosciences, Johann Wolfgang Goethe University, Frankfurt am Main 60438, Germany;* orcid.org/0000-0001-7955-5508; Phone: +49-6979829507; Email: vmueller@bio.uni-frankfurt.de

Authors

Fabian M. Schwarz − *Molecular Microbiology & Bioenergetics, Institute of Molecular Biosciences, Johann Wolfgang Goethe University, Frankfurt am Main 60438, Germany*

Florian Oswald − *Molecular Microbiology & Bioenergetics, Institute of Molecular Biosciences, Johann Wolfgang Goethe University, Frankfurt am Main 60438, Germany;* orcid.org/0000-0003-1783-9841

Complete contact information is available at: https://pubs.acs.org/10.1021/acssuschemeng.1c01062

Author Contributions

V.M. designed and supervised the research, analyzed the data, and wrote the manuscript. F.M.S. designed the research, performed the experiments, analyzed the data, and wrote the manuscript. F.O. supervised the fermentation.

Funding

This project has received funding from the European Research Council (ERC) under the European Union's Horizon 2020 research and innovation program (grant agreement 741791).

Notes

The authors declare the following competing financial interest(s): Goethe-University Frankfurt and V.M. possess a patent on the HDCR-based whole-cell system for storing gaseous hydrogen through producing methanoate (patent number: EP2816119).

REFERENCES

(1) Kumar, M.; Sundaram, S.; Gnansounou, E.; Larroche, C.; Thakur, I. S. Carbon dioxide capture, storage and production of biofuel and biomaterials by bacteria: A review. *Bioresour. Technol.* **2018**, *247*, 1059−1068.

(2) Cheah, W. Y.; Ling, T. C.; Juan, J. C.; Lee, D. J.; Chang, J. S.; Show, P. L. Biorefineries of carbon dioxide: From carbon capture and

storage (CCS) to bioenergies production. *Bioresour. Technol.* **2016**, *215*, 346−356.
(3) Takors, R.; Kopf, M.; Mampel, J.; Bluemke, W.; Blombach, B.; Eikmanns, B.; Bengelsdorf, F. R.; Weuster-Botz, D.; Dürre, P. Using gas mixtures of CO, CO_2 and H_2 as microbial substrates: the do's and don'ts of successful technology transfer from laboratory to production scale. *Microb. Biotechnol.* **2018**, *11*, 606−625.
(4) Bengelsdorf, F. R.; Dürre, P. Gas fermentation for commodity chemicals and fuels. *Microb. Biotechnol.* **2017**, *10*, 1167−1170.
(5) Köpke, M.; Mihalcea, C.; Liew, F.; Tizard, J. H.; Ali, M. S.; Conolly, J. J.; Al-Sinawi, B.; Simpson, S. D. 2,3-butanediol production by acetogenic bacteria, an alternative route to chemical synthesis, using industrial waste gas. *Appl. Environ. Microbiol.* **2011**, *77*, 5467−5475.
(6) Bengelsdorf, F. R.; Poehlein, A.; Linder, S.; Erz, C.; Hummel, T.; Hoffmeister, S.; Daniel, R.; Dürre, P. Industrial acetogenic biocatalysts: A comparative metabolic and genomic analysis. *Front. Microbiol.* **2016**, *7*, 1036.
(7) Jeong, J.; Bertsch, J.; Hess, V.; Choi, S.; Choi, I. G.; Chang, I. S.; Müller, V. Energy conservation model based on genomic and experimental analyses of a carbon monoxide-utilizing, butyrate-forming acetogen, *Eubacterium limosum* KIST612. *Appl. Environ. Microbiol.* **2015**, *81*, 4782−4790.
(8) Köpke, M.; Held, C.; Hujer, S.; Liesegang, H.; Wiezer, A.; Wollherr, A.; Ehrenreich, A.; Liebl, W.; Gottschalk, G.; Dürre, P. *Clostridium ljungdahlii* represents a microbial production platform based on syngas. *Proc. Natl. Acad. Sci. U. S. A.* **2010**, *107*, 13087−13092.
(9) Köpke, M.; Simpson, S. D. Pollution to products: recycling of 'above ground' carbon by gas fermentation. *Curr. Opin. Biotechnol.* **2020**, *65*, 180−189.
(10) Bengelsdorf, F. R.; Beck, M. H.; Erz, C.; Hoffmeister, S.; Karl, M. M.; Riegler, P.; Wirth, S.; Poehlein, A.; Weuster-Botz, D.; Dürre, P. Bacterial anaerobic synthesis gas (syngas) and CO_2+H_2 Fermentation. *Adv. Appl. Microbiol.* **2018**, *103*, 143−221.
(11) Daniell, J.; Köpke, M.; Simpson, S. D. Commercial biomass syngas fermentation. *Energies* **2012**, *5*, 5372−5417.
(12) Drake, H. L. Acetogenesis, Acetogenic Bacteria, and the Acetyl-CoA "Wood/Ljungdahl" Pathway: Past and Current Perspectives. In *Acetogenesis*; Drake, H. L., Ed.; Springer US: New York, 1994; pp 3−60.
(13) Ragsdale, S. W. Enzymology of the Wood-Ljungdahl pathway of acetogenesis. *Ann. N. Y. Acad. Sci.* **2008**, *1125*, 129−136.
(14) Drake, H. L.; Gößner, A. S.; Daniel, S. L. Old acetogens, new light. *Ann. N. Y. Acad. Sci.* **2008**, *1125*, 100−128.
(15) Schuchmann, K.; Müller, V. Autotrophy at the thermodynamic limit of life: A model for energy conservation in acetogenic bacteria. *Nat. Rev. Microbiol.* **2014**, *12*, 809−821.
(16) Schölmerich, M. C.; Müller, V. Energy conservation by a hydrogenase-dependent chemiosmotic mechanism in an ancient metabolic pathway. *Proc. Natl. Acad. Sci. U. S. A.* **2019**, *116*, 6329−6334.
(17) Müller, V. Energy conservation in acetogenic bacteria. *Appl. Environ. Microbiol.* **2003**, *69*, 6345−6353.
(18) Schuchmann, K.; Müller, V. Energetics and application of heterotrophy in acetogenic bacteria. *Appl. Environ. Microbiol.* **2016**, *82*, 4056−4069.
(19) Schuchmann, K.; Müller, V. Direct and reversible hydrogenation of CO_2 to formate by a bacterial carbon dioxide reductase. *Science* **2013**, *342*, 1382−1385.
(20) Schwarz, F. M.; Schuchmann, K.; Müller, V. Hydrogenation of CO_2 at ambient pressure catalyzed by a highly active thermostable biocatalyst. *Biotechnol. Biofuels* **2018**, *11*, 237.
(21) Müller, V. New horizons in acetogenic conversion of one-carbon substrates and biological hydrogen storage. *Trends Biotechnol.* **2019**, *37*, 1344−1354.
(22) Schwarz, F. M.; Müller, V. Whole-cell biocatalysis for hydrogen storage and syngas conversion to formate using a thermophilic acetogen. *Biotechnol. Biofuels* **2020**, *13*, 32.
(23) Kottenhahn, P.; Schuchmann, K.; Müller, V. Efficient whole cell biocatalyst for formate-based hydrogen production. *Biotechnol. Biofuels* **2018**, *11*, 93.
(24) Preuster, P.; Papp, C.; Wasserscheid, P. Liquid Organic Hydrogen Carriers (LOHCs): Toward a Hydrogen-free Hydrogen Economy. *Acc. Chem. Res.* **2017**, *50*, 74−85.
(25) Enthaler, S.; von Langermann, J.; Schmidt, T. Carbon dioxide and formic acid-the couple for environmental-friendly hydrogen storage? *Energy Environ. Sci.* **2010**, *3*, 1207−1217.
(26) An, L.; Chen, R. Direct formate fuel cells: A review. *J. Power Sources* **2016**, *320*, 127−139.
(27) Yishai, O.; Lindner, S. N.; Gonzalez de la Cruz, J.; Tenenboim, H.; Bar-Even, A. The formate bio-economy. *Curr. Opin. Chem. Biol.* **2016**, *35*, 1−9.
(28) Hwang, H. W.; Yoon, J.; Min, K.; Kim, M.-S.; Kim, S.-J.; Cho, D. H.; Susila, H.; Na, J.-G.; Oh, M.-K.; Kim, Y. H. Two-stage bioconversion of carbon monoxide to biopolymers via formate as an intermediate. *Chem. Eng. J.* **2020**, *389*, 124394.
(29) Li, H.; Opgenorth, P. H.; Wernick, D. G.; Rogers, S.; Wu, T. Y.; Higashide, W.; Malati, P.; Huo, Y. X.; Cho, K. M.; Liao, J. C. Integrated electromicrobial conversion of CO_2 to higher alcohols. *Science* **2012**, *335*, 1596.
(30) Kim, S. J.; Yoon, J.; Im, D. K.; Kim, Y. H.; Oh, M. K. Adaptively evolved *Escherichia coli* for improved ability of formate utilization as a carbon source in sugar-free conditions. *Biotechnol. Biofuels* **2019**, *12*, 207.
(31) Oswald, F.; Dörsam, S.; Veith, N.; Zwick, M.; Neumann, A.; Ochsenreither, K.; Syldatk, C. Sequential mixed cultures: From syngas to malic acid. *Front. Microbiol.* **2016**, *7*, 891.
(32) Hu, P.; Chakraborty, S.; Kumar, A.; Woolston, B.; Liu, H.; Emerson, D.; Stephanopoulos, G. Integrated bioprocess for conversion of gaseous substrates to liquids. *Proc. Natl. Acad. Sci. U. S. A.* **2016**, *113*, 3773−3778.
(33) Straub, M.; Demler, M.; Weuster-Botz, D.; Dürre, P. Selective enhancement of autotrophic acetate production with genetically modified *Acetobacterium woodii*. *J. Biotechnol.* **2014**, *178*, 67−72.
(34) Riegler, P.; Bieringer, E.; Chrusciel, T.; Stärz, M.; Löwe, H.; Weuster-Botz, D. Continuous conversion of CO_2/H_2 with *Clostridium aceticum* in biofilm reactors. *Bioresour. Technol.* **2019**, *291*, 121760.
(35) Kantzow, C.; Mayer, A.; Weuster-Botz, D. Continuous gas fermentation by *Acetobacterium woodii* in a submerged membrane reactor with full cell retention. *J. Biotechnol.* **2015**, *212*, 11−18.
(36) Oswald, F.; Stoll, I. K.; Zwick, M.; Herbig, S.; Sauer, J.; Boukis, N.; Neumann, A. Formic acid formation by *Clostridium ljungdahlii* at elevated pressures of carbon dioxide and hydrogen. *Front. Bioeng. Biotechnol.* **2018**, *6*, 6.
(37) Kantzow, C.; Weuster-Botz, D. Effects of hydrogen partial pressure on autotrophic growth and product formation of *Acetobacterium woodii*. *Bioprocess Biosyst. Eng.* **2016**, *39*, 1325−1330.
(38) Weghoff, M. C.; Müller, V. CO metabolism in the thermophilic acetogen *Thermoanaerobacter kivui*. *Appl. Environ. Microbiol.* **2016**, *82*, 2312−2319.
(39) Hungate, R. E. A roll tube method for cultivation of strict anaerobes. In *Methods in Microbiology*; Norris, J. R., Ribbons, D. W., Eds.; Academic Press: New York and London, 1969; Vol. *3b*, pp 117−132.
(40) Bryant, M. P. Commentary on the Hungate technique for culture of anaerobic bacteria. *Am. J. Clin. Nutr.* **1972**, *25*, 1324−8.
(41) Heise, R.; Müller, V.; Gottschalk, G. Sodium dependence of acetate formation by the acetogenic bacterium *Acetobacterium woodii*. *J. Bacteriol.* **1989**, *171*, 5473−5478.
(42) Heise, R.; Müller, V.; Gottschalk, G. Presence of a sodium-translocating ATPase in membrane vesicles of the homoacetogenic bacterium *Acetobacterium woodii*. *Eur. J. Biochem.* **1992**, *206*, 553−557.
(43) Schmidt, K.; Liaaen-Jensen, S.; Schlegel, H. G. Die Carotinoide der *Thiorhodaceae*. *Arch. Microbiol.* **1963**, *46*, 117−126.

https://doi.org/10.1021/acssuschemeng.1c01062
ACS Sustainable Chem. Eng. 2021, 9, 6810−6820

(44) Bredwell, M. D.; Worden, R. M. Mass-transfer properties of microbubbles. 1. Experimental studies. *Biotechnol. Prog.* **1998**, *14*, 31−38.
(45) Schwarz, F. M.; Ciurus, S.; Jain, S.; Baum, C.; Wiechmann, A.; Basen, M.; Müller, V. Revealing formate production from carbon monoxide in wild type and mutants of Rnf- and Ech-containing acetogens, *Acetobacterium woodii* and *Thermoanaerobacter kivui*. *Microb. Biotechnol.* **2020**, *13*, 2044−2056.
(46) Wiechmann, A.; Ciurus, S.; Oswald, F.; Seiler, V. N.; Müller, V. It does not always take two to tango: "Syntrophy" *via* hydrogen cycling in one bacterial cell. *ISME J.* **2020**, *14*, 1561−1570.
(47) Andreesen, J. R.; Schaupp, A.; Neurauter, C.; Brown, A.; Ljungdahl, L. G. Fermentation of glucose, fructose, and xylose by *Clostridium thermoaceticum*: effect of metals on growth yield, enzymes, and the synthesis of acetate from CO_2. *J. Bacteriol.* **1973**, *114*, 743−751.
(48) Kozuch, S.; Martin, J. M. "Turning over" definitions in catalytic cycles. *ACS Catal.* **2012**, *2* (12), 2787−2794.
(49) Mourato, C.; Martins, M.; da Silva, S. M.; Pereira, I. A. C. A continuous system for biocatalytic hydrogenation of CO_2 to formate. *Bioresour. Technol.* **2017**, *235*, 149−156.
(50) Roger, M.; Brown, F.; Gabrielli, W.; Sargent, F. Efficient hydrogen-dependent carbon dioxide reduction by *Escherichia coli*. *Curr. Biol.* **2018**, *28*, 140−145.
(51) Pappenreiter, P. A.; Zwirtmayr, S.; Mauerhofer, L. M.; Rittmann, S. K. R.; Paulik, C. Development of a simultaneous bioreactor system for characterization of gas production kinetics of methanogenic archaea at high pressure. *Eng. Life Sci.* **2019**, *19*, 537−544.

https://doi.org/10.1021/acssuschemeng.1c01062
ACS Sustainable Chem. Eng. 2021, 9, 6810−6820

SUPPORTING INFORMATION

Acetogenic conversion of H_2 and CO_2 into formic acid

and *vice versa*

in a fed-batch operated stirred tank bioreactor

Fabian M. Schwarz †, Florian Oswald† and Volker Müller†*

†Department of Molecular Microbiology and Bioenergetics, Institute of Molecular Biosciences, Johann Wolfgang Goethe University, Max-von-Laue-Str. 9, 60438 Frankfurt am Main, Germany

*Corresponding author: vmueller@bio.uni-frankfurt.de

The Supporting Information consists of 5 pages, including 3 figures and 1 table:

Supplementary Figures

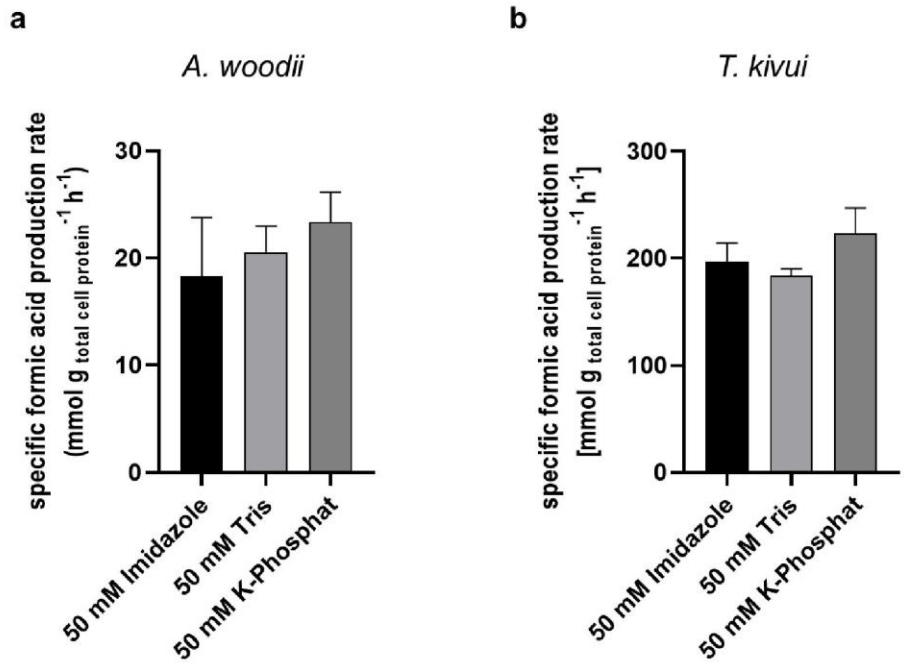

Figure S1. Buffer effect in whole-cell based formic acid production of *A. woodii* and *T. kivui*. Resting cells of *A. woodii* and *T. kivui* were prepared as described and suspended in the corresponding buffer of 50 mM imidazole, 20 mM KCl, 20 mM $MgSO_4$, 20 mM NaCl, pH 7.0 or 50 mM Tris, 20 mM KCl, 20 mM $MgSO_4$, 20 mM NaCl, pH 8.0 or 50 mM K-phosphate, 20 mM KCl, 20 mM NaCl, pH 7.0 to a final concentration of 1 mg/mL. Each buffer contained additional 2 mM DTE and 4 µM resazurin. Prior to the reaction start, 30 µM monensin in case of *A. woodii* and 300 mM $KHCO_3$ in case of *T. kivui* were added. The experiment was started by replacing the gas phase with H_2+CO_2 (80:20 %, 2 × 105 kPa). The specific formic acid production rates of *A. woodii* **(a)** and *T. kivui* **(b)** are shown. All data points are mean ± SD, N = 2.

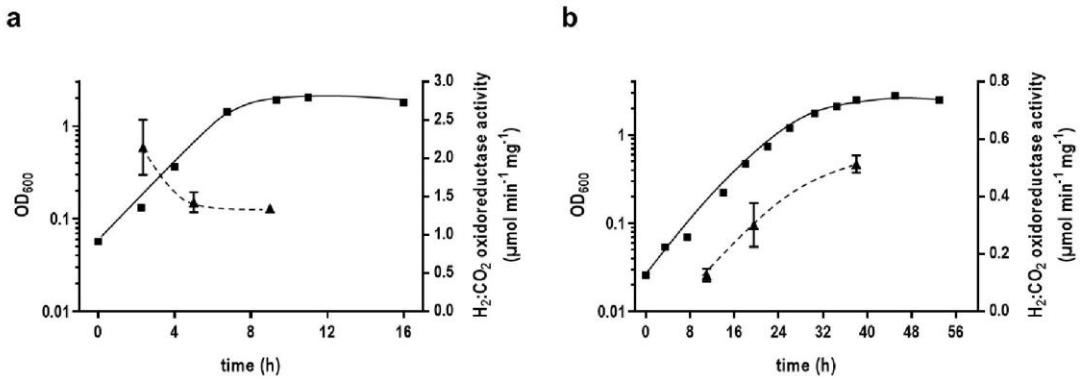

Figure S2. Growth-phase dependent conversion activity of H_2 and CO_2 into formic acid by the HDCR. Cultures of *T. kivui* and *A. woodii* were grown in complex medium with pyruvate (100 mM) or fructose (20 mM) as substrate to the early-, mid- and late-exponential growth phase. Cell were harvested in the appropriate growth phase and cell free extracts were prepared. The H_2:CO_2 oxidoreductase activity was measured in anoxic serum bottles containing a gas atmosphere of H_2+CO_2 (80:20%), buffer (100 mM HEPES, 20 mg MgSO4, 2 mM DTE, 4 µM Resazurin, pH 7.0) and cell free extracts (0.5 mg/ml) of *T. kivui* **(a)** and *A. woodii* **(b)**. Squares, optical density at 600 nm; triangels, H_2:CO_2 oxidoreductase activity. All data points are mean ± SD, N = 2.

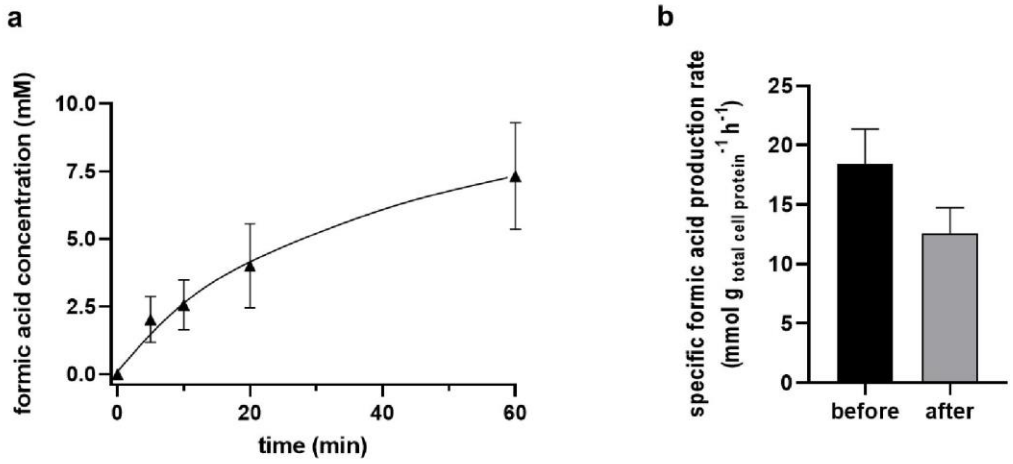

Figure S3. Cell recycling of bioreactor cells. Resting cells of *A. woodii* were prepared as described before and the ability of H_2-driven CO_2 reduction to formic acid was analyzed before and after the use of cells in the bioreactor approach. In both cases *A. woodii* cells were treated the same way with 30 µM monensin as "uncoupler", 50 mM K-phosphate as buffer and a gas atmosphere of H_2 + CO_2 (80:20%, 2 × 105 kPa) was used. Shown is the formic acid production of the recycled cells over the time **(a)** and the comparison of the specific rates before and after the fermentation approach **(b)**. All data points are mean ± SD, N = 2.

Supplementary Table

Table S1. Buffer and substrate effect for formate and formic acid-driven H_2 production using resting cells of *A. woodii*. Resting cells of *A. woodii*, grown on 20 mM fructose were prepared as described before. The cells were suspended in the corresponding buffer to a final concentration of 1 mg/mL. The reaction was started by adding the corresponding substrate to the serum bottles and the H_2 evolution was monitored. Shown is the mean of two biological replicates.

Buffer-substance*	50 mM imidazole	50 mM imidazole	500 mM K-phosphate	500 mM K-phosphate
Substrate	200 mM K-formate	200 mM formic acid	150 mM K-formate	150 mM formic acid
qH_2 (mmol g^{-1} h^{-1})	**70.7**	**0**	**45.3**	**37.4**
pH after substrate addition	7	2.5	7	6.2

*contained additional 20 mM KCl, 20 mM $MgSO_4$, 4 µM Resazurin, 2 mM DTE, pH 7.0. K-phosphate buffer without additional $MgSO_4$

7. Deutsche Zusammenfassung

In Zeiten der globalen Klimaerwärmung und des Klimawandels werden Strategien zur Vermeidung, Reduzierung oder Wiederverwertung von CO_2 - Emissionen sowie die Abkehr von fossilen Energieträgern immer wichtiger. Aus diesem Grund erfreuen sich Technologien zur Bindung, Speicherung und Wiederverwertung von CO_2 immer größerer Aufmerksamkeit und diverse chemische als auch biologische Ansätze werden verfolgt. Eine dieser Möglichkeiten umfasst die Reduktion von CO_2 mit Hilfe von molekularem Wasserstoff. Im Prozess der direkten Hydrogenierung von CO_2 zu Ameisensäure bzw. Formiat wird nicht nur CO_2 gebunden, sondern ebenfalls H_2 in flüssiger Form gespeichert. Wasserstoff als möglicher Energieträger der Zukunft kann hierbei durch die Elektrolyse von Wasser mit Strom aus erneuerbaren Energiequellen wie Solar- und Windenergie erzeugt werden. Da die flüssige Verbindung Ameisensäure gegenüber dem hochflüchtigen Wasserstoffgas verschiedenste Vorteile aufweist (z. B. nicht entflammbar, einfachere Handhabung, höhere volumenbezogene Energiedichte), zählt Ameisensäure zu der Gruppe der flüssigen, organischen Wasserstoffspeicherverbindungen. Daneben ist das Einsatzgebiet von Ameisensäure als Ausgangstoff für Chemikalien oder als mikrobielle Kohlenstoffquelle sehr vielseitig und die Verbindung erfreut sich zunehmenden Interesses.

Die thermodynamische und kinetische Stabilität des CO_2-Moleküls stellt die chemische Katalyse zur Reduktion von CO_2 in Bezug auf Effizienz und ökonomische Rentabilität vor Herausforderungen. Die Natur hält hier biologische Katalysatoren (Enzyme) bereit, die eine Reduktion von CO_2 in den 7 bekannten CO_2-Fixierungswegen ermöglichen. Einer dieser CO_2-Fixierungswege wird auch als Wood-Ljungdahl-Weg (WLP) oder reduktiver Acetyl-CoA-Weg bezeichnet und kommt neben methanogenen Archaeen und Sulfatreduzierern auch in acetogenen Bakterien vor. Acetogene Bakterien sind eine heterogene Gruppe von strikt anaeroben Bakterien die eine hohe metabolische Flexibilität besitzen und eine Vielzahl verschiedener Substrate verwerten können. Neben einem chemoorganoheterotrophem Lebensstil können acetogene Bakterien auch chemolithoautotroph mit H_2 und CO_2 als Energie- und Kohlenstoffquelle wachsen. Zur Reduktion und Fixierung von CO_2 im WLP besitzen acetogene

Bakterien Formiatdehydrogenasen als CO_2-Reduktasen. Diese Enzyme katalysieren die reversible 2-Elektronen Reduktion von CO_2 zu Ameisensäure, wobei die verwendeten Elektronendonoren und Enzymkomplexe innerhalb der Gruppe der acetogenen Bakterien sehr divers sein können. Kürzlich konnte aus dem mesophilen Bakterium *A. woodii* und dem thermophilen Bakterium *T. kivui* ein neuartiger, cytoplasmatischer Enzymkomplex isoliert werden, der die Reduktion von CO_2 direkt an die Oxidation von H_2 koppelt. Der Enzymkomplex wurde als Wasserstoff-abhängige CO_2-Reduktase bezeichnet (engl. hydrogen-dependent CO_2 reductase, HDCR). Nicht nur die Verwendung von molekularem Wasserstoff als direkter Elektronendonor war bis dato neu, sondern die HDCR katalysierte die reversible Hydrogenierung von CO_2 zu Formiat mit annähernd gleicher Kinetik und Umsatzraten. Die hier erreichten Umsatzraten bei der CO_2 Reduktion übertrafen bisherige chemische als auch biologische Katalysatoren um mehre Größenordnungen.

Im Hinblick auf die besonderen katalytischen Eigenschaften der HDCRs wurde in dieser Arbeit die biotechnologische Anwendbarkeit der Enzyme als Biokatalysatoren zur Speicherung und Sequestrierung von H_2 und CO_2 in Form von Ameisensäure untersucht. Im Speziellen wurde ein HDCR-basiertes Ganz-Zell-System für das thermophile Bakterium *T. kivui* entwickelt. Ein Ganz-Zell-System für *A. woodii* wurde bereits zuvor etabliert. Der Einsatz von ganzen Zellen als Biokatalysatoren bietet verschieden Vorteile gegenüber gereinigten Enzymen wie z.B. die Kosten- und Zeitreduzierung im Herstellungsprozess, mögliche Skaleneffekte und der Schutz von Zell-umschlossenen Enzymen vor schädigenden Substanzen aus der unmittelbaren Umgebung. Dies ermöglicht unter anderem einen Schutz der sauerstoffempfindlichen HDCR vor Spuren von O_2, die das aktive Zentrum [H-Cluster] der Hydrogenase-Untereinheit irreversible schädigen können. Auch die Nutzung von thermophilen Organismen in der Anwendung bergen verschiedene Vorteile. So sind zum Beispiel höhere Temperaturen meist mit höheren Umsatzraten verbunden und die Prozesskühlungskosten sowie das Kontaminationsrisiko können reduziert werden. Um eine Ganz-Zell basierte Umwandlung von H_2 und CO_2 zu Formiat zu gewährleisten, wurde zuvor die Weiterverwertung des Formiats zu Acetat im WLP gestoppt. Wie bereits beschrieben ist die Formyl-THF-Synthetase Reaktion, die der HDCR-Reaktion im Methyl-Zweig des WLP nachfolgt, ATP abhängig.

Durch eine Reduktion des zellulären ATP Gehalts konnte eine weitere Prozessierung des aus der HDCR-Reaktion gebildeten Formiats im Zellstoffwechsel des Bakteriums unterbunden werden. Hierzu wurden Inhibitorstudien durchgeführt und eine verminderte Acetatbildung aus H_2 + CO_2 wurde bei ruhenden Zellen beobachtet. Zudem wurde Formiat das dominierende Endprodukt. Interessanterweise hatten höhere Konzentrationen an Bicarbonat (ab 300 mM) ebenfalls eine supprimierende Wirkung auf die Acetatbildung und eine steigernde Wirkung auf die Formiatbildung zur Folge. Mit Hilfe von Membranstudien konnte ein inhibierender Effekt auf die ATP-Synthase-Aktivität von *T. kivui* geschlussfolgert werden, wodurch die Bildung von ATP und damit die Bildung von Acetat gehemmt wurde. In Anwesenheit von Bikarbonat wurde anschließend die Formiatbildung aus H_2 und CO_2 in Zellsuspensionen von *T. kivui* charakterisiert. Hier zeigten *T. kivui* Zellen mit 234 mmol g^{-1} h^{-1} die höchste spezifische Formiatbildungsrate, die bis dato in der Literatur genannt wurde und bis zu 130 mM Formiat wurden innerhalb von 90 min gebildet. Der entkoppelnde Effekt von Bikarbonat auf wachsende *T. kivui* Zellen sowie der Einfluss auf die Produktbildung konnten ebenfalls in einem geschlossenen Wachstumsansatz demonstriert werden. So führte bei heterotroph angezogenen *T. kivui* Zellen die Zugabe von Bikarbonat und H_2 und CO_2 zu einem sofortigen Wachstumsstopp der Zellen und das vorherrschende Produkt verlagerte sich von Acetat zum gewünschten Endprodukt Formiat. Der Wechsel von einer Wachstumsphase in eine Produktionsphase zur Umwandlung von H_2 und CO_2 zu Formiat konnte damit demonstriert werden.

In einer zuvor veröffentlichten Studie konnte *T. kivui* ebenfalls an einen carboxydotrophen Lebensstil mit 100% CO adaptiert werden. CO ist neben H_2 und CO_2 ein wesentlicher Bestandteil von industriellen Abfallgasen (auch Synthesegas genannt), die unter anderem im Stahlherstellungsprozess und bei der Vergasung von Biomasseabfällen und anderen Abfallströmen entstehen. Der Prozess der Synthesegasfermentation wird bereits zur Produktion von diversen Biochemikalien und Biokraftstoffen eingesetzt. Aus diesem Grund wurde in dieser Arbeit ebenfalls die Umwandlung von Synthesegas (H_2 + CO_2 und CO) zu Formiat untersucht. Bioenergetisch entkoppelte und auf CO-adaptierte *T. kivui* Zellen konnten in der Tat Synthesegas exklusiv zu Formiat umsetzen. Dies wurde in der vorgelegten Arbeit erstmalig für die Gruppe der acetogenen Bakterien

demonstriert. Die spezifische Aktivität betrug 8 mmol g^{-1} h^{-1} und ein Verbrauch der CO Bestandteile konnte im Gasgemisch nachgewiesen werden. Die Verwertung und Umwandlung von CO im Gasgemisch rief die Frage auf, ob ruhende Zellen auch CO als alleiniges Substrat zu Formiat umsetzen können. Zur Klärung der Fragestellung wurde in dieser Arbeit die Formiat- und Acetatbildung aus CO untersucht. Dazu wurden ruhende Zellen der beiden bekannten HDCR-enthaltenden Organismen *A. woodii* und *T. kivui* herangezogen. Hier wurde die Produktbildung sowie der Substratverbrauch von bioenergetisch gekoppelten und entkoppelten Zellen untersucht. Auch der Einfluss von variierenden CO-Konzentrationen war Bestandteil der Arbeit. Um die CO-Verwertung zu Acetat und Formiat im Stoffwechsel der Rnf- (*A. woodii*) und Ech-Acetogenen (*T. kivui*) verstehen zu können, wurden Mutanten von *A. woodii* und *T. kivui* zu Hilfe genommen. Die Mutanten von Δ*hdcr*, Δ*cooS*, Δ*hydBA*, Δ*rnf* and Δ*ech2* weisen katalytische Defizite bei den Enzymen des zentralen Zellstoffwechsels auf und ermöglichten so die Feststellung von Unterschieden in der CO-Verwertung der beiden untersuchten Mikroorganismen. In beiden Organismen war die CO-basierte Formiatbildung vom Vorhandensein eines funktionalen HDCR Enzymkomplexes abhängig.

Für eine mögliche biotechnologische Anwendung der beiden acetogenen Bakterien *A. woodii* und *T. kivui* im Bereich der CO_2-Sequestrierung und H_2-Speicherung wurde die Maßstabsvergrößerung des Ganz-Zell-Systems angestrebt. Dazu wurde der Maßstab von Serumflaschenversuchen (120 mL) mit unkontrollierten Prozessbedingungen hin zu einem Bioreaktormaßstab (3 L) mit kontrollierten Prozessbedingungen skaliert. Diese Arbeit demonstriert die effiziente Umwandlung von H_2 und CO_2 zu Formiat unter Verwendung eines Rührkesselreaktors. Der Prozess zeigte eine Effizienz von 100% für die Umwandlung von CO_2 zu Formiat und spezifische Raten von 48.3 mmol g^{-1} h^{-1} wurden von *A. woodii* Zellen erreicht. Zudem wurden verschiedene Faktoren und Parameter des Bioreaktoransatzes optimiert und evaluiert. So konnte unter anderem bei optimierter Gaszusammensetzung eine finale Formiatkonzentration von 73 mM im Reaktor erreicht werden. Ebenso wurde die Reversibilität der direkten Hydrogenierung von CO_2 im Bioreaktoransatz untersucht. Dazu wurde die Oxidation von Ameisensäure mit simultaner Freisetzung von H_2 und CO_2 betrachtet. Für eine mögliche biotechnologische Anwendung ist die Freisetzung

des zuvor gespeicherten H_2 in Form von Ameisensäure bzw. Formiat ein nicht zu vernachlässigender Prozessschritt um den H_2-Kreislauf zu schließen. Durch die kontinuierliche Zufütterung von reiner Ameisensäure in den Bioreaktor, konnte die Substratkonzentration sowie der pH-Wert während der gesamten Prozesszeit auf einem konstanten Niveau gehalten werden. Die spezifische H_2-Produktionsrate (qH_2) betrug 27.6 mmol g^{-1} h^{-1} und mehr als 2.12 M Ameisensäure konnte über einen Zeitraum von 195 h oxidiert werden. Wichtige Parameter der Enzymkatalyse wie Wechselzahl (engl. turnover frequency, TOF) und katalytische Produktivität (engl. turnover number, TON) wurden ebenfalls im Versuch bestimmt.

Nachdem die Umsetzung von H_2 und CO_2 zu Formiat sowie die Formiatoxidation zu H_2 und CO_2 im Rührkesselreaktor demonstriert wurden, stand die Planung und Konstruktion eines HDCR-basierten Anwendungsansatzes im Vordergrund. Basierend auf dem generierten Prozessverständnis und der effizienten Reversibilität der katalysierten Reaktionen wurde ein Ganz-Zell-basierter Bioreaktoraufbau gewählt, der die vielfache Speicherung und Freisetzung von H_2 in einer einzigen Prozesseinheit und unter Verwendung eines einzelnen Katalysators ermöglicht. Die konzipierte Prozesseinheit kann so als „Bio-Batterie“ zur Speicherung und Freisetzung von überschüssiger Energie in Form von H_2 betrachtet werden (siehe Additional results). Über eine Prozesszeit von 2 Wochen und 15 CO_2 Reduktions-/Formiat Oxidations-Zyklen wurde so im Mittel 330 mM Formiat produziert und oxidiert. Die durchgeführten Bioreaktorstudien zeigen das Potential der acetogenen Bakterien in der biotechnologischen Anwendung und geben zudem einen vielversprechenden Ausblick auf weitere Prozessideen mit diversen Reaktortypen.

Zusammenfassend thematisiert diese Arbeit die biotechnologische Anwendbarkeit eines Ganz-Zell-Systems zur Speicherung und Sequestrierung von H_2 und CO_2 in Form von Formiat und *vice versa*. Die katalytische Aktivität der betrachteten Organismen von *A. woodii* und *T. kivui* fußt dabei auf der Aktivität eines neuartigen Enzymkomplexes, der in der Gruppe der acetogenen Bakterien erstmals entdeckt wurde. Der als Wasserstoff-abhängige CO_2-Reduktase bezeichnete Enzymkomplexe könnte zudem die zukünftige Konzipierung Enzym-inspirierter und effizienter chemischer Katalysatoren

vorantreiben. Auch der Einsatz des Enzyms/der Zellen in so genannten Hydrogelen oder die Etablierung elektrochemischer Prozesse sind vorstellbar. Diese Arbeit stellt somit eine Basis für mögliche zukünftige Anwendungen des etablierten Ganz-Zell-Systems von *A. woodii* und *T. kivui* im Bereich der Wasserstoffökonomie dar.